STUDIES ON PROPERTIES OF PREVULCANIZED NATURAL RUBBER LATEX LAYERED SILICATE NANOCOMPOSITES

Thesis submitted to
MAHATMA GANDHI UNIVERSITY
in partial fulfilment of the
requirements for the award of the degree of
DOCTOR OF PHILOSOPHY
in Chemistry under the Faculty of Science

by
SHERA MATHEW
Technical Consultancy Division
Rubber Research Institute of India
Kottayam, Kerala, India-686 009

DECEMBER 2011

...To my
dear husband, kids &
my beloved parents

RUBBER RESEARCH INSTITUTE OF INDIA
RUBBER BOARD
(MINISTRY OF COMMERCE AND INDUSTRY, GOVERNMENT OF INDIA)

Dr. Siby Varghese
Deputy Director, Technical Consultancy Division
JSPS Postdoctoral Fellow, Japan • Humboldt Fellow, Germany

Certificate

This is to certify that the thesis entitled **"Studies on Properties of Prevulcanized Natural Rubber Latex Layered Silicate Nanocomposites"** is an authentic record of the research work carried out by **Ms. Shera Mathew** under my supervision and guidance in partial fulfilment of the requirements for the award of the degree of **Doctor of Philosophy in Chemistry** under the Faculty of Science of the Mahatma Gandhi University, Kottayam. The work presented in this thesis has not been submitted for any other degree or diploma earlier. It is also certified that **Ms. Shera Mathew** has fulfilled all the course requirements.

Kottayam
December 2011

Dr. Siby Varghese
(Supervising Teacher)

Technical Consultancy Division, Kottayam-686 009, Kerala, India.
Phone: +91 481 2354474 (Direct), +91 481 2353311 (10 lines), Fax: +91 481 2353327
E-mail: sibyvarghese100@yahoo.com, siby@rubberboard.org.in

Declaration

    I, Shera Mathew, hereby declare that the thesis entitled **"Studies on Properties of Prevulcanized Natural Rubber Latex Layered Silicate Nanocomposites"** is the original research work carried out by me under the supervision of **Dr. Siby Varghese**, Dy. Director (Technical Consultancy Division), Rubber Research Institute of India, Kottayam and that it has not previously formed the basis of award of any other degree or diploma or other similar title.

Kottayam   **Shera Mathew**
December 2011

Acknowledgement

GLOSSARY

λ	-	wavelength
θ	-	incident angle
δ	-	phase angle
γ	-	shear rate
ε	-	strain
η	-	viscosity
χ	-	interaction parameter
σ	-	stress
ρ	-	specific gravity
τ	-	tortuosity factor
Υ	-	shear rate
k	-	viscosity index
E_a	-	activation energy
R	-	universal gas constant
T	-	absolute temperature
α	-	extension ratio

d	-	interlamellar spacing
V_r	-	volume fraction of rubber
F	-	weight fraction of the filler
ρ_r	-	specific gravity of rubber
ρ_s	-	specific gravity of solvent
v	-	crosslink density
n	-	pseudoplastic index
δ_p	-	solubility parameter of polymer
η_o	-	zeroshear viscosity
Φ_1	-	volume fraction of component 1
Φ_2	-	volume fraction of component 2
T_s	-	yield stress
tpa	-	tonne per annum
nm	-	nanometer
μm	-	micrometer
meq/g	-	milliequivalents per gram
σ	-	surface charge density
S	-	specific surface of the layered silicate
e	-	elementary charge, 1.6022×10^{-19} C
a	-	unit cell parameter
L/h	-	aspect ratio
ν (Si-O)	-	Si-O stretching vibration
δ (Si-O)	-	Si-O bending vibration,
ABS	-	acrylonitrile butadiene styrene
ATH	-	aluminium trihydride
AZO	-	aluminum-doped zinc oxide

BGNF	-	bioactive glass nanofiber
BNNT	-	boron nitride nanotube
BZC	-	basic zinc carbonate
CEC	-	cation exchange capacity
CVD	-	chemical vapor deposition
CVI	-	chemical vapor infiltration
DMTA	-	dyanamic mechanical thermal analysis
DSC	-	differential scanning calorimetry
DTG	-	differentiation of the thermogravimetric curve
DRC	-	dry rubber content
DPNR	-	deproteinized natural rubber
ECM	-	extra cellular matrix
ENR	-	epoxidized natural rubber
EVA	-	ethylene vinyl acetate
FTIR	-	fourier transform infrared
HFIP	-	hexafluoro-2-isopropyl alcohol
HNBR	-	hydrogenated accrylo nitrile-butadiene rubber
HPMC	-	hydroxy propyl methyl cellulose
MA	-	maleic anhydride
MB	-	melt blend
Na-MMT	-	sodium montmorillonite
OMMT	-	organic montmorillonite
PACN	-	poly (acrylonitrile)
PANI	-	poly (aniline)
PC	-	polycarbonate
PDDA	-	polydimethyl diallyl ammonium

PE	-	poly ethylene
PEEK	-	poly (aryl- ether- ether- ketone)
PET	-	poly (ethylene terephthalate)
PLGA	-	poly (glycolic acid)
PNC	-	polymer nanocomposites
PP	-	polypropylene
PPS	-	poly (phenylene sulfide)
PVC	-	poly vinyl chloride
PVD	-	physical vapor deposition
PVP	-	poly (vinylpyrrolidone)
SEM	-	scanning electron micrograph
SF	-	silk fibroin
SP/SA	-	*superior processing grades*
SWNCT	-	single walled carbon nanotubes
TEM	-	transmission electron microscopy
TEOS	-	tetraethyl orthosilicate
TGA	-	thermogravimetric analysis
TPNR	-	thermoplastic natural rubber
TPO	-	thermoplastic olefin
TSR	-	technically specified rubber
UHV	-	ultra-high vacuum
XRD	-	X- ray diffraction
XPS	-	X-ray photo electron spectroscopy
ZDC	-	zinc diethyl dithiocarbamate
ZMBT	-	zinc mercapto benzthiasole

Preface

The field of material science has become quite popular and pragmatic with a tremendous lust for composite materials that exhibit the positive characteristics of both the components. Of late world-wide attempts were made to tailor the structure and composition of materials of nanometer scale. Composites that exhibit a change in composition and structure over a nanometer scale have shown remarkable property enhancements relative to conventional composites. Nanocomposites are a combination of two or more phases containing different compositions or structures where at least one of the phases is in the range of 10 to100 nm. Fillers with a particle size in the nanometer range have small number of atoms per particle and for this reason they have different properties than the bulk material and strong interactions with the matrix. The separation of filler particles is of the order of molecular dimensions, which may modify the properties of polymers. Nanostructured composites based on clay and polymers from methyl methacrylate, styrene, acrylonitrile and pyrrole have been receiving much research attention in view of many improved bulk properties of these composites compared to those of the base polymer.

In this work for the preparation of natural rubber nanocomposites two nanoclays were used: one synthetic (fluorohectorite) and the other natural (bentonite) in origin. English Indian clay, also called china clay, which is amorphous in nature was used as the reference material. These materials are mixed with prevulcanized natural rubber latex and also blended with chloroprene latex. In these studies more emphasis is given to layered silicates with sulphur prevulcanized latex.

The present study is divided into 10 chapters and is described under different headings as follows. First chapter gives a general introduction to nanocomposites. Second chapter deals with the experimental techniques used throughout the study. In the third chapter, the preparation of prevulcanized latex nanocomposites and their characterization using TEM and XRD are given. The mechanical properties are also discussed in this chapter. The preparation of radiation vulcanized latex nanocomposites and their characterization using TEM, XRD are given in the chapter 4. The mechanical and dynamic mechanical properties are also discussed. Fifth chapter is devoted to the rheological properties of sulphur prevulcanized latex compounds. The dipping characteristics of layered silicates nanocomposites using an automatic dipping machine is given in chapter 6. Dipping characteristics such as immersion and withdrawal speeds of the former, immersion time, concentration of the coagulant etc of the layered latex nanocompounds are demonstrated. The effect of layered silicates on the ageing of latex films with degrading agents such as UV, γ- radiations, autoclave ageing, higher temperature, ozone, chlorine, solvents etc are discussed here in chapter 7. Mechanical and morphological properties of natural rubber/chloroprene latex blends nanocomposites are given in chapter 8. In this chapter the effect of layered silicate on chloroprene latex and its blends with natural rubber latex in different proportions is given. The morphological studies were done using FTIR, XRD, TEM and SEM analysis. Finally a suitable latex compound with nanoclays has been developed for the production of Foley catheters and their technological properties are evaluated (chapter 9). The overall conclusion of the research work and future scope are discussed in chapter 10.

CONTENTS

Chapter 1

Introduction

Nanotechnology is recognized as one of the highly promising areas for technological development in the 21st century. In materials research, the development of polymer nanocomposites is rapidly emerging as a multidisciplinary research activity whose results could broaden the applications of polymers to the benefit of many industries. This introductory chapter gives an overview of the recent advances in polymer nanocomposites. The chapter focuses on the general introduction of the nanocomposites, their classification and the synthetic routes of preparation of nanocomposites. The general properties of different nanocomposites are also covered in this section. Specifically recent literature on natural rubber latex based nanocomposites and their blends with synthetic latices are also given. The specific objectives of the present study are discussed.

1. Nanotechnology

Nanotechnology is the study of matter on an atomic and molecular scale. Generally nanotechnology deals with structures of size 100 nm or smaller in dimension, and involves in developing materials or devices within that size. This technology is very diverse, ranging from extensions of conventional methods to completely new approaches based upon new materials with dimensions on the nanoscale.

The particles with small size in the range from a few to several tens of nanometers were explained by Sharma, *et al.* [1]. According Jordan *et al.* [2] the nano-sized inclusions are defined as those that have at least one dimension in the range 1 to 100 nm. There has been much debate on the future implications of nanotechnology. It has the potential to create many new materials and devices with a wide range of applications, especially in medicine, electronics and energy production. On the other hand, nanotechnology raises many of the same issues as with the introduction of any new technology, including concerns about the toxicity and environmental impact of nanomaterials [3], and their potential effects on global economics, as well as speculation about various extremely serious situations.

1.1 Nanotechnology-global outlook

The global outlook series on nanotechnology provides a collection of statistical anecdotes, market briefs, and concise summaries of research findings. The report offers a bird's eye view of this new, promising, and pulsating, potential laden industry. The report provides awareness about the basic facts or principles relating to the concept of nanotechnology, providing selective insights into major technology trends, and its impact on commercial applications in key

end-use industries. Key regional markets briefly researched and abstracted include the US, Canada, Japan, Europe, France, Germany, Russia, UK, Asia, China, Australia, and Israel, among few others. Also included is an indexed, easy-to-refer, fact-finder directory listing the addresses, and contact details of 994 companies world wide [4].

Nanocomposites are expected to penetrate a number of key packaging applications, including soft drinks, beer, food, pharmaceuticals and electronics, driven by the improved barrier strength and conductive properties that they offer. In motor vehicles, automotive manufacturers are increasingly turning to nanocomposites in an effort to replace higher-priced materials, increase production speed of parts and reduce motor vehicle weight in a number of exterior, interior and under-hood applications. As material and production costs of clay-based nanocomposites fall, clays will rise to account for over half of all nanomaterials demand by volume in 2025. Similarly, a decline in price will enable the rapid commercialization of carbon nanotubes, which will eventually gain over 60% of the nanocomposite materials market in value terms (Table 1.1).

Table 1.1 - Percentage annual growths of nanocomposites in US 2005- 2020

	US nanocomposites demand (million pounds)			
	2005	2010	2020 (Projected)	Annual Growth 2005-2020, %
Nanocomposites demand	154	344	7030	29
Thermoplastic	152	329	5600	27
Thermoset	2	15	1430	55

Nanocomposites play a significant role in one of the most promising technologies known as nanotechnology. Worldwide demand for nanocomposites is increasing rapidly in packaging, automotive, electrical, and other applications due to their superior thermal, electrical, conductive and other properties. Development of industrially important nanocomposites with enhanced features and expanding research activities in the development of new nanocomposites are some of the factors that would drive nanocomposites market in the coming years. United States and Europe dominate the global nanocomposites market, with a collective share of over 80 per cent of the volume sales for 2008.

The markets are also projected to witness rapid growth, driven by enhanced volume consumption of nanocomposites in various applications. Research institutions and companies are engaged in the exploration of efficient methods for developing nanocomposites in large volumes, and at lower cost. Applications of nanocomposite plastics are diversified, with automotive and packaging accounting for a majority of consumption. Increased R&D activities and advent of innovative materials is expected to widen the application areas of nanocomposites. Packaging segment represents the largest end-use market for nanocomposites in the world, with consumption estimated at 284 million pounds for 2008. Automotive segment is projected to generate the fastest demand for nancomposites during the period 2001-2010. Rise in demand and easy accessibility of nanocomposites would lead to their extensive usage in a wide range of applications.

Several global plastic suppliers have already commercialized products based on nanocomposite materials, with majority of the efforts focused on either nylons or polyolefins. Other industries are also optimistic about the future role of these novel materials, attributed to the growing volume of research studies being

conducted across the world. The development of innovative nanocomposite polyolefins and an array of other resin matrixes and nanofillers are also expected to bolster the market scenario [5]. Technological advancements would reduce manufacturing costs, enabling the development of low-cost-nanocomposites [6].

Polymer/clay nanocomposites have received a lot of attention over the last decade [7, 8]. Companies such as Nanocor and Honeywell are already commercially exploiting nanocomposite materials. A small amount of nanodispersed filler leads to an improvement in material properties, such as modulus, strength, heat resistance, flame retardancy and lower gas permeability.

Polymer nanocomposite markets have been slow in development till date seems ready to take off with increasing application in the automotive and packaging sector. As commercial interest has moved beyond pilot programs, it appears that nanocomposites are finally ready for a breakthrough in these markets. By 2011, nanocomposite demand will reach 150,000 tpa in USA. Growth will be fueled by declining prices of nanomaterials and composites, as production levels increase and technical issues concerning the dispersion of nanoadditives in the compounds are overcome. By 2025, it is expected that nanocomposites will be a US$9 billion market, with volumes nearing 5 million tons. While thermoplastics currently comprise virtually all demand for nanocomposites, compounds based on thermoset resins will eventually become a substantial part of the market, constituting 20% of demand in 2025. Over the near term, the most rapid gains will be seen in higher-priced resins such as engineering plastics, in applications where the additional cost of nanomaterials is not a critical factor. Looking forward, however, nanocomposites based on commodity plastics, such as polypropylene, polyethylene and PVC will dominate

the market. Among thermosets, nanocomposites will make the strongest impact as enhancements for reinforced polyester and epoxy compounds. Packaging and motor vehicles, two key early markets for nanocomposites, will account for nearly 50 per cent of total demand in 2011 and 40 per cent of demand in 2020. However, by 2025, electrical and electronics applications will gain in prominence, as nanotube-based composites will penetrate a sizable portion of the market as a substitute for other conductive materials. Construction will emerge as a significant market as nanocomposites begin to replace fibre-reinforced plastics in a number of applications.

1.2 Nanomaterials and nanosized dimensions

The common factor in nanotechnology is the lateral dimension, being in the nm (that is 1 billionth of a meter) range, of the structures studied. Atomic or molecular distances, sizes of structures in semiconductor devices and grain sizes in nanopowders are just a few examples out of many that can be considered as nanosized dimensions. Nanomaterials cross the boundary between nanoscience and nanotechnology and link the two areas together. Nanoparticles can come in a wide range of morphologies, from spheres, through flakes and platelets, to dentritic structures, tubes and rods. The sophistication of the production processes for some materials has reached the level in the laboratory where complex three dimensional structures such as springs, coils, and brushes have been made [9].

1.3 Classification

Nanomaterials can be classified according to the nature of the reinforcing agent as nanoparticles, nanoplatelets etc. The following section gives a general idea regarding the various classes of nanomaterials and their preparation.

1.3.1 Nanoparticles

Particulate composites reinforced with micron- sized particles of various materials are perhaps the most widely utilized materials in day to day life. Particles are typically added to improve the elastic modulus and yield strength of polymer matrix. By scaling the particle size down to the nm scale, it has been shown that novel material properties can be obtained. A few systems are reviewed below for illustrating the resulting modification in matrix properties. Micron-scale particles typically scatter light making other wise transparent matrix materials appear opaque. It has been shown that the use of nano-aluminium increases the propellant burning rate further, and gives rise to sub-micron aluminium oxide as a combustion product [10]. This could be useful in reduced smoke applications, since the visibility of the smoke varies as the square of the product-oxide size. Thus, the use of aluminium at the nano-particle size level enables reduced smoke while still ensuring the high specific impulse offered by aluminized propellants De Luca *et al.* [11].
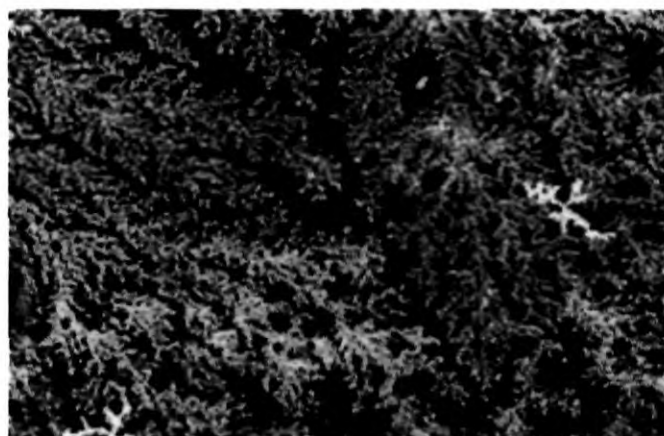
Figure 1.1 SEM image (scale bar 10µm) obtained for the Al in PMMA (Al: PMMA=1 : 1) [12]

The reduction of aluminium trichloride by lithium aluminium hydride in the presence of poly (vinylpyrrolidone) or poly (methylmethacrylate) in mesitylene yielded nano aluminium particles in the matrices of respective polymers (Figure 1.1) [12]. Alumina nanoparticles were introduced in epoxidized natural rubber by melt intercalation method [13]. Study on nickel oxide with flexible polyimide substrate via ion exchange technique was studied by Mu.*et al.* [14]. Silver impregnated on polymer-titania nanocomposite films exhibit excellent antibacterial properties with the added advantage of repeated use [15]. Studies of Ash *et al.* explained that when a weak particle/matrix interface exists, the mode of yielding of amorphous polymers changes from cavitational (normal) to shear, which leads to a brittle-to-ductile transition [16]. This behavior is attributed to increased polymer chain mobility, due to the presence of smaller particles. Chen *et al.* reported the successful development of a NR nanocomposite reinforced with nano silica (SiO_2) [17].

Solution phase synthesis methodology was used successfully to produce composites of various Al/polymer ratios. Nano-sized powders of transparent conductive aluminum-doped zinc oxide (AZO) have been successfully prepared by electrolysis-modified co-precipitation method. By adding ammonium hydroxide into the precursor solution prepared by electrolytic dissolution of zinc metal in a buffered electrolyte solution of nitric acid and ammonium nitrate with adequate addition of aluminum nitrate, co-precipitate precursors of AZO with particle size between 30 to 60 nm. After washing, filtering, and drying of the co-precipitates, nano-powders of AZO with wurtzite structure were produced when the dried co-precipitate precursors were calcined at temperature above 800°C. By ageing at pH 5 and co-precipitating at pH 8.0, the atomic ratio of Al/Zn of the nano-powders could be maintained throughout the synthesis. After calcining at 1000°C in air for 2 h, nano-sized

powders of AZO with ZnO wurtzite structure and particle size between 200 to 500 nm were synthesized [18]. Zinc oxide nano-particles coated with aluminum were prepared using reagent grade $ZnSO_4.7H_2O$ and NH_4HCO_3 dissolved in distilled water. The concentrations were 1.5mol/L zinc sulphate and 2.5mol/L NH_4HCO_3. 100mL $ZnSO_4$ solution was added to the 126 mL NH_4HCO_3 solution while stirring, and the reaction temperature was kept at 45°C. The slurry of basic zinc carbonate (BZC) white precipitate was obtained. Then $Al_2(SO_4)_3$ and NH_4HCO_3 solution with appropriate concentrations were slowly added to the above slurry while stirring. When the above processes finished, it was stirred for another 30 min. The precursor powders were obtained after the precipitate was filtered, washed and dried. Finally, zinc oxide nano-particles coated with aluminium were prepared by calcining the resulting precursor powders at 500°C for 1h [19].

1.3.2 Nano platelets or layered silicates

The generic term "layered silicates" not only refers to natural clays but also to synthesized layered silicates such as magadiite [20], mica, laponite [21] and flurohectorite [22]. Both natural clays and synthetic layered silicates have been successfully used in the synthesis of polymer nanocomposites [23-26].

Because of its suitable layer charge density, montmorillonite, discovered in 1847 in France (Montmorillon) by Damour and Slavetat [27], is nowadays the most widely used clay as nanofiller. Montmorillonite is a common clay mineral, formed in most cases, by the weathering of eruptive rock material, usually tuffs and volcanic ash (bentonite) [28]. In its pristine form, montmorillonite contains varying amounts of crystobalite, zeolite, biotite, quartz, feldspar, zircon and other minerals found in volcanic rocks. Therefore, a purification [29] of the clay is required prior to its use in the nanocomposites synthesis.

Somasif ME-100 is a fluorohectorite prepared by heating talcum in the presence of Na_2SiF_6 for several hours at high temperature in an electric furnace. Its crystallographic structure is similar to montmorillonite. Some hydroxyl groups of the octahedral sheet are replaced by fluorine atoms [30].

1.3.2.1 Morphology-crystallography

The suggested crystallographic structure for montmorillonite is based on that of pyrophyllite (Figures 1.2a & b). It must be emphasized that the structure proposed is idealized and that in reality the lattice is distorted [31]. The model structure, proposed by Hoffmann, Endell and Wilm [32], consists of two fused silica tetrahedral sheets sandwiching an edge-shared octahedral sheet of either aluminium or magnesium hydroxide.
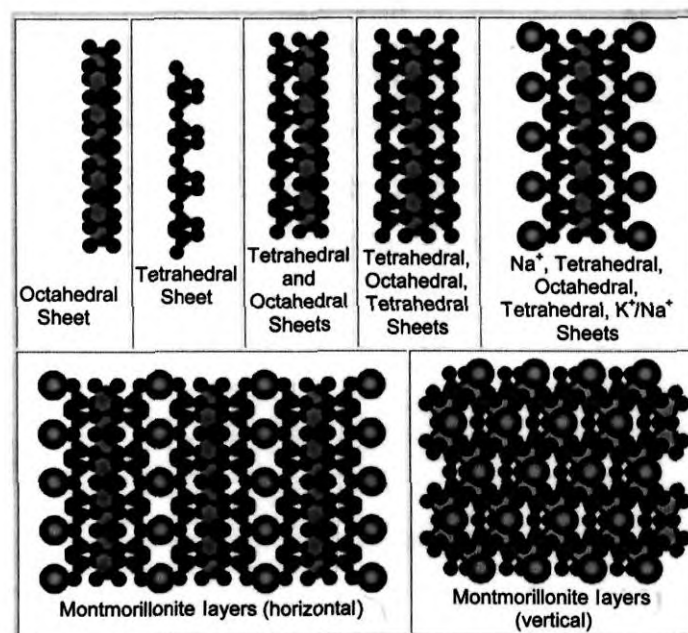
Figure 1. 2a   Portions of the montmorillonite structure [32]
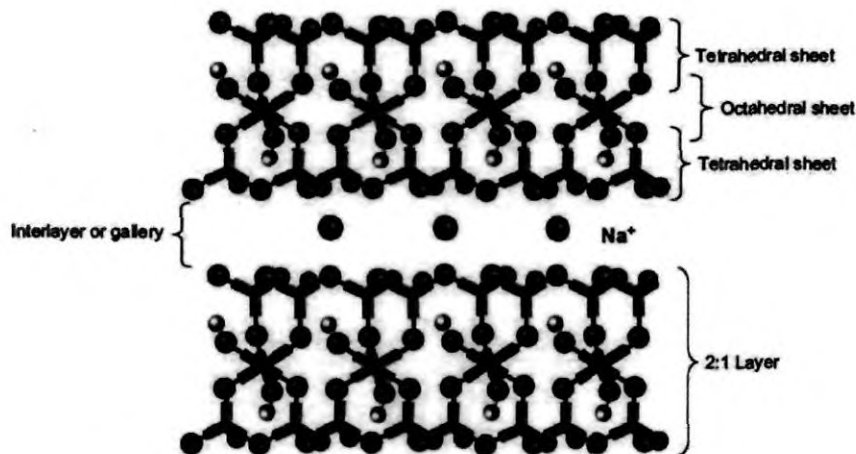
Figure 1. 2b Structure of sodium montmorillonite [33]

Isomorphous substitution of Si^{4+} for $A1^{3+}$ in the tetrahedral lattice and of $A1^{3+}$ for Mg^{2+} in the octahedral sheet cause an excess of negative charges within the montmorillonite layers. These negative charges are counterpoised by cations such as Ca^{2+} and Na^+ situated between the layers. Due to the high hydrophilicity of the layered silicate, water molecules are also present between the layers. Stacking of the layers leads to regular van der Waals gaps called inter- layers or galleries.

The sum of the single layer thickness (9.6 A°) and the interlayer represents the repeat unit of the multilayer, so called d- spacing or basal spacing, and is calculated from the (001) harmonics obtained from X-ray diffraction patterns using Bragg's law. The d-spacing between the silica alumina-silica units for a Na-montmorillonite varies from 9.6 A° for the clay in the collapsed state to 20 A° when the clay is dispersed in water solution [34].

The crystallographic structure of montmorillonite can be characterized by X- ray diffraction (XRD) (Figure 1. 3). XRD patterns of layered silicates give basically two categories of information on the crystallographic structure [35].
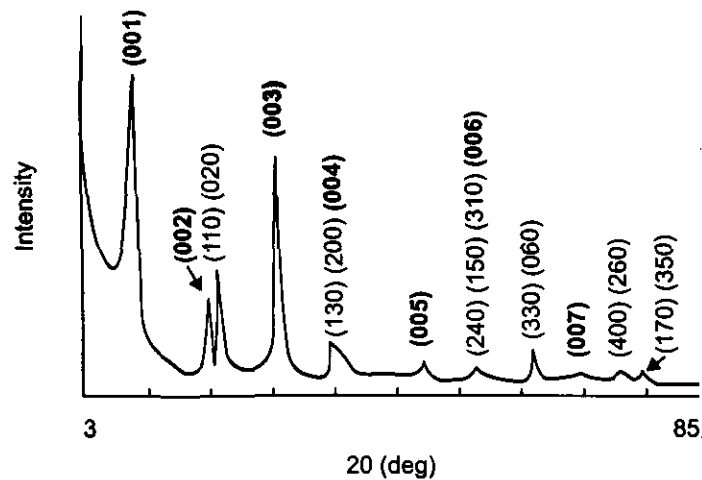
Figure 1.3 X- ray diffraction pattern of sodium treated montmorillonite showing the (001) basal reflections (in bold) and the (hk$_o$) diffraction bands. In some cases, both reflections are overlapping [36].

One class consists of the basal 001 reflections which depend on the nature of the interlayer cations, the state of hydration of the mineral-*i.e.*, the thickness and regularity of the water layers between the silica sheets and the presence of other intercalated molecules (such as ammonium salts for instance). Because of the variability of the basal 001 reflections caused by intercalated water molecules, no table can be given for them.

The second class consists of the two dimensional *hk* diffraction bands which are characteristic of the structure of the smectite layers themselves and are independent from the basal spacing. These *hk* diffraction bands are the same in all smectites. They are not very useful in structural determination because each observed band is the summation of several *hk* index pairs. Thus, only a "trial and error" procedure is possible in which bands are calculated for

different structural models and compared with the observed data. Moreover, montmorillonite cannot be totally isolated from impurities, which makes analysis by XRD even more difficult.

1. 3. 2. 2 Microstructure

On a higher scale, each layer of montmorillonite can be seen as a high aspect ratio lamella of about 100-200 nm in diameter and 1 nm in thickness (Figure 1. 4).

lamella   primary particle   aggregate
(1 nm)   (8-10 nm)   (0.1-10 μm)
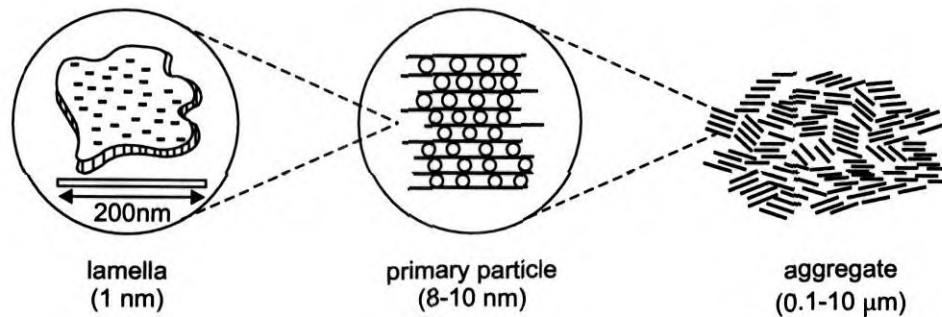
Figure 1. 4. Microstructure of montmorillonite. The circles in the primary represent he intercalated inorganic cations (Na^+, Ca^{2+}, K^+ etc) [37].

In primary particles (8-10nm in the "transverse" direction), five to ten lamellae are associated by interlayer ions [38], which in turn, form larger irregular aggregates (0.1-10μ m in diameter) giving to the layered silicate its turbostratic structure [39]. Usually, the individual particles of montmorillonite can barely be distinguished using scanning electron microscopy (Figure 1. 5). Finely divided platy forms usually with poorly defined shapes and very crumpled layers can be seen in different studies [40].

The capacity of layered silicates to exchange cations between each of their individual layer is a unique characteristic, which makes layered silicates attractive for a number of uses. The following section describes the steps of the cation exchange process as well as several relevant measurement techniques.

Figure 1. 5 Scanning electron micrograph of montmorillonite. Divided platy forms with poorly defined shapes and very crumpled layers

1. 3. 2. 3 Cation exchange

1.3.2.3.1 Cation exchange capacity

For a given layered silicate, the maximum amount of cations that can be taken up is constant and is known as the cation exchange capacity (CEC). It is measured in milli equivalents per gram (meq/g) or more frequently per 100g (meq /100g). Although the convention is to use this unit, it represents a charge per unit mass and, in SI units, is expressed in "coulombs per unit mass." A CEC of 1 meq/g is 96.5 C/g SI units. Cation exchange capacity measurements are performed at a neutral pH of 7. The CEC of montmorillonite varies from 80 to 150 meq/100 g.

Determination of the cation exchange capacity is a more or less arbitrary matter and no high degree of accuracy can be claimed. The measurement is generally made by saturating the layered silicate with NH_4^+ or Ba^{2+} and determining the amount held at pH 7 by conductometric titration [41-42]. Another method consists of saturating the layered silicate with alkyl ammonium ions and evaluating the quantity of ions intercalated by pyrolysis of the sample [43].

1.3.2.4 Surface charge density

Surface charge density σ can be estimated in different ways. If the CEC and the specific surface of the layered silicate (S) are measured:

$$\sigma = CEC/S$$

Since S can be calculated based on the structural formula and the unit cell parameters, σ can be expressed as:

$$\sigma = e. \frac{\sum (\text{interlayer cation charge})}{2. a. b}$$

Where e is the elementary charge, 1.6022×10^{-19} C, a and b are the unit cell parameters. This formula gives an average value of the surface charge density in the layered silicate but the heterogeneity of the surface charge density in montmorillonites was suggested by Stul and Mortier [44].

1.3.2.5 Compatibilising agents

Dispersing layered silicates in a polymer is like trying to mix oil with water. Oil can be dispersed in water with the use of detergent. The role of a compatibilising agent is similar to that of a detergent. It is a molecule constituted

of one hydrophilic function (which likes polar media such as water or layered silicate) and one organophilic function (which likes organic molecules such as oil or polymer). In the case of the detergent, this permits to disperse oil in the water. In the present case, compatibilising agents allow us to disperse layered silicates in polymers.

Aminoacids are the first compatibilising agents used in the synthesis of nanocomposite [45]. Numerous other kinds of compatibilising agents have been used in the synthesis of nanocomposites. The most popular are alkyl ammonium ions because they can be exchanged easily with the inorganic ions situated between the layers. Moreover, because of the nonpolar nature of their chain, they reduce the electrostatic interactions between the silicate layers so that an optimal diffusion of the polymer during the exfoliation process can be obtained. The most widely used alkyl ammonium ions are based on primary alkyl amines. The basic formula is $[(CH_3\text{-}CH_2\text{-}) n\ NH_3^+]$, where n is in between 1 and 18. It is interesting to note that the length of the ammonium ions has a strong influence on the resulting structure of nanocomposites. Lan *et al.* [46] observed that alkyl ammonium ions with chain length larger than eight carbon atoms were favoring the synthesis of exfoliated nanocomposites whereas ammonium ions with chain length shorter than eight carbon atoms were lead to the formation of intercalated nanocomposites.

A modifier used in epoxy systems consists of using adducts made from the reaction of epoxy resin and alkyl amines or even protonated polyoxyalkylene mono-, di- or triamines as compatibilising agents. Silanes have also been used because of their ability to react with the hydroxyl groups situated possibly at the surface and at the edges of the clay layers.

1.3.2.6 Nanoclay modifications

Nanoclay is described as a clay mineral having a 2:1 expanding crystal lattice. Synonyms of nanoclays (montmorillonite, bentonite, smectite) are montmorillonite, smectite, sodium montmorillonite (sodium bentonite (wyoming bentonite (US)), swelling bentonite (western bentonite (US), sodium-activated bentonite (bentonite (UK)), sodium-exchanged bentonite, (synthetic bentonite)), calcium montmorillonite (calcium bentonite (Mississippi bentonite (US)), sub-bentonite (Texas bentonite (US)), magnesium montmorillonite (saponite & armargosite), potassium montmorillonite (metabentonite), and lithium montmorillonite (hectorite). Nanoclays are clays from the smectite family which have a unique morphology: They form platelets about 1 nm thick and 100 nms in diameter. Chemical name is hydrated sodium calcium aluminum magnesium silicate and the chemical formula is $(Na, Ca)(Al,Mg)_6(Si_4O_{10})_3(OH)_6\text{-}nH_2O$.

Isomorphous substitution gives the various types and causes a net permanent charge balanced by cations in such a manner that water may move between the sheets, giving reversible cation exchange and very plastic properties. Smectite refers to a family of non-metallic clays primarily composed of hydrated sodium calcium aluminum silicate. Common names for smectite include montmorillonite or sodium montmorillonite ("sodium bentonite" or "Wyoming bentonite") and swelling bentonite ("Western bentonite"). Its chemical composition (%) is Al= 9.98, Si= 20.78, H= 4.10 and O=65.12. It is a powder as fine as 20 nm.

1.3.2.7 Nanoclay-physical constants

Fillers of different types are used in polymer compounding. The introduction of nano-sized particle has generated considerable interest in the

polymer industry because of some very attractive performance benefits derived from properly dispersed composite materials. Common nanoclay physical constants are given in Table 1.2. Early claims involving dramatically improved barrier properties, improved flame retardancy, improved stiffness, as well as improved tensile and flexural properties, have often been unfulfilled. This is because the existing mixing and blending technologies were not sufficient to achieve the necessary dispersions of particles. Moreover, the host resin suffered some molecular degradation, because of the high pressure and heat involved in the operation.

Table 1.2 - Nanoclay - physical constants

Molecular weight (g/mol.)	540.46
Average density (g/cm³)	2.35
Crystal system	Monoclinic
Member of	Smectite group
Fracture	Uneven to lamellar
Luster	Earthy (dull)
Mohs hardness @20°C	1.5- 2.0
Average specific gravity (g/cc)	2.3- 3
Colour	White, yellow
Cleavage	Perfect in one direction, basal
Characteristics [47]	Crystals expand to many times their volume when added to water
Field indicators	Softness and soapy feel

The essential nanoclay raw material is montmorillonite; a 2:1 layered smectite clay mineral with a platy structure. Individual platelet thicknesses are

just one nm (one-billionth of a meter), but surface dimensions are generally 300 to more than 600 nm, resulting in an unusually high aspect ratio. Naturally occurring montmorillonite is hydrophilic. Since polymers are generally organophilic, unmodified nanoclay disperses in polymers with great difficulty. Through clay surface modification, montmorillonite can be made organophilic and, therefore, compatible with conventional organic polymers. Surface compatibilization is also known as "intercalation". Compatibilized nanoclays disperse readily in polymers. Nanoclays are known as nanoclays because of 1 nm spacing between layers. The modified nanoclays are, 2:1 layered silicates modified to contain an ammonium cation that is stable at the temperature required for forming the polymer and is compatible with the polymer.

The term "2:1 layered silicates" is a known term and describes silicates with lattice layers containing two tetrahedral sheets that share an edge with an octahedral sheet of either aluminum or magnesium hydroxide. The stacking of the layers provides interlayer or galleries between the layers. The galleries are normally occupied by the hydrated cations which balance the charge deficiency that is generated by the isomorphous substitution within the layers in the tetrahedral sheets. Besides the charge-balancing cations, water is also present in the galleries where it tends to associate with the cations. The silicates may be referred to as gallery-containing to describe this characteristic of 2:1 layered silicates which allows for intercalation therein of polymers. The silicates may be either natural or synthetic. The natural silicates include, for example, smectite clay minerals (*e.g.*, montmorillonite, saponite, beidellite, nontronite, hectorite and stevensite), vermiculite and halloysite. The synthetic silicates include, for example, laponite, fluoromica, fluorohectorite, hydroxyl hectorite, boron fluophlogopite, hydroxyl boron phlogopite. These normally are associated with,

i.e., in the pristine state contain, charge balancing cations selected from the group consisting of sodium, potassium, lithium, calcium and magnesium ions. The 2:1 layered silicate preferably has a cation exchange capacity of 60 -190 meq/100 grams. To provide the modified nanoclays herein, charge-balancing ammonium cation that is stable at the temperature required for forming the polymer and which provides a modified nanoclay compatible (miscible) with the polymer, is exchanged.

Nanoclays are nanoparticles of layered mineral silicates. Depending on chemical composition and nanoparticle morphology, nanoclays are organized into several classes such as montmorillonite, bentonite, kaolinite, hectorite, and halloysite. Organically-modified nanoclays (organoclays) are an attractive class of hybrid organic-inorganic nanomaterials with potential uses in polymer nanocomposites, as rheological modifiers and drug delivery carriers [48-50].

Nanoclay also has proved effective as a flame retardant: It improves UL ratings by eliminating dripping and promoting formation of stable char (UL): Most roofs at that time were made of wooden shingles, but in 1916 UL gave a time rating for three kinds of roofing. In 1924 tests began on new roofing. For example, Sud-Chemie's new nanoclay (Nanofil SE 3000) is used commercially in an EVA/PE compound to provide halogen-free flame retardancy in wire and cable coatings. At only 3 to 5% loading, it improves flame retardancy to the level that aluminium trihydride (ATH) or magnesium hydroxide flame retardants can offer from 52% to about 65% by weight. Besides, mechanical and surface properties improve, and extrusion rates are higher for Nanofil SE 3000.

Nanomaterials weigh less, mold more easily on smaller presses, process dramatically faster, and produce better properties. For example,

nanoblend MB (melt blend) concentrate, a nanoclay master batch introduced in 2003 by PolyOne Corp., is used commercially in a thermoplastic olefin (TPO) automotive rocker panel(Rocker panel is a component of the car's body panel found under the compartment of the passenger) replacing talc-filled TPO. Nanoblend has better low-temperature ductility and lower specific gravity. Because of the lower amount of nano-filler, color matching was less expensive with nanoblend. Moreover the lower density, led to a projected higher economic savings per year, despite somewhat higher material cost/weight.

1.3.3 Nanofibres

Carbon nanofibres are cylindrical nanostructures with graphene layers arranged as stacked cones, cups or plates. Vapour grown carbon nanofibres have been used to reinforce the polymers such as acrylonitrile butadiene styrene (ABS), epoxy, polypropylene (PP), polycarbonate (PC), poly (ethylene terephthalate) (PET), poly (phenylene sulfide) (PPS) etc [51-53].

Figure 1. 6   Carbon nanofibres

Carbon nanofibres (Figure 1. 6) typically have diameters of the order of 50-200nm. Finegan and co-workers [54-55] have investigated the processing and properties of carbon nanofibre with polypropylene. They used a variety of grown nanofibres.

Bio-nanofibres are also under study of many research groups. The importance of 'green' properties such as biodegradability and favourable CO_2 balance grows with the awareness of consumers and engineers for sustainability in the use of materials. Thus cellulose fibrils from various plants such as soya bean stock [56], wood pulp [57], sugar beet pulp [58, 59] potato pulp [60], swede root [61], and cactus, Opuntia ficus-Indica were investigated [62]. In medicine nanofibres are used for cartilage regeneration [63]. Lenaghan *et al.* reported the identification of nanofibres in Chinese herbal medicine for wound healing. Atomic force microscopic images revealed uniform nanofibres present in relatively high abundance in a solution of this medicine. Fibres were typically 25.1 nm in diameter and ranged in length from 86-726 nm due to processing [64]. Attempts have been made to fabricate nanofibrous scaffolds to mimic the chemical composition and structural properties of the extracellular matrix (ECM) for tissue/organ replacement. Nanofibre scaffolds with various patterns have been successfully produced from synthetic and natural polymers through a relatively simple technique of electro spinning. Furthermore, clinical application of electro spun nanofibres including wound healing, tissue regeneration, drug delivery and stem cell therapy are highly feasible due to the ease and flexibility of fabrication [65]. Other type of nanofibre is titanium foam-bioactive nanofibre. This is used in bone repair and in bone regeneration [66].

Mechanical fibrillation process for the preparation of cellulose nanofibres from two commercial hard and softwood cellulose pulps was done by W. Stelte

and A. R. Sanadi [67]. The process consisted of initial refining and subsequent high-pressure homogenization. The progress in fibrillation was studied using different microscopy techniques, mechanical testing and fibre density measurements of cellulose films prepared after different processing stages.

Various polymers have been utilized in tissue engineering. A copolymer of poly (lactic acid) and poly (glycolic acid) (PLGA) is one of the most widely used synthetic polymer [68]. Fibroin is a main component of silkworm silk, and has been frequently used in the areas of biomedical science and engineering [69]. In this study, nanofibre matrices were prepared as synthetic extracellular matrices by electrospinning a solution of either PLGA or silk fibroin (SF), dissolved in hexafluoro-2-isopropyl alcohol (HFIP), and were collected on a target drum. A voltage of 16 kV was applied to the collecting target, and the flow rate of the solution was 2 mL/min [70].

The bioactive glass nanofibre (BGNF) was observed to be distributed uniformly within the collagen reconstituted nanofibrous matrix that can be used as a novel bone regeneration matrix [71]. Bioactive glass nanofibre (BGNF) is a sol-gel derived glass with a bioactive composition ($58SiO_2 \cdot 38CaO \cdot 4P_2O_5$) was electro spun to a nanoscale fibre with an average diameter of ~ 320 nm. The bioactive glass nanofibre was then hybridized with collagen.

1.3.4 Nanotubes

A nanotube has a nm-scale tube-like structure. Nanotubes, depending on their structure, can be metals or semiconductors. They are also extremely strong materials and have good thermal conductivity. The above

characteristics have generated strong interest in their possible use in nano-electronic and nano-mechanical devices. For example, they can be used as nano-wires or as active components in electronic devices such as the field-effect transistor.

Carbon nanotubes are extremely thin (their diameter is about 10,000 times smaller than a human hair), hollow cylinders made of carbon atoms. Figure 1.7 shows single walled and multi-walled carbon nanotubes. Carbon nanotubes are molecular-scale tubes of graphitic carbon with outstanding properties. They are among the stiffest and strongest fibres known, and have remarkable electronic properties and many other unique characteristics. For these reasons they have attracted huge academic and industrial interest, with thousands of papers on nanotubes being published every year. Commercial applications have been rather slow to develop, however, primarily because of the high production costs of the best quality nanotubes. The current huge interest in carbon nanotubes is a direct consequence of the synthesis of buckminsterfullerene, C_{60}, and other fullerenes, in 1985. The discovery that carbon could form stable, ordered structures other than graphite and diamond stimulated researchers worldwide to search for other new forms of carbon. The search was given new impetus when it was shown in 1990 that C_{60} could be produced in a simple arc-evaporation apparatus readily available in all laboratories. It was using such an evaporator that the Japanese scientist Sumio Iijima discovered fullerene-related carbon nanotubes in 1991. The tubes contained at least two layers, often many more, and ranged in outer diameter from about 3 nm to 30 nm. They were invariably closed at both ends.

Single walled carbon nanotube   Multi-walled carbon nanotube
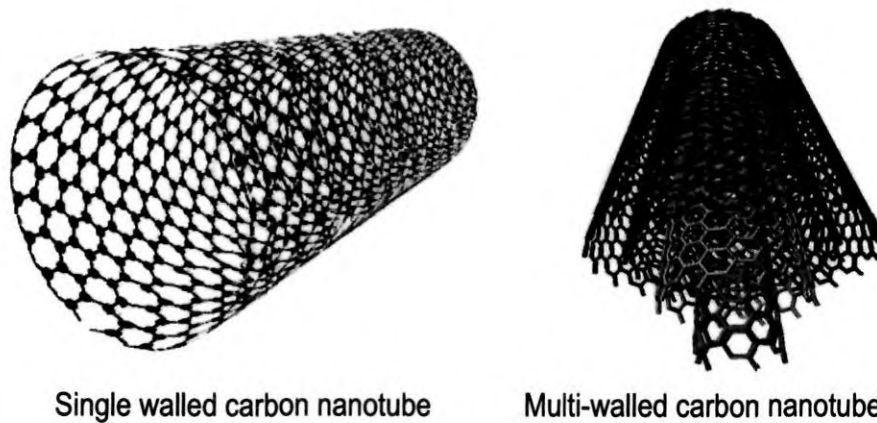
Figure 1.7 Carbon nanotubes

Single walled nanotubes are generally narrower than the multi-walled tubes, with diameters typically in the range 1-2 nm, and tend to be curved rather than straight. The bonding in carbon nanotubes is sp^2, with each atom joined to three neighbors, as in graphite. The tubes can therefore be considered as rolled-up graphene sheets (graphene is an individual graphite layer). There are three distinct ways in which a graphene sheet can be rolled into a tube, the first two of these known as "armchair" and "zigzag" have a high degree of symmetry. The terms "armchair" and "zigzag" refer to the arrangement of hexagons around the circumference. The third class of tube, which in practice is the most common, is known as chiral, meaning that it can exist in two mirror-related forms. The strength of the sp^2 carbon-carbon bonds gives carbon nanotubes amazing mechanical properties. The stiffness of a material is measured in terms of its Young's modulus, the rate of change of stress with applied strain. The young's modulus of the best nanotubes can be as high as 1000 GPa (approximately 5x higher than steel) and the tensile strength, or breaking strain of nanotubes can be up to 63 GPa(around 50x higher than steel). They have a density of 1.33-1.4g/cm^3; elastic modulus is comparable with diamond (1.2TPa). These

properties, coupled with the lightness of carbon nanotubes, give them great potential in applications such as aerospace. It has even been suggested that nanotubes could be used in the "space elevator", an earth-to-space cable first proposed by Arthur C. Clarke. The electronic properties of carbon nanotubes are also extraordinary. Especially notable is the fact that nanotubes can be metallic or semiconducting depending on their structure. Thus, some nanotubes have conductivities higher than that of copper, while others behave more like silicon. There is great interest in the possibility of constructing nanoscale electronic devices from nanotubes, and some progress is being made in this area. However, in order to construct a useful device we would need to arrange many thousands of nanotubes in a defined pattern, and we do not yet have the degree of control necessary to achieve this. There are several areas of technology where carbon nanotubes are already being used. These include flat-panel displays, scanning probe microscopes and sensing devices. The unique properties of carbon nanotubes will undoubtedly lead to many more applications.

1. 3. 5 Nanofibrils

The potential for development of advanced continuous fibres with nanoscale diameter is attractive. Conventional mechanical spinning techniques are limited to producing fibres of micrometer diameters. Nanofibres are produced with a diameter ranging from about 4 Å to 1 nm, and a nano denier of about 10^{-9}. The use of electro-spinning process permits production of desired nanofibrils. These fibrils in combination with a carrier or strengthening fibres/filaments can be converted directly into nonwoven fibrous assemblies or converted into linear assemblies (yarns) before weaving, braiding or knitting into 2-dimensional and 3-dimensional fabrics. The electrospun fibre can be

fed in an air vortex spinning apparatus to form a linear fibrous assembly. The process makes use of an air stream in a properly confined cavity. The vortex of air provides a gentle means to convert a mixture of the fibril fed directly or indirectly from the ESP unit and a fibre mass or filament into an integral assembly with proper level of orientation. For example, wood is a material perfectly adapted to the functions it has to fulfill. It combines high strength and elasticity at very low weight. Responsible for its extraordinary properties is the composite structure of its cell walls. If it is possible to transfer this composite principle and embed cellulose fibrils or threads from wooden cell walls in a polymer matrix, a functional and sustainable material should emerge, which could be used in a wide range of technical applications.

The wood structure of softwood is composed to 90 per cent of tracheids (Figure 1.8). These are the basic fibres of sulphite pulp, which serves as raw material to separate cellulose fibrilar structures [72].
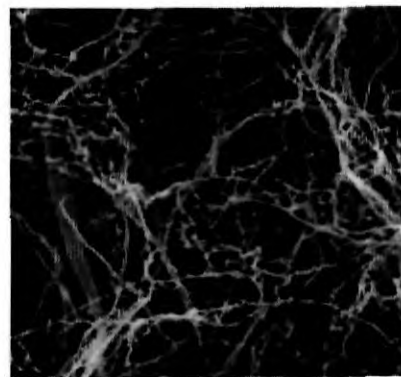
Cellulose nanofibre   Cellulose nanofibrile

Figure 1. 8 Cellulose nanofibre and nanofibrile

Even though the fibrils are oriented at random in the matrix material, tensile strength arises by a factor of five compared to the unfilled polymer. Pure films of cellulose fibrils are reaching almost the same strength properties of clear wood. Application areas of fibril reinforced biopolymers are conceivable where biodegradability and at the same time a high strength and visual transparency are required. Further, the fibrils could be used in adhesives (*e.g.* instead of synthetic fibres) to improve systematically their application and exploitation as well as thermal creep. In next steps, larger quantities of cellulose fibrils are produced and are embedded into different polymers for getting it optimized.

1.4 Preparation of nanomaterials

Preparation of nanoparticles can be achieved through different routes. Nanomaterials (nano particles, layered silicates, nanotubes, nanofibres, nanofibrils etc) can be dispersed in different matrices in nanoscale, which will give high modulus, high strength, solvent resistance etc. But the first step is the preparation of uniform nanomaterials arrays with correct chemical composition and structure. There are four major methods to make nanomaterials: wet chemical, mechanical, form-in-place, and gas phase synthesis.

1.4.1 Major preparation methods

1.4.1.1 Wet chemical process

This includes hydrothermal methods, colloidal chemistry, sol gel, and other precipitation processes. Solutions of different ions are mixed in well defined quantities and under controlled conditions of heat, temperature and pressure to promote the formation of insoluble compounds, which precipitate out of solution. These precipitates are then collected through spray drying and/

filtering to produce dry powder. Main advantages of wet chemical processes are that a large variety of compounds can be fabricated and the nanomaterials can be produced. Another important factor is the ability to control particle size to produce highly monodisperse materials. However, there are limitations with the range of compounds possible, bound water molecules specially for sol-gel processing, the yields can be quiet low. High-through put micro reactors might overcome some of these problems [73]. For bulk production, large quantities of starting materials may be required. For some nanomaterials surface coating has to be given to encapsulate or functionalize their surface [74]. The formation of metal-encapsulated carbon nanomaterials by using metallic catalysts (iron, cobalt, and nickel) has been studied by U. Narkiewicz *et al.* [75].

1.4.1.2 Mechanical process

Milling, grinding and mechanical alloying techniques are included in this category. At present, the most common process is ball milling. The advantages of this technique are low cost equipment and relatively small quantity of starting material. However, there can be difficulties such as agglomeration of the powders, broad particle size distributions, contamination from the process equipment itself and often difficulty in getting to the very fine particle sizes with viable yields. It is commonly used for inorganic materials.

1.4.1.3 Gas-phase synthesis

Flame pyrolysis, laser ablation, high temperature evaporation, electro-explosion and plasma synthesis are included in this type of synthesis. Flame pyrolysis has been used in the fabrication of simple materials like carbon black, fumed silica etc. Laser ablation is capable of making almost all nonmaterial, since

it utilizes a mix of physical erosion and evaporation. However, the production rates are extremely slow and most suited for research applications. The heat source is very clean and controllable and the temperatures in the plasmas can reach in excess of 9000°C, which means that even highly refractory materials can be processed and this technique is unsuitable for processing organic materials.

The production of fullerenes and carbon nanotubes is a specific subset of gas phase synthesis techniques. No variations have been explored and patented in the years since they were discovered [76]. All the techniques essentially involve the controlled growth of a nanotube on a catalyst particle through the cracking of carbon rich gases such as methane.

As can be seen, there are numerous methods employed to manufacture nanoparticles and carbon nanotubes. All are being used, some commercially, and each has its merits and drawbacks. However, it is clear that most of the methods will be utilized in commercial production at some stage since, although the materials are nominally the same, the characteristics of the materials produced by each process are not always equivalent and can have different properties. The manufacturing routes that become commercially successful, therefore, will predominantly be those for which the materials have been developed at the same time as the application. Some of these preparation techniques commonly employed are described briefly with some specific examples in the corresponding sections.

1.4.1.4 Form-in-place process

These include lithography, vacuum deposition processes such as physical vapor deposition (PVD) and chemical vapor deposition (CVD),

and spray coatings. These processes are more geared to the production of nanostructure layers and coatings, but can be used to fabricate nanoparticles by scraping the deposits from the collector. However, they tend to be quite inefficient and are generally not used for the fabrication of dry powders, although some companies are beginning to exploit these processes. A number of universities and companies are developing variations on these processes, such as the electrostatic spray assisted vapor deposition process [77].

1.4.2 Micro-emulsion methods

Preparation of nanoparticles using reverse micelles can be dated back to the pioneer work of Boutonnet et al. [78]. In 1982 they first synthesized monodispersed Pt, Rh, Pd and Ir nanoparticles with diameters 3-6 nm. After that, many nanoparticles were synthesized and the method of preparing nanoparticles using reverse micelles became a matter of interest in nanoscience and nanotechnology.

The general method to synthesis nanoparticles using reverse micelles can be divided into three cases. The first one is the mixing of two reverse micelles. Due to the coalescence of the reverse micelles, exchange of the materials in the water droplets occurs, which causes a reaction between the cores. Since the diameter of the water droplet is constant, nuclei in the different water cores cannot exchange with each other. As a result, nanoparticles are formed in the reversed micelles. The second case is that one reactant (A) is solubilized in the reversed micelles while another reactant (B) is dissolved in water. After mixing the two reverse micelles containing different reactants (A and B), the reaction can take place by coalescence or aqueous phase exchange between the two reverse micelles.

There are essentially three procedures to form nanoparticles by reversed micelles: precipitation, reduction and hydrolysis. Precipitation is usually applied in the synthesis of metal sulphate, metal oxide, metal carbonate and silver halide nanoparticles. In this method two reverse micelles containing the anionic and cationic surfactants are mixed. Because every reaction takes place in a nanometer-sized water pool, water-insoluble nanoparticles are formed. Platinum, palladium, rhodium, iridium, gold, silver, PbS, $CaCO_3$ nanomaterials and $BaCO_3$ nano wires are prepared by this process [78, 79- 93].

Method developed at the University of Ulm (Germany), the first step is the diblock-copolymer based micelle structures are formed in solution with a hydrophobic outer shell and a hydrophilic inner core. This hydrophilic core is capable of legating defined amounts of a metal salt by complexation or protonization, thus acting as a nano-reactor. After transfer of the metal-salt loaded micelles onto a flat substrate by dip-coating, the polymer is removed by means of different plasmas (oxygen and/or hydrogen) which also allow reducing the metal salt into the metallic state. Thus, the micelles are simply used as carriers for the metal precursor exploiting their self-assembly into ordered structures during dip-coating. This way, arrays of metal nanodots (elemental or alloy) can be prepared on various substrates exhibiting a high degree of hexagonal order. By adjusting corresponding experimental parameters, the size of the final dots as well as their interparticle distance can easily be varied and controlled over a large range of values (size: 1-10nm, distance: 20-150nm). To determine their purity, their chemical state and surface cleanliness (all being crucial for subsequent experiments since nanoscale structures are intrinsically surface dominated), *in-situ* x-ray photo electron spectroscopy (XPS) is required. A corresponding ultra-high vacuum (UHV) system has been built up and

optimized for the *in-situ* transfer of samples between the plasma etcher system and the XPS system. Both major parts (analysis chamber and plasma chamber) are close to operation, allowing the study the size-dependent physical and chemical properties of size-selected nanoparticles. Here, the electronic and magnetic properties as well as the chemical reactivity of elemental and alloy nanostructures will be in the focus of interest.

1.4.3 Pyrolysis

Pyrolysis is the chemical decomposition of condensed substances by heating that occurs spontaneously at high enough temperatures. There are several methods for creating nanoparticles, including both attrition and pyrolysis. In pyrolysis, a vaporous precursor (liquid or gas) is forced through an orifice at high pressure and burned. The resulting solid (a version of soot) is air classified to recover oxide particles from by-product gases. Pyrolysis often results in aggregates and agglomerates rather than singleton primary particles. More and more nanomaterials have been prepared using this method and modified processing. This method has some advantages: the reaction process is easy to control, the as-prepared substances are of variety, and the product is of high purity. The drawbacks are that the high temperature may lead to wide size distribution and particle agglomeration. The selective precipitation could be used to compensate above method for obtaining specific sized nanoparticles after pyrolysis. Silver, gold, spherical nickel, ZnS and CdS fine particles are produced mainly by this method [94-99]. Al_2O_3-TiO_2 composite oxide nanocrystals, carbon nanotubes and single crystalline ZnO nanoparticles also can be prepared through this route [100-103]. A new method, laser induced pyrolysis is also used for the preparation of nanoTiO$_2$ [104].

1.4.4 Sol-gel processing

The sol-gel process is a wet-chemical technique (also known as chemical solution deposition) widely used recently in the fields of materials science and ceramic engineering. Such methods are used primarily for the fabrication of materials (typically a metal oxide) starting from a chemical solution (*sol*, short for solution) which acts as the precursor for an integrated network (or *gel*) of either discrete particles or network polymers [105].

Typical precursors are metal alkoxides and metal chlorides, which undergo hydrolysis and polycondensation reactions to form either a network "elastic solid" or a colloidal suspension (or dispersion) - a system composed of discrete (often amorphous) submicrometer particles dispersed to various degrees in a host fluid. Formation of a metal oxide involves connecting the metal centers with oxo (M-O-M) or hydroxo (M-OH-M) bridges, therefore generating metal-oxo or metal-hydroxo polymers in solution. Thus, the sol evolves towards the formation of a gel-like diphase system containing both a liquid phase and solid phase whose morphologies range from discrete particles to continuous polymer networks [106]. In the case of the colloid, the volume fraction of particles (or particle density) may be so low that a significant amount of fluid may need to be removed initially for the gel-like properties to be recognized. This can be accomplished in any number of ways. The simple method is to allow time for sedimentation to occur, and then pour off the remaining liquid. Centrifugation can also be used to accelerate the process of phase separation.

Removal of the remaining liquid (solvent) phase requires a drying process, which is typically accompanied by a significant amount of shrinkage and densification. The rate at which the solvent can be removed is ultimately

determined by the distribution of porosity in the gel. The ultimate microstructure of the final component will clearly be strongly influenced by changes implemented during this phase of processing. Afterwards, a thermal treatment, or firing process, is often necessary in order to favour further polycondensation and enhance mechanical properties and structural stability. One of the distinct advantages of using this methodology as opposed to the more traditional processing techniques is that densification is often achieved at a much lower temperature.

The precursor sol can be either deposited on a substrate to form a film (*e.g.* by dip-coating or spin-coating), cast into a suitable container with the desired shape (*e.g.* to obtain a monolithic ceramics, glasses, fibres, membranes, aerogels), or used to synthesize powders (*e.g.* microspheres, nanospheres). The sol-gel approach is a cheap and low-temperature technique that allows for the fine control of the product's chemical composition. Even small quantities of dopants, such as organic dyes and rare earth metals, can be introduced in the sol and end up in uniformly dispersed in the final product. It can be used in ceramics processing and manufacturing as an investment casting material, or as a means of producing very thin films of metal oxides for various purposes. Sol-gel derived materials have diverse applications in optics, electronics, energy, space, (bio)sensors, medicine (*e.g.* controlled drug release) and separation (*e.g.* chromatography) technology [107].

The interest in sol-gel processing can be traced back in the mid-1880s with the observation that the hydrolysis of tetraethyl orthosilicate (TEOS) under acidic conditions led to the formation of SiO_2 in the form of fibres and monoliths. Sol-gel research grew to be so important that in the 1990s more

than 35,000 papers were published worldwide on the process [108-116]. Sol-gel processing can control the structure of a material on a nanometer scale from the earliest stage of processing. The size of the sol-gel particles and the cross linking between the particles depend upon some variable factors such as pH, solution composition, and temperature etc. Thus by controlling the experimental conditions, one can obtain the nanostructured target materials in the form of powder or thin film.

A sol-gel method followed by a hydrogen reduction procedure was used in the preparation of metal nanotubes. The tube length, diameter, wall thickness and, most importantly, the chemical components can be adjusted conveniently. Several examples of metal nanotubes (Fe, Ni, Pb. and CoFe) were prepared by using anodic aluminium oxide (AAO) templates [117]. Fabrication of ZnO nanotubes using AAO template and sol-gel method was reported by S. Ozturk *et al.* [118].

1.4.5 Forced hydrolysis and chemical co-precipitation

The simple forced hydrolysis and chemical co-precipitation technique is widely used in industry and research to synthesize oxide complexes. The processing parameters of starting raw materials, reaction temperature, solution pH, titration rate and even stirring rate have effect on properties of final precipitates, such as particle size, particle size distribution, particle shape, even stoichiometry. Jiang prepared nanoparticles of yttrium oxide of 10nm by this method [119]. A number of metal hydroxides or oxides have been prepared by using the hydrolysis technique *viz.* Gadolinium, Terbium, Samarium, Cerium [120] and Zirconium [121-122].

1.4.6 Chemical vapour deposition

Chemical vapor deposition or CVD is a generic name for a group of processes that involve depositing a solid material from a gaseous phase and is similar in some respects to physical vapor deposition (PVD). PVD differs in that the precursors are solid, with the material to be deposited being vaporized from a solid target and deposited onto the substrate.

Chemical vapor deposition (CVD) is a chemical process used to produce high-purity, high-performance solid materials. The process is often used in the semiconductor industry to produce thin films. In a typical CVD process, the wafer (substrate) is exposed to one or more volatile precursors, which react and/or decompose on the substrate surface to produce the desired deposit. Frequently, volatile by-products are also produced, which are removed by gas flow through the reaction chamber. In chemical vapor deposition (CVD), the vaporized precursors are introduced into a CVD reactor, where the precursor molecules adsorb on to a substrate held at an elevated temperature. These adsorbed molecules will be either thermally decomposed or reacted with other gases/ vapors to form a solid film on the substrate.

CVD covers processes such as: i) atmospheric pressure chemical vapor deposition (APCVD) ii) low pressure chemical vapor deposition (LPCVD) iii) metal-organic chemical vapor deposition (MOCVD) iv) plasma assisted chemical vapor deposition (PACVD) or plasma enhanced chemical vapor deposition (PECVD) v) laser chemical vapor deposition (LCVD) vi) photochemical vapor deposition (PCVD) vii) chemical vapor infiltration (CVI) and viii) chemical beam epitaxy (CBE)

Micro fabrication processes widely use CVD to deposit materials in various forms, including: monocrystalline, polycrystalline, amorphous, and epitaxial. These materials include: silicon, carbon fibre, carbon nanofibres, filaments, carbon nanotubes, SiO_2, silicon-germanium, tungsten, silicon carbide, silicon nitride, silicon oxynitride and titanium nitride. The CVD process is also used to produce synthetic diamonds.

David Boyd and his colleagues reported that the new vapor deposition process known as plasmon-assisted chemical vapor deposition can be used with a variety of materials by focusing a low-powered laser beam onto a substrate coated with gold nanoparticles [123]. Nanomaterials like semiconductor quantum dots [124-127], nanosized ZnO, Fe_2O_3, SnO_2 [128-130], TiO_2 [131], SiC [132], TiN [133], carbon nanotubes [134-136] can be prepared using this technique.

1.4.7 Aerosol methods

Starting with the methods previously applied to atmospheric aerosol condensation Sutugin and Fuchs [137] were able to apply the classical theory to get a first glimpse at the importance that the competing processes of coalescence and aggregation play. The work done in the 1960's by Flagan and co-workers [138] and Windier *et al.* [139] have greatly improved the understanding and application of condensation theory. With the process of initial nucleation of nanocrystal nuclei unknown, they were still able to formulate a theory that incorporates Brownian collisions, aggregations and coalescence growth through surface area minimization and solid state diffusion and agglomerate versus single particle formation. There are three essential processing stages. Evaporation of the bulk material in an inert environment, transport of the vapor through a temperature gradient and collection of

the produced nanocrystals are the vey general ideas. A brief account of the nanomaterials prepared by this technique are titania [138,140-142], nickel nanocrystals [143], luminescent Si nanoparticles [144-145], nanocrystals of W, Cu and Ag [146]and nanoparticles of Au, TiO_2[147].

1.4.8 Polyol method or induced crystallization

The polyol method is a low-temperature process and is environmentally benign because the reactions are carried out under closed system conditions. The growth of a particular crystalline phase or modification of certain materials has been the goal of material scientists over past several years. It has been known that inorganic materials such as alkali halides, talc, clay, minerals etc., especially in fine particulate form act as nucleating agent for crystallization of polymers [148-152], and in some instance the polymer grows epitaxial on the inorganic substrates [153-154]. However, the influence of polymers on the growth of inorganic crystals has not been studied very extensively. Biomineralization especially has drawn considerable interest because of the fascinating features observed, such as growth of certain inorganic compounds (calcium carbonate, phosphates, iron oxides etc.) by the biological systems in most unusual morphological forms which at the same time show single crystal type diffraction patterns [155-157]. These systems are quite complex, involving many types of macromolecules, and the exact role of the polymeric substances- proteins, long chain fatty acids etc in controlling the morphology is not yet fully understood. Studies on the crystallization behavior of inorganic salts such as cupric chloride, calcium chloride, potassium carbonates etc in polymeric media have shown that the crystallization of the polymer or its orientation can influence the inorganic salts [158-161].

1.5 Nanocomposites

The term "nanocomposites" describes a two-phase material where one of the phases has at least one dimension in the nm (10^{-9}m) range. This term is commonly used in two distinct areas of material science: ceramics and polymers. However, nanocomposites based on polymers will only be considered here. Thus, nanocomposites can be reinforced by iso-dimensional phases, which have three dimensions in the nm range such as precipitated silica [162], silica – titania oxides synthesized by the solgel process [163-164], silica beads [165] but also colloidal dispersion of rigid polyamides[166], and many others [167]. They can also be reinforced by a phase, which has only two dimensions in the nm scale. This is the case for polymer matrices reinforced by cellulose whiskers [168-171] or nanotubes [172]. The third type of nanocomposites corresponds to the case where the reinforcing phase, in the shape of platelets, has only one dimension on a nano level. Polymer- layered silicate nanocomposites belong to this class.

Polymer- layered silicate interaction have been actively studied during the sixties and the early seventies [173] and it is as early as 1961 that Blumstein demonstrated polymerization of vinyl monomers intercalated into montmorillonite clay [174]. Recently, researchers from Toyota discovered the possibility to build a nanostructure from a polymer and an organophilic layered silicate [7]. Their new material based on polyamide 6 and organophilic montmorillonite showed dramatic improvements of mechanical properties, barrier properties and thermal resistance as compared with the pristine matrix even at low layered silicate content (4 wt per cent) . Since then, polymer - layered silicate composites are ideally divided into three general types (Figure 1.9): conventional composite or micro composite where the layered silicate

acts as a conventional filler, intercalated nanocomposite consisting of a regular insertion of the polymer in between the silicate layers and exfoliated or delaminated nanocomposite where 1 nm - thick layers are dispersed in the matrix forming a monolithic structure on the micro scale. Because thermoset layered silicate nanocomposites are synthesized by *in-situ* polymerization, silicate layers separated by 5 to 10 nms remain parallel if the extent of intragallery polymerization is uniform. Nanocomposites are considered as exfoliated when it has a structure of long-range order [20].
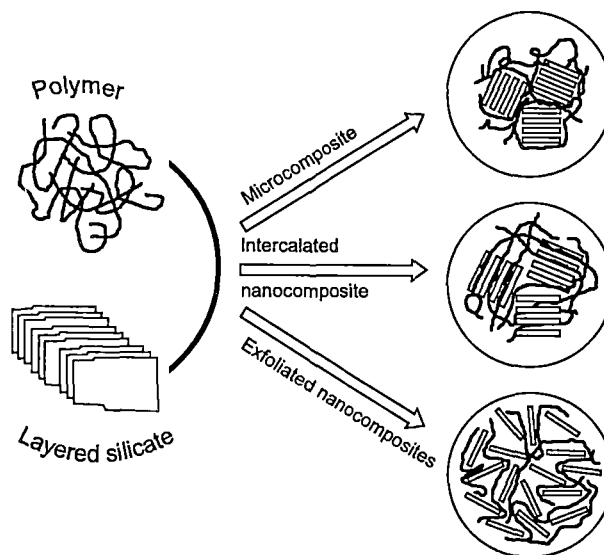
Figure 1.9 The three idealized structures of polymer- layered silicate composites. In reality, several of them are often co-exist in a nanocomposite.

The exfoliated configuration maximizes the polymer-layered silicate interactions making the entire surface of the layers available for interactions with the polymer. This should lead to most dramatic changes in mechanical and physical properties [175].

1.5.1 Critical issues in nanocomposites

Just as in traditional fibre composites, the major challenges in the research of nanocomposites can be categorized in terms of the structures from nano to micro levels. There is still considerable uncertainty in theoretical modeling and experimental characterization of the nano-scale reinforcement materials, particularly nanotubes. Then, there is a lack of understanding of the interfacial bonding between the reinforcements and the matrix material from both analytical and experimental viewpoints. Lastly, the challenges at the level of nanocomposites have mainly to do with the following issues related to composites processing [176, 177].

1.5.1.1 Dispersion

Uniform dispersion of nanoparticles and nanotubes against their agglomeration due to van der Waals bonding is the first step in the processing of nanocomposites. Besides the problems of agglomeration of nanoparticles, exfoliation of clays and graphitic layers are essential. SWCNTs tend to cluster into ropes and MWCNTs produced by chemical vapor deposition are often tangled together like spaghettis. The separation of nanotubes in a solvent or a matrix material is a prerequisite for aligning them.

1.5.1.2 Alignment

Because of their small sizes, it is exceedingly difficult to align the nanotubes in a polymeric matrix material in a manner accomplished in traditional short fibre composites. The lack of control of their orientation diminishes the effectiveness of nanotube reinforcement in composites, whether for structural or functional performance.

1.5.1.3 Volume and rate

High volume and high rate fabrication is fundamental to manufacturing of nanocomposites as a commercially viable product. The lessons learned in the fabrication of traditional fibre composites have clearly demonstrated that the development of a science base for manufacturing is indispensable. Efficiency in manufacturing is pivotal to the future development of nanocomposites.

1.5.1.4 Cost effectiveness

Besides high volume and high rate production, the cost of nanocomposites also hinges on that of the nano reinforcement material, particularly, nanotubes. It is anticipated that as applications for nanotubes and their composites increase the cost will be drastically reduced.

1.5.2 Polymer nanocomposites

Polymer nanocomposites (PNC) are polymers (thermoplastics, thermosets or elastomers) that have been reinforced with small quantities (less than 5 per cent by weight) of nano-sized particles having high aspect ratios (L/h >300) (Denault and Labrecque) [178]. The subject of hybrids based on layered inorganic compounds such as clays has been studied for a considerable time, but the area is enjoying a resurgence of interest and activity as a result of the exceptional properties which can be realized from such nanocomposites [179].

Material variables which can be controlled and which can have a profound influence on the nature and properties of the final nanocomposite include the type of clay, the choice of clay pre-treatment, the selection of polymer component and the way in which the polymer is incorporated into the nanocomposite.

The purpose of this chapter is to give an overview of polymer- layered silicate nanocomposites and to provide the reader with the necessary background to understand the papers of this thesis. First of all emphasis is given to polymer layered silicate nanocomposites. Then after a description of the characterization methods, properties specific to nanocomposites are discussed.

1.5.3 Polymers used in nanocomposites synthesis

Polymer- layered silicate nanocomposites have been synthesized from various polymers. An overview of the advances that have been made during the past 10 years in the intercalation and the exfoliation of organophilic layered silicates in different polymeric media are given here.

This part has been divided into two sections. First, the use of thermosets as matrices for nanocomposites is discussed. Epoxy and unsaturated polyester resins used in this as well as their chemistry are described here.

1.5.3.1 Thermosets

1.5.3.1.1 Epoxies

Both the prepolymer and the cured resin can be termed as "epoxy resin"; the former contains reactive epoxy groups (Figure 1.10) hence their name. In order to convert epoxy resins into hard, infusible thermoset networks, it is necessary to use curing agents. Diamines are the most widely used curing agents because they offer good reactivity with the epoxy groups and exist in wide variety. The diversity of curing agents gives to epoxies their wide versatility since their glass transition temperature may vary from under room temperature to 200°C or more.

Epoxy group

R-NH$_2$ + H$_2$C-CH-CH$_2$-O... $\longrightarrow$ R-NH-CH$_2$-CH-CH$_2$O...
|
OH

+ H$_2$C-CH-CH$_2$-O... $\longrightarrow$ R-N
CH$_2$-CH-CH$_2$O...
|
OH

CH$_2$-CH-CH$_2$O...
|
OH
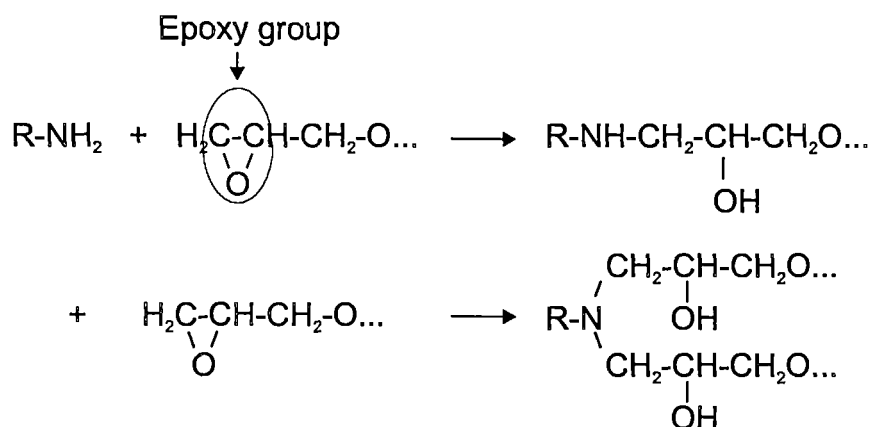
Figure 1.10 Mechanism of cure of epoxy with primary amines: - CH$_2$O indicates that only the reactive epoxy group is shown [180].

Figure 1.10 illustrates the initial step, which involves the primary amine active hydrogen adding to the epoxy group. This is followed by the resulting secondary amine adding to another epoxy group. Hydroxyl groups, including those generated during cure, accelerate the reaction by favoring the epoxy ring opening.

Epoxy-layered silicate nancomposites have been extensively studied [181-185]. The reason for this is that the reactants of epoxy systems have a suitable polarity in order to diffuse between the silicate layers and form a nanocomposite upon polymerization. Many researchers have studied the epoxy-clay nanocomposites in detail [180-192], one of the most important phenomenon they discovered is the self-polymerization of epoxy resin in organophilic smectite clays due to the presence of alkyl ammonium ions [193]. The mechanism is described in Figure 1.11, where in the dissociation of the alkyl ammonium cations in the clay galleries generates protons that attack the epoxy ring causing acid catalyzed ring opening homopolymerisation.
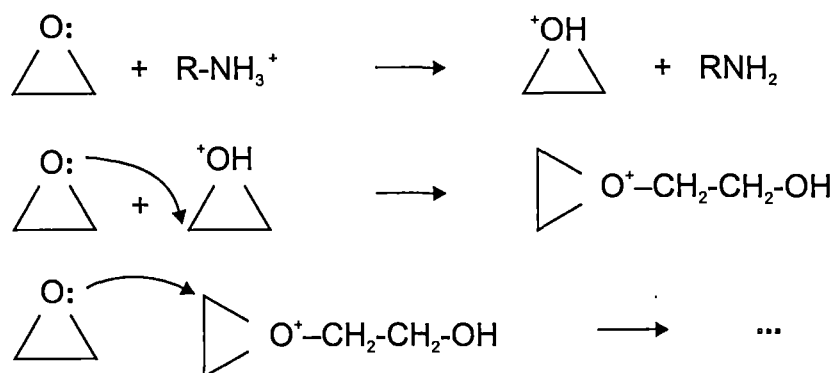
Figure 1.11   Homopolymerisation mechanism of epoxy resin catalyzed
by alkyl ammonium ions [194]

1.5.3.1.2 Unsaturated polyesters

Unsaturated polyester resins are bicomponent systems where polar unsaturated prepolymers are dissolved in styrene monomer (usually around 30 wt %). The unsaturated prepolymer is obtained by the polycondensation of the following components: a glycol, a saturated acid used to control the flexibility of the prepolymer chain and an unsaturated acid which provides the reactive double bonds. The resin is cured by free-radical polymerization. Initiators used to start the polymerization, are chemical entities (peroxides or azo-compounds) which produce free radicals during their dissociation. A catalyst is also used in order to speed up the dissociation of the initiator [195]. During the polymerization, unsaturated polyesters build a complex network with styrene bridges with the formation of micro gels. In the synthesis of unsaturated polyester-clay nanocomposites [196], it was noticed that the chain polymerization was partially inhibited by the presence of the clay. Apparently, the clay consumed free radicals. The mechanical properties of the nanocomposites were substantially improved as compared with the pristine polymer at low clay content (less than 5 vol %).

In recent times, a new method has been reported for the synthesis of unsaturated polyester-clay nancomposites [197] using dodecylmethyl ammonium bromide as surface modifier. Two different ways of mixing the organoclay with the unsaturated polyester were used. Simultaneous mixing, which consists in mixing directly the prepolymer and the styrene with the organoclay was compared with a second method, sequential mixing, which consists in pre-swelling the prepolymer in the organoclay with subsequent mixing with styrene for different durations. Results recommended that a more homogeneous network was obtained for nanocomposites prepared with sequential mixing.

1. 5. 3. 2 Thermoplastics

The first and the most studies carried out on thermoplastic for the synthesis of polymer clay nancomposites has been polyamide 6 [198-199]. As before indicated, polyamide 6–clay hybrids were first synthesized by Toyota researchers and physical properties of their polyamide 6 clay hybrids as compared with the pristine polymer find their origin in the presence of a constrained region [200] around the clay particles combined with the crystallinity of the pure polymer.

Other thermoplastics such as poly (ethylene oxide) [201], poly (methyl methacrylate) [202-203] polybutadiene acrylonitrile [204], polycarbonate [205], polydiacetylene [206], poly(ε-caprolactone) [207], polyvinyl pyridne [208], polystyrene [209-212], polyimide [213-216], polyethylene [217], and poly (ethylene terephthalate) [218] have since been used to synthesize polymer layered silicate nancomposites by different methods.

Polypropylene-layered silicate nanocomposites have also been actively studied by researchers from Toyota [219-223] and chemists from the

Institute for Macromolecular Chemistry in Freiburg [224-225] used a maleic anhydride-modified polypropylene oligomer to separate the silicate layers in the polypropylene matrix, maleic anhydride gives a sufficient polarity to the modified polypropylene to diffuse between the silicate layers in order to obtain an intercalated nancomposite. Polypropylene-nanocomposites constitute a major challenge for industry since they represent the route to substantially increase the mechanical and physical properties of one of the most used thermoplastics.

1.6 Synthesis of polymer-layered silicate nanocomposites

Maleic anhydride (MA) grafted polyethylene/clay nanocomposites were prepared by simple melt compounding [226]. The exfoliation and intercalation behaviours depended on the hydrophilicity of polyethylene grafted with maleic anhydride and the chain length of organic modifier in the clay. When polyethylene has a higher grafting level of MA than the critical grafting level of MA (0.1 wt per cent) and the number of methylene groups in alkyl amine chain has more than 16, polyethylene/clay nanocomposites are completely exfoliated. The main chemical routes for the synthesis of polymer-inorganic nancomposites is schematically represented by Sanchez *et al.* [227].

Mainly two different approaches have been usually employed in nanocomposites production. One approach involves enhancing the mobility of the polymer chain, in the presence of silicate layers, and with thermodynamic compatibility between the two, in order to achieve silicate layer dispersion. Currently, numerous procedures for the preparation of polymer nanocomposites have been proposed [228] using the following approaches

> 1. Direct intercalation of nanoscale building blocks into a polymer melt or solution.

2. *In situ* generation of nanoscale building blocks in a polymer matrix.

3. Polymerization of monomers in presence of nanoscale building blocks.

4. A combination of polymerization and formation of nanoscale building blocks. (*e.g.* sol-gel method, intercalation of monomers into layered structures followed by polymerization, etc)

The key issue of these techniques is that the geometry, spatial distribution and volume content of the nanofillers must be effectively controlled through adjusting the preparation conditions so as to ensure the structural requirements of nanocomposites.
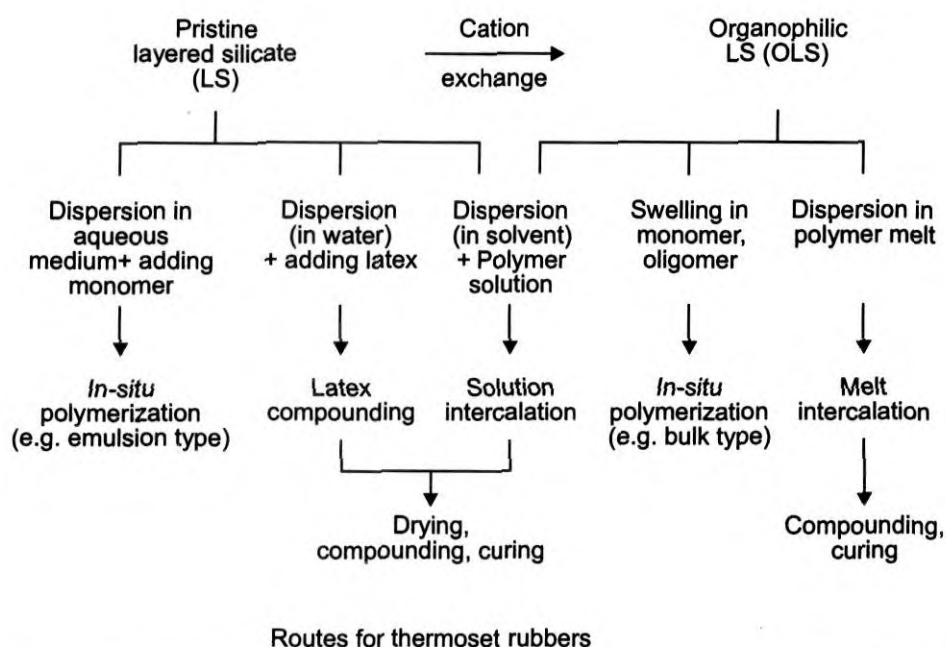
Figure 1.12 Possible preparation routes of rubber layered silicate nanocomposites

Then preparation of rubber/clay nanocomposites slightly differs from the above scenario as some methods are not ideal (*e.g. in-situ* polymerization) and rubbers are available in various forms (latex, solution and dry) which offer additional possibilities (*e.g.* latex compounding). Figure1.12 shows the possible production routes of thermoset rubber/ layered silicate nanocomposites at a glance. Further, the melt intercalation method, which is strongly recommended for dry form of rubber are not included here as the main theme of our discussion is latex based nanocomposites [229].

1.6.1 *In-situ* intercalative polymerization method

In-situ polymerization was the first method used to synthesize polymer layered silicate nanocomposites based on polyamide [7]. Nowadays, it is the conventional process used to synthesize thermoset-layerd silicate nanocomposites. The strategy is described schematically in Figure 1.13.
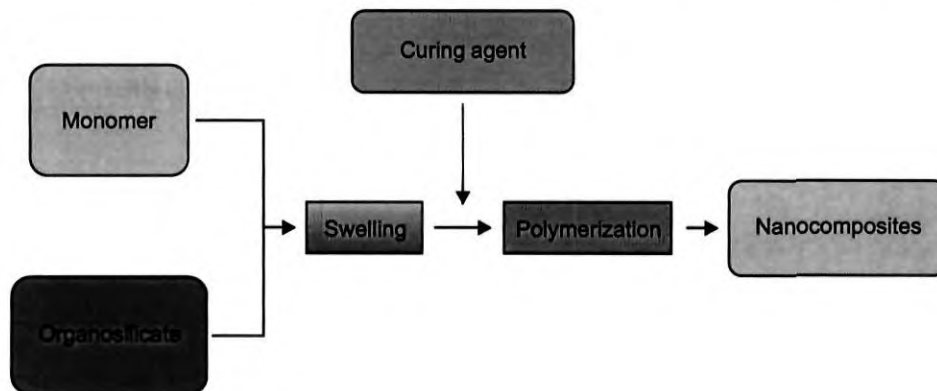
Figure 1.13 Flowchart presenting the different steps of the "*in-situ* polymerization" approach.

First, the organosilicate is swollen in the monomer. This step requires a certain amount of time, which depends on the polarity of the monomer

molecules, the surface treatment of the oragansilicate, and the swelling temperature. Then, the reaction is initiated. For thermosets such as epoxies or unsaturated polyesters, respectively, a curing agent or peroxide is added to initiate the polymerization [195, 230]. For thermoplastics, the polymerization can be initiated either by the addition of a curing agent or by an increase of temperature [231].

The key of this method is to control the polymerization occurring between the silicates layers (intragallery polymerization). If the cure kinetics is lower between the layers than outside the layers (extragallery polymerization), then separation of the silicate layers is impeded. Therefore, one needs to find ways to favour the intragallery polymerization as compared with the extragallery polymerization.

The driving force of the "*in-situ* polymerization" method in epoxy systems is linked to the polarity of the monomer molecules. During the swelling phase, the high surface polarity of layered silicate attracts polar monomer molecules so that they diffuse between the silicate layers.

When equilibrium is reached the diffusion stops and the layered silicate is swollen in the monomer to a certain extent corresponding to a perpendicular orientation of the alkyl ammonium ions [183, 232]. When polymerization is initiated, the monomer intercalated starts to react with the curing agent, which has diffused between the silicate layers. This reaction lowers the overall polarity of the intercalated molecules and displaces the thermodynamic equilibrium so that more polar molecules are driven between the silicate layers. As this mechanism occurs, the organic molecules can eventually separate the silicate layers.

Polymer-layered silicate nanocomposites based on thermosets such as epoxies [233] unsaturated polyester and polyurethanes [234-235] have been synthesized by this method as well as thermoplastic nanocomposites based on polyethylene terephthalate [236] polystyrene and PMMA[237]. Natural rubber (NR)/sodium-montmorillonite (Na-MMT) nanocomposites were prepared by co-coagulating the mixture of NR latex and various amounts of Na-MMT aqueous suspension [238]. Polyacrylate/organic montmorillonite (OMMT) nanocomposite was synthesized by *in-situ* emulsion polymerization with intercalated structure [239].

1.6.2 Intercalation of polymer or pre-polymer from solution

Polar solvents can be used to synthesize intercalated polymer – layered silicate nanocomposites. The strategy is similar to the one used in the "*in-situ* polymerization" approach.
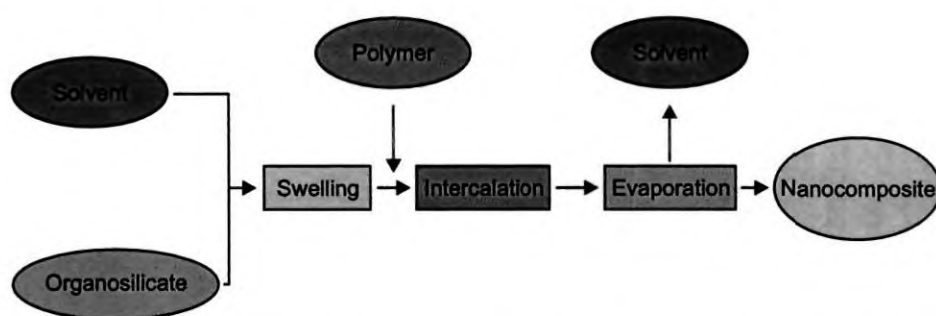
Figure 1.14 Flow chart presenting the different steps of the "solution" approach

Figure 1.14, describes the different steps of the synthesis. First, the organosilicate is dispersed in a polar solvent such as toluene or N, N-dimethyl formamide. Alkyl ammonium treated clays swell considerably in polar organic solvents, forming gel structures.

Once the organosilicate is swollen in the solvent, the polymer, dissolved in the same solvent, is added to the solution so that polymer chains intercalate between the silicate layers. The last step consists in removing the solvent by evaporation usually under vacuum.

The driving force for polymer intercalation from solution is the entropy gained by desorption of solvent molecules, which compensates for the decrease in conformational entropy of the intercalated polymer chains [173, 240]. Therefore, a relatively large number of solvent molecules need to be desorbed from the layered silicate to accommodate the incoming polymer chains.

Nanocomposites based on high-density polyethylene [241], polyimide [242], and liquid crystal polymers [243] have been synthesized by this method. Nanocomposites based on untreated clays have also been synthesized using this approach. In this particular case, the polar solvent was deionised water. The polymer must be either able to be dispersed in water like poly (ethylene) oxide [244] or synthesized by emulsion polymerization as was reported for polymethylmethacrylate [245] and epoxy [246, 247].

The possibility to synthesize intercalated nanocomposites based on polymers with low or even no polarity is the major advantage of this method. However, the "solution" approach is difficult to apply in industry due to problems associated with the use of large quantities of solvent.

1. 6. 3 Melt-Intercalation or melt blending method

Vaia *et al.* [209] was the one who first reported about the melt intercalation process in 1993. The strategy consists in blending molten thermoplastic with an organosilicate in order to optimize the polymer –

layered silicate interactions (Figure 1.15). The mixture is then annealed at a temperature above the glass transition temperature of the polymer and forms a nanocomposite.
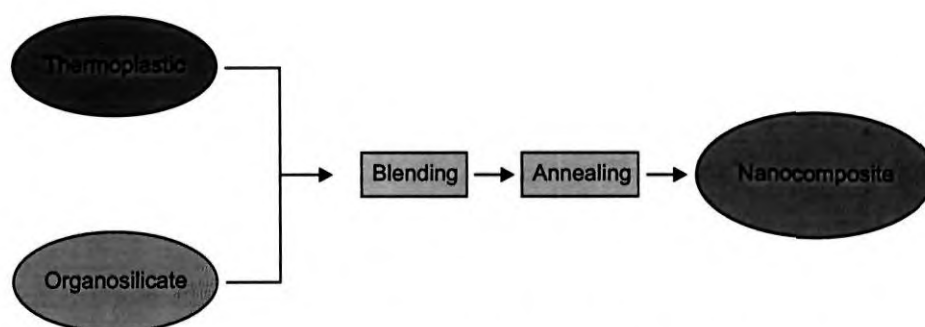
Figure 1.15 Flowchart presenting the different steps of the "melt intercalation" approach.

The fact that polymer chains can undergo centre of mass transport in between the silicate layers is surprising because the unperturbed radius of gyration of the polymer is roughly an order of magnitude greater than the interlamellar spacing [248]. Polymer chains experience a dramatic loss of conformational entropy during the intercalation. The proposed driving force for this mechanism is the important enthalpic contribution of the polymer/ organosilicate interaction during the blending and annealing steps.

Because of its great potential for application with rapid processing methods such as injection moulding, the melt intercalation process has become increasingly popular. Polymer – layered silicate nanocomposites have been successfully produced by extrusion [249]. A wide range of thermoplastics from strongly polar polyamide 6 [250-251] to styrene [252] have been exfoliated or intercalated between silicate layers. However, polyolefins which represent

the biggest volume of polymers produced have so far only been successfully intercalated to a limited extent [253-254]. PS/MMT [255-256], PEO/Na+MMT [257-259], N6/clay [260-264], HDPE [265], PCL/clay [266] PE/clay [267] etc are examples for this type of synthesis. Melt intercalation of natural rubber, epoxidized natural rubber and styrene butadiene rubbers are also reported [268]. The polymer, hydrogenated nitrile-butadiene rubber (HNBR) was melt compounded with organophilic montmorillonite (OMMT) [269]. Study of interlayer spacing collapse during polymer/clay nanocomposite melt intercalation was done by Benali *et al* .[270]. Bio-degradable poly (lactic acid)/clay nanocomposites can also prepared by melt intercalation [271].

1.6.4 *In-situ* formation of silicate layers

A relatively new approach proposed by Carrado *et al.* [272] is the *in-situ* hydrothermal crystallization of silicate layers (hectorite) in an aqueous polymer gel medium. This method is particularly suited for water soluble polymers such as poly (acrylonitrile) (PACN), poly (aniline) PANI) poly (vinylpyrrolidone) PVP), hydroxy propyl methyl cellulose (HPMC) and polydimethyl diallyl ammonium (PDDA). To make these synthetic polymer- layered silicate nanocomposites, dilute solutions of precursor hectorite gel are refluxed for various lengths of time, then isolated *via* centrifugation, washed, and air - dried. Polymer loading up to 86% can be attained by this method. The driving force of this synthesis is the balance between the negatively charged sites on the silicate lattice with those on the cationic polymer chain. Beyond charge compensation, the formation of the layers stops. If this method presents certain advantages, it must be noted that the size of the synthesized layers cannot compete with natural layered silicate for kinetic reasons and their average length is limited, at best,

to about one - third of their natural counterparts. Ring opening polymerization of caprolactum in N6/MMT, *in-situ* polymerization in PA12/MMT, dispersion of MMT in liquid caprolactone follow this route.

1.7 Thermoset nanocomposites

Thermoset nanocomposites are complex hybrid materials which integrate nanoparticles with polymers to produce a novel nanostructure, with extraordinary properties. Organic/inorganic hybrids are some of the most challenging nanostructures investigated to date. What differentiates nanocomposite materials from classical composites is the degree of control of fabrication, processing and performance that can be achieved down to a very small scale.

Thermoset polymer nanocomposites have received less interest in their scientific development and engineering applications than thermoplastic nanocomposites. However, some of these materials may be relatively easy to bring into production. The understanding of characteristics of the interphase region and the estimation of technology are the current research frontier in nanocomposite materials. The engineering resin nanocomposites are restricted to the most commonly used thermosets, such as epoxy resins, unsaturated polyesters, acrylic resins, and so on. Various nanoparticles have been found to be useful for nanocomposite preparation with thermosetting polymers, along with smectite clay, diamond, graphite, alumina and ferroxides. Thermoset nanocomposites represent a new technology solution. These new formulations benefit from improved dimensional/thermal stability, flame retardancy and chemical resistance; and have potential applications in marine, industrial and construction markets.

Adding clay nanofillers to biodegradable polymers has also been shown to enhance composite properties. The enhancement of material properties has been linked to the interfacial interaction between the polymer matrix and the organically modified layered silicate filler structure.

The filler particles provide a very high surface area. Montmorillonite, hectorite and saponite are the most commonly used layered silicates. For a nanocomposite to be formed successfully, the mineral must disperse into separate layers. The surface chemistry is also important - ion exchange reactions with cations (commonly alkyl ammonium or alkyl phosphonium cations) allow the silicate to be compatibilised with the polymer matrix. The strong interaction between the two materials leads to dispersion at the nanometer level.

Polymer/layered silicate nanocomposites are prepared by a variety of routes. One of the first materials, a nylon 6 nanocomposite, was prepared by *in-situ* polymerization of e-caprolactam in a dispersion of montmorillonite. The silicate can be dispersed in liquid monomer or a solution of monomer. It has also been possible to melt-mix polymers with layered silicates, avoiding the use of organic solvents. The latter method permits the use of conventional processing techniques such as injection molding and extrusion. Nanocomposites have been formed with a wide variety of polymers including: epoxy, polyurethane, polyetherimide, poybenzoxazine, polypropylene, polystyrene, polymethyl methacrylate, polycaprolactone, polyacrylontrile, polyvinyl pyrrolidone, polyethylene glycol, polyvinylidene fluoride, polybutadiene, copolymers and liquid crystalline polymers. Many studies have been carried out to characterize different nanocomposites. Techniques in use include wide-angle X-ray diffraction and transmission electron microscopy. Processing techniques are critical

in polymer manufacturing and this holds true for nanocomposites. Several processing methods and innovative techniques are discussed. For example, nylon 6 clay nanocomposites have been electrospun from solution, which resulted in highly aligned clay particles. Two other types of nanofiller are briefly described here. Polyhedral oligomeric silsesquioxane (POSS) nanoparticles combine organic and inorganic segments with nanosized cage structures.

Carbon nanotubes have also been examined as they offer unique mechanical and electrical properties.

1.8 Characterization of polymer- layered silicate nanocomposites

There are mainly two methods to characterize the nanostructure of polymer- layered silicate nanocomposites. The most up-front is X- ray diffraction (XRD) because it is a simple way to evaluate the spacing between the silicate layers. The sample preparation is relatively easy and the X- ray analysis can be performed within a short time [273]. However, one needs to be very careful with the interpretation of the results. Lack of sensitivity of the analysis and limits of the equipment can lead to misleading conclusions about the nanocomposites structure. The lack of peak at low angle is not a definite proof of nanocomposite structure. Therefore, transmission electron microscopy (TEM) is a necessary complement to X-ray diffraction. TEM gives a direct measure of the spatial distribution of silicate layers but requires substantial skills in specimen preparation and analysis. Concerning the determination of the microstructure of polymer – layered silicate nanocomposites, scanning electron microscopy (SEM) is the most appropriate method.

Nanocomposites have also been characterized by differential thermal analysis such as dynamic mechanical thermal analysis (DMTA) differential scanning calorimetry (DSC) or thermogravimetric analysis (TGA).

1.8.1 Structural characterization

1.8.1.1 XRD analysis

Nanocomposites generally contain a fairly small amount of layered silicate (typically less than 5vol per cent). Therefore, the XRD analysis must be sensitive enough to detect the crystalline structure of the layered silicate in the polymer. If this is not the case, no peaks appear in the diffraction pattern and the false conclusion that an exfoliated nanocomposite has been synthesized might be drawn. A simple method to verify the sensitivity consists in looking if crystallographic planes belonging to the silicate layers themselves (*hk* bands) can be detected. If so, the analysis is sensitive enough to detect (001) reflections. Then, the analysis is performed at low angle ($2\theta < 9°$, i.e. d> 9.8 Å) in order to detect the 001 reflection and evaluate the d- spacing between the silicate layers. It means that the irradiated surface may include not only the sample but also the sample holder. This might create a large amount of noise and complicate the interpretation of the XRD patterns to the diffraction angle θ. It means that the X-ray analysis at low angle will only reflect the structure present in a thin sample and a large surface area is recommended for the analysis in order to obtain the best response.

After all, XRD analysis is not well adapted to evaluate the structure of long-range ordered layered silicate, as it is often the case in thermoset layered silicate nanocomposites. Indeed, if the layered silicate embedded in a

matrix presents a large distribution of interlameller spacing, this will result in a smooth shoulder rather than a distinct peak in the XRD-spectrum so that the nanocomposites might appear exfoliated. Besides, conventional XRD equipment cannot usually detect an interlamellar spacing larger than 10 mm. For all these reasons, it is highly recommended to compare the results measured with XRD with the ones obtained with transmission electron microscopy.

1.8.1.2 Transmission electron microscopy

Transmission electron microscopy (TEM) is a powerful technique whereby a beam of electrons is transmitted through an ultra thin specimen, interacting with the specimen as it passes through it. An image is formed from the electrons transmitted through the specimen, magnified and focused by an objective lens and appears on an imaging screen, a fluorescent screen in most TEMs. The first TEM was built by Max Knoll and Ernst Ruska in 1931, with this group developing the first TEM with resolving power greater than that of light in 1933 and the first commercial TEM in 1939.

Modern TEMs are often equipped with specimen holders that allow the user to tilt the specimen to a range of angles in order to obtain specific diffraction conditions, and apertures placed above the specimen allow the user to select electrons that would otherwise be diffracted in a particular direction from entering the specimen.TEM pictures give a direct measure of the spatial distribution of silicate layers, morphology, and structural effects of a selected *area of the sample; however, the limitation is that it requires substantial skill in* specimen preparation and analysis.

1.8.1.2.1 Correlation between XRD and TEM

XRD and TEM measurements showed a very good correlation for materials where the layered silicates were ordered in a short range (14 to 20 Å).

However, epoxy-layered silicate nanocomposites presenting long range ordered structures were best characterized with TEM. Indeed, the XRD analysis of these materials showed no peak at low angle, suggesting that the silicate layers were exfoliated, whereas TEM measurements indicated that the interlamellar spacing of the silicate layers was about 50Å and that the layers were parallel to each other. TEM and XRD are complementary methods but the last remarks illustrate the fundamental importance of TEM in the characterization of the nanostructure of polymer layered silicate nanocomposites.

1.8.1.3 Scanning electron microscopy

Scanning electron microscopy (SEM) was used to characterize the microstructure of polymer-layered silicate nanocomposites. This method has the advantages to give a board overview of the micro scale dispersion of the silicate layers in these materials.

1.8.1.4 Fourier transform spectroscopy

Fourier transform spectroscopy is a measurement technique whereby spectra are collected based on measurements of the temporal coherence of a radiative source, using time-domain measurements of the electromagnetic radiation or other type of radiation. It can be applied to a variety of spectroscopy including optical spectroscopy, infrared spectroscopy (IR), nuclear magnetic resonance, mass spectrometry and electron spin resonance spectroscopy. The infrared spectrum shows the most characteristic properties of a compound. It provides a finger print for identification and is a powerful tool for the study of molecular structure. The correlation between the vibrating groups and the observed adsorption bands offer the possibility of chemical identification and the intensity measurements for quantitative determinations. The range in the

electromagnetic spectrum from 0.8 to 200μm (66 to 16520cm^{-1}) is referred to as infrared. However, the discussions will be limited to those regions from 400-4000 cm^{-1} which can be explored with commercial IR instruments. The spectra originate primarily from the vibrational stretching and bending modes within the molecules. Most organic and inorganic material show a rich array of absorption bands in the IR regions in contrast to that observed in the ultraviolet region.

Spectra obtained will either be of the polymer itself or its pyrolizate, in both cases matching to reference spectra gives the quickest means of identification of both blends and single polymer systems.

1.8.2 Thermal characterization

The term" thermal analysis" now applies to a series of techniques all of which subject a sample to a programmed temperature treatment, but which use a variety of transducers to sense the property changes continuously and automatically. Main analysis techniques used are thermo gravimetry (TGA) and differential scanning calorimetry (DSC). These techniques can be used to characterize different rubbers form their glass transition temperature, determining the microstructure, compatibility etc.

1.8.2.1 Thermogravimetric analysis

Thermogravimetric analysis (TGA) is a technique by which the mass of the sample is monitored as function of temperature or time, while the sample is subjected to a controlled temperature programme. The plot of the mass change versus temperature is termed as thermo gravimetric curve. Generally, the mass parameter in the TG curve is plotted on the ordinate decreasing downwards and the temperature on abscissa increasing from left to right. Often the differentiation

of the thermo gravimetric curve (DTG) proves extremely useful. It consists essentially of the plot of the rate of mass change with respect to temperature on the ordinate and temperature on the abscissa.

1.8.2.2 Differntial scanning calorimetry (DSC)

The differential scanning calorimeter consists of a specimen holder assembly, furnace having low thermal temperature- programmer- controller, system for atmosphere control and a recording system. In DSC, the sample and the reference are heated separately by individually controlled elements. The power to these heaters is adjusted continuously in response to any thermal effects in the sample so as to maintain sample and reference at identical temperatures. The differential power required to achieve this condition is recorded as the ordinate with the programmed temperature of the system as the abscissa.

1.9 Properties of polymer-layered silicate nanocomposites

The increasing interest devoted to polymer layered silicate nanocomposites arises from the fact that exfoliation of a relatively low amount of layered silicate gives the possibility to modify drastically not only the mechanical properties of the polymer but also some of its physical properties. In this section, the most characteristic changes brought by the nanocomposites structure are described and possible explanations about the origin of those changes are given. During testing the specimen is subjected to stretching at constant speed. Figure 1.16 show the stretched state, position of nanoclay and NR crystallization during the process of experimentation.

stretched state

nanoclay

sulphur bridges   NR crystallites
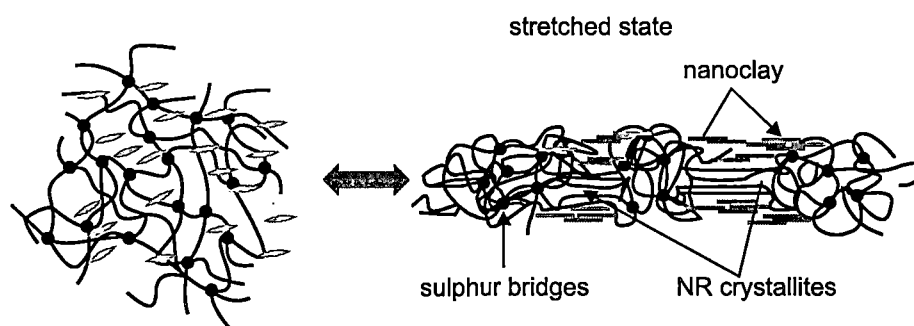
Figure 1.16 Stretched state position of nanoclay and NR crystallization
during the process of experimentation

1.9.1 Mechanical properties

1.9.1.1 Modulus

The drastic improvement in modulus provided by the exfoliated nanocomposites structure on polyamide 6 – clay hybrids was first reported by the Toyota researchers [7]. The modulus increased by 90 per cent with the addition on only 4 wt per cent of exfoliated clay. They also showed that the extent of improvement in modulus in their material was related to the average length of the silicate layers (i.e. aspect ratio of the dispersed nanoparticles) [274]. Later, Lan *et al.* [181] used rubbery epoxy matrix with only 15 wt per cent (= 7.5 vol per cent) of exfoliated organoclay. Similar improvements were also reported by Sreekala *et al.* [275] for nanocomposites based on anhydride-cured epoxy resins.

This short review concerning the moduli of polymer-layered silicates nanocomposites that the stiffness of nanocomposites is related to the degree of exfoliation of the layered silicate in the polymer matrix possibly because it increases the interaction between the silicate layers and the polymer. Several

explanations have been given about the reinforcement observed in polymer-layered silicate hybrids based on interfacial properties and interfacial effects where the direct binding (adsorption) of the polymer to the silicate layers would be the dominant factor. Shia *et al.* [276] has developed an interface model to predict the Young's modulus of elastomer-layered silicate nanocomposites suggesting also the important role of the interface. Usuki *et al.* [277] also suggested that the strong ionic crystallinity at the interface, explaining part of the reinforcement effect. Another explanation related also to interactions between the layered silicate and the polymer at the interface is the formation of a constrained region in the vicinity of the silicate layers. Kojima *et al.* [199] described a concept where the improvement of tensile modulus in polyamide 6-clay hybrids was well described by the contribution of a constrained region where the polymer chains have a restricted mobility.

1.9.1.2 Tensile strength

The tensile strength of polyamide 6 was substantially increased by 55 per cent with only 4 wt per cent of exfoliated clay [7] and in PMMA, Lee *et al.* [246] reported an improvement in strength of 15 per cent with 10 wt per cent of montmorillonite in their intercalated nanocomposites. These improvements have been explained by the presence of polar (PMMA) and ionic interaction (polyamide 6) between the polymer and the silicate layers. The lack of interfacial adhesion explains why no improvement in strength was observed for nanocomposites based on this polymer [278].

In rubbery epoxies, Lan *et al.* [181] reported a more than ten–fold increase in strength of their nanocomposites. Substantial increase of tensile strength

was also observed in elastomeric polyurethanes [221]. These enhancements in strength were attributed to the reinforcement effect of the nanolayers. In contrast, the tensile strength of nanocomposites based on glassy epoxies was not improved [279] and was sometimes even lower than the pristine epoxy [184]. Nevertheless, increasing the compatibility of strength in glassy epoxy-layered silicate nanocomposites [280]. This suggests that the strength of glassy epoxy-layered silicate nanocomposites is mainly controlled by the quality of the dispersion of the layered silicate on a micro-scale.

The compressive yield strength of glassy epoxy-clay nanocomposites was also studied by Massam *et al.* [281]. It was increased by 17 per cent with clay loading of 10 wt per cent whereas a conventionally filled composite with the same clay loading provided no compressive yield strength improvement. According to the authors, a total exfoliation of the clay was required to obtain such improvement. Differences in interfacial interaction, platelet aspect ratio, and layer charge densities had also a direct impact in the compression behavior of the nanocomposites.

1.9.1.3 Elongation at break

The elongation at break of nanocomposites based on thermoplastics and thermosets is usually reduced as the content of layered silicate increases [245, 278]. However, in nanocomposites prepared with elastometric epoxy [282] and polyurethane matrices [221-222], the addition of organosilicates increases the elongation at break of the material as compared with the pristine thermoset. This effect was attributed to the plasticizing effect of alkyl ammonium ions, which contributes to dangling chain formation in the matrix.

1.10 Barrier properties

1.10.1 Solvent resistance

The enhanced barrier properties of polymer-layered silicate nanocomposites increase solvent resistance also. A study performed on epoxy-clay nanocomposites [283] demonstrated that these materials offer a better resistance to organic solvents (alcohols, toluene, and chloroform). This was particularly the case for solvent molecules that are small enough to penetrate into the polymer network so that once they were absorbed, they caused molecular damage to the epoxy matrix, as with propanol or toluene. The exfoliated silicate layers prevent this type of solvent molecules from diffusing and damaging the polymer network.

1.10.1.1 Equilibrium swelling

The equilibrium swelling of a vulcanized rubber in a solvent is dependent on the density of crosslinks, the nature of the solvent, and the rubber. With a given rubber-solvent system, therefore, the equilibrium swelling value becomes a measure of the crosslink density of the vulcanization.

1.10.2 Permeability

The substantial decrease of permeability brought by nanocomposite structure is also a major advantage of polymer-layered silicate nanocomposites. Their polyamide 6-clay hybrid had a rate of water absorption reduced by 40 per cent as compared with the pristine polymer. Later Messersmith *et al.* [284] observed a dramatic decrease of water permeability with their poly (ε-caprolactone) - layered silicate nanocomposites up to 80 per cent with only 5 vol of clay. The gas permeability in rubber-clay hybrids was also reduced by 30 per cent with 4 vol per cent of exfoliated clay [285].
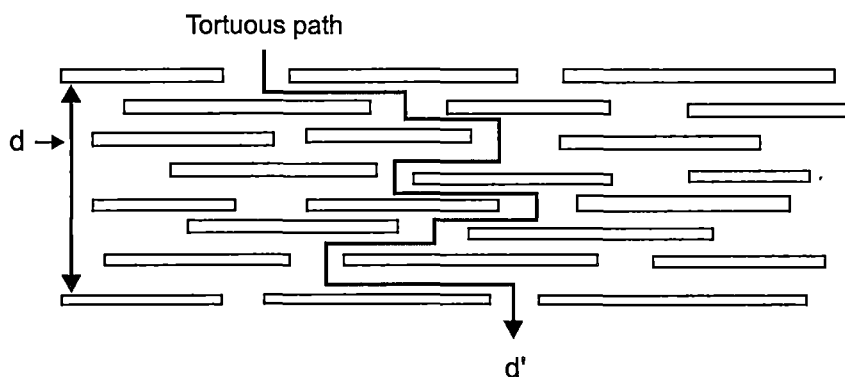
Figure1. 17 Model describing the path of the diffusing gas through the nanocomposite the tortuosity factor τ = d/d'. [286]

Until recently, the impressive decrease of permeability was only attributed to the large aspect ratio of the silicate layers which should increase the tortuosity of the path of the gas as it diffuses into the nanocomposites. As described in Figure 1. 17, the tortuosity factor, defined as τ = d/d', increases with the aspect ratio of the silicate layers. Measurements of the permeability of polyimide-clay hybrids [209] using clays with different aspect ratios confirm this idea.

However, a scrutiny [287] on a new nanocomposite based on polyamide 6, MXD6, has shown a reduction of water permeability by a factor of 40 as compared with the pristine polymer and contradicts this idea. Indeed, the aspect ratio of the silicate layers in this material was lower than that of the clay used in polyamide 6-clay hybrids, which brings a decrease of water permeability of only 40 per cent. The conclusion was that the constraint brought by the nanocomposite structure to the polymer chains situated in the neighborhood of the silicate layers may be the essential factor contributing to the decrease of permeability.

1.11 Thermal properties

1.11.1 Thermal stability

Toyota researchers also showed that their new material had an improved thermal stability [7]. The heat distortion temperature of their nanocomposites was 87°C higher than that of unfilled polyamide 6 extending the use of this polymer to under the hood structural parts in the engine compartment. This property was combined with a reduction of the thermal expansion coefficient up to 45 per cent. The improvement of heat distortion temperature was increased with the length and the content of silicate layers and was attributed to the presence of a constrained region in the nanocomposites [31].

The improved thermal stability of polymer-layered silicate nanocomposites based on poly (dimethylsiloxane) [225] and poly (imide) [274, 288] was also shown using thermo gravimetric analysis. The thermal stability of these two polymers was increased, respectively, of 60° and 25°C at 50 per cent of weight loss. Y.Cai *et al.* [289] demonstrated also by TGA that poly (styrene-acrylonitrile) (SAN)/clay nanocomposites have been prepared by melt intercalation method from pristine montmorillonite (MMT). SAN/clay nanocomposites have remarkably enhanced thermal stability as compared with the pristine polymer. They attributed this improvement to the confinement of SAN polymer chains between the silicate layers and polymer / clay interactions. The extent of thermal stability brought by the nanocomposite structure for a given polymer appears to be related to the chemical nature and the degradation mechanism of the pristine polymer.
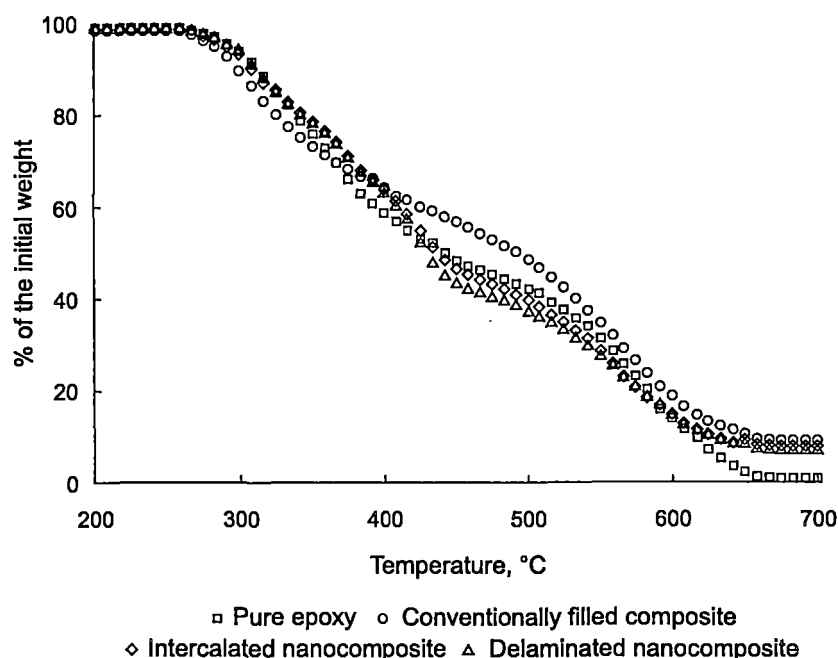
Figure 1.18 Thermogravimetric analysis of pure epoxy, conventionally filled compounds and intercalated and delaminated nanocomposites under nitrogen.

Thermogravimetric analysis under nitrogen of a conventionally filled epoxy-clay composite and two epoxy-clay nanocomposites (intercalated and exfoliated) containing approximately the same true clay content and compared their thermograms with that of the pure epoxy. The results, presented in Figure 1.18, indicate that at 50 per cent of weight loss the conventionally filled composite. This counter performance is apparently due to the low thermal stability of the compatibilising agent (octadecylammonium ions) used in the synthesis of these two nanocomposites and is lower than that of the conventionally filled composite. This shows that the choice of the compatibilising agent is also important to optimize the thermal properties of the resulting nanocomposites.

1.11.2 Flammability

The flame retardant properties of polymer-layered silicate nanocomposites have been recently reviewed by Gilman [290]. Polymer-layered silicate nanocomposites usually exhibit low flammability. Thus, the peak heat release rate during the combustion of polyamide 6–clay nanocomposites is reduced by 63 per cent at only 5 wt per cent of clay [291]. Moreover, the nanocomposites structure appears to enhance the performance of the char through reinforcement of the char layer. This means that nanocomposite parts conserve their shape during combustion.

1.12 Optical properties

Conventional composites tend to be largely opaque because of light scattering by the particles or fibres embedded within the continuous phase [292]. In nanocomposites, the domain sizes are reduced to a level such that true "molecular composites" are formed. As a result of this intimate mixing these hybrids are often highly transparent, a property which renders them ameanable to applications outside the boundaries of traditional composites. Wange *et al.* [186] demonstrated that magadite-nanocomposites based on an epoxy matrix were much more transparent than corresponding smectite-nanocomposites at the same loading. They attributed this phenomenon to the possibility that the magadite was more fully exfoliated than smectite. Later, they reported the high transparency of smectite nanocomposites based on a polyurethane matrix [221].

1.13 Natural rubber based nanocomposites

1.13.1 Natural rubber

The natural rubber (NR) presently used by industry is obtained by tapping the sap known as 'latex', from the tree *Hevea brasiliensis* [293].Tapping is usually done by shaving about one or two millimeters thickness of bark with each cut, usually in the early morning hours, after which latex flows for several hours and gets collected in cups mounted on each tree. The latex having an initial DRC 30-35% may either be concentrated to about 60% dry rubber content (DRC), usually by centrifuging or evaporation, or alternatively coagulated and dried. The two approaches lead to two distinct branches of rubber technology, namely latex technology and dry rubber technology.

1.13.1.1 Compounding of natural rubber-dry stage

Natural Rubber (NR) is a very versatile engineering material. The applications of NR are still increasing both in diversity and extent. A few examples are automobile components, dock fenders, spring insulated buildings, bridge bearings, marine engineering, seals for structures such as tunnels, sluices, aqueducts, basements, structural bearings used as structural components to provide flexible support for concrete panels, bridges and viaducts, anti-earthquake systems.

The characteristics of natural rubber as an engineering material are listed below.

   • hardness adjustable from very soft to very hard (ebonite);

- appearance from translucent (soft) to black (hard);

- electrically insulating or fully conductive;

- compounded to meet almost any mechanical requirement;

- silence noise and absorb vibration;

- protect, insulate and seal;

- available in any shape and surface roughness.

Uncured natural rubber behaves like a viscoelastic fluid during mixing. Under processing conditions, various rubber chemicals, fillers and other additives can be added and mixed into the rubber to form an uncured " rubber compound." These compounding ingredients are generally added to the rubber through one of two basic types of mixers, the two roll mill and the internal mixer.

The choice of type of natural rubber depends on the purpose for which it will be used. Several marketable forms of natural rubber are available which meet the requirement of various products. The different types of NR are specified in the Technical Specified Rubber (TSR) bulletin which was first introduced by Malaysia (SMR). Now-a-days, also new types of NR are available such as superior processing grades (SP/SA), epoxidized natural rubber (ENR), thermoplastic natural rubber (TPNR), deproteinized natural rubber (DPNR) and SUMAR (low smell natural rubber). A feature of natural rubber is that the desired physical properties can be achieved by compounding. Figure 1.19 shows the effect of crosslink density at various vulcanize properties.
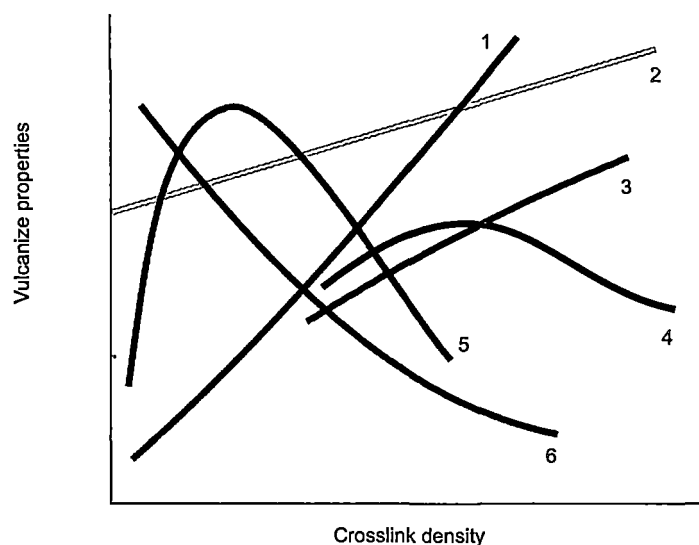
Crosslink density

Figure 1.19 Vulcanizate properties *vs.* crosslink density [294]. 1. Static modulus, extrusion resistance and blister resistance. 2. High speed dynamic modulus. 3. Hardness. 4. Tensile strength. 5. Tear strength, fatigue life and toughness. 6. Hysteresis, permanent set, coefficient of friction, elongation and compression set.

1.13.1.2 Compounding of natural rubber latex

Compounding is the process of incorporation of various chemicals such as vulcanizing agents (*eg.*: sulphur), accelerators (ZDC, ZMBT etc), activators(ZnO), fillers etc in to latex, before they are converted in to finished products [295]. The major requirements of compounding are to provide 1) the rheological, gelling, or other characteristics required for processing 2) to get good physical properties to the final product 3) a suitable vulcanizing system with desired tensile properties within the time/ temperature cycles available on the production line in use. Sulphur is the common vulcanizing agent, where vulcanization is the process in which rubber is converted to a condition in

which the elastic properties are conferred, over a higher range of temperature. Important accelerators are the salts of various dithiocarbamic acids. Zinc oxide is the usual activator.

1.13.2 Natural rubber latex nanocomposites

As most of the rubber exists in latex form and layered silicates can be easily dispersed in water, the production of nanocomposites from latices is rather easy. Here the latex should be blended with the clay/water slurry without causing coagulation of the rubber. In order to get better mechanical properties, there must be a strong interaction between the matrix and the stiffer silicate phase and this can be achieved using filler with a large interlayer distance. In this situation, nano-concept is highly relevant for rubber compounds since their applications require filler reinforcement [296-300]. The mechanical mixing is the most popular method for the incorporation of filler in the polymer. Other methods include *in-situ* filler synthesis [301-304] or polymerization around the filler particles [305].

Rubber nanocomposites can be considered as an important category of organic-inorganic hybrid materials, in which inorganic nanoscale building blocks (*e.g.* nanoparticles, nanotubes or nm-thick sheets) are dispersed in an organic polymer matrix [306]. Now-a-days rubber nanocomposites are of great importance because of the high reinforcement property associated with very small concentration [307]. An updated survey of literature covering the field of nanocomposites of polymer latices and their blends are available [308-314].

Rubber layered-silicate nanocomposites (PLSN) are the foremost members of such high performance nanocomposites. Improvements in mechanical, thermal and barrier properties, flame retardency etc [315-322] are

claimed for this class of polymer nanocomposites that could not be achieved by conventional fillers at such low loading (typically < 10 phr). This class of material uses different types of clay, such as smectite, laponite, kaolinite, etc. Among which smectite group of clays are most widely used due its layered structure, very high surface area (700– 800 m²/g), higher cation exchange capacity (90–125 meq/100g clay) and high aspect ratio (100–1000). Cations like ammonium ion with long aliphatic hydrocarbon chains compatibilise the silicates with polymers and enhance the interaction with a polymer by enlarging the interlayers (lamina), generating organically modified layered silicates or simply organoclays. Each layer is constructed from two silicon tetrahedron fused to an alumina octahedron [323]. They have properties that are superior to conventional microscale composites and can be synthesized using simple and inexpensive techniques.

Latest reports available in literature about natural rubber nanocomposites are listed in Table 1. 3.

Table 1. 3

No	Nanocomposite	Method/ result	Ref
1	ENR-pristine layered silicate composites	Melt mixing and sulphur curing	324
2	NRL&PVNRL + colloidal suspension of chitin whiskers	Two aqueous suspensions were mixed and solid composite films were obtained either by freeze-drying and hot-pressing or by casting and	325

		evaporating. Better resistance of evaporated samples than hot-pressed ones against swelling in an organic solvent medium is good evidence for the existence of a rigid chitin network.	
3	NRL&PVNRL + colloidal suspension of chitin whiskers	Structural morphology and swelling behaviour shows high mechanical property	326
4	NR / MWCN	By increasing the amount of CNTs added into the rubber the ductility decreased and the material become stronger and tougher but at the same time more brittle	327
5	NR/ Silica	Payne effect becomes more pronounced at higher silica loading.	328
6	NR/SWNTs/ SiC	Modulus and strength of natural rubber with 1.5 per cent SiC nanoparticles appear to be superior to those of SWNTs	329
7	NR +MMT/ sepolite / hectorite/Carbon nanofibre/ expanded graphite.	SP filled nanocomposite exhibited 26 per cent increase in modulus and F increased the tear strength by 18 per cent, over the gum. Supported by AFM, XRD, TEM, SEM analysis	330

8	NR/ nano SiO_2	Nano SiO_2/NR composites were prepared through blending nano SiO_2 emulsion with natural rubber latex and then concreting with acetic acid. The emulsion nano SiO_2 was prepared with $Na_2SiO_3 \cdot 9H_2O$ and hydrochloric acid under the reaction of the assistant agents. This was analyzed effect of the application rates of assistant agents such as silane coupling agent, surfactant, nucleating agent and dispersant on the properties and interface structure of the nano SiO_2/ NR composites with IR, TEM, SEM, DMA was analyzed.	331
9	NR/nano organoclay	Mechanical properties were improved at 2 phr organoclay. Further loading decreases these properties.	332
10	ENR as compatibilizer in SBR cloisite 20A nanocomposites	Morphology observed through XRD and HRTEM shows that the nanoclay is highly intercalated in ENR, and further incorporation of organically modified clay in SBR matrix leads to partial exfoliation of the nanoclay.	333
11	ENR/ Alumina nanoparticles	ENRAN were produced by melt compounding followed by sulphur curing.	334

12	Radiation crosslinked NR/EVA/organo clay nanocomposite	The NR/EVA blend with a ratio of 40/60 was melt blended with different concentrations of either dodecyl ammonium montmorillonite (DDA-MMT) or dimethyl dihydrogenated tallow quarternary ammonium montmorillonite (C20A).	335
13	NR/Organo modified bentonite	Filler ODTMA-JP A030 appears to be the most effective among the organoclays; surprisingly similar values of composite elongation and strength were obtained with unmodified bentonite JP A030	336
14	NR/ Nano SiO$_2$	Nanocomposite is developed by combining self-assembly and latex-compounding techniques	337
15	NR/Nano organoclay compatibilized with ENR	The tensile strength, elongation at break, and tear strength increases as a function of the organoclay content	338
16	ENR/Organoclay	The addition of nanoclay 15A and 20A improved the mechanical properties of ENR, while the properties of ENR/10A were enhanced indistinctively	339

17	NR/LDPE / BSCCO nanoparticles	NR filled with Bi-based superconductor BSCCO nanoparticles was successfully fabricated using a traditional milling rubber technique.	340
18	NR/ Montmorillonite nanoclay	NR/clay aerogel nanocomposites were produced via freeze–drying technique. clay - filled NR vulcanizates' crosslink density increase with the pristine clay content in both thermal and microwave curing methods.	341
19	NR/C nanotubes	R V(NRL/CNTs)were prepared using solvent casting method. Tensile modulus of the nanocomposites increases with the increase of carbon nanotubes.	342
20	NR/ Nano-organoclay	The nanocomposites of natural rubber (NR) and organoclay are prepared by the grafting and intercalating method in latex in the presence of butyl acrylate (BA) monomer	343
21	NR/starch/ nano-clay	Effect of operating variables such as natural rubber type, clay, glycerol and natural rubber contents on mechanical properties of NR/starch/ clay nanocomposites	344

22	NRL/ Nanoclays	Transport properties of natural rubber latex layered clay nanocomposites	345
23	Rubber (NR/PUR/NR+PUR) /layered silicate	Used broad band dielectric spectroscopy (BDS) to investigate relaxation phenomena in NR, PUR, PUR/NR blend based nanocomposites (10 phr LS).	346
24	NR/ Cellulose nanofibre	Nanocomposite dried in air. Prepared by blending natural rubber latex and cellulose nano-fibres using a home-use mixer. Higher glass transition temperature, lower tan δ peak value, slightly broader glass transition region and increased tortuosity compared with pure NR	347
25	NR/ cassava starch and mineral clay composite	SEM shows no trace of starch granules in the tensile fracture surface of composites. XRD shows dispersed clay platelets provided more surface area for the rubber and starch interactions which resulted in better reinforcing and improved mechanical properties.	348

| 26 | NR/SWNT | Ultrasonication dispersed SWNTs in water and stabilized by the addition of a surfactant. The SWNTs dispersion was mixed with NR latex and the effect of nanofiller on the flow properties was noted. Casting and curing gave good quality composite. Thermal stability of NR remained unaffected by the presence of SWNTs at low concentrations. | 349 |

1.13.3 Nanocomposites from latex blends

Blending of polymers in the latex stage will give a final product of better properties, depending on the miscibility and properties of individual components [159-160]. The main advantage of latex stage blending is the finer scale dispersion of the components and there is no contamination of any type of solvents. The control of phase morphology during blend processing is a key issue for the production of new materials with improved properties. Thomas and co-workers have studied properties of NR/SBR and NR/XSBR blends [161-169]. The properties of layered silicate reinforced NR and polyurethane rubber latex blends were extensively studied. Improvement in static dissipative properties of cast films prepared from blends of natural rubber latex and 2-(Dimethylamino) ethyl methacrylate (DMAEMA)-grafted NR latex was demonstrated in literature [169]. A new method has been developed to determine the probability of miscibility in binary polymer blends through hydrodynamic interaction. This is achieved by the measurement of the free volume content in blends of carefully selected systems-styrene acrylonitrile (SAN)/poly(methyl methacrylate)

(PMMA), PMMA/poly(vinyl chloride) (PVC), and PVC/polystyrene (PS)-with positron annihilation lifetime spectroscopy [170]. Important latest works done in latex blends nanocomposites is given in Table 1. 4

Table 1. 4

No	Nanocomposite	Method/ result	Ref
1	PP-NR /clay (Na-MMTs)	PP-NR /clay nanocomposite prepared by octa and dodecylamine modified natrium- montmorillonites using an internal mixer. Studied blending speed, temperature and period. Maximum property was obtained at 80 r.p.m. of rotor speed, temperature of 180°C and 6 m of period	350
2	NR-EVA blends with organoclay	NR/EVA (40/60) nanocomposite prepared with various amounts of organoclay using an internal mixer followed by compression molding. XRD, TEM, SEM confirmed homogeneous distribution of the organoclay in the polymer matrix	351
3.	PP/LNR/NR(TPNR) with KF, GF nano fibres	TPNR hybrid composite prepared via melt blending using internal mixer, at various temperatures, speed and	352

time. Reinforced TPNR-KF-GF hybrid composites (0-20 per cent by volume), with and without silane coupling agent and maleic anhydride grafted polypropylene, using the optimum processing parameters.

4.	NR -EVA/ unmodified MMT	Nanocomposites of natural rubber (NR) /poly(ethylene-co-vinyl acetate) (EVA)/ unmodified montmorillonite (MMT) were prepared by latex compounding. 90NR/10EVA/4MMT exhibited the highest property. XRD, TEM pictures showed an exfoliated structure and SEM micrographs revealed the well dispersed MMT particles in the polymer matrix	353
5.	ENR-cloisite nanocomposites+ NR-SBR blend+ varying types of carbon blacks	ENR and Organoclay (Cloisite 20A) nanocomposites were incorporated in NR and SBR blends in presence of varying types of carbon black as reinforcing fillers. The rubber compound containing 70 wt per cent of NR, 30 wt per cent of SBR and 10 wt per cent of ENR/nanoclay with ISAF N231 are found to be the toughest rubber.	354

6. NR-SBR blend/ Na-MMT	50/50 (wt per cent) NR/SBR blend/clay (10 phr) nanocomposite was prepared by mixing the latex blend with aqueous clay dispersion and co-coagulating the mixture. TEM and XRD characterized nanocomposites showed better mechanical properties than clay-free NR/SBR blend vulcanizate.	355
7. TPNR/ $BaFe_{12}O_{19}$	TPNR filled $BaFe_{12}O_{19}$ nanocompasites were prepared by melt blending at $180°$ C with mixing speed 110 and 13 min mixing time. TPNR nanocomposites with only 4 per cent nanoparticles exhibited good mechanical properties. Magnetization (Ms), and remagnetization (Mr) increased with increasing ferrite content	356
8. NR-CR blend/ OMMT	The effect of dispersed OMMT on curing behaviors of NR/ CR blend (75/25) was investigated. TEM showed dispersion of OMMT in the rubber blends and found little OMMT migrated into the NR phase. Results verified that addition of OMMT can obviously modify the reversion resistance of the binary blend	357

9. NR/[P(S-BA)], P(S- BA)/ PVC & NR/ Starch nanocomposites	Studies on three blends (natural rubber [NR]/poly (styrene–butyl acrylate) [P(S-BA)], P(S–BA)/poly(vinyl chloride) [PVC], and NR/starch) showing low contrast between the polymer phases in the 40–60 eV range. In the NR/ P(S–BA) and P(S–BA)/PVC blend nanocomposites, the clay platelets accumulate in the P(S–BA) phase, while in the P(S–BA)/ PVC nanocomposites, clay is also found at the interfaces. In the NR/starch blend, clay concentrates at the interface, but it also penetrates the two polymer phases. These observations reveal that nanostructured soft materials can display complex morphochemical patterns.	358
10. NR-PUR/sodium fluorohectorite	NR/PUR-based nanocomposites were produced by adding LS; sodium fluorohectorite 10(phr) in latex blends. The LS is more compatible and thus better intercalated by PUR than by NR. Nano-reinforcement confirmed by XRD, TEM, FTIR was best reflected in stiffness and strength-related properties of the rubber composites	359

11.	CR-CSM/ Nano/Micro Silica particles	Investigated, the rheological, mechanical properties and thermal stability of CR/CSM rubber blends filled with nano and micro-silica particles. Nano-silica filled CR/CSM rubber blends shows lower density, higher V_{r0}/V_{rf} values, higher tensile properties, higher Tg and increased stability than micro-silica filled compounds.	360
12.	NR-PB/ organo clay	Nanocomposites based on NR and PB rubber blend were prepared by adding different amounts of organic layered silicate. Tensile strength, modulus, abrasion resistance and tear strength improved significantly, elongation decreases slightly on adding organoclay. Thermal stability of the blend was improved by using 5 phr organoclay	361
13.	(Silicone based oligomer/ cloisite 20A, $2C_{18}$ MMT)-Polyolefin	Novozyme-435 catalyzed amidation reaction with silicone-based oligomer was carried out to scale up the synthesis of co-polymer which was compounded with nanoclays Cloisite 20A, $2C_{18}$ MMT. The resulting compound mixed with polyolefins for thermal and flame retardant applications.	362

| 14 | Nylon 6- ABS rubber/ nano-SiO$_2$ | The mechanical properties and morphology of the composites of nylon 6, ABS rubber, and nano-SiO$_2$ particles were examined. At higher nano-SiO$_2$ content obvious agglomeration appeared and decreased impact strength. At lower nano-SiO$_2$ content, a mixture with separation and encapsulation microstructures existed in the nylon 6/ABS/ nano-SiO$_2$ and ABS and nano-SiO$_2$ improved the toughness synergistically. | 363 |

1.14 Motivation and objectives of the present work

From the ongoing discussion it can be concluded that the area of polymer nanocomposites is the topic of this era. Their preparation, characterization, properties and application will be beneficial to the mankind in a long way. Natural rubber latex is a naturally occurring material with high wet gel strength, excellent physical properties and used in the manufacture of various latex goods. Polymer nanocomposites are well noted for their excellent barrier properties and flame retardness.

Usually fillers are incorporated in rubbers to modify certain properties to an acceptable level. The selection and the optimum loading of filler vary from polymer to polymer. Among black fillers carbon black is the most widely used filler in rubber industry. Clay and silica are the important white fillers. It is well known that the particle size, structure and surface characteristics of

reinforcing materials are the three factors, which influence the final properties of vulcanizates. The reinforcing capability of conventional clay is poor owing to its large particle size and low surface activity. Nanoclays have high aspect ratio, intrinsically anisotropic character, swelling capabilities and the ability to separate into individual layers in the aqueous medium. The aqueous phase of the latex can easily disperse unmodified layered silicates without the aid of the dispersing agent. Nanocomposites exhibit markedly improved properties as compared to pristine polymer and traditional micrcomposites. The superior mechanical properties thus obtain can be easily tailored to useful applications.

In this study prevulcanized natural rubber latex is used as the base material, chloroprene latex was also used for the study for making NR/CR blend. Sodium bentonite and sodium fluorohctorite are the layered silicates, in which bentonite is natural in origin and fluorohectorite is synthetic. English Indian clay and the gum compounds are used as the reference materials.

The main objectives of the present study are the following:

1.   Preparation of prevulcanized natural rubber latex nanocomposite.

2.   Characterization of natural rubber latex composites using TEM, XRD and evaluation of mechanical properties.

3.   Preparation of radiation vulcanized latex nanocomposite and their characterization.

4.   To study the rheological properties at different temperatures, shear rate and at different loadings of nanoclay.

5.   To study the dipping characteristics such as immersion and withdrawal speeds of the former, immersion time, temperature, concentration of the

coagulant etc on the thickness of the layered latex nanocompounds. This would be beneficial to the manufacturing units of catheter, bladder etc.

6.   To study the effect of nanofillers on ageing of rubber nanocomposite under different conditions like UV, γ- radiations, autoclave ageing, higher temperature, ozone, chlorine and solvents.

7.   To study the effect of nanofillers on chloroprene latex and their blends with natural rubber latex in different proportions and their characterization with FTIR, XRD, TEM and SEM.

8.   To develop a suitable latex compound formulation for the production of latex Foley catheter as per the IS specifications.

1.15 References

1.   P. Sharma, S. Raghunathan, A. Giri, W. Miao, Nanomaterials; Manufacturing, processing and applications, In; Dekker Encyclopedia of Nano Science, Eds. J. A. Schwarz and C. I. Contescu, Dekker, NewYork, 2004

2.   J. Jordan, K. Jacobb, R.Tannenbaumc, M. Sharafb, I. Jasiukd, *Materials Science and Engineering* A, **393**, 1 - 11, 2005

3.   C. Buzea, I. Pacheco, K. Robbie. *Biointerphases,* **2**, MR17, 2007

4.   Global Industry Analysts, Inc., 153 p, 2008

5.   S. Bakshi, P. R. Basak, S. Biswas, Nanocomposites - Technology Trends & Application Potential, TIFAC, 2009

6.   K. C. Arup, *Rubber World,* **236**, 6, 27, 2007

7.   A. Okada, M. Kawasumi, A. Usuki, Y. Kojima, T. Kurauchi, O. Kamigatio, *Mater. Res. Soc. Proc.*, **171**, 45 - 50, 1990

8.   T. Lan, T. J. Pinnavaia, *Mat. Res. Soc. Symp. Proc.*, **435**, 79 - 84, 1996

9.   R. M. Al- Habashi, Characterization of Aluminum-Substituted Yttrium-Iron Garnet Nanoparticles Prepared Using Sol-Gel Technique, Masters Thesis, University Putra Malaysia, 1 - 134, 2006

10. T. K. Sindhu, R. Sarathi, S. R.chakravarthy, *Bull. Mater. Sci.*, **30**, 2, 187 - 195, 2007

11. L. T. De Luca, L. Galfetti, F. Severini, L. Meda, G. Marra, A. B. Vorozhtsov, V. S. Sedoi, V. A. Babuk, *Combust. Expl. Shock Waves.*, **41**, 6, 680 - 692, 2005

12. S. R. Ghanta, K. Muralidharan, *Nanoscale*, **2**, 976 - 980, 2010

13. N. Mohamad, A. Muchtar, M. J. Ghazali, D. Hj. Mohd, C. H. Azhari, *Euro. Jl Sci. Res.*, **24**, 4, 538 - 547, 2008

14. S. Mu, D. Wu, Y. Wang, Z. Wu, X. Yang, W. Yang, *ACS Appl.Mater. interfaces*, **2**, 111 - 118, 2010

15. M. S. A. S. Shah, M. Nag, T. Kalagara, S. Singh, S. V Manorama, *Chem. Mater.*, **20**, 7, 2455 - 2460, 2008

16. B. J. Ash, R.W. Siegel, L.S. Schadler, *Macromolecules*, **37**, 1358 - 1369, 2004

17. Y. Chen, Z. Peng, L. X. Kong , M. F. Huang , P. W. Li, *Polym. Eng. Sci.*, **48**, 9, 1674 - 1677, 2008

18. H. C. Lu, C. S. Chang, C. W. Li, Y. S. Lin, C. L. Chu , C. Lai, *Nanoelectronics Conference, 2008. INEC 2008, 2nd IEEE International*, 917 -920, 2008

19.   Y. Fangli, H. Shulan, L. Jinlin, *J. Mat. Sci. Letters*, **20**, 16, 1549 - 1551,
       2001

20.   Z. Wang, T. Lan, T. J. Pinnavaia, *Chem. Mater.*, **8**, 2200 - 2204, 1996

21.   C. D. Munzy, B. D. Butler, H. J. M. Hanley, F. Tsvetkov, D. G. Pfeiffer,
       Materials Letters, **28**, 379 - 384, 1996

22.   E. G. William, A. B. Aldo, Z. Jinwen, *Maderas. Ciencia y tecnología*, **7**,
       3, 159 - 178, 2005

23.   H. Shioyama, *Carbon*, **35**, 1664 - 1665, 1997

24.   L. Hernan. J. Morales, J. Santos, *J. Solid State Chem.*, **141**, 327 - 329,
       1998

25.   Y. Ding, D. J. Jones, P. Maireless – Torres, *Chem. Mater.*, **7**, 562 - 571,
       1995

26.   O. C. Wilson, Jr., T. Olorunyolemi, A. Jawokrski, L. Borum, D. Young, A.
       Siriwat, E. Dickens, C. Oriakhi, M. Lerner, *Appl. Clay Sci.*, **15**, 265 - 279,
       1999

27.   A. A. Damour, D. Salvetat, Ann. Chim. *Phys. Ser.*, **21**, 376 - 383, 1847

28.   W. A. Deer, R. A. Howie, *Rock - Forming Minerals*, **3**, 240 p, 1962

29.   J. W. Earley, B. B. Osthaus, I. H. Milne, *Am. Miner.*, **38**, 707-724, 1953

30.   M. Jaber , J. Miehe-Brendle, *Microporous and Mesoporous Materials*,
       107, 1-2, 121 - 127, 2008

31.   S. I. Tsipursky, V. A. Drits, *Clay Minerals*, **19**, 177 - 193, 1984

32.   U. Hoffman, K. Endell, D. Wilm, Kristallstruktur , Z. Quellung, *Krist.*, **86**,
       340 - 348, 1933

33.   D. R. Paul, L. M. Robeson, *Polymer*, **49**, 3187 - 3204, 2008

34. J. Mering, *Trans. Faraday Soc.*, **42** B, 205 - 219, 1946

35. G. W. Brindley, G. Brown, Crystal Structures of Clay Minerals and Their X-ray Identification, Mineralogical Society, London, 169 - 171,1980

36. G. Brown, The X-Ray Identification and Crystal Structures of Clay Minerals, 2nd Ed., Mineralogical Society, London, 191 - 192, 1972

37. A. Akelah, N. Salahuddin, A. Hiltner, E. Baer, A. Moet, *Nanostructured Materials*, **4**, 965 - 978, 1994

38. A. Mathieu- Sicaud, J. Mering, I. Perrin- Bonnet, *Bull.Soc. Miner. Cristal.*, **74**, 439 - 455, 1951

39. G. Sides, L. Barden, *Can. Geotch. J.*, **8**, 391 - 299, 1971

40. R. E. Grim, Clay Mineralogy, 2nd Ed., Mc. Graw- Hill, New York, 175 - 176, 1968

41. E. Busenberg, C. V. Clemency, *Clays & Clay Minerals*, **21**, 213 - 215, 1973

42. M. M. Mortland, J. L. Mellor, *Soil Sci. Proc.*, **18**, 363 - 364, 1954

43. J. L. Mc Atee, *Am. Miner.*, **44**, 1230 - 1236, 1959

44. M. Stul, W. J. Mortier, *Clays & Clay Minerals*, **22**, 391 - 396, 1974

45. A. Usuki, M. Kawasumi, Y. Kojima, A. Okada, T. Kurauchi, O. Kamigatio, *J. Mater. Res.*, **8**, 1179 - 1184, 1993

46. T. Lan, P. D. Kaviratna, T. J. Pinnavia, *Chem. Mater.*, **7**, 2144 - 2150, 1995

47. Nanoclays at READE http://www.reade.com/component/content/article/597- montmorillonite-smectite

48. W. Liu, G. He, Z. He, *J. Appl-polym, Sci*, **115**, 3, 1630 - 1634, 2010

49. M. C. Floody, B. K. G. Theng, P. Reyes, M. L. Mora, *Clay Minerals*, **044**, 2,161 - 176, 2009

50. P. Bertoglio, S. E. Jacobo, M. E. Daraio, *J. Appl. Polym. Sci.*, **115**, 3, 1859 - 1865, 2010

51. V. Khanna, B. R. Bakshi, *Environ. Sci. Technol.*, **43**, 6, 2078 - 2084, 2009

52. Z. Zhao, J. Gou, Sci. *Technol. Adv. Mater.*, **10**, 015005, 2009

53. Y. Il. Yoon, J. M. Ko, *Int. J. Electrochem. Sci.*, **3**, 1340 - 1347, 2008

54. I. C. Finegan. G. G. Tibbetts, D. G. Glasgow, *J. Mater.Sci.*, **38**, 3485 - 3490, 2003

55. I. C. Finegan. G. G. Tibbetts, R. F. Gibson, *Compos. Sci. Technol.*, **63**, 1629 - 1635, 2003

56. B. Wang, M. Sain, Cellulose nanocomposites, In; ACS Symposium Series 938, Eds. K. Oksman and M. Sain, American Chemical Society, Washington DC, 187- 208, 2006

57. A. Chakraborty, M. Sain, M. Kortschot, *Holzforschung*, **59**, 102 - 107, 2005

58. A. N. Nakagaito, H. Yano, *Appl. Phys. A*, **78**, 547 - 552, 2004

59. A. N. Nakagaito, H. Yano, *Appl. Phys. A*, **80**, 155 - 159, 2005

60. A. Dufresne, D. Dupreyre, M. R. Vignon, *J. Appl. Polym. Sci.*, **76**, 2080 - 2092, 2000

61. D. M. Bruce, R. N. Hobson, J. W. Farrent, D. G. Hepworth, *Comp. Part A: Appl. Sci. Manf.*, **36**, 1486 - 1493, 2005

62. M. E. Malainine, M. Mahrouz, A. Dufresne, *Comp. Sci. Technol.*, **65**, 1520 - 1526, 2005

63. R. N. Shah, N. A. Shah, M. M. D. Lim, C. Hsieh, G. Nuber, S. I. Stupp, *Proc. Natl. Acad. Sci. U. S. A*, **107**, 8, 3293 - 3298, 2010

64. S. C. Lenaghan, L. Xia, M. Zhang, *J. Biomed. Nanotechnol.* **5**, 5, 472 - 476, 2009

65. S. Liao, C. K. Chan, S. Ramakrishna, *Frontiers of Materials Science in China*, **4**, 1, 29 - 33, 2010

66. T. D. Sargeant, S. M. Oppenheimer, D. C. Dunand, S. Stupp, *J. Tissue Engin. Regen. Medic.*, **2**, 8, 455 - 462, 2008

67. W. Stelte, A. R. Sanadi, *Ind. Eng. Chem. Res.*, **48**, 24, 11211 - 11219, 2009

68. R. C. Thomson, A. G. Mikos, E. Beahm, J. C. Lemon, W. C. Satterfield, T. B. Aufdemorte, M. J. Miller, *Biomaterials*, **20**, 2007 - 2018, 1999

69. A. Motta, C. Migliliaresi, F. Faccioni, P. Torricelli, M. Fini, R. Giardino, *J Biomater Sci Polymer Ed.*, **15**, 851 - 64, 2004

70. H. H. Park, K. E. Park, K. Y. Lee, W. H. Park, *Euro. Cells. Mater.*, **11**, 1, 2006

71. H. W. Kim, J. H. Song, H. E. Kim, *J. Biomed. Mater. Res. Part A*, **79A**, 3, 698 - 705, 2006

72. T. Zimmermann, E. Pohler, T. Geiger, *Adv. Eng. Mat.*, **6**, 9, 754 - 761, 2004.

73. The Micro Jet Reactor for Producing Nanoparticles, Synthesechemie GmbH, home.t- online.de/home/penth/ebesch.htm

74. A. L. Martin, B. Li, E. R. Gillies, *J. Am. Chem. Soc.*, **131**, 2, 734 - 741, 2009

75.   U. Narkiewicz, I. Pełech, M. Podsiadły, M. Cegłowski, G. Schroeder, J. Kurczewska, *J. Mater. Sci.*, **45**, 4, 1100 - 1106, 2010

76.   M. J. Pitkethly, *Materials today*, **7**, 12, 20 - 29, 2004

77.   K. L. Choy, In; Innovative Processing of Films and Nanocrystalline Powders, World Scientific Publishing, Singapore, 2002

78.   M. Boutonnet, J. Kizling, P. Stenius, G. Maire, *Colloids Surfaces*, **5**, 209 - 225, 1982

79.   B. H. Robinson, A. N. Khan-Lodhi, T. Towey, In; Structure and Reactivity in Reverse Micelles, Ed, M. P. Pileni, Elsevier, Armsterdam, 198 - 220, 1989

80.   P. Barnickel, A. Wokaun, W. Sager, H. F. Eicke, *J. Colloid Interface Sci.*, **148**, 80 - 90, 1992

81.   M. P. Pileni, *Phys. Chem. Chem. Phys.*, **12**, 11821 - 11835, 2010

82.   J. P. Chen, K. M. Lee, C. M. Sorensen, K. J. Klabunde, G. C. Hadjipanayis, *J. Appl. Phys.*, **75**, 5876 - 5878, 1994

83.   Z. J. Chen, X. M. Qu, F. Q. Tang, L. Jiang, *Colloids Surf.* B **7**, 173 - 179, 1996

84.   A. J. I. Ward, E.C. O Sullivan, J. C. Rang, J. Nedeljkovic, R. C. Patel, *J. Colloid Interface Sci.*, **161**, 316 - 320, 1993

85.   J. Eastoe, B. Warne, *Curr. Opin. Colloid Interface Sci.*, **1**, 800 - 805, 1996

86.   K. Kandori, K. Kon-No, A. Kitahara, *J. Colloid Interface Sci.*, **122**, 78 - 82, 1988

87. K. Kandori, K. Kon-No, A. Kitahara, *J. Dispersion Sci. Technol.*, **9**, 61 - 73, 1988

88. S. Y. Chang, L. Liu, S. A. Asher, *J. Am. Chem. Soc.*, **116**, 6739 - 6744, 1994

89. E. Joselevich, I. Willner, *J. Phys. Chem.*, **98**, 7628 - 7635, 1994

90. V. Chhabra, V. Pillai, B. K. Mishra, A. Morrone, D. O. Shah, *Langmuir*, **11**, 3307 - 3311, 1995

91. A. Fujino, K. Kon-No, *Colloids Surfaces A*, **100**, 245 - 253, 1996

92. V. Pillai, P. Kumar, M. S. Multani, D. O. Shah: *Colloids Surf. A*, **80**, 69 - 75, 1993

93. L. M. Qi, J. Ma, H. Cheng, Z. Zhao, *J. Phys. Chem.*, **B 101**, 3460 - 3463, 1997

94. K. C. Pingali, D. A. Rockstraw, S. Deng, *Aerosol Sci. Technol.*, **39**, 10, 1010 - 1014, 2005

95. W. Cai, L. Zhang, *J. Phys. Condens. Matter.*, **9**, 7257 - 7267, 1997

96. L. Maya, M. Paranthaman, T. Thundat, M. L. Bauer, *J. Vac. Sci. Technol.*, **B14**, 15 - 21, 1996

97. R. Subramanian, P. E. Denney, J. Singh, M. Otooni, *J. Mater. Sci.*, **33**, 3471 - 3477, 1998

98. S. L. Che, K. Takada, K. Takashima, O. Sakurai, K. Shinozaki, N. Mizutani, *J. Mater. Sci.*, **34**, 1313 - 1318, 1999

99. K. Okuyama, I. W. Lenggoro, N. Tagami, S. Tamaki, N. Tohge. *J. Mater. Sci.*, **32**, 1229 - 1237, 1997

100. G. Xiong, X. Wang, L. Lu, X. Yang, Y. Xu, *J. Solid State Chem.*, **141**,1,70 - 77, 1998

101. C. N. R. Rao, A. Govindaraj, R. Sen, B. C. Satishkumar, *Mater. Res. Innovations*, **2**, 128 - 141, 1998

102. W. Li, B. Chang, S. Qian, X. Zou, W. Zhou, *Science*, **274**, 1701 - 1703, 1996

103. C. Panatarani, I. W. Lenggoro, K. Okuyama, *J. Nanopart. Res.*, **5**, 1/2, 47 - 53, 2003

104. R. Alexandrescu, I. Morjan, M. Scarisoreanu, R. Birjega, E. Popovici, I. Soare, L. Gavrila-Florescu, I. Voicu, I. Sandu, F. Dumitrache, G. Prodan, E. Vasile, E. Figgemeier, *Thin Solid Films*, **515**, 24, 8438 - 8445, 2007

105. M. Suganeswari, A. M. Shering, P. Bharathi, J. J. Sutha, *Int. J. Pharma. & Biolo. Arch.*, **2**, 2, 847 - 854, 2011

106. A. Sadeghi Nik, A. Bahari , A. Sadeghi Nik, *Am. J. Sc. Res.*, **25**, 104 - 111, 2011

107. T. K. Tseng, Y. S. Lin, Y. J. Chen, H. Chu, *Int. J. Mol. Sci.*, **11**, 2336 - 2361, 2010

108. R. S. Sonawane, M. K. Dongare, *J. Mol. Catal. A*, **243**, 68 - 76, 2006

109. H. Dislich, *Angewandte Chemie International Edition in English*, **10**, 363 - 370, 1971

110. E. Matijevic, *Langmuir*, **2**, 12 - 20, 1986

111. C. J. Brinker, S. P. Mukherjee, *J. Mater. Sci.*, **16**, 1980 - 1988, 1981

112. S. Sakka, K. Kamiya, *J. Non-Cryst. Solids*, **42**, 403 - 422, 1980

113. B. E. Yoldas, *J. Mater. Sci.*, **14**, 1843 - 1849, 1979

114. S. Prochazka, F. J. Klug, *J. Amer. Cera. Soc.*, **66**,12, 874 - 880, 1983

115. A. Ikesue, T. Kinoshita, K. Kamata, K. Yoshida, *J. Am.Ceram. Soc.*, **78**, 1033 - 1040, 1995

116. A. Ikesue, *Opt. Mater.*, **19**, 183 - 187, 2002

117. Z. Hua, S. Yang, H. Huang, L. Lv, M. Lu, B. Gu, Y. Du, *Nanotechnology*, **17**, 20, 5106 - 5110, 2006

118. S. Ozturk, N. Tasaltin, N. Kilinc, Z. Z. Ozturk, *J. Optoelectro. Biomed. Mater.*, **1**, 1, 15 - 19, 2009

119. Y. D. Jiang, M Phil Thesis, Georgia Institute of Technology, 1999

120. E. Matijevic, W. P. Hsu, *J. Colloid Interface Sci.*, **118**, 2, 506 - 523, 1987

121. Y. X. Huang, C. J. Guo, *Powder Technology*, **72**, 101 - 104, 1992

122. A. P. Kumar, D. Depan, N. S. Tomer, R. P. Singh, *Prog. Polym. Sci.*, **34**, 6, 479 - 515, 2009

123. D. A. Boyd, L. Greengard, M. Brongersma, M. Y. El- Naggar, D. G. Goodwin, *Nano Lett.*, **6**, 11, 2592 - 2597, 2006

124. M. Kitamura, M. Nishioka, J. Oshinowo, Y. Arakawa, *Jpn. J. Appl. Phys.*, **34**, 4376 - 4379, 1995

125. F. Heinrichsdorff, A. Krost, N. Kirataedter, M. H. Mao, M. Grundmann, D. Bimberg, A. O. Kosogov, P. Werner, *Jpn. J. Appl. Phys. Part1*, **36**, 4129 - 4133, 1997

126. S. Ishida, Y. Arakawa, K. Wada, *Appl. Phys. Lett.*, **72**, 7, 800 - 802, 1998

127. K. Tachibana, T. Someya, Y. Arakawa, *Appl. Phys. Lett.*, **74**, 383 - 385, 1999

128. T. Seto, K. Okuyama, A. Hirota, *J. Aerosol. Sci.*, **26**, suppl.1, 5601, 1995

129. Y. Liu, W. Zhu, O. K. Tan, Y. Shen, *Mater. Sci. Eng.*, **B 47**, 171 - 176, 1997

130. Y. Liu, W. Zhu, O. K. Tan, X. Yao, Y. Shen, *J. Mater. Sci.: Mater. Electro.*, **7**, 279 - 282, 1996

131. M. K. Akhtar, S. E. Pratsinis, S. V. R. Mastrangelo, *J. Mater. Res.*, **9**, 1241 - 1249, 1994

132. W. Z. Zhu, M. Yan, *Mater. Chem. Phys.*, **53**, 262 - 266, 1998

133. J. P. Dekker, P. J. van der Put, H. J. Veringa, J. Schoonman, *J. Amer. Ceram. Soc.*, **80**, 3, 629 - 636, 1997

134. M. Yudasaka, R. Kikuchi, Y. Ohki, E. Ota, S. Yoshimura, *Appl. Phys. Lett.*, **70**, 1817 - 1818, 1997

135. L. C. Qin, D. Zhou, A. R. Krauss, D. M. Gruen, *Appl. Phys. Lett.*, **72**, 26, 3437 - 3439, 1998

136. G. Che, B. B. Lakshmi, C. R. Martin, E. R. Fisher, Brinda B. Lakshmi, C. R. Martin, E. R. Fisher, *Langmuir*, **15**, 3, 750 - 758, 1999

137. A. G. Sutugin, N. A. Fuchs , *J. Colloid Interface Sci.*, **27**, 216 - 228, 1968

138. R. C. Flagan, M. M. Lunden, *Mater. Sci. Eng.*, **A 204**, 113 - 124, 1995

139. R. S. Windeler, S. K. Friedlander, K. E. J. Lehtinen, *Aerosol. Sci. Tech.*, **27**, 174 - 190, 1997

140. W. Mahoney, R. P. Andres, *Mater. Sci. Eng.*, **A 204**, 1 - 2, 160 - 164, 1995

141. W. Mahoney, M. D. Kempe, R. P. Andres, *Mater. Res. Soc. Symp. Proc.*, **400**, 65p, 1996

142. R. S. Windeler, Thesis, University Of California, Los Angeles, 1995

143. H. Huang, S. Yang, G. Gu, *J. Phys. Chem. B*, **102**, 3420 - 3424, 1998

144. W. A. Saunders, P. C. Sercel, R. B. Lee, H. A. Atwater, K. J. Vahala, R.C. Flagan, E. J. E. Aparcio. *Appl. Phys. Lett.*, **63**, 1549 - 1551, 1993

145. R. P. Camata, H. A. Atwater, K. J. Vahala, R. C. Flagan, *Mat. Res. Soc. Symp. Proc.*, **405**, 259 - 264, 1996

146. S. Yatsuya, T. Kamakura, K. Yamauchi, K. Mihama, *Jpn. J. Appl. Phys.*, **2**, 25, L42, 1986

147. M. Hirasawa, H. Shirakawa, H. Hamamura, Y. Egashira, H. Komiyama, *J. Appl. Phys.*, **82**, 1404 - 1407, 1997

148. B. Wunderlich, *Macromolecular Physics*, Academic Press, New York, **2**, 1 - 35, 1976

149. E. P. Chang, R. Kirsten, E. L. Sagowski, *Polym. Eng. Sci.*, **18**, 932 - 936, 1978

150. B. Y. Shekunov, P. Taylor, J. G. Grossmann, *J. Crystal Growth*, **198-199**, 2, 1335 - 1339, 1999

151. E. Morales, J. R. White, *J. Mater. Sci.*, **23**, 3612 - 3522, 1988

152. P. D. Calvert, S. Mann, *J. Mater. Sci.*, **23**, 3801 - 3815, 1988

153. K. A. Mauritz, E. Baer, A. J. Hopfinger, *J. Polym. Sci. Polym. Phys. Macromol. Rev.*, **13**, 1 - 185, 1978

154. S. K. Peneva, J. M. Schuitz, *J. Polymer Sci. Polymer Phys.*, **25**, 185 - 193, 1987

155. J. Petermann, G. Broza, *J. Mater. Sci.*, **22**, 1108 - 1112, 1987

156. A. Lowenstam, S. Weiner, In: Biomineralization, Oxford University Press, London, 1989

157. M. A. Crenshaw, In: Biological Mineralization and Demineralization, Ed. G. H. Nancollas, Springer, Berlin, 243, 1982

158. V. Kapustianyk, M. Partyka, V. Rudyk, M. Piasecki, M. G. Brik, S. Tkaczyk, K. Ozga, K. Plucinski, S. Romanyshyn, I. V. Kityk, *J. Alloys and Compounds*, **493**, 1 - 2, 26 - 30, 2010

159. S. Radhakrishnan, J. M. Schultz, *J. Crystal Growth*, **116**, 378 - 386, 1992

160. C. Saujanya, S. Radhakrishnan, *J. Mater. Sci.*, **33**, 4, 1069 - 1074, 1998

161. S. Mishra, S. Sonawane, A. Mukherji, H. C. Mruthyunjaya, *J. Appl. Polym. Sci.*, **100**, 5, 4190 - 4196, 2006

162. M. Motomatsu., T. Takahashi, H. Y. Nie, W. H. Mizutani, H. Tokumoto, *Polymer*, **38**, 1, 177 - 182, 1997

163. J. Wen, J. E. Mark, *Rubber Chem. & Tech.*, **67**, 806 - 819, 1994

164. J. E. Mark, *Polym. Eng. Sci.*, **36**, 2905 - 2920, 1996

165. Z. Pu, J. E. Mark, J. M. Jethmalani, W. T. Ford, *polymer Bulletin*, **37**, 545 - 551, 1996

166. E. Ruckenstein, Y. Yuan, *Polymer*, **38**, 3855 - 3860, 1997

167. Y. Godovski, Thermal and Electrical Conductivity of Polymer Materials, Springer-Verlag, Heidelberg, Germany, 79 - 122, 1995

168. W. Helbert, J. Y. Cavaille, A. Dufresne, *Polym. Comp.*, **17**, 604 - 611, 1996

169. G. Siqueira, J. Bras, A. Dufresne, *Polymer*, **2**, 728 - 765, 2010

170. S. Kamel, *eXPRESS Polym. Letter.*, **1**, 9, 546 - 575, 2007

171. L. Chazeau, J. Y. Cavaille, G. R. Canova, R. Dendievel, B. Boutherin, *J. Appl. Polym. Sci.*, **71**, 1797 - 1808, 1999

172. H. L. Frisch, E. J. Mark, *Chem. Mater.*, **8**, 1735 - 1738, 1996

173. B. K. G. Theng, Formation and Properties of Clay - Polymer Complexes, Elsevier, Amsterdam, 133 - 154, 1979

174. A. Blumstein, Etude des polymerisations en couche adsorbee, Bull. Soc. Chim. France, 899 - 905, 1961

175. S. Pavlidou, C. D. Papaspyrides, *Progr.Polym. Sci.*, **33**, 12, 1119-1198, 2008

176. B. Li, W. H. Zhong, *J. Mater. Sci.*, **46**, 17, 5595 - 5614, 2011

177. E. T. Thostenson, C. Li, T. W. Chou, *Compos. Sci. Tech.*, **65**, 491 - 516, 2005

178. J. Denault, B. Labrecque, Technology Group on Polymer Nanocomposites -PNC-Tech. Industrial Materials Institute. National Research Council Canada, 75 de Mortagne Blvd. Boucherville, Quebec, J4B 6Y4, 2004

179. J. N. Hay, S. J. Shaw, Nanocomposites - Properties and Applications, abstracted from A Review of Nanocomposites, 2000

180. B. Ellis, Chemistry and Technology of Epoxy Resins. Blackie A & P, Chapamn & Hall, London p 39, 1993

181. T. Lan, T. J. Pinnavaia, *Chem. Mater.*, **6**, 2216- 2219, 1994

182. P. Kelly, A. Akelah, S. Qutubuddin, A. Moet, *J. Mater. Sci.*, **29**, 2274 - 2280, 1994

183. P. B. Messersmlth, E. P. Giannelis, *Chem. Mater.*, **6**, 1719 -1725, 1994

184. C. Zilg, R. Mulhaupt, J. Finter, *Macromol. Chem. Phys.*, **200**, 661 - 670, 1999

185. C. Zilg, PhD Thesis, Epoxid.Thermoplast.- und Polyurethan - Nanokomposite auf Basis Organophil Modifizierter Dreischichisilikate, Faculty for Chemistry and Pharmacy, Albert Ludwigs University Freiburg J. Br, 2000

186. M. A. Osman, V. Mittal, M. Morbidelli, U. W. Suter, *Macromolecules*, **37**, 19, 7250 - 7257, 2004

187. T. P. Mohan, M. R. Kumar, R. Velmurugan, *J. Mater. Sci.*, **41**, 18, 5915 - 5925, 2006

188. G. Lagaly, *Solid State Ionics*, **22**, 43 - 51, 1986

189. L. Shen, L. Wang, T. Liu, *Macromolec. Mater. Engin.*, **291**, 11, 1358 - 1366, 2006

190. I. M. Daniel, H. Miyagawa, E. E. Gdoutos, J. J. Luo, *Exper. Mech.*, **43**, 3, 348 - 354, 2003

191. L. Chang, Z. Zhang, L. Ye, K. Friedrich, *Wear*, **262**, 699 - 706, 2007

192. H. B. Hsueh, C. Y. Chen, *Polymer*, **44**, 18, 5275 - 5283, 2003

193. T. Lan, P. D. Kaviratna, T. J. Pinnavaia, *J. Phys. Chem Solids*, **57**, 1005 - 1010, 1996

194.   T. J. Pinnavaia, T. Lan, Z. Wang, H. Shi, P. D. Kaviratna, *ACS Polym. Mat. Sci. Eng. Proc.* **73**, 250 - 261, 1995

195.   G. Lubin, Handbook of Fibreglass and Advanced Plastics Composites,. Polym. Techn Ser., New York, 1969

196.   X. Kornmann, L. A. Berglund, J. Sterte, E. P.Giannelis, *Polym. Eng. Sci.,* **38**, 1351 - 1358, 1998

197.   D. J. Suh, Y. T. Limand, O. O. Park, *Polymer,* **41**, 8557 - 8563, 2000

198.   A. Okada, A. Usuki, T. Kurauchi, O. Kamigaitio, American Chemical Society, 55 - 65, 1995

199.   Y. Kojima, A. Usuki, M. Kawasumi, A. Okada, T. Kurauchi, O. Kamigaitio, K. Kaji, *J. Polym. Sci. Part B,* **33**, 1039 - 1045, 1995

200.   D. Adame, G.W. Beall, *Applied Clay Science,* **42**, 3 - 4, 545 - 552, 2009

201.   J. P. Lemmon, J. Wu, C. Oriakhi, M. M. Lerner, *Electrochimica Acta,* **40**, 2245 - 2249, 1995

202.   L. Biasci, M. Aglietto, G. Ruggeri, F. Ciardelli, *Polymer,* **35**, 3296 - 3304, 1994

203.   F. Dietsche, Y. Thomann, R. Thomann, R. Muihaupt, *J. Appl. Polym. Sci.,* **75**, 3, 396 - 405, 2000

204.   A. Moet, A. Akelah, N. Salahuddin, A. Hiltner, E. Baer, *Mat. Res. Soc. Proc.,* **351**, 163 - 170, 1994

205.   X. Huang, S. Lewis, W. J. Brittain, R. A. Vaia, *Macromolecules,* **33**, 2000 - 2004, 2000

206.   T. Srikhirin, A. Moet, J. B. Lando, *Polym. Adv. Tech.*, **9**, 491 - 503, 1998

207.   E. Ruiz - Hitzkya, A. V. Meerbeek, In; Handbook of Clay Sci., Eds. F. Bergaya, B.K.G. Theng and G. Lagaly, Developments in Clay Science, Vol. 1, Elsevier, Amsterdam, 583 - 621, 2006

208.   K. G. Fournairs, M. A. Karakassides, D. Petridis, K. Yiannakopoulou, *Chem. Mater.*, **11**, 2372 - 2381, 1999

209.   R. A. Vaia, H. Ishil, E. P. Giannelis, *Chem. Mater.*, **5**, 1694 - 1696, 1993

210.   A. Moet, A. Akelah, A. Hiltner, E. Baer, *Mater. Res. Soc. Symp. Proc.*, **351**, 91 - 96, 1994

211.   B. Hoffmann, C. Dietrich, R. Thomann, C. Friedrich, R. Mulhaupt, Macromol. *Rapid. Commun.*, **21**, 57 - 61, 2000

212.   X. Fu, S. Qutubuddin, *Polymer*, **42**, 807 - 813, 2001

213.   T. J. Pinnavaia, T. Lan, P. D. Kaviratna, M. S. Wang, *Mater. Res. Symp. Proc.*, **346**, 81 - 87, 1994

214.   K. Yano, A. Usuki, A. Okada, *J. Polym. Sci. Part A*, **35**, 2289 - 2294, 1997

215.   Y. H. Cho, J. M. Park, Y. H. Park, *Macromolecu. Res.*, **12**, 1, 38 - 45, 2004

216.   H. L. Tyan, K. H. Wei, T. E. Hsieh, *J. Polym. Sci., Part B: Polym. Phys.*, **38**, 22, 2873 - 2878, 2000

217.   J. Heineman, P. Rechert, R. Thommann, R. Mulhaupt, *Macromol. Rapid. Commun.*, **20**, 8, 423 - 430, 1999

218.   Y. Ke, C. Long, Z. Qi, *J. Appl. Polym. Sci.*, **71**, 1139 - 1146, 1999

219.   A. Usuki, M. Kato, A. Okada, T. Kurauchi, *J. Appl. Polym. Sci.*, **63**, 137 - 139, 1997

220. Q. Zhang, X-I. Gao, K. Wang, Q. Fu, *Chin. J. Polym. Sci.*, **22**, 2, 175 - 182, 2004

221. M. Kato, A. Usuki, A. Okada, *J. Appl. Polym. Sci.*, **66**, 1781 - 1785, 1997

222. N. Hasegawa, M. Kawasumi, M. Kato, A. Usuki, A. Okada, *J. Appl. Polym. Sci.*, **67**, 87 - 92, 1998

223. M. Kawasumi, N. Hasegawa, M. Kato, A. Usuki, A. Okada, *Macromolecules*, **30**, 6333 - 6338, 1997

224. P. Walter, D. Mader, P. Reichert, R. Mulhaupt, *J.Mater. Sci. Pure Appl. Chem., A* **36**, 11, 1613 - 1639, 1999

225. M. L. L. Quintanilla, S. S. Valdes, L. F. Ramos de Valle, R. G. Miranda, *Polymer Bulletin*, **57**, 3, 385 - 393, 2006

226. K. Wang, M. Choi, C. Koo, Y. Choi, I. Chung, *Polymer*, **42**, 9819 - 9826, 2001

227. C. Sanchez, B. Julian, P. Belleville, M. Popall, *J. Mater. Chem.*,**15**, 3559 - 3592, 2005

228. P. H. C. Camargo, K. G. Satyanarayana, F. Wypych, *Mat. Res.*, **12**, 1, 2009

229. K. Friedrich, S. Fakirov, Z. Zhang, Polymer Composites- From Nano- to Macro Scale, Springer, Newyork, 2005

230. M. Worzakowska, *J. Therm. Anal. Calorim.*, **105**, 987 - 994, 2011

231. H. P. Wang, Y. C. Yuan, M. Z. Rong, M. Q. Zhang, *Macromolecules*, **43**, 595 - 598, 2010

232. A. J. Jacobson, L. F. Nazar, Intercalation Chemistry, Encyclopedia of Inorganic Chemistry, John Wiley & Sons, 2006

233. R. K. Gupta, S. N. Bhattacharya, *Indian Chem. Engin.*, **50**, 3, 242 - 267, 2008

234. Z. Wang, T. J. Pinnavia, *Chem. Mater.*, **10**, 3769 - 3771, 1998

235. I. V. Khudyakov, R. D. Zopf, N. J. Turro , *Designed Monomers and Polymers*, **12**, 279 - 290, 2009

236. J. P. He, H. M. Li, X. Yu Wang, Y. Gao, *Europ. Polym. J.*, **42**, 1128 - 1134, 2006

237. J. M. Yeh, K. C. Chang, C. W. Peng, B. G. Chand, S. C. Chiou, H. H. Huang, C. Y. Lin, J. C. Yang , H. R. Lin , C. L. Chen, *Polym. Compos.*, **30**, 6, 715 - 722, 2009

238. M. Abdollahi, A. Rahmatpour, J. Aalaie, G. Khanbabae, *Iran. Polym. J.*, **17**, 7, 519 - 529, 2008

239. L. Wu, M. Wang, X. Zhang, D. Chen, A. Zhong, *Iran. Polym. J.*, **18**, 9, 703 - 712, 2009

240. V. Mittal, *Materials*, **2**, 992-1057, 2009

241. H. G. Joen, H. T. Jung, S. D. Hudson, *Polymer Bulletin*, **41**, 107 - 113, 1998

242. T. Tanaka, G. C. Montanari, R. Mulhaupt, *Dielectr. Electr. Insul., IEEETrans.*, **11**, 5, 763 - 784, 2004

243. M. Kawasumi, N. Hasegawa, A. Usuki, O. Akane, *Mater. Eng. Sci. C*, **6**, 135 - 143, 1998

244. R. A. Vaia, B. B. Sauer, O. K. Tse, E. P. Giannelis, *J. Polym. Sci. : Part B*, **35**, 59 - 67, 1997

245. D. C. Lee, L. W. Jang, *J. Appl. Polym. Sci.*, **61**, 1117 - 1122, 1996

246. D. C. Lee, L. W. Jang, *J. Appl. Polym. Sci.*, **68**, 1997 - 2005, 1998

247. M. J. Yang, J. D. Zhang, *J. Mater. Sci.*, **40**, 16, 4403 - 4405, 2005

248. R. A. Vaia, K. D. Jandt, E. J. Karmer, E. P. Giannelis, *Macromolecules*, **28**, 8080 - 8085, 1995

249. Y. Kojima, A. Usuki, M. Kawasumi, A. Okada, T. Kurauchi, O. Kamigaito, K. Kaji, *J. Polym. Sci.*, B, **32**, 625 - 630, 1994

250. L. Liu, Z. Qi, X. Zhu, *J. Appl. Polym. Sci.*, **71**, 1133 - 1138, 1999

251. J. W. Cho, D. R. Paul, *Polymer*, **42**, 1083 - 1094, 2001

252. R. A. Vaia, K. D. Jandt., E. J. Kramer, E. P. Giannelis, *Chem. Mater.*, **8**, 2628 - 2635, 1996

253. A. K. Kulshreshtha, A. K. Maiti, M. S. Choudhary, K. V. Rao, *J. Appl. Polym. Sci.*, **99**, 3, 1004 - 1009, 2006

254. P. Reichert, PhD Thesis, Faculty for Chemistry and Pharmacy, Albert Ludwigs- University., Freiburg I Br, 2000

255. R. A. Vaia, E. P. Giannelis, *Macromolecules*, **30**, 8000 - 8009, 1997

256. L. Abate, I. Blanco, F. A. Bottino, G. D. Pasquale, E. Fabbri, A. Orestano, A. Pollicino, *J. Therm. Anal. Calor.*, **91**, 3, 681 - 686, 2008

257. F. L. Beyer, N. C. B. Tan, A. Dasgupta, M. E. Galvin, *Chem. Mater.*, **14**, 2983 - 2988, 2002

258. R. A. Vaia, S. Vasudevan, W. Krawiec, L. G. Scanlon, E.P. Giannelis. *Adv. Mater.*, **7**, 154 - 156, 1995

259.   Z. Shen, G. P. Simon, Y. B. Cheng, *Polymer*, **43**, 4251 - 4260, 2002

260.   L. M. Liu, Z. N. Qi, X. G. Zhu, *J. Appl. Polym. Sci.*, **71**, 1133 - 1138, 1999

261.   D. L. Vanderhart, A. Asano, J. W. Gilman, *Chem. Mater.*, **13**, 3781 - 3795, 2001

262.   T. D. Fornes, P. J. Yoon, H. Keskkula, D. R. Paul, *Polymer*, **42**, 9929 - 9940, 2001

263.   T. D. Fornes, P. J. Yoon, D. L. Hunter, H. Keskkula, D. R. Paul, *Polymer*, **43**, 5915 - 5933, 2002

264.   N. Hasegawa, H. Okamoto, M. Kato, A. Usuki, N. Sato, *Polymer*, **44**, 2933 - 2937, 2003

265.   J. X. Li, J. Wu, C. M. Chan, *Polymer*, **41**, 6935 - 6937, 2000

266.   P. Nadege, M. Alexandre, P. Degee, C. Calberg, R. Jerome, R. Cloots, *e- Polymers*, **09**, 2001

267.   X. Zheng, C. A. Wilkie, *Polym. Degrad. Stab.*, **82**, 441 - 450, 2003

268.   M. Arroyo, M. A. L. Manchado, J. L. Valentín, J. Carretero, *Compos. Sci. Tech.*, **67**, 7 - 8, 1330 - 1339, 2007

269.   R. L. Zhang, L. Liu, Y. D. Huang, Y. R. Tang, T. C. Zhang, S. Z. Zhan, *J. Appl. Polym. Sci.*, **117**, 5, 2870 - 2876, 2010

270.   S. Benali, S. Peeterbroeck , J. Larrieu , F. Laffineur, J. J. Pireaux, M. Alexandre, P. Dubois, *J. Nanosci. Nanotechnol.*, **8**, 4, 1707 -1713, 2008

271.   P. Krishnamachari, J. Zhang, J. Lou, J. Yan, L. Uitenham, *Int. J. Polym. Anal. Char.*, **14**, 4, 336 - 350, 2009

272.   K. A. Carrado, L. W. Xu, *Chem. Mater.*, **10**, 1440 - 1445, 1998

273.   H. P. Klug, L. E. Alexander, X - Ray Diffraction Procedures for Polycrystalline and Amorphous Materials, Wiley & Sons, 1974

274.   E. W. Gacitua, A. A. Ballerini, J. Zhang, Maderas. *Ciencia y tecnología*, **7**, 3, 159 - 178, 2005

275.   M. S. Sreekala, C. Eger, Property Improvements of an Epoxy Resin by Nanosilica Particle Reinforcement, *Polymer Composites*, part 1, 91 - 105, 2005

276.   D. Shia, C. Y. Hui, S. D. Burnside, E. P Giannelis, *Polym. Comp.*, **19**, 608 - 617, 1998

277.   A. Usuki, A. Koiwai, Y. Kojima, M. Kawasumi, A.Okada, T. Kurauchi, O. Kamigatio, *J. Appl. Polym. Sci.*, **55**, 119 -123, 1995

278.   P. C. Ma, N. A. Siddiqui, G. Marom, J. K. Kim, *Composites: Part A*, **41**, 1345 - 1367, 2010

279.   C. S. Triantafillidis, P. C. Le Baron, T. J. Pinnavaia, *J. Solid State chem.*, **167**, 2, 354 - 362, 2002

280.   X. Kornmann, M. Rees, Y. Thomann, A. Necola, M. Barbezat, R. Thomann, *Comp. Sci. Tech.*, **65**, 14, 2259 - 2268, 2005

281.   J. Massam, T. J. Pinnavaia, *Mat. Res. Soc. Symp. Proc.*, **520**, 223-232, 1998

282.   Z. Wang, T. J. Pinnavaia, *Chem. Mater.*, **10**, 1820 - 1826, 1998

283. R. Kotsilkova, P. Pissis, Thermoset Nanocomposites for Engineering Applications, Ed., R. Kotsilkova, Smithers Rapra Technology, Shawbury, UK, 1 - 328, 2007

284. P. B. Messersmith, E. P. Giannelis, *J. Appl. Polym. Sci., Part A,* **33,** 1047 - 1057, 1995

285. Y. Kojima, K. Fukumori, A. Usuki, A. Okada, T. Kurauchi, *J. Mats. Sci. Letters.,* **12,** 889 - 890, 1993

286. K. Yano, A. Usuki, A. Okada, T. Kurauchi, O. Kamigaito, *J. Polym.Sci., Part A, Polym. Chem,* **31,** 2493 - 2498, 1993

287. G. W. Beall, *Antec,* **11,** 2398 - 2401, 1999

288. Y. Zhou, F. Pervin, R. K. Vijaya, *J. Mater. Process. Tech.,* **191,** 1/3, 347 - 351, 2007

289. Y. Cai, Y. Hu, S. Xuan, Y. Zhang, H. Deng, X. Gong, Z. Chen, W. Fan, *J. Mater. Sci.,* **42,** 14, 5524 - 5533, 2007

290. J. W. Gilman, *Appl. Clay. Sci.,* **15,** 31 - 49, 1999

291. A. B. Morgan, L. L. Chu, J. D. Harris, *Fire Mater.,* **29,** 213 - 229, 2005

292. N. A. Salahuddin, *Polym. Adv. Techno.,* **15,** 5, 251 - 259, 2004

293. H. Y. Yeang, *J. Rubb. Res.,* **8,** 3, 160 - 181, 2005

294. B. van Baarle, LPRI, TNO Institute of Industrial Technology, Delft, The Netherlands, *Natuurrubber,* **13,** 10 - 11, 1999

295. D. C. Blackley, Polymer Latices: Applications of latices, Eds. Chapman & Hall, John Wiley, London, Vol. 3, 34 - 37, 1997

296. C. X. Viet, H. Ismail, A. A. Rashid, T. Takeichi, V. H. Thao, *Polymer-Plastics Tech. Eng.*, **47**, 11, 1090 - 1096, 2008

297. A. I. Nakatani, W. Chen, R. G. Schmidt, G. V. Gordon, C. C. Han, *Polymer*, **42**, 3713 - 3722, 2001

298. S. Westermann, M. Kreitschmann, W. Pyckhout-Hintzen, D. Richter, E. Straube, B. Farago, G. Goerigk, *Macromolecules*, **32**, 18, 5793 - 5802, 1999

299. M. Arroyo, M. A. L. Manchado, B. Herrero, *Polymer*, **44**, 8, 2447 - 2453, 2003

300. A. Usuki, A. Tukigase, M. Kato, *Polymer*, **43**, 8, 2185 - 2189, 2002

301. C. J. T. Landry, B. K. Coltrain, J. A. Wesson, N. Zumbulyadis, J. L. Lippert, *Polymer*, **33**, 1496 - 1506, 1992

302. D. W. Mc Carthy, J. E. Mark, D. W. Schaefer, *J. Polym. Sci., Part B: Polym. Phys.*, **36**, 7, 1167 - 1189, 1998

303. L. Matejka, O. Dukh, J. Kolarik, *Polymer*, **41**, 1449 - 1459, 1999

304. D. W. Mc Carthy, J. E. Mark, S. J. Clarson, D. W. Schaefer, *J. Polym. Sci., Part B: Polym. Phys.*, **36**, 7, 1191 - 1200, 1998

305. Z. Pu, J. E. Mark, J. M. Jethmalani, W. T. Ford, *Chem. Mater.*, **9**, 2442 - 2447, 1997

306. Y. Kojima, A. Usuki, M. Kawasumi, Y. Fukushima, A. Okada, T. Kurauchi, O. Kamigato, *J. Mater. Res.*, **8**, 5, 1185 - 1189, 1993

307. R. A. Vaia, E. P. Giannelis, *Macromolecules*, **30**, 25, 7990 - 7999, 1997

308. R. Dagani, *Chem. Eng. News*, **70**, 47, 18 - 24, 1992

309. M. Z. Rong, M. Q. Zhang, Y. X. Zheng, H. M. Zeng, R. Walter, K. Friedrich, *Polymer*, **42**, 3301 - 3304, 2001

310. R. A. Vaia, J. F. Maguire, *Chem. Mater.*, **19**, 11, 2736 - 2751, 2007

311. A. Okada, Y. Fukushima, S. Inagaki, A. Usuki, S. Sugiyama, T. Kurashi, O. Kamigaitov, *U.S. patent 4739007*, 1988

312. C. Zilg, F. Dietsche, B. Hoffmann, C. Dietrich, R. Mulhaupt, In: "Eurofiller '99", Proceedings

313. C. Zilg, P. Reichert, F. Dietsche, T. Engelhardt, R. Mulhaupt, *Kunstoffe*, **88**, 1812 - 1820, 1998

314. R. Stephen, S. Thomas, K. V. S. N. Raju, S. Varghese, K. Joseph, Z. Oommen, *Rubb. Chem. Tech.*, **80**, 4, 672 - 689, 2007

315. L. Theodore, R. G. Kunz Nanotechnology: Environmental Implications and Solutions, John Wiley & Sons, Hoboken, New Jersey, 61 - 102, 2005

316. P. Uthirakumar, Ph.D Thesis, School of Chonbuk National University, Chonju, Korea, 2005

317. R. A. Vaia, G. Price, P. N. Ruth, H. T. Nguyen, J. Lichtenhan, *Appl. Clay Sci.*, **15**, 67 - 92, 1999

318. J. S. Murday, *The AMPTIAC New. Lett.*, **6**, 1, 5 - 11, Spring 2002

319. K. M. Lee, C. D. Han, *Macromolecules*, **36**, 19, 7165 - 7178, 2003

320. M. Maiti, M. Bhattacharya, A. Bhowmick, *Rubb. Chem. Tech.*, **81**, 3, 384 - 469, 2008

321. Y. Kojima, A. Usuki, M. Kawasumi, A. Okada, T. Kurauchi, O. Kamigaito, *J. Appl. Polym. Sci.*, **49**, 1259 - 264, 1993

322. E. P. Giannelis, R. Krishnamoorti, E. Manias, *Adv. Polym. Sci.,* **138**, 107 - 147, 1999

323. T. J. Pinnavaia, G. W. Beal, Polymer–Clay Nanocomposites, John Wiley & Sons, Chichester, England, 2001

324. S. Varghese, J. Karger-Kocsis, K. G. Gatos, *Polymer,* **44**, 14, 3977 - 3983, 2003

325. K. G. Nair, A. Dufresne, *Biomacromolecules,* **4**, 3, 657 - 665, 2003

326. K. G. Nair, A. Dufresne, *Biomacromolecules,* **4**, 3, 666 - 674, 2003

327. M. A. Atieh, N. Girun, E. S. Mahdi, H. Tahir, C. T. Guan, M. F. Alkhatib, *Fullerenes Nanotubes Carbon Nanostruct.,* **14**, 4, 641 - 649, 2006

328. A. P. Meera, S. Said, Y. Grohens, S. Thomas, *J. Phys. Chem. C,* **113**, 42, 17997 - 18002, 2009

329. K. Kueseng, K. I. Jacob, *Euro. Polym. J.,* **42**, 1, 220 - 227, 2006

330. M. Bhattacharya, M. Maiti, A. K. Bhowmick, *Rubb. Chem. Tech.,* **81**, 782 - 808, 2008

331. T. Zhao, Y. Xu, J. Wang, X. Fu, J. Wuhan University of Techno. Mater. Sci. Edit., **24**, 3, 387 - 392, 2009

332. P. L. Teh, Z. A. Mohd ishak, U. S. Ishiaku, J. Karger-Kocsis, *Jurnal Teknologi,* **39(A)**, 1 - 10, 2003

333. R. Rajasekar, G. Heinrich, A. Das, C. K. Das, *Res. Lett. Nanotech.,* **2009**, Article ID 405153, 5 p, 2009

334. N. Mohamad, A. Muchtar, M. J. Ghazali, H. M. Dahlan, C. H. Azhari, *Solid State Sci. Tech.*, **17**, 2, 133 - 143, 2009

335. J. Sharif, K. Z. M. Dahlan, W. M. Z. W. Yunus, *J. Nucl. Relat. Technols.*, **5**, 1, 65 - 80, 2008

336. J. Hrachova, P. Komadel, I. Chodak, *Clays and Clay Minerals*, **57**, 4, 444 - 451, 2009

337. Z. Peng, L. X. Kong, S. D. Li, Y. Chen, M. F. Huang, *Compos. Sci. Tech.*, **67**, 15-16, 3130 - 3139, 2007

338. P. L. Teh, Z. A. M. Ishak, A. S. Hashim, J. Karger-Kocsis, U. S. Ishiaku, *J. Appl. Polym. Sci.*, **100**, 2, 1083 - 1092, 2006

339. X. Wang, D. Jia, M. Chen, *Nanoelectronics Conference, 2008. INEC 2008. 2nd IEEE International*, Shanghai, 335 - 339, 2008

340. A. A. Al-Ghamdi, S. Al-Heniti, F. Salman, N. Abdel Aal, E. H. El-Mossalamy, F. El-Tantawy, *International Journal of Nanoparticles*, **2**, 1-6, 458 - 466, 2009

341. T. Pojanavaraphan, R. Magarapha, *Eur. Polym. J.*, **44**, 7, 1968 - 1977, 2008

342. M. A. Atieh, N. Nazir, F. Yusof, M. Fettouhi, C. T. Ratnam, M. Alharthi, F. A. Abu-Ilaiwi, K. Mohammed, A. Al-Amer, *Fullerenes, Nanotubes and Carbon Nanostructures*, **18**, 1, 56 - 71, 2010

343. L. Liu , Y. Luo , D. Jia , W. Fu , B. Guo, *J. Elast. Plast.*, **38**, 2, 147 - 161, 2006

344. K. M. Ardakani, Sh. S. Ardakani, *Dig. J. Nanomater. Bios.*, **5**, 2, 307 - 316, 2010

345. A. Jacob, P. Kurian, A. S. Aprem, *J. Appli. Polym. Sci.*, **108**, 4, 2623 - 2629, 2008

346. G. C. Psarras, K. G. Gatos, P. K. Karahaliou, S. N. Georga, C. A. Krontiras, J. Karger-Kocsis, *eXPRESS Polymer Letters*, **1**, 12, 837 - 845, 2007

347. E. Abraham, B. Deepa, L. A. Pothan, T. Sabu, 2nd International IUPAC Conference on Green Chemistry, Russia, 14 - 19 September 2008

348. R. Tantatherdtam, K. Sriroth, *Kasetsart J. Nat. Sci.* **41**, 279 - 285, 2007

349. A. K. Anand, S. T. Jose, R. Alex, R. Joseph, *Int. J. Polym. Mater.*, **59**, 33 - 44, 2010

350. W. C. Goh, Preparation and Characterization of Polypropylene-Natural Rubber/ Clay Nanocomposites. Masters Thesis, Universiti Putra Malaysia, 2007

351. J. Sharif, W. M. W. Yunus, K. H. Dahlan, M. H. Ahmad, *J. Appl. Polym. Sci.*, **100**, 1, 353 - 362, 2006

352. H. Anuar, W. N. W. Busu, S. H. Ahmad, R. Rasid, *J. Comp. Mat.*, **42**, 11, 1075 - 1087, 2008

353. S. Chuayjuljit, B. Nonthaboonlert, S. Limpanart, *Polym. Comp.*, **16**, 4, 277 - 282, 2008

354. K. Pal, R. Rajasekar, S. K. Pal, J. K. Kim, C. K. Das, *J. Nanosci. Nanotech.*, **10**, 5, 3022 - 3033, 2010

355. A. Rahmatpour, M. Abdollahi, M. Shojaee, *J. Macromol. Sci., Part B*, **47**, 3, 523 - 531, 2008

356. M. M. M. Milad, Hj. A. Sahrim, S. Y. Yahya, A.T. Mou'ad, Nanosci. Nanotech: Internat.Confer.Nanosci. and Nanotech.-2008. *AIP Confer. Proc.*, **1136**, 46 - 50, 2009

357. P. Zhang, G. Huang, Z. Liu, *J. Appl. Polym. Sci.*, **111**, 2, 673 - 679, 2009

358. E. M. Linares, M. M. Rippel, F. Galembeck, *ACS Appl. Mater. Interfaces*, **2**, 12, 3648 - 3653, 2010

359. S. Varghese, K. G. Gatos, A. A. Apostolov, J. Karger-Kocsis, *J. Appl. Polym. Sci.*, **92**, 543 - 551, 2004

360. G. Markovic, S. S. Jovanovic, V. Jovanovic, M. M. Cincovic, *J. Therm. Analy. Calori.*, **100**, 3, 881 - 888, 2010

361. M. M. Kooshki, A. J. Arani, *e-Polymers*, **132**, 2009

362. V. Kumar, B. Gupta, P. K. Sharma, R. Mosurkal, V. S. Parmar, J. Kumar, L. A. Samuelson, A. C. Watterson, *J. Macromol. Sci., Part A*, **46**, 12, 1199 - 1204, 2009

363. J. Ren, J. Wang, H. Wang, J. Zhang, S. Yang, *J. Macromol. Sci., Part B*, **48**, 6, 1069 - 1080, 2009

Experimental

The materials and methods used for the present study are discussed in this chapter. It gives a detailed description of the formulations used for the preparation of latex film vulcanizates. It also deals with different characterization techniques used for evaluating the properties such as mechanical, dynamic mechanical, rheological, gas barrier, solvent diffusion and different types of degradation resistance. Experimental methods involved in the evaluation of a catheter prepared using the latex compound with nanomaterial is also discussed here.

2.1 Centrifuged natural rubber latex

High Ammonia (HA) centrifuged natural rubber latex conforming to BIS-5430-1981 was used for the production of prevulcanized latex [1]. The characteristic tests were carried out with test methods as shown in Table 2.1.

Table 2.1 - IS specification numbers for latex tests

Test	Test method
Dry rubber content	IS 3708 (part1); 1985
Coagulum content	IS 9316 (part3); 1987
Sludge content	IS 3708 (part 2); 1985
Alkalinity as ammonia	IS 3708 (part4); 1985
Potassium hydroxide number	IS3708 (part5); 1985
Mechanical stability time	IS 3708 (part-6); 1985
Volatile fatty acid number	IS 3708 (part-7); 1986
Copper content	IS 9316 (part-8); 1987
Manganese content	IS 9316 (part-9); 1987
Total solids content	IS 9316 (part4); 1988

A test method for non-rubber solids was also conducted, by taking the difference between total solids content and dry rubber content.

2.2 Neoprene latex

It was supplied by Polymer Latices, Germany.

2.3 Compounding ingredients

2.3.1 Sulphur (Rhombic type)

Industrial grade manufactured by Emerk Ltd., Bombay was used in this study. Yellow crystals stable at room temperature has a specific gravity of 2.06.

2.3.2 Zinc diethyldithiocarbomate (ZDC)

An ultra accelerator manufactured by R.T. Vanderbuilt Company Inc, USA is a white powder having specific gravity 1.24 and its melting range is 104-108°C. It is soluble in CS_2, benzene, chloroform and insoluble in water [2].

2.3.3 Zinc oxide

Laboratory grade manufactured by Emerk Ltd., Bombay was used in this work. It is a coarse white powder having specific gravity 5.47 [3].

2.3.4 Dispersol F

It is a dispersing agent manufactured by ICI Ltd., Calcutta, and its chemical name is sodium naphthalene formaldehyde sulphonate, also known as sodium methylene *bis*-(naphthalene sulphonate) [3].

2.3.5 Fillers

2.3.5.1 English Indian clay

English Indian clay was collected from M/s. English Indian Clays Ltd., Thiruvananthapuram, Kerala. The composition of the clay is given in Table 2.2

Table 2.2 - Composition of the English Indian clay

English Indian Clay	Contents, mass per cent
SiO_2	45
Al_2O_3	38
Fe_2O_3 (max)	0.5
TiO_2	0.55
CaO (max)	0.06
MgO (max)	0.07
Na_2O (max)	0.25
K_2O (max)	0.10
Loss of Ignition	15.47

2.3.5.2 Sodium bentonite

Sodium bentonite (EXM 757) of Sud Chemie, Germany is a purified natural layered silicate. The details are given in Table 2.3.

Table 2.3 - Details of the bentonite clay

Trade name	Chemical name	Chemical formula	Ion exchange capacity, meq/100g	Layer distance, nm
EXM 757	Sodium bentonite	$(Al_{3.2} Mg_{0.8})$ $Si_8O_{20} (OH)_4 Na_{0.8}$	80	1.24

2.3.5.3 Sodium fluorohectorite

Sodium fluorohectorite (Somasif ME-100) of Coop Chemicals, Japan is a synthetic layered clay. Details are furnished in Table 2.4.

Table 2. 4 Details of fluorohectorite

Trade name	Chemical name	Chemical formula	Ion exchange capacity, meq/100g	Layer distance, nm
Somasif ME - 100	Sodium fluorohectorite	$(Mg_{5.2} Li_{0.8}) (Si_8)O_{20}$ $(OH)_{4-x} (F)_x Na_{0.8}$	100	0.94

2.4 Preparation of dispersions

50 per cent dispersion of sulphur, zinc oxide, and zinc diethyl dithio carbomate were prepared using a ball mill with dispersol F (sodium methylene *bis*-(naphthalene sulphonate) as the dispersing agent. The recipes used for making dispersions are given in Table 2.5.

A. 50% Chemical Dispersion

Table 2.5 - Recipes for dispersions

Ingredients	Parts by Weight
Chemical (S/ ZDC/ ZnO)	100
Dispersol F	3
Water	97
Ball milled 48-72h	

B. Layered silicate dispersion (10%)

Aqueous dispersions of layered silicates were prepared as 10 per cent solutions using a mechanical stirrer at an rpm of 1200 for 24 h.

2.5 Prevulcanization of latex

For prevulcanization, the concentrated, high ammonia (1per cent) latex having 60 per cent dry rubber content was mixed with the ingredients as listed in Table 2.6 under slow stirring at 55°C for 4h in a circulating water bath. Loss of ammonia was compensated by adding freshly prepared 1 per cent ammonia solution. The prevulcanized latex thus obtained was cooled to room temperature and kept in sealed plastic containers.

Table 2.6 - Formulation of sulphur prevulcanized NR latex compound

Ingredients	Dry	Wet
60% Natural rubber latex	100	167
10% Potassium hydroxide	0.25	2.5
10% Potassium oleate	0.16	1.6
50% Sulphur dispersion	1.25	2.5
50% Zinc diethyl dithiocarbamate dispersion	0.8	1.6
50% ZnO dispersion	0.25	0.5

2.6 Chloroform test

This is probably the most widely used procedure for determining the crosslink density of vulcanized latex. A sample of the latex is coagulated by mixing with an equal volume of chloroform. After two to three minutes the coagulum is examined and graded. The grading is defined in Table 2.7

Table 2.7 - Grading as per chloroform test

Chloroform number	Nature of coagulum
Number1	The coagulum is a tacky mass and break in a stringy manner when stretched
Number 2	The coagulum is a weak lump which breaks short when stretched
Number 3	The coagulum is in the form of non- tacky agglomerates
Number 4	The coagulum is in the form of small dry crumbs

2.7 Brookfield viscosity (ASTM D 2526-229)

Brookfield viscometer (LVT Model) supplied by Brookfield Engineering Laboratories, Inc, Strongton, MA 02072, USA was used in this study.

It consists of a rotating cylinder driven by a synchronous motor through a beryllium-copper torque spring. The viscous drag on the cylinder cause an angular deflection of the torque spring which is proportional to the viscosity of the fluid in which the disk is rotating. The torque and therefore, the viscosity are indicated by means of a pointer and scale. The pointer is attached to the cylinder spindle and the scale of the drive spindle above the spring so that both pointer and scale rotate.

To measure the viscosity of the compound, 200ml latex compound was taken and placed it below the viscometer by fitting the spindle No. 2 in correct

position and placed it such a position as to dip in the compound up to the cut mark of the spindle. Then allowed the spindle to rotate at a particular speed (60 rpm) to obtain a reading. The pointer and scale are clamped tighter and the reading is noted and it is multiplied by a factor 5 and the result is expressed in cPs (mPa.s).

2.8 Mechanical stability apparatus

Mechanical stability of latex means the ability of latex to withstand the colloidal destabiliative effects of mechanical origin such as shearing and agitation. This was determined by the mechanical stability apparatus supplied by Birmingham, England. 80 grams latex or compound of 55 per cent total solid content, after reaching 35°C was subjected to mechanical agitation using the MST tester at 14000 rpm. The time elapses before gross colloidal destabilization appearance was denoted as MST in seconds.

2.9 pH meter

Digital pH meter 335 supplied by M/s Systronics, India was used to measure the pH of the latex compound.

2.10 Rheology measurements

The rheological measurements were carried out using a viscometer, Haake-VT 550, Germany (Figure 2.1). This instrument has provisions for measuring shear values continuously at different rotational speeds from 0.5 to 800 min (rpm). The machine consists of a steel cup attached to a temperature-controlled system, a cylindrical sensor and a rotor, and can be rotated at preset speed. In the experiment, 9ml of latex nanocomposite was pippetted out into

the gap between the cup and the sensor system. The temperature was set at a desired value in the range 25 to 45°C and the speed of rotation varied to get shear rates in the range 1-200 s^{-1}. The apparent viscosity (mPa.s), shear rate (s^{-1}) and shear stress (Pa) can be read directly from the machine.
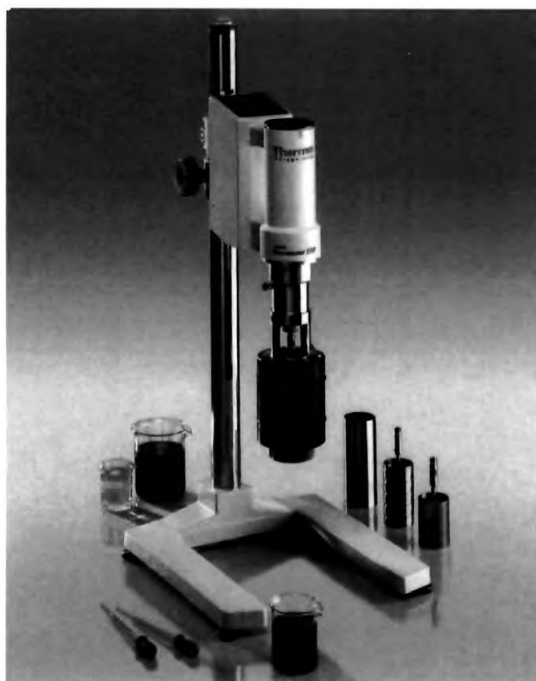
Figure 2.1 Haake viscometer

2.11 Preparation of the vulcanizate

2.11.1 Film casting

The prevulcanized latex was mixed with aqueous dispersion of silicates at different loading, after removing the dirt and coarse particles by filtering through a sieve (opening: 250 micron). It is then casted on side-raised glass plates having dimensions 13cm x l0cm x 2mm. The casting was allowed to

dry at room temperature till transparent and post-vulcanized at 70°C for 2h in an air-circulated oven. The vulcanized samples thus obtained were kept in a desiccator for mechanical testing.

2.11.2 Dipping process
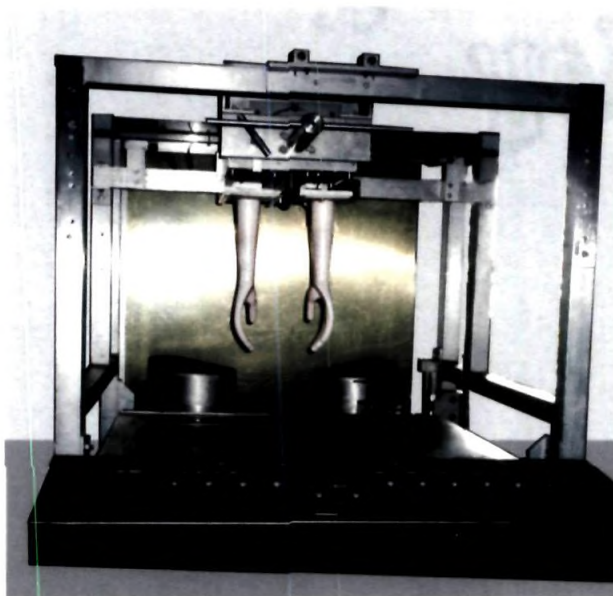
Figure 2.2 Laboratory model dipping equipment

Laboratory model dipping equipment supplied by Diptech (Stroud, UK) was used for dipping studies (Figure 2.2). The machine has a dipping unit of 430 mm depth. The dipping unit has two tanks, one for the latex and the other for the coagulant. Dipping can be performed either manually or automatically where the speed of immersion as well as withdrawal can be controlled. For the dipping studies, films were prepared using glass formers. Calcium nitrate and formic acid were used as coagulants. The dipped films were dried at room temperature till transparent and vulcanized at 70°C for 2h in an air-circulated

oven. A digital micrometer supplied by Cadar Electronics (Sheffield, UK) was used for measuring the thickness of latex films.

2.12 Dynamic mechanical thermal analysis

The dynamic mechanical thermal analysis (DMTA) spectra were recorded on rectangular casted specimens (6cm x 1cm x 0.25mm) in tensile mode at a frequency of 10Hz using an Eplexor 150N device, Gabo Qualimeter, Germany. DMTA spectra, *viz.* storage modulus (E′) and mechanical loss factor (tanδ) were measured in the temperature range ⁻120 to 100°C at a heating rate of 2°C min⁻¹.

2.13 Mechanical properties

The tensile properties of the nanocomposites and the control compounds at different loadings were tested using dumbbell shaped specimens according to the ASTM D-412 on a Zwick 1485 universal testing machine at a crosshead speed of 500 mm per minute. The tear strength, stress relaxation, tension set were also performed on the same machine. The stress relaxation was carried out on samples elongated to 500 per cent at a strain rate of 25 mm min⁻¹. All mechanical tests were carried out at ambient temperature (28°C). Force and elongation are continuously monitored by the electronic circuit. As soon as the test specimens break, test results are displayed and printed as a table using the following formula. The tensile curves obtained were analyzed for strain at break and modulus.

$$\text{Tensile strength} = \frac{\text{Load (N)}}{\text{Area of cross section (mm}^2\text{)}} \quad \dots\dots\dots\dots \quad 1$$

The tear strength of the samples were carried out according to ASTM D-624-2000 using an unnicked 90° angle test piece at a cross head speed of 500mm per min at 25°C.

$$\text{Tear strength} = \frac{\text{Load (N)}}{\text{Thickness (mm)}} \quad \dots\dots\dots\dots 2$$

2.14 Equilibrium swelling and crosslink density

For swelling studies, circular specimens of 1.98 cm diameter were punched using a sharp edged circular die. The quantity of solvent absorbed was expressed as weight in grams of solvent absorbed per gram of the composite (swell index). Volume fraction of rubber (V_r) was calculated using the Ellis and Welding equation [4].

$$V_r = \frac{(D-FT)\,\rho_r^{-1}}{(D-FT)\,\rho_r^{-1} + A_0\,\rho_s^{-1}} \quad \dots\dots\dots\dots 3$$

Where D is the deswollen weight, F is the weight fraction of the filler, A_0 is the solvent absorbed, T is the sample weight, ρ_r - specific gravity of rubber (0.92), ρ_s - specific gravity of solvent (0.86) [5].

The crosslink density (v) of those samples were also calculated from the stress-strain curves using the equation,

$$v = \frac{F}{2A_0\,R\,Tp(\alpha - 1/\alpha^2)} \quad \dots\dots\dots\dots 4$$

F is the maximum load, A_0 is the area of cross section of the tensile specimen, p is the density, R is the universal gas constant, T is the absolute temperature, α is the extension ratio. The equilibrium swelling of a vulcanized rubber in a solvent is dependent on the density of crosslinks, the nature of the solvent, and the rubber. With a given rubber-solvent system, therefore, the equilibrium swelling value becomes a measure of the crosslink density of the vulcanization.

Equilibrium swelling values are determined by immersing a thin film of the rubber in the solvent, usually toluene, and measuring the increase in weight, or the linear dimensions, at equilibrium.

Equilibrium swelling ratios are usually calculated in the following manner:

$$\text{Weight swelling index, } Q = \frac{W_2 - W_1}{W_1} \qquad \text{.................... 5}$$

Where W_1 = Initial weight and W_2 = swollen weight

The variation of 'Q' with crosslink density, for conventionally-cured natural rubber in toluene, may be broadly described as follows:

Unvulcanized rubber,	Q = >15
Lightly vulcanized,	Q = 7-15
Moderately vulcanized,	Q = 5-7
Fully vulcanized,	Q = < 5

Advantages of the swelling test are the results are directly related to crosslink density and are also quite reproducible.

2.15 Gas permeation analysis

Permeabilities of pure gases like N_2 and O_2 through filled and unfilled latex films were carried out using ATS FAAR gas permeability tester in accordance with ASTM D 1434-2003. Circular samples (about 9 cm diameter) were used for the analysis. Permeability was calculated using the equation,

$$P= p.d \qquad\qquad\qquad .... 6$$

where, d is the thickness of the sample and p is the permeance obtained from the equation,

$$p= \frac{g(h)}{(t-t_0)} \qquad\qquad .... 7$$

where, t is the time and g(h) is the gas transmission rate.

2.16 Characterization of polymer- layered silicate nanocomposites

There are mainly two methods to characterize the nanostructure of polymer- layered silicate nanocomposites. The most straight forward route is X- ray diffraction (XRD) because it is a simple way to evaluate the spacing between the silicate layers. The sample preparation is relatively easy and the X- ray analysis can be performed within a short time. However, one needs to be very careful with the interpretation of the results. Lack of sensitivity of the analysis and limits of the equipment can lead to misleading conclusions about the nanocomposites structure. The lack of peak at low angle is not a definite proof of nanocommposite structure. Therefore, transmission electron

microscopy (TEM) is a necessary complement to X-ray diffraction. TEM gives a direct measure of the spatial distribution of silicate layers but requires substantial skills in specimen preparation and analysis. Concerning the determination of the microstructure of polymer layered silicate nanocomposites; scanning electron microscopy (SEM) is the most appropriate method.

Nanocomposites have also been characterized by differential thermal analyses such as dyanamic mechanical thermal analysis (DMTA) differential scanning calorimetry (DSC) or thermogravimetric analysis (TGA)

2.16.1 Structural characterization

2.16.1.1 X-ray diffraction

The X-ray diffractometry (XRD), was used to determine the inter-spatial distance between the clay platelets. X-ray diffractograms were obtained by a D500 diffractometer (Siemens, Munchen, Germany) using Ni-filtered Cu-K$_\alpha$ radiation (λ = 0.1542 nm). The samples were scanned in step mode at a scan rate of 1.5°/min in the range 2θ< 12°.

2.16.1.2 Transmission electron microscopy

Transmission electron microscopic (TEM) studies were carried out with a LEO 912 Omega transmission electron microscope (Carl Zeiss, Oberkochen, Germany) with an acceleration voltage of 120 keV. The specimens were prepared using an Ultracut E ultramicrotome (Leica Microsystems, Wetzlar, Germany) equipped with a cryochamber. Thin sections of about 100 nm were cut with a diamond knife at -120°C.

Transmission electron microscopy (TEM) is a microscopy technique whereby a beam of electrons is transmitted through an ultra thin specimen, interacting with the specimen as it passes through it. An image is formed from the electrons transmitted through the specimen, magnified and focused by an objective lens and appears on an imaging screen, a fluorescent screen in most TEMs, plus a monitor, or on a layer of photographic film, or to be detected by a sensor such as a CCD camera. The first TEM was built by Max Knoll and Ernst Ruska in 1931, with this group developing the first TEM with resolving power greater than that of light in 1933 and the first commercial TEM in 1939.

Modern TEMs are often equipped with specimen holders that allow the user to tilt the specimen to a range of angles in order to obtain specific diffraction conditions, and apertures placed above the specimen allow the user to select electrons that would otherwise be diffracted in a particular direction from entering the specimen.

A transmission electron microscope can be divided into three components, the illumination system, the objective lens and state, and the imaging system (see Figure 2.3) [6].

The illumination system comprises the gun (1), which produces the electrons and the condenser lenses (2) equipped with a diaphragm (3), which provides the beam onto the specimen (4). The lenses use an electromagnetic field to focus the beam. The electrons are scattered as they pass through the specimen. Then, they are transferred to the objective lens, which is the heart of the TEM. The first image of the specimen is formed by the objective

lens (5). The objective aperture (6) controls the spread of the electron beam and gives contrast to the image. The imaging system uses several lenses (intermediate lens (7) and projector (8) to magnify the image and focus it on the viewing screen (9) where the operator can observe the magnified image of the specimen.
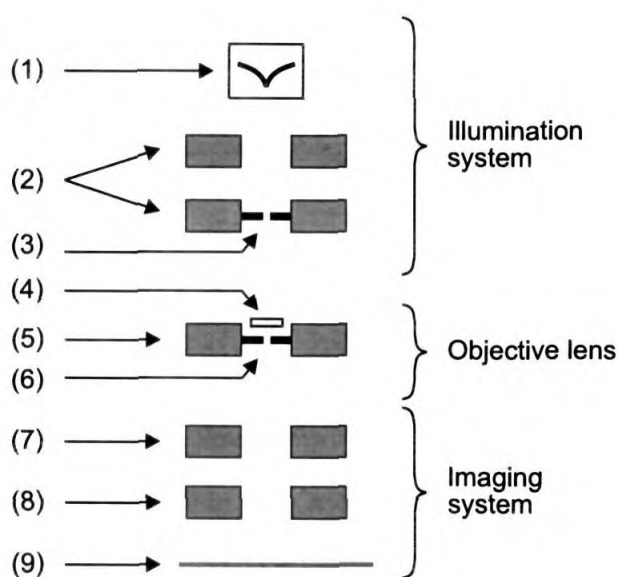
Figure 2. 3 Schematic description of a transmission electron microscope (bright field imaging).

2.16.1.2.1 Specimen preparation

Specimen preparation constitutes a major difficulty in transmission electron microscopy analysis. TEM specimens need to be sufficiently thin in order to optimize the so- called mass - thickness contrast. It means that their thickness should be in order of 100 nm or less. One way to prepare TEM specimen from polymer samples is ultramicrotomy (see Figure 2. 4)
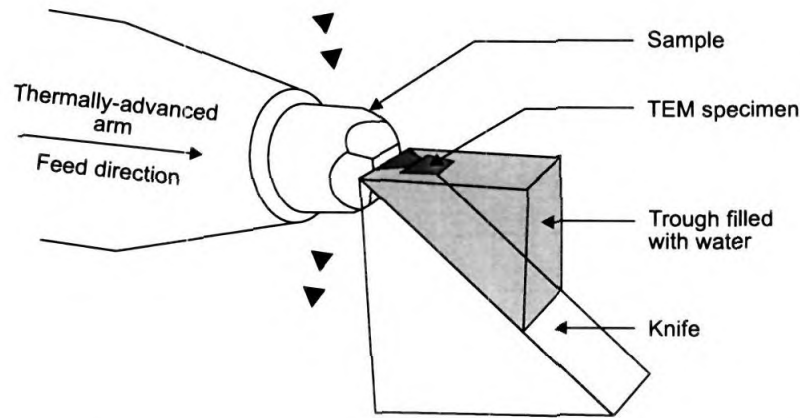
Figure 2.4 Ultramicrotomy: the sample is moved across a knife - edge (of glass or diamond). The ultrathin flakes (10-100 nm thick) float off onto water, from where they are collected on grids.

A thermally advanced   arm moves the sample block vertically (mesa about 1x1 mm^2) past a knife, which can either be of glass or diamond. The ultrathin specimens, floating on the water surface are collected on grids and dried at room temperature. The grids are then transferred directly to the TEM column for observation of the specimen. Due to the energy transferred to the organic specimen, the intensity of the electron beam should be minimized in order to prevent degradation of the sample [7].

2.16.1.3 Scanning electron microscopy (SEM)

For SEM studies the samples were cryogenically fractured and the morphology was analyzed with a Philips XL-30 scanning electron microscope (North Billerica, Massachusetts, USA).

Scanning electron micrographs of nanocomposites and conventionally filled composites were taken using backscattered imaging. This means that backscattered electrons were collected by the detector to form the image. Contrary to micrographs taken by TEM the areas of high density appear in bright. Therefore, the bright spots correspond to region rich of layered silicates.

2.17 Degradation studies

Degradation studies were performed with the following equipment.

2.17.1 UV-irradiation chamber

The exposure of UV radiation was conducted using a UV chamber PHILIPS TLD 30W, Holland. The UV source used was of two 15W capacity fluorescent tubes. One fitted at the top and the other at the bottom of the chamber in a face to face manner. A plane glass sheet of area 2580 cm^2 fitted inside the middle of the chamber holds the dumb-bell shaped tensile test samples for irradiation. Both the sides of the samples were simultaneously exposed to UV- radiation.

2.17.2 Gamma chamber

Dumbbell shaped tensile test samples were irradiated with γ-rays from a ^{60}Co source in a gamma chamber model 5000 supplied by Board of Radiation and Isotope Technology, Bhabha Atomic Research Centre, Mumbai. The size of the unit is 125cm x 106.5 cm x 150 cm. The samples were irradiated for different radiation doses at a dose rate of 2.82 kGy/h, in the atmospheric conditions.

2.17.3 Ozone test chamber

Ozone test chamber used was manufactured by MAST Development Company, USA. The chamber provides an atmosphere with controlled concentration of ozone and ambient temperature. Ozone concentrations used were 50 and 100 pphm for 24 h, which is generated by a UV- quartz lamp. Dumb-bell shaped tensile test samples were placed in an ozone test chamber. The percentage retention of tensile properties after the exposure of ozone was calculated.

2.17.4 Ageing oven

Ageing studies were conducted with dumbbell shaped tensile test samples at 100°C for 22h in an air circulated oven.

2.17.5 Autoclave

Latex articles for medical purposes often need sterilization before subsequent uses. During this process, high pressure and the elevated temperature cause degradation of rubber films. Here the test specimen was sterilized at 115 to 120°C in steam under a pressure of 1 kgf/cm^2 for 20 minutes in the autoclave and the process was repeated five times with 20 minutes interval between the successive sterilizations [8].

2.17.6 Chlorination

Chlorination is a usual procedure for removing the extractable protein from natural rubber latex products, especially surgical gloves and catheters.

Chlorination causes degradation of mechanical properties [9]. Chlorination was done in a closed vessel with 0.3 per cent chlorine solution. After chlorination the product was washed thoroughly in dilute ammonia solution (1 per cent) and dried at 50°C. The tensile properties of the films were measured thereafter.

2.17.7 Swelling studies

Common solvents encountered with latex products during their service life are water and organic solvents. Hence the effect of two solvents namely water and toluene on tensile properties were noted. The procedure for swelling studies is described in section 2.14.

2.18 Fourier infrared spectroscopy

In order to get a deeper insight of the possible interaction between layered silicates and rubber, Fourier transform infrared spectroscopic (FTIR) measurements were conducted in the ATR (attenuated total reflection) mode. FT-IR spectra of thin films were recorded using a Fourier transform infrared (FTIR) spectrophotometer (Nicolet, Model 410, USA) using attenuated total reflection. Pure layered silicates were mixed and pressed with KBr pellets for FTIR measurements.

2.19 Thermal characterization

2.19.1 Thermogravimetric analysis

Thermogravimetry is a technique in which the mass of the material under investigation is continuously followed as a function of temperature

or time as it is heated or cooled at a predetermined rate. This technique is used for examining the degradation behavior of the composites. The thermal degradation of the nanocomposites was studied using a TGA-50 Shimadzu instrument (Japan). TGA measurements were carried out on 5-10 mg samples at a heating rate of 10°C min⁻¹ in nitrogen atmosphere under a constant flow rate of 20 mL min⁻¹. The samples were placed in the platinum sample pan and heated from 30 to 700°C. The degradation temperature and the activation energy for degradation were computed. Figure 2.5 presents a schematic description of a thermo-balance used to carry out thermogravimetric measurements.
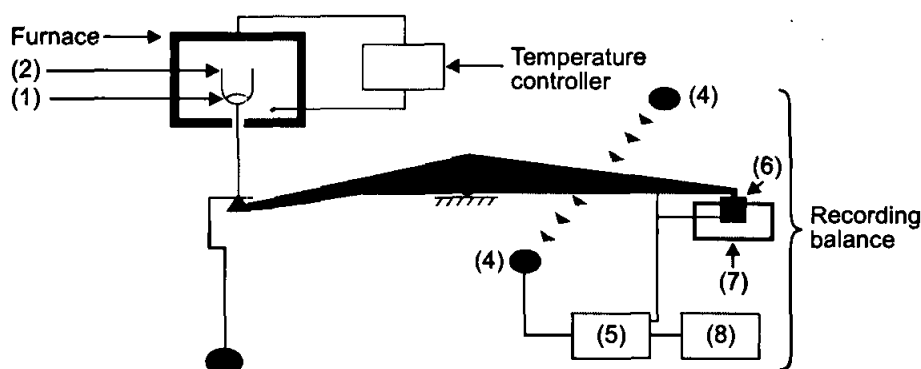
Figure 2. 5 Schematic description of a thermo-balance [10]

It is constituted of a recording balance, a furnace and a temperature controller. The sample (1) (typically few mg) is placed in a crucible (2) inside the furnace. A change in sample mass causes a deflection of the beam (3), which interposes a light shutter between a lamp and one of two photodiodes (4). The resulting imbalance in the photodiode is amplified (5) and fed into a coil (6) which is situated between the poles of a permanent magnet (7). The magnetic field

generated by the current in the coil restores the beam to its original position. The amplified photodiode current is monitored and transformed into mass or mass loss information by the data acquisition system (8). Analyses can be performed under different types of atmosphere and at temperature up to 1000°C and at a heating rate up to 20°C/min. It should be noted that the sample size and shape have an influence on the thermo gravimetric curve also called thermogram.

TGA was used to determine the quality or organic ions exchanged between silicate layers. Indeed, knowing the mass loss of the organic silicate after pyrolysis and the molecular weight of the organic ions, TGA allows a fast determination of the quantity of organic ions retained between the silicate layers. It is also commonly used to evaluate the thermal stability of organic species.

2.20 Protein estimation

A colorimetric test method is used for the determination of protein levels in NR and its products. This test method involves the extraction of soluble proteins from NR followed by precipitation to remove the interfering substances. The protein content was then determined by the Lowry method of protein analysis ASTM D 5712-2005 [11]. Spectrometric measurement was performed at a wavelength of 750 nm, using a UV-visible spectrophotometer, UV-1601 PC of Shimadzu Corporation, Japan.

2.21 Bio-burden test

Bio-burden test was conducted in the pathology lab of Rubber Research Institute of India. This test is to determine the pre-sterilization microbial load on medical products. Bio-burden test samples must be refrigerated on collection and tested within 24h of sampling. Sterilized equipment was used for the test

and it should be used before 48h after autoclaving. The testing was conducted in the laminar flow cabinet. A negative control for each test session was included. Incubated plates were kept at 30 to 35°C for 48h and examined and counted the number of colonies present.

2.22 Development of latex Foley catheter

Since the latex Foley catheter is a medical product, the chemicals and other materials used are of high purity and devoid of toxic materials.

A latex compound as per the requirement of the latex Foley catheter was prepared. Latex thread used for channel production was of count - 30, modulus 1.5 MPa, tensile strength- 20 MPa and having an elongation at break of 700 per cent. Coagulant used was 25 per cent Ca $(NO_3)_2$. The protein content of the catheter was then determined by the Lowry method of protein analysis ASTM D 5712-2005 and powder content as per ASTM D 6124. The properties of the latex nanocomposite were compared with a commercial compound and fine- tuning was done accordingly.

2.22.1 Development of compound formulation

2.22.1.1 Double centrifuged natural rubber latex

Table 2.8 Specification of double centrifuged natural rubber latex

Characteristics	Double centrifuged (BIS 11001-1984)
1. Dry rubber content, per cent by mass, min.	60
2. Non rubber solids, per cent by mass, max.	0.8

3. Sludge content, per cent by mass, max.	0.01
4. Ammonia content, per cent by mass, min	0.70
5. KOH number, max.	0.50
6. Mechanical stability time, seconds, min.	650
7. Volatile fatty acid content, max.	0.05
8. Coagulam content, percent by mass, max.	0.01
9. Copper, ppm. max.	5.0
10. Iron, ppm, max.	8.0
11.Manganese, max.	8.0

2.22.1.2 Other chemicals

Table 2.9 Properties of chemicals used

1. Caustic potash - Analar grade	
2. Sulphur powder conforming to BIS 8851 – 1978	
1. Assy,per cent mass, (min)	- 99
2. Colour	- Bright, whitish yellow
3. Ash, per cent mass, (max.)	- 0.25
4. Sulphuric acid, per cent mass, (max.)	- 0.03
5. Chloride, per cent mass (max.)	- 0.0012
6. Selinium, per cent mass (max.)	- 0.0002
7. Tellurim, per cent mass (max.)	- 0.0002
8. Arsenic, ppm (max.)	- 0.25

3. ZDC (Zinc diethyl dithio carbamate) conforming to BIS 13978 – 1994

1. Assy, per cent by mass (uncoated)	- 97
2. Assy, per cent by mass (surface coated)	- 95
3. Melting point, °C	- 175
4. Residue on 150 micron sieve, (max.)	- 0.5
5. Loss on drying for 2 h at 150°C, per cent mass (max.)	- 1.5
6. Copper ppm, (max.)	- 20
7. Manganese ppm, (max.)	- 20

4. Zinc oxide: White seal conforming to BIS 3399 – 1973

1. Assy per cent mass, (max.)	- 99
2. Relative density	- 5.5 to 5.65
3. Matter soluble in water, per cent mass (max.)	- 0.9
4. Moisture content, per cent mass (max.)	- 0.5

5. Antioxident 2246, 2,2 methylene - bis (4 methyl - 6 - tertiary butyl phenol)

1. Appearance	- Creamy white powder
2. Specific gravity	- 1.08
3. Melting point, °C	- 125 – 130
4. Solubility	- Soluble in acetone and aliphatic solvents

6. Layered silicates

1. Chemical name	- Na- bentonite
2. Trade name	- EXM 757
3. Ion exchange capacity, meq./100g	- 80
4. Layer distance, nm	- 1.24

7. Calcium nitrate which conforms to BIS 0821 – 1984

1. Purity, per cent	- 98
2. Chloride, ppm	- 10
3. Sulphate, ppm	- 10
4. Iron, ppm	- 7
5. Heavy metals, ppm	- 5
6. Calcium, per cent	- 16.6
7. NH_4, ppm	- 30

2.23 References

1. Specification for Centrifuged Natural Rubber Latex, HA type, BIS 5430 - 1981

2. D. C. Blackely, Polymer Latices, Volume 3, Eds. Chapman & Hall, John Wiley, London, 34 - 99, 1997

3. Girraj Mal, Dictionary of Rubber Chemicals, Modi Rubber, Modipuam, Meerat, India, 1983

4. K. C. Choi, E. K. Lee, S. Y. Choi, *Korean J. Chem. Eng.*, **26**,1, 295 - 299, 2009

5. M. Jacob, S. Thomas, K. T. Varughese, *Compos. Sci. Tech.*, **64**, 7 - 8, 955 - 965, 2004

6. D. B. Williams, C. B. Carier, Transmission Electron Microscopy, Plenum Press, New York, 1996

7. P. J. Goodhew, F. J. Humphreys, Electron Microscopy and Analysis, 2nd Edn, Taylor and Francis, NewYork, 1996

8.   Specification for the testing of surgical gloves as per BIS 4148 - 1989

9.   O. Vandenplas, *Eur. Respir. J.*, **8**, 1957 - 1965, 1995

10.   D. A. Skoog, F. J. Holler, T. A. Nieman, Principles of Instrumental Analysis 5th Edn., Saunders College Publishing, Philadelphia, 698 - 801, 1998

11.   Standard Test Method for Analysis of Aqueous Extractable Protein Content in Natural Rubber and its Products Using the Modified Lowry Method, ASTM D5712 - 05e1, 2005

Sulphur Prevulcanized Natural Rubber Latex-Based Nanocomposites with Layered Silicates

Sulphur prevulcanized natural rubber latex (PVNRL) nanocomposite was produced by mixing dispersions of layered silicates with prevulcanized latex. In this chapter layered silicates such as bentonite (natural) and flurohectorite (synthetic) were used in addition to a nonlayered amorphous filler (English Indian clay) as reference material. After compounding the layered silicate dispersions with PVNRL, films were prepared by casting. The post-vulcanized films of PVNRL nanocomposites were subjected to mechanical, swelling, XRD and TEM studies. In all respects layered silicate nanocomposites registered maximum properties compared to the reference material. This was explained to be due to the intercalation/exfoliation of the silicate layers by the natural rubber. It was found that the fine silicate layers form a skeleton network structure (house of cards) in the vulcanizate.

3.1 Introduction

Vulcanized rubbers are usually reinforced by carbon black and also by inorganic minerals (talc, TiO_2, silicates etc) to improve the mechanical properties. Carbon black has an excellent reinforcement owing to its strong interaction with rubbers, but its presence especially at high loading often decreases the processability of rubber compounds. The reinforcing capacity of silicates is poor because of their large particle size and low surface activity. Now-a-days there is a great interest in the development of polymeric nano-composites using layered silicates as reinforcing material [1-6]. Provided that the layered silicates fully delaminate (termed exfoliation) dispersing less than 10 percent of them may replace 3-4 times higher amount of traditional fillers without sacrificing the processability and mechanical properties. Though the concept of nano-reinforcement with layered silicates is credited to researchers at Toyota Central Research Laboratories (Japan): it became very popular in late1980s, which has been well reviewed [6-7]. Polymer nanocomposites represent a new alternative to conventionally (macroscopically) filled polymers. Because of their nanometer level filler dispersion, nanocomposites exhibit markedly improved properties when compared to the pure polymers or their traditional composites. These include increased modulus and strength, outstanding barrier properties, improved solvent and heat resistance and decreased flammability [7-10].

A powerful approach to produce layered silicate polymer nanocomposites is melt intercalation of polymers. This is a common method and is generally applicable to a range of plastics from essentially non-polar to weakly polar to strongly polar polymers. Layered silicate polymer nanocomposites are processable using latest technologies. In general two types of organic/inorganic hybrids are distinguished: intercalated (polymer

chains are diffused between the silicate layers preserving however some short range order of the latter) and dispersed (in which the silicate layers of ca. 1 nm thick are exfoliated and dispersed in the polymer matrix). Pristine layered silicates usually contain hydrated Na+ or K+ ions. Ion exchange reactions with cationic surfactants, including ammonium ions render the normally hydrophilic silicate surface organophilic. This is the prerequisite for intercalation with many engineering polymers. The role of the alkyl ammonium cations in the "usual" organosilicates is to lower the surface energy of the silicate and to improve its wettability by the polymer. Additionally, the alkyl ammonium compounds may contain functional groups, which can react with the polymer or initiate the polymerization of monomers. This may strongly improve the strength of the interface between the silicate and the polymer [11-12].

Minerals have a variety of shapes suitable for reinforcement of polymers, such as fibrils and platelets. Layered silicate is comprised of platelets having a planar structure of I nm thick and 200-300 nm length. The layers cannot be separated from each other through general rubber processing. Since inorganic ions absorbed by silicates can be exchanged with organic ions, research succeeded in intercalating many kinds of polymers and to prepare clay/polymer nanocomposites [13-17]. It has been shown that the silicate layers can be dispersed at molecular level (nanometer scale) in a polymer matrix [8]. Rubber-clay nanocomosites were prepared from latex by a coagulation method and an improvement in mechanical properties was reported [14-15]. Some layered silicates are suitable additives for latex, provided that they can form dispersions adequate for latex compounding [16]. In aqueous dispersions, the clay "swells" (*i.e.* its layers are separated by hydration) which makes the intercalation due to rubber molecules possible. In this chapter natural (NR) latex

in the prevulcanized form was used to prepare nanocomposites. Properties of the nanocomposites were compared with vulcanizates containing an inert filler called English Indian clay (commercial or non-layered silicate).

3.2 Results and discussion

3.2.1 XRD analysis

The XRD spectrum of the layered silicates showing the interplannar distances is given in Figure 3.1. The XRD spectrum of fluorohectorite showed 3 peaks, which from left correspond to an interlayer distances of 1.35, 1.24 and 1.05 nm respectively. The strong peak at 1.24 nm showed that majority of the layers in fluorohectorite have an interlayer distance of 1.24 nm.
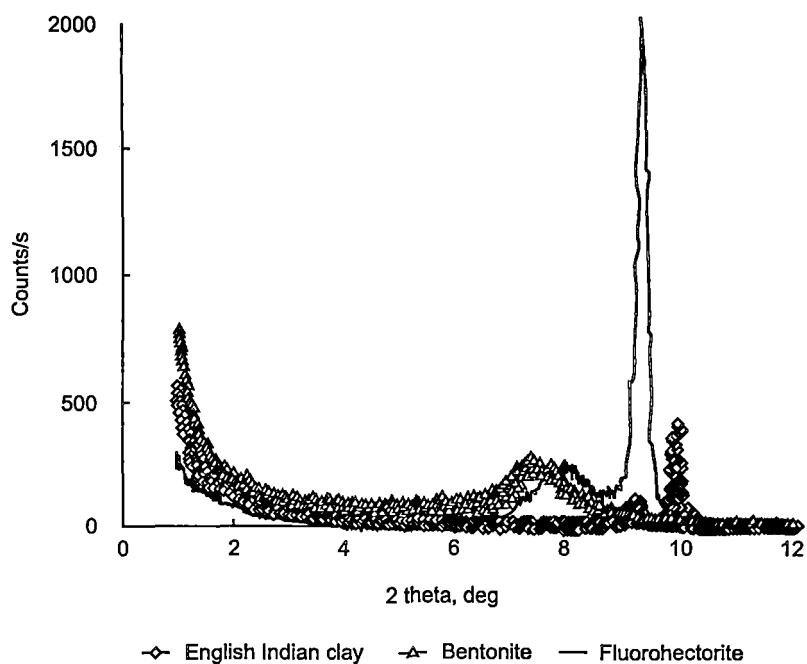
Figure 3.1 XRD of layered silicates (bentonite and fluorohectorite) and the non-layered silicate material (English Indian clay).

The bentonite showed one peak which corresponds to an interlayer distance of 1.35 nm. The commercial clay has one narrow peak at 0.96 nm, which is not at all ideal for polymer intercalation.

3.2.2 TEM analysis

It will be interesting now to analyze the transmission electron microscopic (TEM) pictures of the composites. All the composites are loaded with 10 phr filler. In Figure 3.2a, the TEM picture of commercial clay (English Indian clay) loaded vulcanizate is given.

Figure 3. 2a TEM picture of commercial clay (English Indian clay) loaded vulcanizate

Here the filler exist as large particles and the bulk of the polymer did not contain any filler particle for reinforcement. This means, 10 phr loading of the

commercial clay is not enough to saturate the polymer phase as they exist as big particles distributed unevenly which in effect weaken the matrix. Recall that this clay was not a layered version.

500 nm
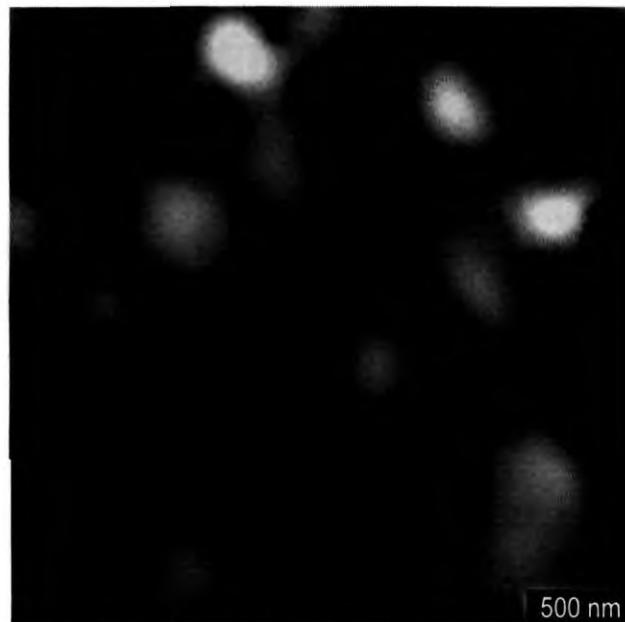
Figure 3. 2b TEM pictures of bentonite filled (nano)composites.

However in bentonite filled vulcanizate (Figure 3.2b), the filler exist as a network structure around the rubber particles (white portion). This is because the bentonite clay underwent some level of intercalation, and the silicate layers form 'clusters or house of cards structure'. The high compound viscosity, which have experienced during mixing might be due to the formation of the layer network structure. The polymer phase is reinforced to a great extent as it is saturated with this network structure which in turn contributed to the high mechanical properties of the vulcanizate.

However a fully saturated structure was observed in the case of fluorohectorite filled vulcanizate Figure 3.2c). Here, the silicate layers were intercalated to a great extent and a small level of exfoliation was also observed which exist as thin black strands in the photograph. Some level of network structure and orientation were also visible here which may be responsible for the higher modulus of fluorohectorite filled vulcanizate compared to that of bentonite. Moreover the exfoliated structure gives a several fold increase in surface area.
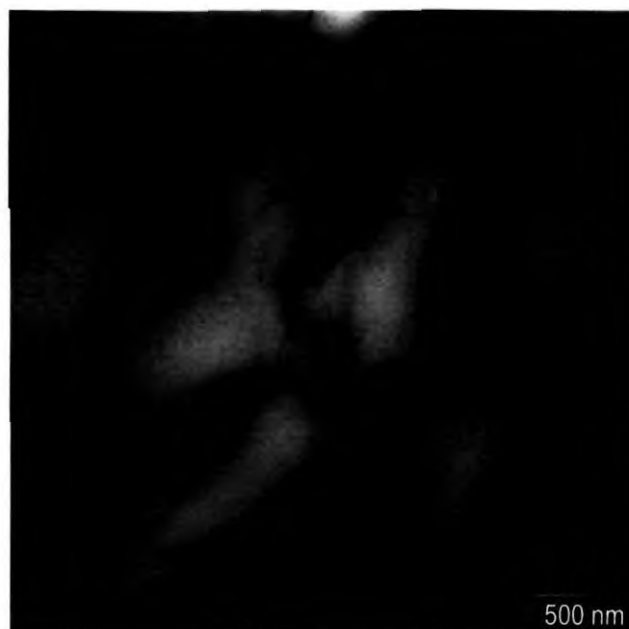
Figure 3. 2c TEM pictures of fluorohectorite filled (nano)composites

3.2.3 Mechanical properties

Figures 3.3a, b and c show the modulus at various elongations for different silicate filled vulcanizates Figure 3.3a illustrates the results of 3 phr

loaded vulcanizate. It is to be noted that at low elongation (100%) there is a gradual increase in modulus, which is in the order gum < English Indian clay < bentonite < flurohectorite. As the elongation is increased the modulus also increased which is maximum at 300% elongation. It is to be noted that the maximum increase in modulus is with flurohectorite at 300% elongation followed by bentonite.
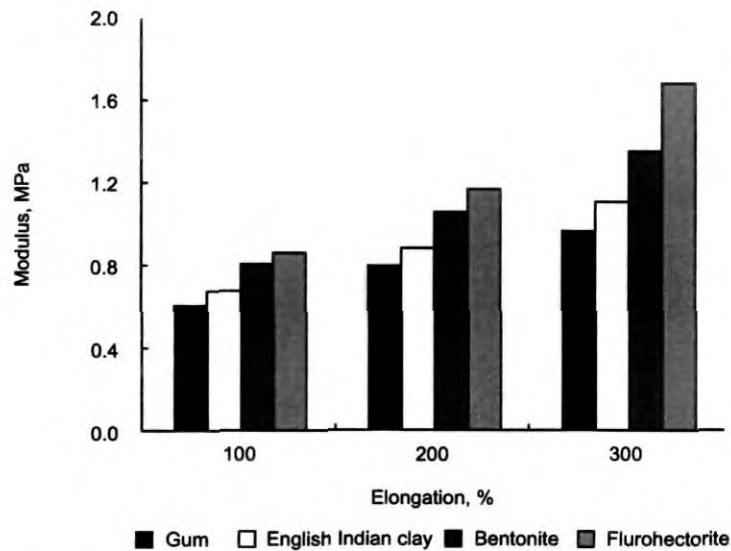
Figure 3. 3a Moduli at different elongations for different silicates filled (nano)composites at a loading of 3 phr

Figure 3.3b represents the modulus change with various silicates at 5phr loading. Here also the change in modulus at various elongations is of the same order as we have discussed earlier. However at same elongation the magnitude of the modulus at 5 phr loading is higher when compared to that at 3phr loading (Figure 3.3a) especially with layered silicates. In the case of gum and commercial clay filled vulcanizates this difference

is negligible. The silicate layers may favour the formation of immobilized or partially immobilized polymer phases, which may contribute for high modulus [17]. Moreover the sheets of layered silicates orient along the strain direction, which increases with increased strain. The low stiffening effect of commercial clay can be attributed to its high particle size and poor dispersion. In the vulcanizate containing layered silicate, a part of the silicate were exfoliated which offers high surface area for reinforcement. When the silicate loading is increased to 10phr (Figure 3.3c) layered silicates showed comparatively high modulus.
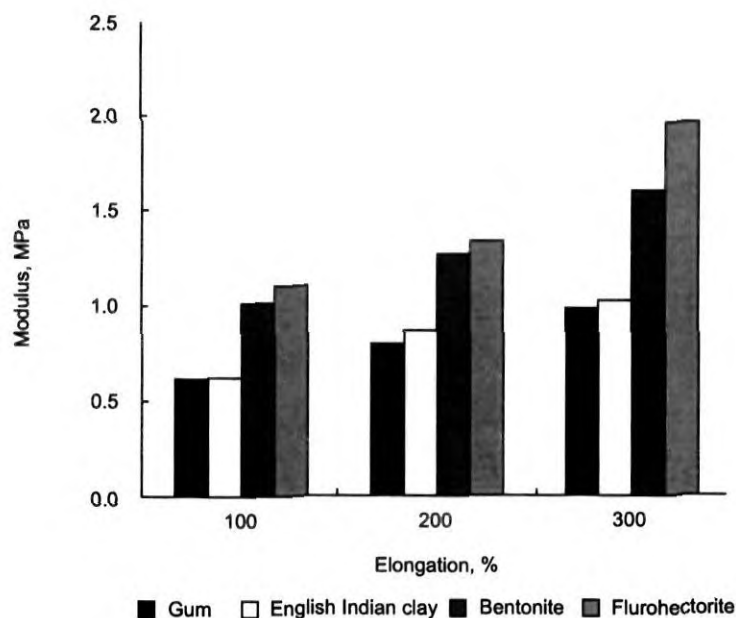
Figure 3. 3b Moduli at different elongations for different silicates filled (nano) composites at a loading of 5phr
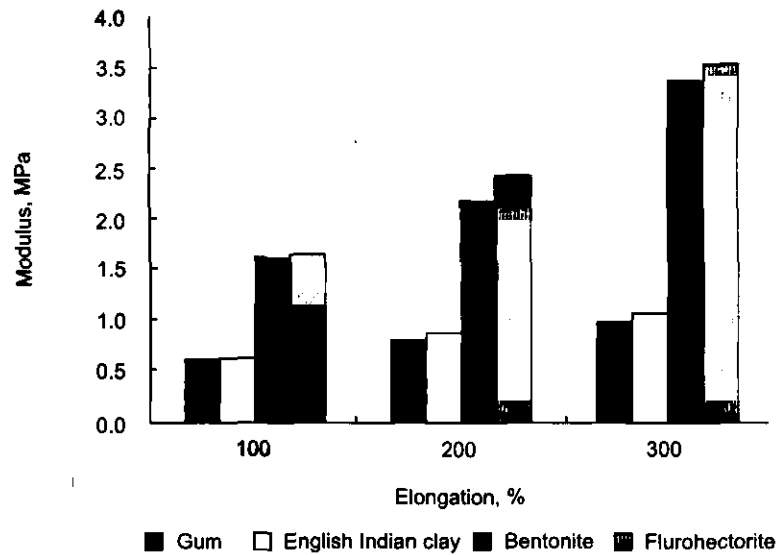
Figure 3. 3c Moduli at different elongations for different silicates filled
(nano)composites at a loading of 10phr.
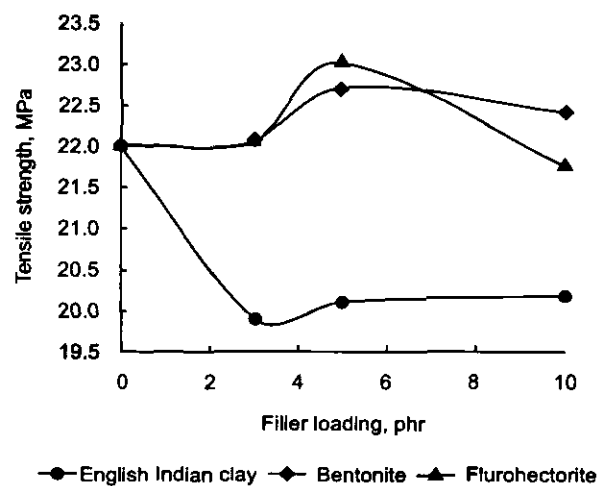
Figure 3. 4 Tensile strength of different silicates filled (nano) composites
at different loading

The effect of filler loading on tensile strength of the composites is shown in (Figure 3.4) which was found to increase up to 5 phr loading of layered silicates and thereafter it decreases. This might be due to the agglomeration of the fine silicate layers beyond a particular concentration in the polymer. In the case of layered silicates the critical concentration was found to be 5 phr.

Tear strength values of the composite are given in (Table 3.1). Addition of small amount of layered silicate (3phr) increased the tear strength considerably. It has been reported that exfoliated layered silicates can increase the tear strength considerably [17].

Table 3.1 Tear strength of layered silicate filled vulcanizates

Silicate	Loading, phr			
	0	3	5	10
Flurohectorite, kN/m	47.98	60.53	58.21	28.88
Bentonite, kN/m	47.98	51.44	48.91	23.22
English Indian clay, kN/m	47.98	41.17	48.86	41.84

However as the amount of silicates increased, the tear strength decreased whereas for English Indian clay, addition of filler decreased the tear strength irrespective of the amount of loading. From this it can be concluded that exfoliated silicate layers hinter/divert the tear path which results in high tear strength value in flurohectorite and bentonite. At high loading (above 5phr) the silicate layers agglomerate and exist as stacks, which can not orient in the strain direction. In the case of tear strength, the threshold level of silicate (layered) loading was observed to be 3phr.
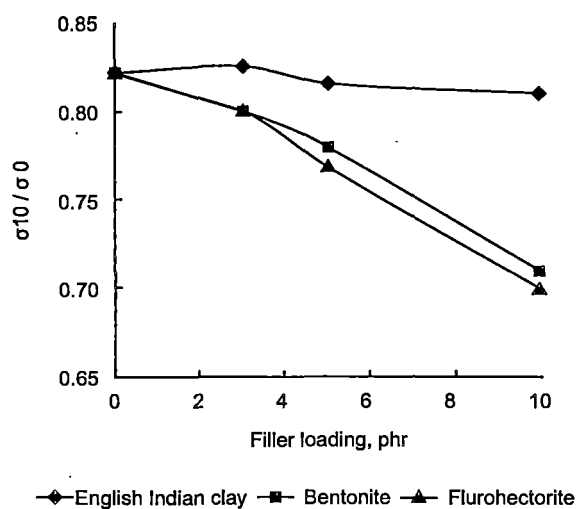
Figure 3. 5. Relaxation of stress after 10 minutes for different silicate filled (nano)composites

The rate of relaxation of the composites with stress was fast in the case of layered silicate (Figure 3.5) incorporated vulcanizates and it is in the order flurohectorite> bentonite> commercial clay. At high elongation the chain slip along the filler surface is the major factor, which contribute to the stress decay and is proportional to the surface area of the filler in contact with the polymer. As the extend of exfoliation was high in fluorohectorite, the surface area and hence the stress decay at a given elongation was proportionately higher in fluorohectorite.

Table 3.2 Tension set (%) of layered silicate filled vulcanizates.

Silicate	Loading, phr			
	0	3	5	10
Flurohectorite	2	10	16	36
Bentonite	2	8	14	18
English Indian clay	2	2	6	10

Tension set of the composites was determined and is given in (Table 3.2). Set was maximum with flurohectorite, which is typical for reinforcing fillers. The results showed that as the loadings of layered silicate increased the set also increased. The tension set increase in the order English Indian clay < bentonite < flurohectorite.

3.2.4 Sorption behaviour

Table 3.3 shows the weight in grams of toluene absorbed per gram of the composite at 25°C. The gum vulcanizate has the maximum toluene uptake at equilibrium swelling.

Table 3.3 Sorption behaviour of layered silicate incorporated vulcanizates

Silicate	Loading, phr			
	0	3	5	10
Flurohectorite	4.93	4.74	4.49	4.312
Bentonite	4.93	4.85	4.6	4.35
English Indian clay	4.93	4.89	4.83	4.73

This was expected, since there was less restriction for the penetrant to diffuse into the vulcanizate. At equal volume loading of filler, the amount of solvent absorbed at equilibrium swelling is less for the composites containing layered silicate - especially with fluorohectorite - compared to that containing commercial clay. During swelling the solvent can enter in the polymer along or transverse to the aligned silicate platelets. The presence of impermeable clay layers decreases the rate of transport by increasing the average diffusion path length in the specimen [18-19]. In commercial clay filled rubber, the solvent uptake is high because of the weak interface and also due to poor

clay dispersion. In well-oriented composites, the penetration perpendicular to the orientation is highly restricted. The Kraus plots, which show the ratio of the crosslink-density of the unfilled material (gum sample) to that of the filled vulcanizate are given Figure 3. 6.

If the value V_{r0}/V_{rf} is less than unity the filler rubber interactions are more and vice versa. It is interesting to note that for layered silicates V_{r0}/V_{rf} is always less than one and the magnitude of the ratio decreases with filler loading. However in the case of English Indian clay the V_{r0}/V_{rf} is always higher than 1 hence these composites showed low reinforcement and poor mechanical properties.
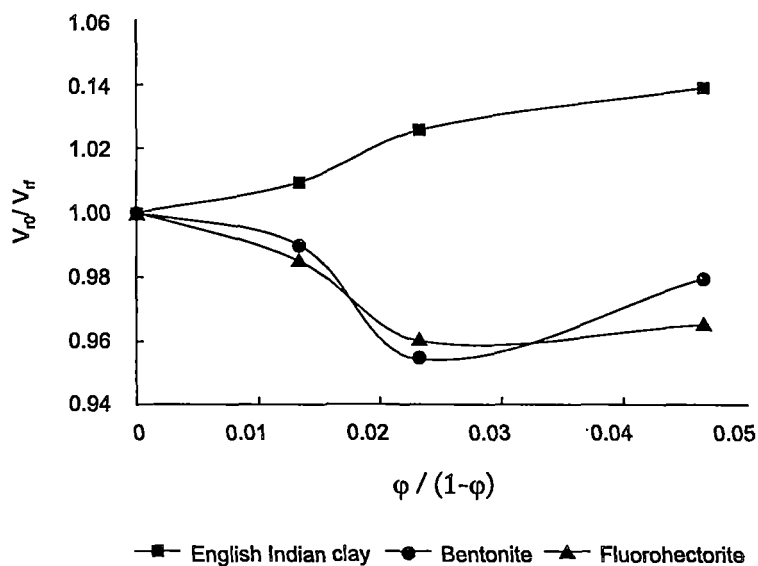
Figure 3.6. Plots of V_{r0}/V_{rf} against volume fraction of filler for different silicates-filled (nano) composites.

3.3 Conclusion

Nanocomposites based on sulphur prevulcanized natural rubber latex and layered silicates were prepared. The vulcanized nanocomposite was subjected to mechanical analysis. It is found that the modulus and tear strength of the vulcanizate increases with the incorporation of layered silicate and in the case of layered silicates 3phr loading was found to be the threshold level for most of the mechanical properties. Higher loading leads to agglomeration or filler networking in the rubber. It was also found that the rate of relaxation of stress and tension set were higher for layered silicate incorporated materials. The solvent resistance of the material is comparably better compared to the reference. The filler-rubber interactions are strong in layered silicate incorporated vulcanizate as evident from Kraus plots.

3.4 References

1. M. Kato, A. Usuki, *Polymer-Clay Nanocomposites*, Eds. T. J. Pinnavaia and G. W. Beall, J Wiley, New York, 97 - 109, 2000

2. B. B. Boonstra, Role of Particulate Fillers in Elastomer Reinforcement: A review, *Polymer*, **20**, 691 - 704, 1979

3. S. Joly, G. Garnard, R. Ollitrault, L. Bokobza, *Chem. Mater.*, **14**, 4202 - 4208, 2002

4. F. Schon, W. Gronski, *KGK Kautschuk Gummikunststoffe*, **56**, 4, 2003

5. M. Arroyo, M. Lopez, A. Manchado, B. Herrero, *Polymer*, **44**, 2447 - 2453, 2003

6. A. Usuki, A. Tukigase, M. Kato, *Polymer*, **43**, 2185 - 2189, 2002

7.   Y. Kojima, A. Usuki, M. Kawasumi, A. Okada, T. Kurauchi, O. Kamigaito, *J. Appl. Polym. Sci.*, **49**, 1259 - 1264, 1993

8.   M. Alexandre, P. Dubois, Polymer-Layered Silicate Nanocomposites: Preparation, Properties and Uses of a New Class of Materials. *Mater. Sci. Eng.*, **28**, 1 - 63, 2000

9.   E. P. Giannelis, Polymer-Layeredsilicate Nanocomposites: Emerging Scientific and Commercial Opportunities. *SPE-ANTEC*, **45**, 3966 - 3968, 1999

10.   J. W. Gilman, T. Kashiwagi, Polymer- Layered Silicate   Nanocomposites with Conventional Flame Retardents, Eds. T. J. Pinnavaia, G. W. Beall, Special Properties and Applications, 193 - 205, 2000

11.   J. Oberdisse, B. Deme, *Macromolecules*, **35**, 4397 - 4405, 2002

12.   Z. Wang, J. Massam, T. J. Pinnavaia, *Epoxy-Clay Nanocomposites*, (Pinnavaia, T. J. and Beall, G. W, Eds.) New York, J. Wiley, 127 - 148, 2000

13.   M. Mousa, J. Karger - Kocsis, *J. Macromol. Mater. Eng.*, **286**, 260 - 266, 2001

14.   Y. Wang, L. Zhan, C. Tang, D. YU, *J. Appl. Polym. Sci.*, **78**, 1879 - 1883, 2000

15.   M. Chen, N. J. Ao, Y. Chen, , H. P. Yu, H. L. Qian, C. Wang, H. L, zhou, J. L. Qu, C. K. Guo, *J Appl.   Polym. Sci.*, **82**, 338 - 342, 2001

16.   S. Varghese, J. Karger-Kocsis, *Polymer*, **44**, 4921 - 4927, 2003

17.   M. Ganter, W. Gronski, P. Reichert, R. Mulhaupt, *Rubb. Chem. Technol.*, **74**, 221 - 235, 2001

18.   S. Varghese, B. Kuriakose, S. Thomas, *Rubb. Chem. Technol.*, **68**, 37 - 49, 1995

19.   Y. Kojima, K. Fukumori, A. Usuki, A. Okada, T. Kurauchi, *J. Materi. Sci. Letters*, **12**, 889 - 890, 1993

Radiation Prevulcanized Natural Rubber Latex Layered Silicate Nanocomposites

Aqueous dispersions of layered silicates of natural and synthetic in origin (sodium bentonite and fluorohectorite) were mixed with radiation vulcanised natural rubber latex (RVNRL) up to 10 wt %. Dried films after sufficient mixing were subjected to mechanical and instrumental analysis. Commercial clay (non-layered version) was selected as the reference material. Layered silicate nanocomposites, expressed good mechanical properties compared to the reference material. Fluorohectorite showed the better properties compared to bentonite. Gas barrier properties were observed to be high in nanocomposites than the reference material (commercial clay). TEM studies revealed that silicate layers were exfoliated and network was formed around the rubber particles.

4.1 Introduction

When rubber is irradiated with high energy radiation, hydrogen atoms of the trunk chain, mainly of methylene groups α to the double bonds, are ejected and radicals are formed and these radical sites are combined into C-C crosslinks [1-3]. Heat vulcanizing ingredients such as sulphur, accelerators, benzoyl peroxide and other peroxides are known to have very little effect on this reaction but it is possible that these ingredients acting as radical acceptors hinder the radicals from combining with each other and thus retard the radiation vulcanization. Since the radiation vulcanization is carried out in the absence of sulphur and accelerators, the products can be obtained uncontaminated by poisonous residues, therefore the future of radiation curing looks bright.

In recent years vulcanized latex is playing a more important role in the rubber industry since it is a good protection material against the AIDS virus. Moreover natural rubber latex is used in a wide variety of products that come in contact with human skin and other body surfaces. Radiation vulcanized natural rubber latex (RVNRL) has many advantages over the conventional sulfur vulcanized latex, such as absence of nitrosamines, very low cytotoxicity, good degradability and low emission of gases when incinerated [4-7]. However radiation vulcanized latex is not fully accepted in industry. The lack of interest of RVNRL is due to high initial investment and poor technological properties such as low tensile properties and poor ageing properties.

Organically modified layered silicates are recently used as excellent reinforcing materials in elastomers [7-11]. In this study, RVNRL is mixed with unmodified layered silicates so as to retain its bio-friendly characteristics. Layered clays are comprised of silicates layers having a planar structure of

1nm thickness. Cations in the gallery of layered silicates undergo hydration in water, which cause swelling of layers. When polymer solutions were mixed with such water swollen layered silicates, polymer intercalation takes place. This is the driving force for reinforcement of polymers by layered silicates in aqueous solutions [12-14]. Layered silicates are supposed to impart improved mechanical properties and ageing resistance to the polymers. Two layered silicates, namely bentonite and fluorohectorite were selected for the study whereas commercial clay (which has no layer structure) was used as the reference material.

4.2 Materials and methods

Raditaion vulcanized latex was obtained from Rubber Research Institute of India. The latex was first diluted to 50 per cent total solids with ammonia solution followed by 0.2 phr of 10 per cent KOH solution. The sensitizer n-butyl acrylate (5phr) was then added with constant stirring. The irradiation was carried out with γ-rays from a Co-60 source at a dose rate of 10 kGy/h for 2h. The irradiated latex is then mixed with different layered silicate dispersions (10 per cent). The films were then cast on raised glass plates and air dried until transparent. The dried films were then leached in 1 per cent ammonia solution for 24h, and post-cured in an air oven at 80°C for 1 h. Other details of the materials used are given in chapter 2.

4. 3 Results and discussion

The XRD spectrum of the layered silicates showing the interplannar distances is given in Figure 3.1. Figure 4.1 shows the storage modulus as a function of temperature. Since radiation vulcanized latex with fluorohectorite showed maximum mechanical properties, dynamic mechanical analysis was

done in detail only for the fluorohectorite filled vulcanizates. The highest storage modulus is registered by nanocomposites with 10 phr loading of fluorohectorite and it decreases with decreasing loading of fluorohectorite. The least value is shown by commercial clay. It is to be noted that the storage modulus of 3phr pf fluorohectorite is almost equivalent to 10 phr of commercial clay. This is attributed to the high in-plane strength of the fine silicate layers separated by intercalation/exfoliation. This is evident from the TEM results, which will be discussed later.

-o- RVNRL gum   -◊- English Indian clay, 10 phr
-+- Flurohectorite-3 phr   -*- Flurohectorite-5 phr   —— Flurohectorite-10 phr
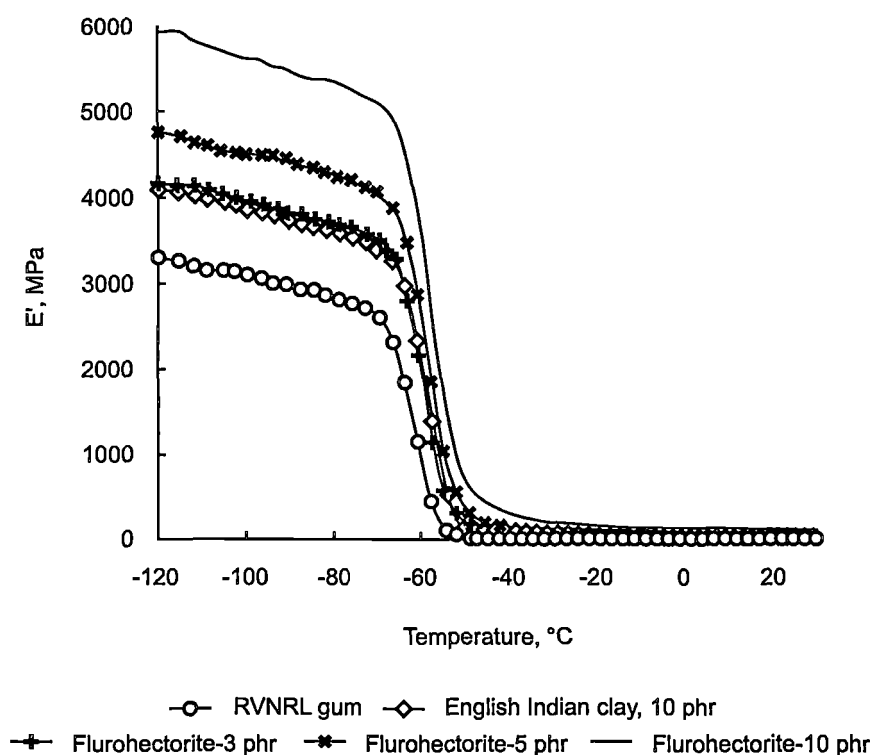
Figure 4.1 Variation of storage modulus with temperature at different loadings of fluorohectorite

The mechanical loss factor as a function of temperature is depicted in Figure 4.2. Tan δ peak is maximum for the gum material. The peak height decreases with increasing loading of layered silicate (fluorohectorite).
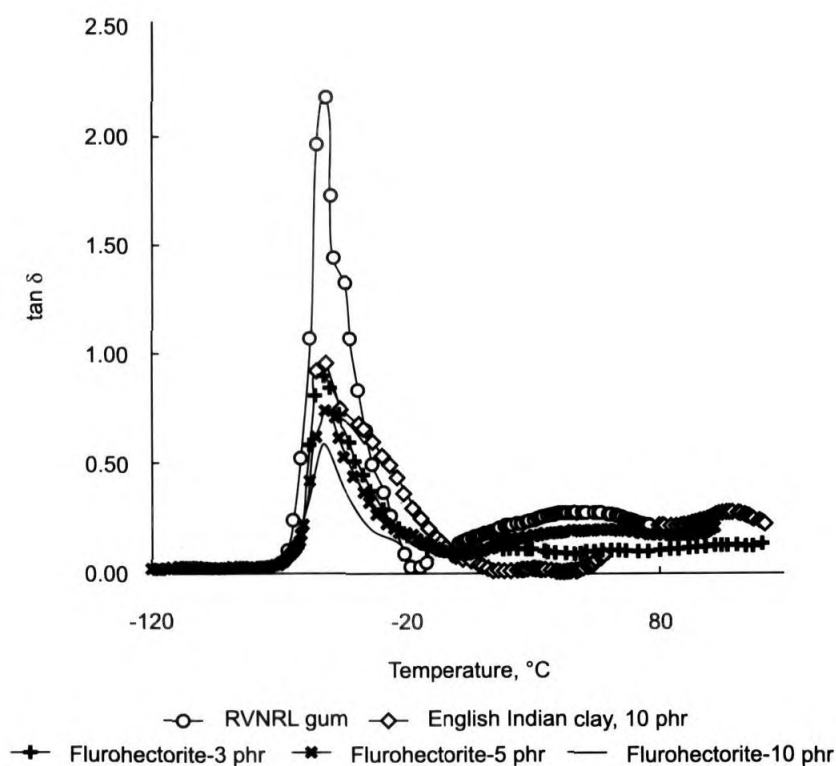
Figure 4. 2 Variation of mechanical loss factor with temperature at different loadings of fluorohectorite

The mechanical anchoring of the polymer chains in to the finely separated silicate sheets cause restriction to the chain mobility, which will reduce the tan δ considerably.

The stress strain curves of different silicate filled rubber nanocomposites are given in Figure 4.3
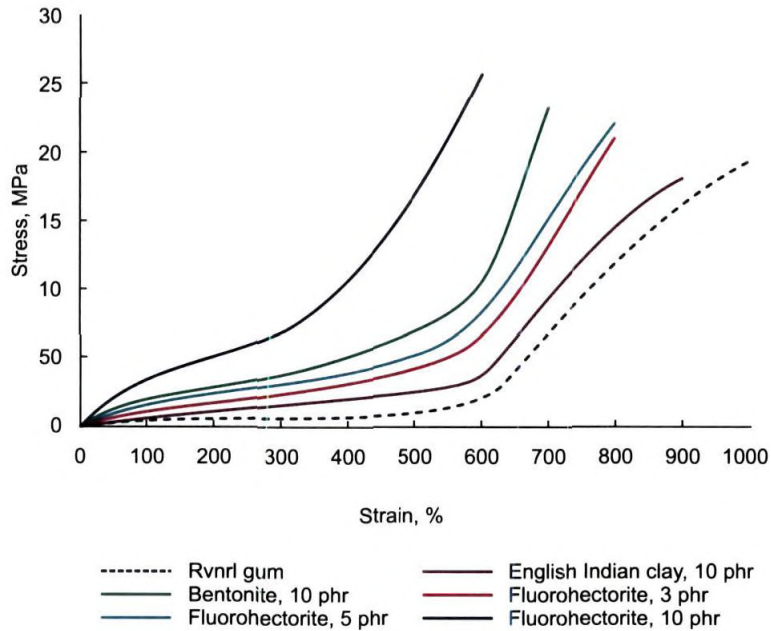
Figure 4. 3 Stress-strain curves of different silicate filled rubber nanocomposites

It can be seen that the gum compound has the lowest stress at all strain levels except at the breaking point where the stress-induced crystallization plays a major role. As the loading of fluorohectorite increases the stress-strain curve occupiers a upper positions and 10 phr loaded composites showed the maximum values. It is interesting to note that 10 phr loaded commercial clay has lower stress values than 3 phr loaded fluorohectorite. The high surface area achieved through exfoliation (approximately 10 fold increase in surface area *via.* exfoliation) is the reason for this. The stress values of 10 phr loaded bentonite are lower at all elongations compared to the 10 phr loaded fluorohectorite. The high reinforcement in fluorohectorite loaded composites may be due to its high aspect-ratio of the layers. The stress at lower elongations (which is a

good measure of the reinforcement) is high for layered silicate filled composites especially with fluorohectorite.

The transmission electron microscopic (TEM) picture of the composites loaded with bentonite (10phr) is given in Figure 4.4

500 nm
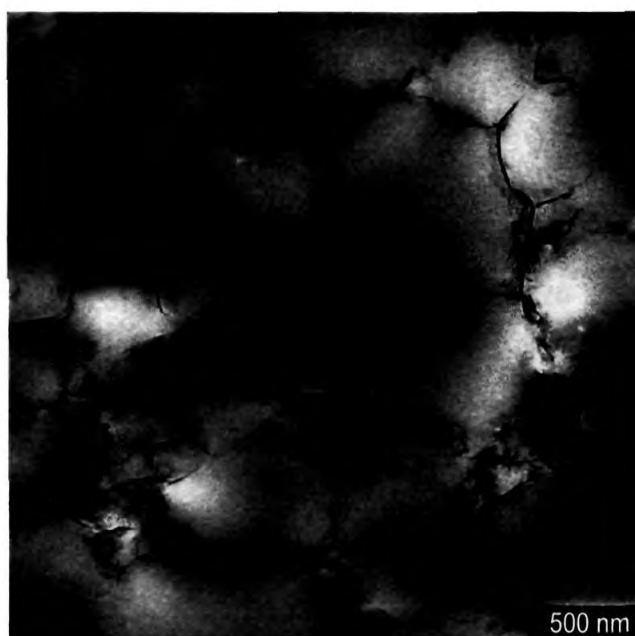
Figure 4. 4 TEM picture of the composite loaded with 10phr bentonite

It can be seen that the bentonite layers are exfoliated well in the latex. It is interesting to note that there is some network formation of the silicate layers in rubber matrix. It is also interesting to note that the filler network is concentrated mainly at the boundary of the rubber particles, which fused together during vulcanization. Since the layered silicate solutions are added to the already vulcanized latex and as the crosslinked rubber cannot diffuse in to the silicate gallery region the layers are supposed to occupy the boundary region. Figure 4.5 represent the TEM picture of fluorohectorite loaded to rubber vulcanizates.

1000 nm
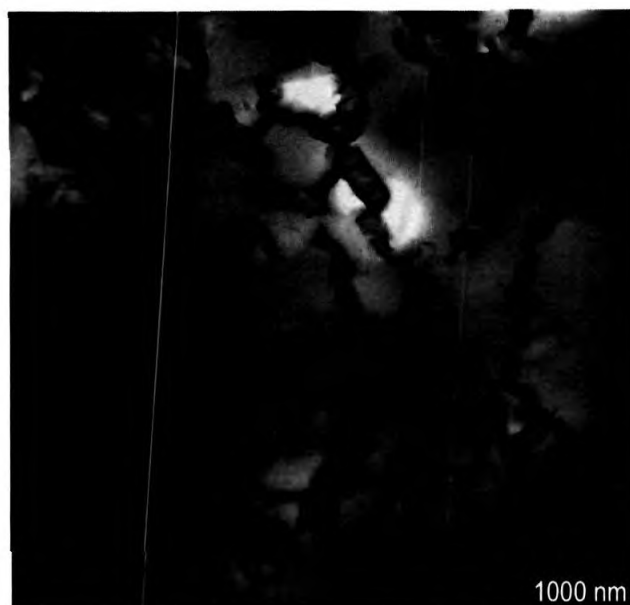
Figure 4.5 TEM picture of the composite loaded with 10 phr
fluorohectorite

Completely exfoliated silicate layers can be seen here. The network
structure is also visible here. The layers of bentonite are needle like whereas that
in fluorohectorite is ribbon shaped. This ribbon shape structure offers high aspect
ratio, which in turn impartshigh mechanical properties to its composites.

The mechanical properties of the nanocomposites are given in Table
4.1. The change in modulus at different elongations for pure rubber and that
of 10 phr loaded commercial clay are as expected. Bentonite filled composites
showed a marginal increase in modulus with elongations. Though the effect is
same in fluorohectorite the magnitude of the stress values are higher especially
at 10 phr loading of the fluorohectorite. In commercial clay there is no chance of
polymer intercalaion and the reinforcement will be very low, whereas in bentonite

there is a good level of intercalation followed by exfoliation. High mechanical properties of the fluorohectorite composites are due to fully exfoliated silicate layers. After ageing properties of the selected composites are also given. Comparatively better retention of mechanical properties in the layered silicate composites are due to the protection of polymer chains by the silicate network structure.

Table 4.1 - Mechanical properties (before and after ageing)

Sample	Silicate loading, phr	Modulus at different elongations, %				Elongation at break, %	Tensile strength, MPa
		100	200	300	600		
Pure rubber	0	0.37	0.51	65	1.72	1040	19.42
		(0.21)	(0.28)	(0.34)	(0.85)	(1002)	(6.38)
Comm.clay	10	0.74	1.05	1.41	3.56	946	18.36
		(0.30)	(0.42)	(0.58)	(1.64)	(700)	(8.54
Bentonite	3	0.72	1.03	1.41	4.83	907	20.41
	5	0.98	1.32	1.73	5.01	901	21.8
	10	2.04	2.72	3.71	10.35	700	23.18
		(1.45)	(1.76)	(2.01)	--	653	(11.65
Fluorohectorite	3	1.08	1.61	2.21	6.44	844	21.57
	5	1.61	2.32	3.17	8.14	811	22.19
	10	3.52	4.98	6.83	16.82	633	25.61
		(2.30)	(3.15)	(3.98)	--	598	(14.77)

Air permeability values of the composites are shown in Figure 4. 6. It can be seen that the fluorohectorite imparts lowest air permeability. High

air impermeability of the layered silicates are attributed to the fact that, the silicate sheets prevents the passage of the penetrant molecules through the rubber film.
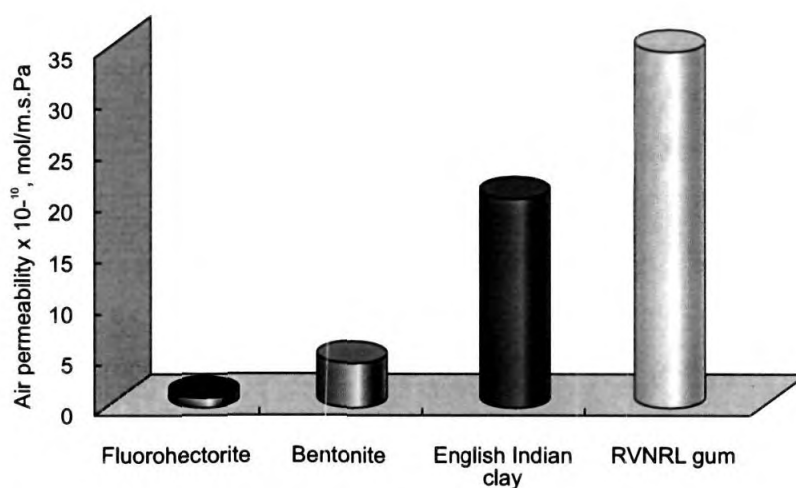
Figure 4.6 Air permeability of different silicates at 10 phr loading

4.4 Conclusion

Unlike the commercial silicate, XRD spectrum of layered silicates revealed that they contain interlayer distance ideal for rubber intercalation. Dispersions of layered silicates showed excellent miscibility with radiation vulcanized latex. Among the layered silicates, fluorohectorite showed good mechanical properties compared to bentonite. There is a continuous increase in storage modulus with fluorohectorite concentration and the trend was reverse with tan δ values. TEM pictures showed good exfoliation of silicate layers. After ageing properties and thermal degradation were better for layered silicates incorporated nanocomposites. Several fold increase in surface area by clay

exfoliation and the filler network structure is main reasons improved properties.

4.5 References

1. T. Ichikawa, Ken-ichi Oyama, T. Kondoh, H. Yoshida JI **32**, 13, 2487 - 2492, 1994

2. J. W. Rygan, *SPE Journal*, **10**, 11, 40 - 44, 1954   I

3. B. A. Dogadkin, Z. N. Tarasova, M. Ia. Kaplunov, V.'. Klauzen, *Rubber Chem. Technol.*, **32**, 3, 785 - 799, 19

4. T. Adul, K. Makuuchi, F. Yoshii, *J. Appl. Polym. Sci.*, **54**

5. K. Makuuchi, F. Yoshii, I. Ishigaki, K. Tsushima, M. M/ *J. Radiat. Appli. Instru., Part C. Radi. Physi. and Ch* 154 - 157,1990

6. S. Varghese, Y. Katsumura, K. Makuuchi, F. Yoshii *Technol.*, **72**, 308 - 317,1999

7. Y. Kojima, K. Fukumori, A. Usuki, A. Okada, T. Kurauci *Letters.*, **12**, 889 - 890,1993

8. M. Ganter, W. Gronski, H. Semke, T. Zilg, C. Thomaı *Kautschuk Gummi Kunststoffe*, **54**, 166 - 171, 2001

9. A. Usuki, A. Tukigase, M. Kato, *Polymer*, **43**, 2185 - 2"

12.   Y. Wang, L. Zhang, C. Tang, D. Yu, *J. Appl. Polym. Sci.*, **78**, 1879 - 1883, 2000

13.   M. Chen, N. J. Ao, Y. Chen, H. P. Yu, H. L. Qian, C. Wang, H. L. Zhou, J. L. Qu, C. K. Guo, *J. Appl. Polym. Sci.*, **82**, 338 - 342, 2001

14.   S. Varghese, J. Karger-Kocsis, *Polymer*, **44**, 4921 - 4927, 2003

Rheological Behaviour of Layered Silicate Natural Rubber Latex Nanocomposites

The rheological behaviour of prevulcanized natural rubber (NR) latex nanocomposites based on layered silicates such as sodium bentonite and sodium fluorohectorite was studied. A typical commercial clay (nonlayered grade) was chosen as the reference material. The effect of layered silicates on flow properties has been analyzed by investigating latex viscosity as a function of shear rate, temperature and filler loading. In presence of layered silicates, latex compounds showed enhanced viscosity, probably due to a network formation of silicate layers in the latex phase. The shear thinning behaviour exhibited by the nanocomposites at high temperature may be due to the network breakdown of silicate layers. Latex - layered silicate systems showed pseudoplastic behaviour, increased zero shear viscosity and yield stress.

5.1 Introduction

In recent years much attention has been paid to polymer nanocomposites based on layered silicates (LS) having platelets with nanometer dimensions [1-8]. The layers cannot be separated from each other through general rubber processing techniques. The most commonly used layered silicates are monmorillonite (MMT) hectorite and saponite. The important characteristic of layered silicates is its ability to disperse into individual layers. According to the strength of interfacial interaction between polymer matrix and the layered silicates, three different types of polymer-layered silicates can be thermodynamically possible and are 1) intercalated 2) flocculated and 3) exfoliated. Due to the high surface area, exfoliated system exhibits better properties.

A deep knowledge of the flow behaviour of compounds containing layered silicates is essential to understand the processability and structure property relations of the materials. The viscosity of latex plays a critical role in the flow and shaping behaviour of latex compounds. Several investigations have been made to understand the rheological behaviour of polymers in view of their relevance to processing [9-12].

Melt rheology has been utilized as a method to characterize polymer-clay nanocomposites. Thomas and co-workers have studied the flow properties of NR/SBR latex blends in the presence of surface active agents with reference to various parameters such as shear rate, temperature and blend ratio [13, 14]. The flow properties of compounded latices are strongly influenced by shear rate, particle size, presence of electrolytes, temperature etc. Prevulcanized natural rubber latex is an industrially important raw material for the production of

many latex articles like condoms, catheters, gloves etc. It has very low residual chemical content and the various tailor made forms make it suitable for the production of many latex articles. Data regarding the processing and rheological behaviour of nanocomposites are very important to design end products [15–16]. The rheological behaviour of prevulcanized natural rubber latex modified with different types of layered silicates is discussed in this paper.

5.2 Results and discussions

5.2.1 Rheological measurements

The dynamic oscillatory and shear rheology studies of the layered silicate modified latex revealed enhanced viscosity as compared to that modified with conventional clay, which can be attributed to the formation of intercalated or exfoliated network structure of clay platelets [17-20]. The rheological behaviour of latex nanocomposites has been analyzed using the Ostwalds power law equation [21].

$$\tau = k \, \dot{Y}^n \qquad \text{.............................. 1}$$

Where τ is the shear stress (Pa), k is the viscosity index, $\dot{Y}$ the shear rate (s^{-1}), and n is the pseudoplasticity index. The n and k values were obtained by regression analysis of the values of τ and $\dot{Y}$ obtained from the experimental data.

The apparent viscosity (η) was calculated using the equation

$$\eta = k \, (\dot{Y})^{n-1} \qquad \text{.............................. 2}$$

Each rheogram was analyzed for yield stress (τ_o), viscosity index (k), and pseudoplasticity index (n). The variations of viscosity with shear rate of different filler incorporated nanocomposites at 25°C are given in Figure 5.1.

-◇- English Indian clay -○- Fluorohectorite
-✕- Gum compound -✳- Bentonite
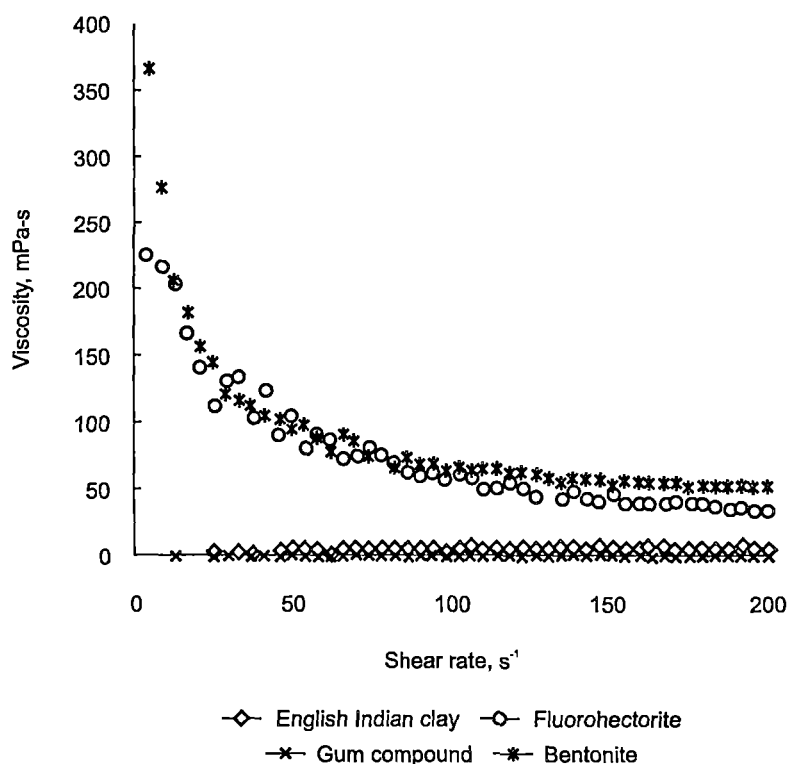
Figure 5. 1 Effect of viscosity on shear rate of NR latex nanocomposites at 5phr loading, temperature 25°C.

The flow behaviour of latex nanocomposites may exhibit the degree of compatibility between polymer matrix and the layered silicate. Moreover, the interlayer distance of the clay also plays an important role in the intercalation and hence the viscosity. It is found that viscosity decreases with shear rate for all silicates and the higher viscosity values are registered by layered silicates (fluorohectorite and bentonite). The interlayer distance of fluorohectorite is 0.94 nm and that of bentonite is 1.25 nm. However the cation exchange capacity

of fluorohectorite and bentonite are 100 and 80 respectively. In dispersions, greater extent of exchange reactions is possible with fluorohectorite as the CEC is higher. In dispersion, fluorohectorite undergoes hydration, which further increases its interlayer distance, and the exchange reaction is faster with fluorohectorite than bentonite. When the latex is mixed with the layered silicate dispersion, rubber molecules can easily intercalate in between the layers. As a result the viscosity of layered silicate–latex mix is higher compared to the control or to the corresponding nonlayered version.

The rheological behaviour of polymer suspensions depends on their liquid binding or immobilization mechanism. The polymer dispersed in the aqueous phase is immobilized within the layers of silicates. It is well known that the layered silicate has the ability to separate the layers and can intercalate the polymers in between the layers. According to Lazzeri and coworkers, the polymer molecules when immobilized in the filler surface are considered as a contribution to the dispersed phase with the effect of raising the effective filler volume fraction [15]. Since at each shear rate there is a structural equilibrium between the immobilized and mobilized part, the effective volume fraction is a function of shear rate. This may the reason behind the shear thinning behaviour of layered silicates reinforced latex samples. From the viscosity curve it is clear that layered silicate modified latex exhibit non-Newtonian behaviour.

The variations of viscosity with shear rate at 5 phr loading of different silicates are also seen in the same Figure 5. 1. Here the gum latex sample and the commercial clay modified latex do not show any change in viscosity with shear rate. However, the shear thinning behaviour is obvious in the case of layered silicates compositions at higher loadings, which indicates the network

formation at low shear rate and its linear alignment along the shear direction at higher shear rates. The viscosity of the latex compounds is found to increase by the addition of silicates. It can be seen that at low shear rates the filled latex compounds show higher viscosity than the unfilled compound. The difference narrows down at higher shear rates. The restriction offered by the fillers to the Brownian movement of the latex particles seems to overcome at the higher shear rates. A schematic model explains the formation of networks and its orientation of the exfoliated or intercalated structure along the shear direction (at higher shear rates) is shown in Figure 5. 2.

Unvulcanized latex   Prevulcanized latex   Layered silicate

Layered silicate latex   Network formation of layers   Orientation of the
nanocomposite   in the latex phase   exfoliated or
                                                                  intercalated structure
                                                                   along the shear
                                                                       direction
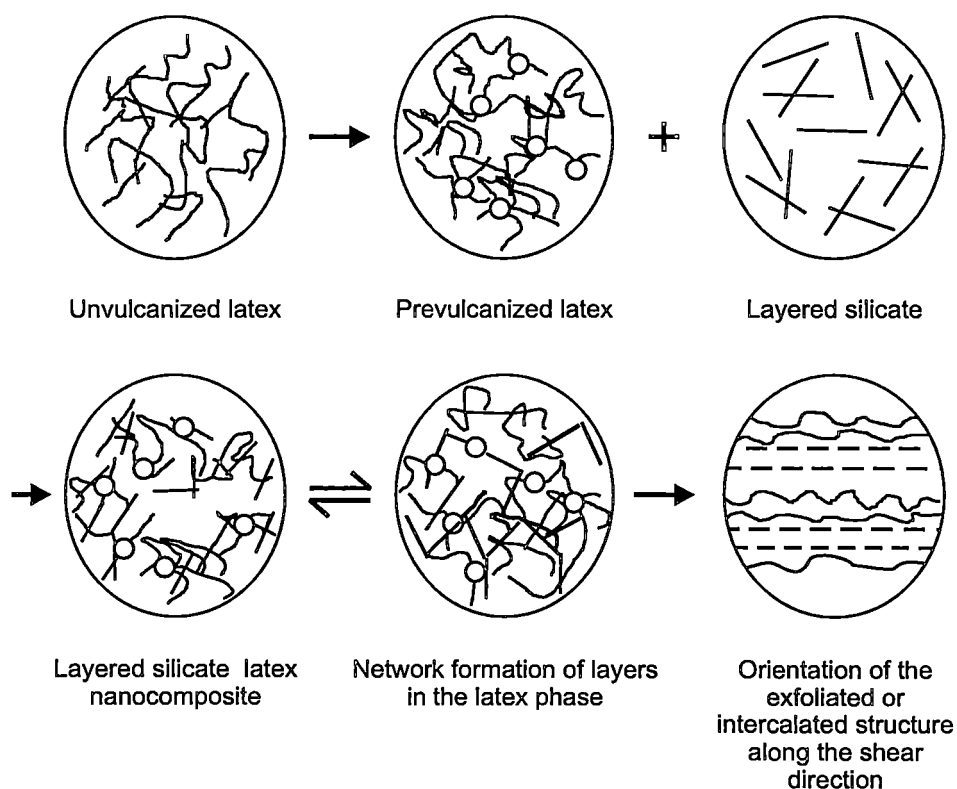
Figure 5.2 Schematic representation of rubber hydrocarbon and layered silicate and their alignment in the shear direction

The network formation of the layers in the nanocomposites at small shear rates and their orientation along with the rubber molecule is illustrated in the scheme.

The variation of viscosity with shear rate at different temperatures is given in Figure 5.3.
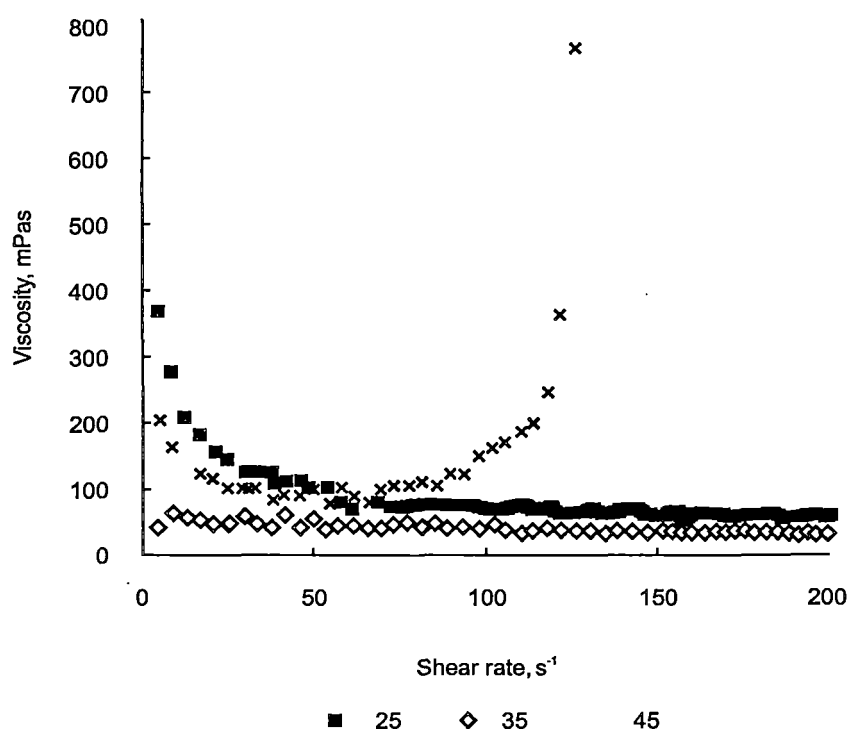
Figure 5. 3 Effect of viscosity on shear rate of bentonite-nanocomposite at different temperatures (5 phr loading)

Due to the non-Newtonian behaviour, a single viscosity measurement of latex at a particular temperature is not enough to understand its flow behaviour. The study was conducted at three different temperatures 25, 35 and 45°C, which are the conventionally adopted ranges of temperatures for the manufacture of

latex goods. The viscosity shows only minor changes with temperature, which might be due to the small differences in the selected temperatures. However at 45°C, there is a sudden increase in viscosity (> 50s^{-1}) which may be due to the coagulation of latex at high temperature and shear rate. As the temperature increases the networks gets aligned so as to increase the free volume and as a result the flow units become less restricted and less organized [22]. At 1phr loading of fluorohectorite, the viscosity rises first and then remains almost constant with rise in temperature. In all systems the viscosity of layered silicates reinforced latex samples decrease with increase in shear rate representing pseudoplastic nature or shear thinning behaviour.
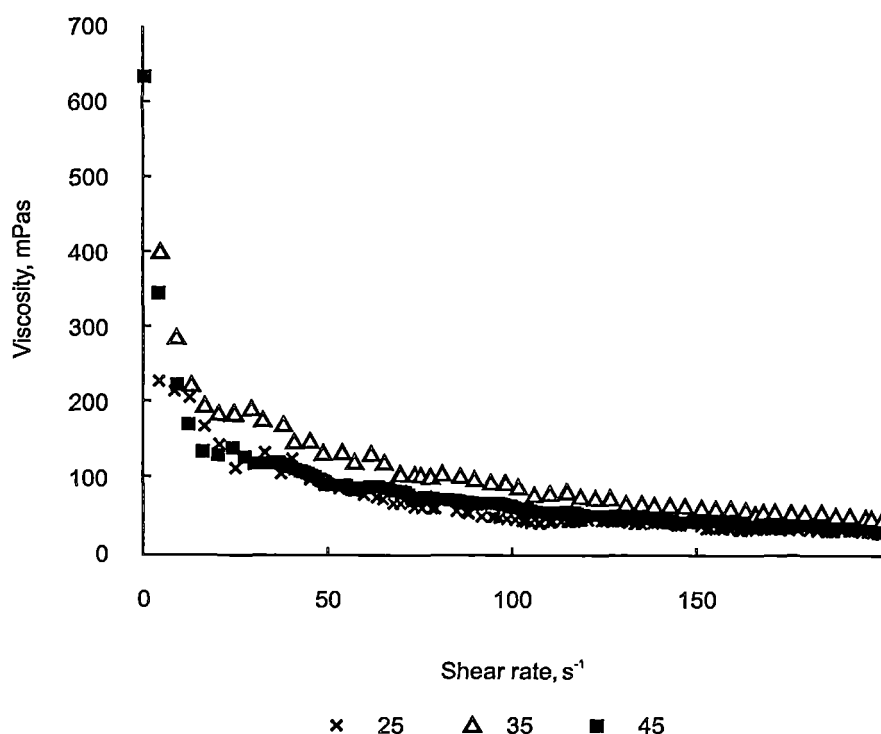
Figure 5.4 Effect of viscosity on shear rate of fluorohectorite-nanocomposite at different temperatures (5 phr loading)

However in the case of fluorohectorite (Figure 5.4) modified latex, the change in viscosity with temperature is negligible. The process stability and consistency at elevated temperature are much better with fluorohectorite compared to bentonite. This might have practical significance in heat sensitized dipping of prevulcanized latex nanocomposites.
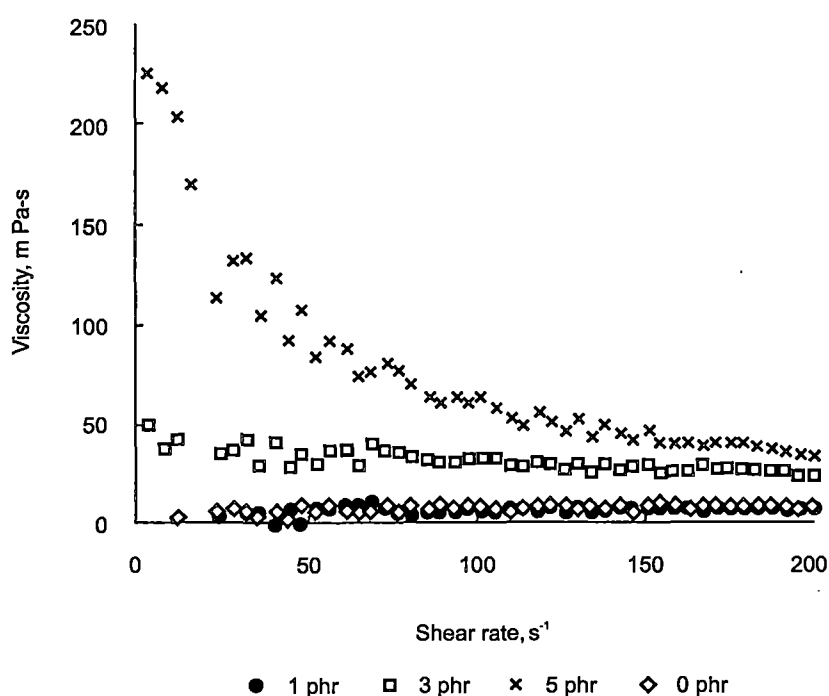
Figure 5.5 Effect of viscosity on shear rate of fluorohectorite-nanocomposites at different loading (temperature 25°C)

The effect of viscosity of the latex at different loading of fluorohectorite (25°C) is given in Figure 5.5. There is a steady increase in viscosity with higher levels of fluorohectorite. For every nano-filler there is a threshold level, above which the filler particle agglomerates in the medium, which leads to poor

mechanical properties. It has been found that for NR latex – fluorohectorite system, 3phr loading is sufficient for reinforcement [23]. At 5 phr loading of fluorohectorite, there is structure formation at low shear rate (>75 s^{-1}) whereas at high shear rates shear thinning occurred.

The viscosity changes for different silicates at a shear rate of 78s^{-1} are given in Figure 5.6.
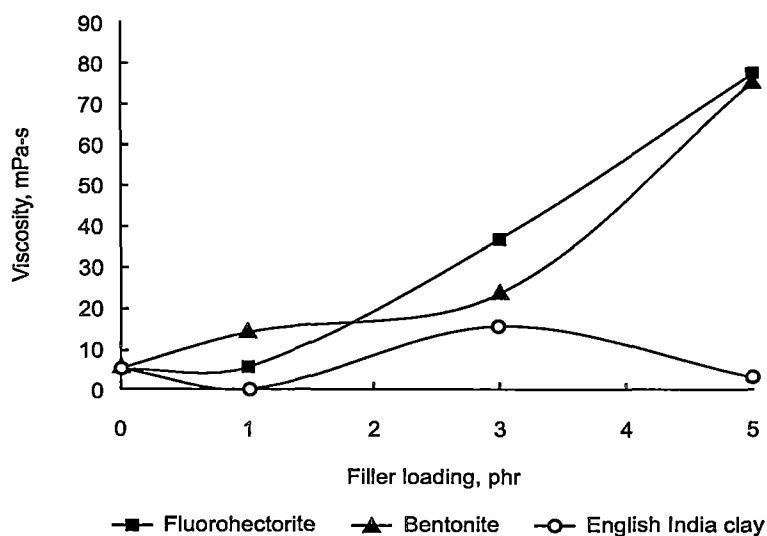
Figure 5. 6 Effect of viscosity on filler loading of NR latex nanocomposites at a shear rate of 78 s^{-1} at 25°C

Initially there is very little change in the viscosity whereas higher viscosity values were recorded for further addition of the layered silicates. However this change is minimum with English Indian clay (non layered version). The surface area of non-layered silicate is 10 m^2/g whereas the effective surface area is in a partially exfoliated system is 790 m^2/g. This accounts for the higher viscosity

of the layered silicate-latex system. The restriction offered by the filler to the Brownian movement of the latex particles seems to overcome at higher shear rates.

5. 2. 2 Activation energy (E$_a$)

The effect of temperature on the viscosity of latex nanocomposites is shown in Figure 5.7. The viscosities of all systems decrease with increase in temperature as the networks get collapsed and the flow units become less restricted and organized.
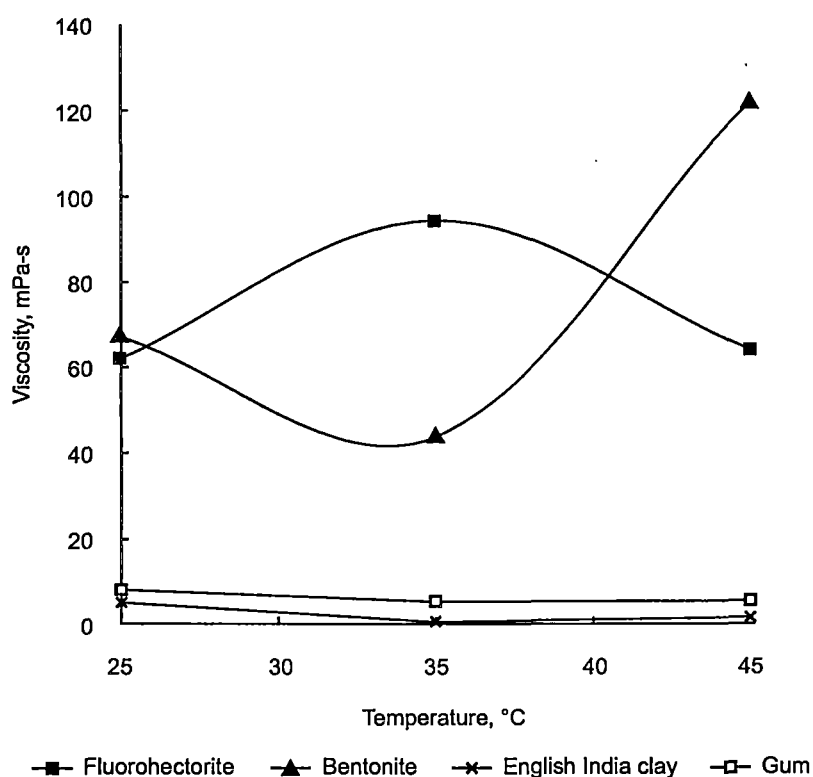
Figure. 5. 7 Effect of viscosity on temperature of NR latex nanocomposites at 5 phr loading (shear rate 95s^{-1})

The effect of temperature on the flow behaviour of layered silicates reinforced latices is further analyzed from the Arrhenius plots using the equation,

$$\eta = \eta_0\, e^{-E_a/RT} \qquad\qquad\qquad\qquad \dots\dots\dots\dots\dots\dots\dots\dots 3$$

Where, E_a is the activation energy, R is the universal gas constant and T is the absolute temperature.

-◇- Gum   -✕- English Indian clay   -○- Bentonite   -■- Fluorohectorite
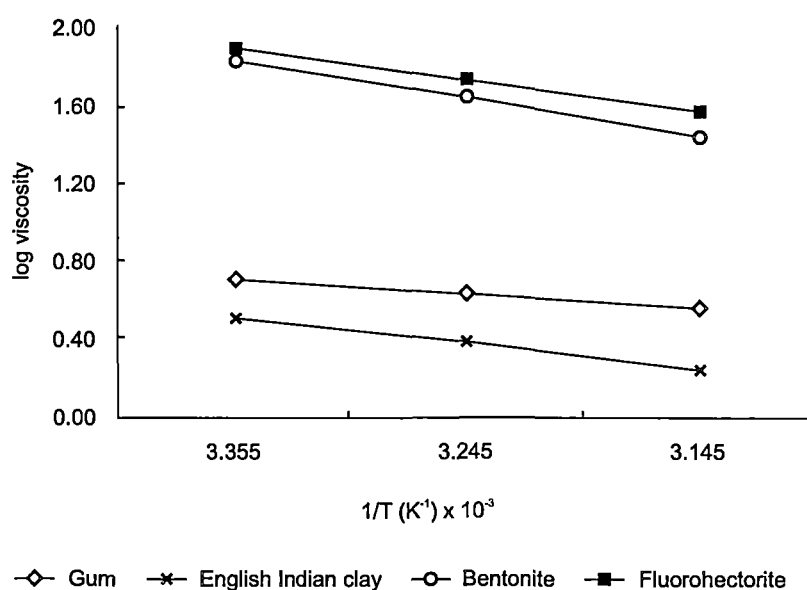
Figure 5.8 Arrhenius plots of nanocomposites at 5 phr loading (shear rate 95 s⁻¹)

Arrhenius plot at a specific shear rate (95s⁻¹) and at 5 phr loading is given in Figure 5.8. The activation energy of different silicates at 5 phr loading at a specific shear rate (95s⁻¹) was calculated and is given in Table 5.1.

Table 5.1 Activation energy at a shear rate of 95 s^{-1} (filler loading 5 phr)

Sample	Activation energy (kJ/mol)
Gum compound	80.15
English Indian clay	151.60
Bentonite	222.38
Fluorohectorite	186.18

From this it is clear that the activation energy is higher for layered silicates than the gum compound. This may be due to the higher level of intercalation of the rubber molecules with layered silicates.

5.2.3 Zero shear viscosity (η_0)

Figure 5.9 shows the effect of filler loading on zero shear viscosity at 25°C. The general trend observed is the decrease of zero shear viscosity with temperature. This was associated with the temperature-induced molecular network break down.
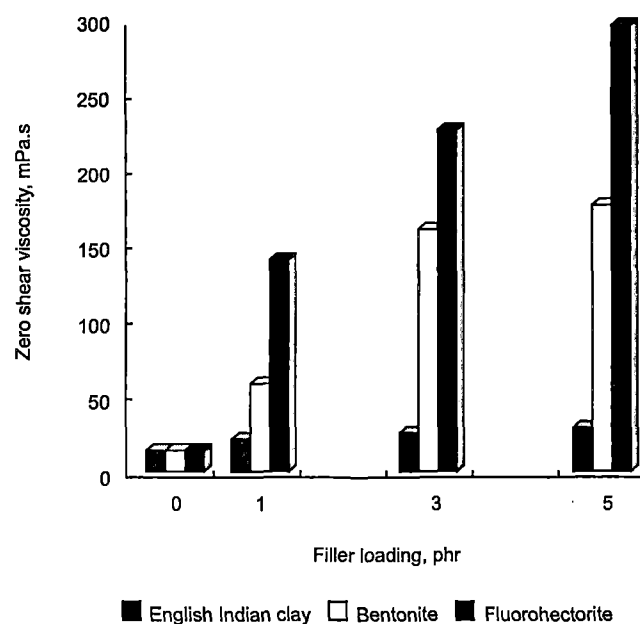
Figure 5.9 Zeroshear viscosity versus filler loading at 25°C

It was also noticed that η_0 of nanocompounds show a sharp increase compared to the English Indian clay-compound. This shows influence of high aspect ratio in polymer-filler intercalation.

5.2.4 Yield stress (τ_0)

Figure 5.10 shows the effect of filler loading on yield stress at 25°C. Yield stress (τ_0) of a polymer can be assessed as a measure of the extra shear stress due to interparticle interactions.

Filler loading, phr

■ English Indian clay ☐ Bentonite ■ Fluorohectorite
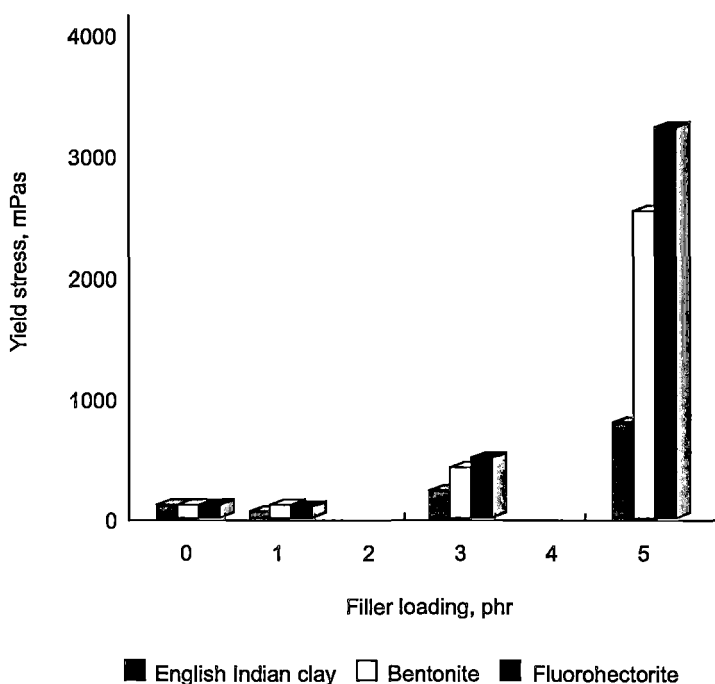
Figure 5.10   Yield stress versus filler loading of latex-nanocomposites at 25°C

There is an initiating force to start the flow in a colloid. Therefore, a finite stress is to be applied to initiate the flow in these systems. At that point the network begins to break. Thus the flocculated system has containing aggregated

particles divided into single units. Yield stress represents the maximum value of force per unit area that the network can withstand before breaking. The nanocomposites show high values of yield stress than the compound with English Indian clay.

5.2.5 Pseudoplasticity index (*n*)

Natural rubber latex is a pseudoplastic fluid and when sheared the rubber particles are progressively aligned and offers less resistance to flow. So the apparent viscosity of the latex decreases on increasing shear rate and continues until the flow curve becomes linear. The extent of non-Newtonian behaviour of the system can be rated from the n values. The effects of temperature and filler content (5 phr) on the flow behaviour indices of the samples are given in Table 5.2.

Table 5.2 - Pseudoplasticity index (n) of nanocomposites at 5 phr loading

| | Pseudo plasticity index (n) | | |
| | Temperature, °C | | |
Sample	25	35	45
Gum compound	0.93	0.86	0.76
Fluorohectorite	0.42	0.406	0.38
Bentonite	0.39	0.346	0.29
English Indian clay	0.79	0.71	0.66

The pseudoplastic, dilatant and Newtonian behaviour of polymers are characterized by *n* which have values *n* <1, *n* >1 and *n* =1 respectively. A high

value of '*n*' shows less pseudoplastic nature of the material. The increase in pseudoplasticity shows a higher extent of silicate exfoliation associated with network build-up of layers.
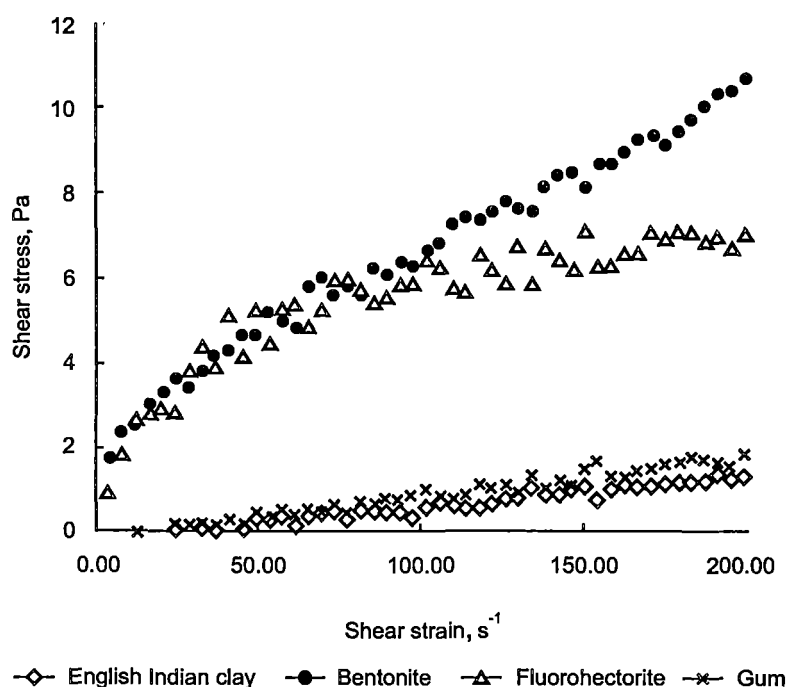
Figure 5.11 Stress - strain curves of latex nanocomposites at 5 phr loading of layered silicates (temperature 25°C)

As the strain increases the shear stress also increases in all cases (Figure 5.11). In the case of gum and English Indian clay there is not much increase in stress values but in the case of nanofillers there is very appreciable change especially in the case of bentonite. This may be because of the network formation and the stress for the alignment of the filler-polymer network. The fine sheets of silicate layers formed during exfoliation align along the direction of the rubber hydrocarbon at elevated stress.

5.3 Conclusion

The flow behaviour of latex nanocomposites depends on the nature of the silicates (layered or non-layered). It is found that viscosity decreases with shear rate for all silicates and layered silicates register the higher shear viscosity values. The higher viscosity of layered silicates nanocomposites is due to the intercalation of rubber hydrocarbons. Natural rubber latex nanocomposites show shear thinning behaviour at higher shear rates due to orientation of the exfoliated or intercalated structure along the shear direction. As the loading of layered silicate increased, the viscosity of the compound also increased especially at low shear rates. The intercalation/ exfoliation can be related to the higher zeroshear viscosity, higher yield stress, higher activation energy (E_a) and higher pseudoplasticity index (n).

5.4 References

1.   A. Mousa, J. Karger-Kocsis, *Macromol. Mater. Eng.*, **286**, 260 - 266, 2001

2.   K. M. Lee, C. D. Han, *Macromolecules*, **36**, 19, 7165 - 7178, 2003

3.   Y. Wang, L. Zhang, C. Tang, D. Yu, *J Appl.Polym Sci*, **78**, 1879 - 1883, 2000

4.   M. Chen, N. J. Ao, Y. Chen, H. P. Yu, H. L. Qian , C. Wang , H. L. Zhou, J. L. Qu, C. K. Guo, *J. Appl. Polym. Sci.*, **82**, 338 - 342, 2001

5.   S. Varghese, J. Karger-Kocsis, *Polymer*, **44**, 17, 4921 - 4927, 2003

6.   S. Varghese, J. Karger-Kocsis, K. G. Gatos, *Polymer*, **44**, 3977 - 3983, 2003

7.   M. Alexander, P. Dubois, *Mater. Sci. Eng.*, **28**, 1 - 63, 2000

8.   S. S. Ray, M. Bousmina, *Progr. in Mater. Sci.*, **50**, 962 - 1079, 2005

9.   D. J. Weeks, W. J. Allen, *Mech. Eng. Sci.*, **4**, 380 - 400, 1962

10.   R. F. Heitmiller, R. Naar, H. H. Zabusky, *J. Appl Polym Sci.*, **8**, 873 - 880, 1964

11.   K. A. Moly, Z. Oommen, S. S. Bhagawan, G. Groeninckx, S. Thomas, *J. Appl. Polym. Sci.*, **86**, 3210 - 3225, 2002

12.   P. Mukhopadhyay, G. Chowdhury, C. K. Das, *Polymer-Plastics.Techn. Enginee.*, **28**, 5 & 6, 517 - 535, 1989

13.   R. Stephen, R. Alex, T. Cherian, S.Varghese, K. Joseph, S.Thomas, *J. Appl. Polym. Sci.*, **101**, 2355 - 2362, 2006

14.   J. T. Varkey, S. Thomas, S. S. Rao, *J. Appl. Polym. Sci.*, **56**, 4, 451 - 460, 1995

15.   A. Lazzeri, S. M. Zebarjad, M. Pracella, K. Cavalier, R. Rosa, *Polymer*, **46**, 827- 844, 2005

16.   J. A. Lee, M. Kontopoulou, J.S.Parent, *Polymer*, **45**, 6595 - 6600, 2004

17.   K. M. Lee, C. D. Han, *Polymer*, **44**, 16, 4573 - 4588, 2003

18.   J. Ren, B. F. Casanueva, C. A. Mitchell, R. Krishnamoorti, *Macromolecules*, **36**, 11, 4188 - 4194, 2003

19.   T. G. Gopakumar, J. A. Lee, M. Kontopoulou, J. S. Parent, *Polymer*, **43**, 5483 - 5491, 2002

20.   A. Lele, M. Mackley, G. Galgali, C. Ramesh, *J. Rheol.*, **46**, 1091 - 1110, 2002

21.   J. A. Brydson, Flow Properties of Polymer Melts, 2nd edn, Eds, George Godwin Plastics Rubber Institute, London, 1981

22.   R. S. Lenk, Polymer Rheology, Applied Science Publishers, London, 1978

23.   S. Mathew, S.Varghese, *J Rubb. Res*, **8**, 1, 1 - 15, 2005

Dipping Characteristics of Layered Silicate-Natural Rubber Latex Nanocomposites

The dipping characteristics of prevulcanized natural rubber latex containing three different types of silicates (fluorohectorite, bentonite and English Indian clay) were studied using a semi-automatic dipping machine. The effect of variation in the speed of immersion and withdrawal of the glass former, dwell time and concentration of the coagulant *etc.* on the thickness of the latex deposit were investigated. Characterization of the composites was done using X-ray diffraction (XRD) and transmission electron microscopy (TEM). The viscosities of these compounds were measured using a Brookfield viscometer. The results of the studies showed that the deposit thickness depends on the withdrawal speed of the glass former, the concentration of the coagulant, dwell time and the viscosity of the latex compound. Higher film thickness was noticed for the bentonite clay filled composites. This was believed to be due to the formation of clay network formation in the composites.

6.1 Introduction

Natural rubber latex is a macroscopic dispersion of rubber particles in an aqueous medium. This macroscopic viscous rubber medium (latex) is converted to elastic rubber through crosslinking of the macromolecules at their reactive sites (vulcanization). The introduction of organic accelerators in the vulcanization process enabled to reduce the vulcanization time and impart optimum physical properties [1, 2]. This prevulcanized latex is an important raw material for the production of many dipped goods. Approximately 600,000 tonnes of latex concentrate is consumed in this way. In the case of dry rubber, carbon black and other inorganic minerals (calcium carbonate, silicates etc) are used to improve the mechanical properties of the vulcanized rubbers. Carbon black offers excellent reinforcement owing to its strong interaction with rubbers, but at high loading, it decreases the processability of rubber compounds. The reinforcing capacity of silicates is poor due to the large particle size and low surface activity. Now-a-days there is great interest in the development of polymeric nanocomposite using layered silicates as reinforcing material [3-8]. Provided that the layered silicates fully delaminate (termed exfoliation) dispersing less than 10% of them may replace 3-4 times higher amount of traditional fillers without sacrificing the processability and mechanical properties. The concept of nano-reinforcement with layered silicates became very popular in late 1980s [8-9]. Polymer nanocomposites represent a new alternative to conventionally (macroscopically) filled polymers. Because of their nanometer level dispersion, nanocomposites exhibit markedly improved properties when compared to pure polymers or traditional analogues. These include increased modulus and strength, outstanding barrier properties, improved solvent and heat resistance and decreased flammability [9-12].

Layered silicate polymer nanocomposites are processable using latest technologies. Layered silicate is comprised of platelets having a planar structure of 1 nm thick and 100-300 nm length. The layers cannot be separated from each other through general rubber processing. Since inorganic ions absorbed by silicates can be exchanged with organic ions, efforts in intercalating many kinds of polymers and to prepare clay/polymer nanocomposites have been reported [13-17]. It has been shown that the silicate layers can be dispersed at molecular level (nanometer scale) in a polymer matrix [10]. In general two types of organic/inorganic hybrids are distinguished: intercalated (polymer chains are diffused between the silicate layers preserving, however, some short range order of the latter) and dispersed (in which the silicate layers of ca.1 nm thick are exfoliated and dispersed in the polymer matrix). Pristine layered silicates usually contain hydrated Na+ or K+ ions. Ion exchange reactions with cationic surfactants, including ammonium ions render the normally hydrophilic silicate to organophilic. This is the prerequisite for intercalation with many engineering polymers. The role of the alkyl ammonium cations in the "usual" organosilicates is to lower the surface energy of the silicate and to improve its wettability by the polymer. Additionally, the alkyl ammonium compounds may contain functional groups, which can react with the polymer or initiate the polymerization of monomers. This may strongly improve the strength of the interface between the silicate and the polymer [18-19]. Rubber-clay nanocomposites were prepared from latex by a coagulation method and an improvement in mechanical properties was reported [14, 15]. Some layered silicates are suitable additives for latex, provided that they can form dispersions adequate for latex compounding [16]. In aqueous dispersions, the clay "swells" (i.e. its layers are separated by hydration) which makes the intercalation due to rubber molecules more feasible.

In this study, the dipping characteristics of prevulcanized latex compounded with layered silicates are illustrated. Compounds are also prepared from an amorphous silica (English Indian clay) for comparison. Parameters such as viscosity, film thickness on rate of immersion and withdrawal of the glass former and dwell time are studied in detail.

6.2 Experimental

The materials, preparation of prevulcanized latex compounds and equipment used are given in chapter 2 and the details of the dipping studies are given below.

6. 2.1 Dipping process

Rate of immersion of the glass former in prevulcanized natural rubber latex (PVNRL) containing two different layered silicates (fluorohectorite and bentonite) and a non-layered silicate on the thickness of the latex deposit was noted. A clean cylindrical glass former (diameter 25 mm and length 300 mm) was fixed on the former supporting bar of the dipping machine and kept over the coagulant tank. A 10% solution of calcium nitrate as coagulant was taken in the coagulant tank. The former was then immersed in the coagulant by lifting the tank hydraulically at a speed of 100 cm/min. The former was then moved over to the tank containing compounded latex and dipped in it by raising the tank at a speed of 100 cm/min, and allowed to dwell for 30 s and then withdrawn (by lowering the tank) at the same speed. The former was inverted and rotated mechanically to obtain a uniform latex deposit on the former. The former was then dried to get a transparent film in the room temperature and vulcanized in an air-circulating oven at 70°C for 2h. The former was then cooled, and the deposit was removed

from the former by applying talc. The thickness of the deposit was measured with a digital micrometer having a sensitivity of 0.001mm. The arithmetic mean of ten measurements was taken as the thickness of the film. The speed of immersion of the former in to the latex tank was changed to 110, 120, 130, 140, and 150 cm/min keeping all the other parameters constant and the thickness of the deposit was recorded. Similarly the effect of other parameters like rate of withdrawal, dwell time, concentration of the coagulant was also studied.

6. 3 Results and Discussion

6. 3.1 Viscosity studies

Figure 6.1 shows viscosity of the latex compounds mixed with different silicates. The viscosity of latex compound has a critical role in most of the manufacturing processes. Bentonite incorporated latex compound showed higher viscosity than other fillers at all loading followed by fluorohectorite. When bentonite is mixed with water, it undergoes considerable swelling due to hydration [1]. Due to this hydration, the initial interlayer distance increases which facilitates the intercalation of rubber molecules. Moreover, the ion-exchange capacity of bentonite is comparatively higher which also influences the intercalation process. Fiurohectorite has lower cation exchange capacity and higher interlayer distance compared to bentonite which registers viscosity values little lower than bentonite except at high loading.
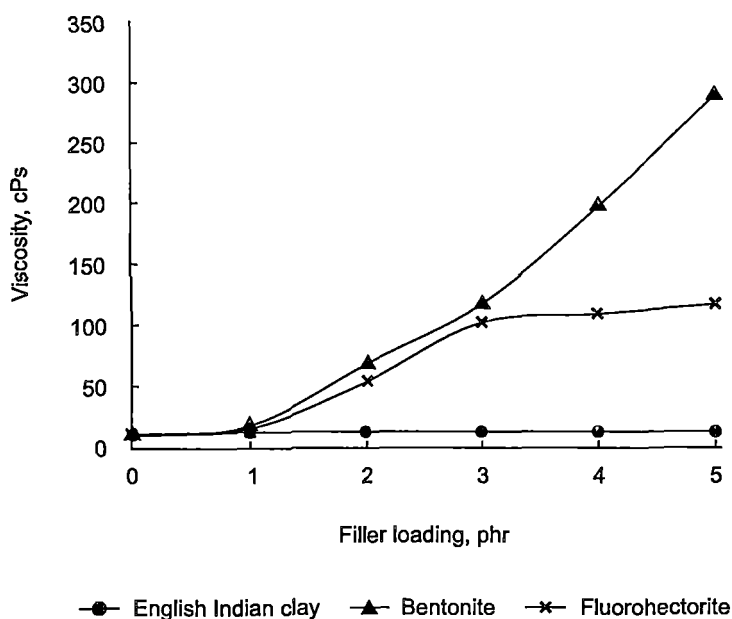
Figure 6.1 Viscosity of the latex compounds mixed with different silicates

However as the O-H bonds in English Indian clay are strong and the layers are resistant to swelling by hydration. Moreover the very low cation exchange capacity (8 meq/100 mg) of English Indian clay makes it impossible to undergo any exchange reactions.

6.3.2 Dipping studies

Figure 6.2 shows the variation in latex film thickness with the speed of immersion of the glass former at a filler loading of 3 phr. As the speed of immersion increased from 100 to 150 cm/min, the thickness of the films show very little change at 1 phr loading (average film thickness 0.15 mm) of the silicates. Though the experiments were conducted with 3 different filler loading

(1, 3 and 5 phr) the shape of the curves were almost identical and hence the discussion was limited only to 3 phr loaded composite. As the filler loading was increased (Figure 6.1) to 3 phr the film thickness of bentonite filled compounds was higher than the other two versions. The film thickness are in the order bentonite> fluorohectorite> gum > English Indian clay.
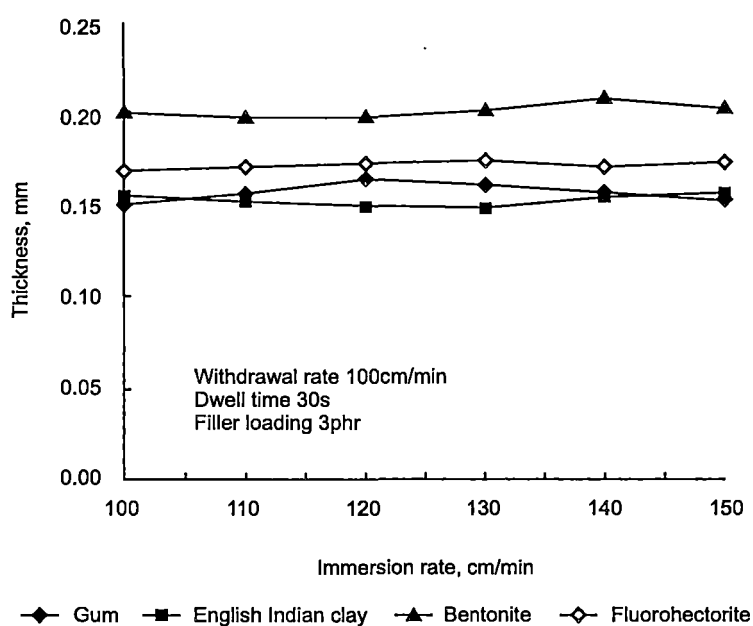
Figure 6.2 The variation in latex film thickness with the speed of immersion of the glass former at a filler loading of 3 phr

Figure 6.3 shows the variation in thickness of the deposit with dwell time. As dwell time increased the film thickness also increased.
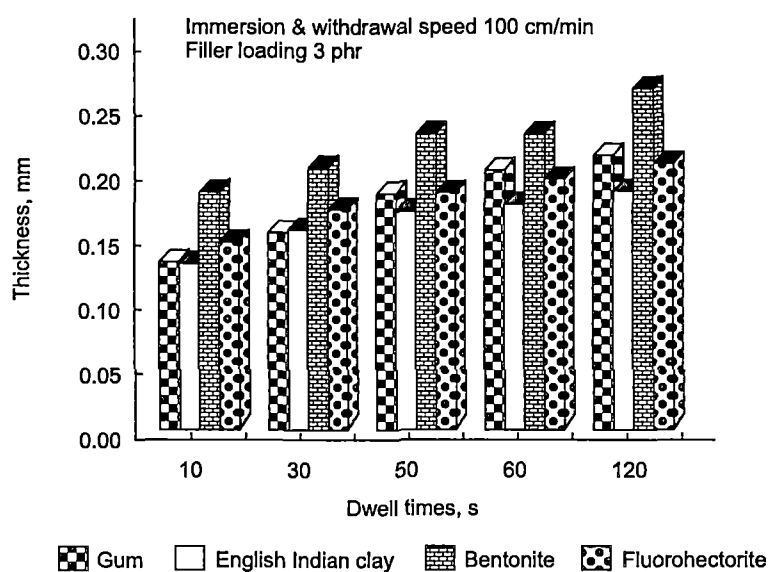
Figure 6.3   The variation in thickness of the deposit with dwell time

Initially there is a gradual increase and thereafter a change is marginal. However bentonite showed high film thickness at all points compared to other clays. As the former with coagulant was immersed in latex, a layer of rubber coagulum was formed immediately, as the dwell time increases, the coagulant ions get more time to diffuse into the latex to form a thick latex deposit [20, 21]. Fluorohectorite showed slight increase in thickness which ranged from 0.15 to 0.22 mm. However in the case of bentonite, the thickness of the deposit increased considerably (0.22-0.32). This may be due to the greater volume of wet latex retained on the former due to the high viscosity of the compound [1, 21, 23].

Figure 6.4 shows the effect on the rate of withdrawal of the glass former on thickness of the deposit.
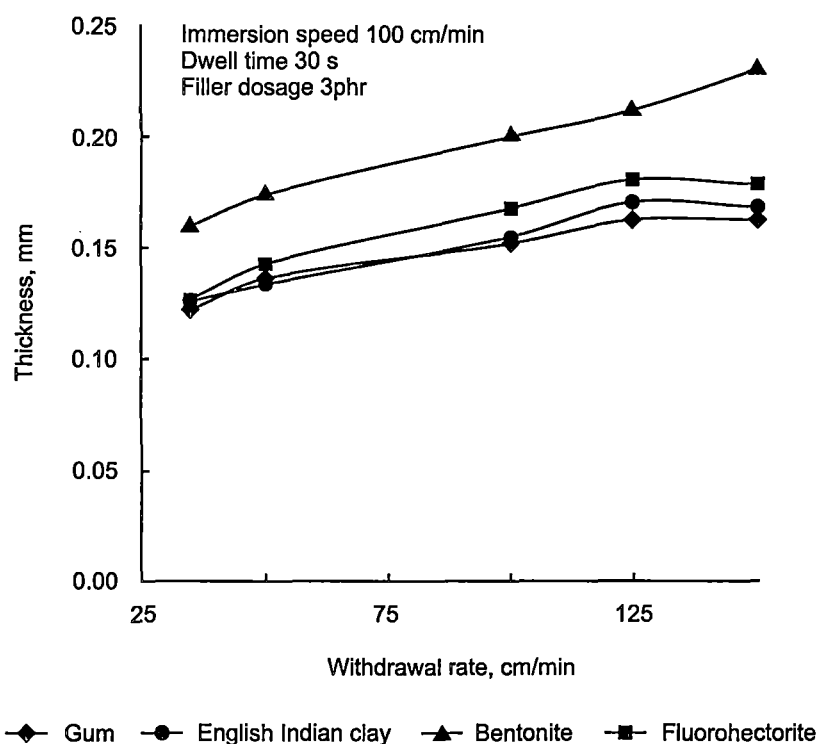
Figure 6.4 The rate of withdrawal of the glass former with thickness of the deposit.

As the rate of withdrawal increased the deposit thickness increased slightly. At 3 phr loading the film thickness did not change considerably, except in the case of bentonite. As the withdrawal speed of the glass former from the latex compound increased, the time obtained to drain the latex deposited on the former decreased, which gives a thick latex deposit on the former [21, 23].

When the immersion and the withdrawal speed are equal the change in deposit thickness is given in Figure 6.5
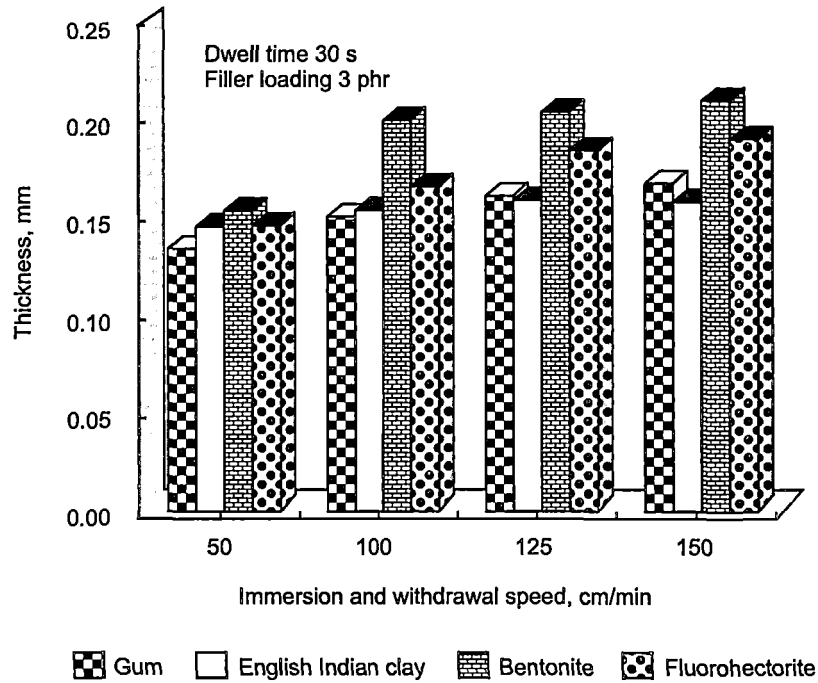
Figure 6.5   The effect of thickness of the deposit at the same immersion and withdrawal rate of the glass former.

At higher speed, the deposit thickness increased. At higher withdrawal rate of the former, the coated latex gets little time for dripping which impart a thick deposit.

Table 6.1 shows the variation of dwell time and coagulant concentration on the deposit thickness. As the dwell time and the concentration of the coagulant increased, the deposit thickness increased. This is due to the fact that as the concentration of the coagulant increased, the amount of coagulant deposit on the former increased and, hence the rate of diffusion of the coagulant into the latex was higher, which lead to a greater thickness [21, 22, 24].

Table 6.1. Effect of concentration of coagulant on deposit thickness, mm

10% Ca $(NO_3)_2$

Dwell time, s	English Indian Clay, phr				Bentonite, phr				Fluorohectorite, phr			
	0	1	3	5	0	1	3	5	0	1	3	5
10	0.130	0.131	0.129	0.126	0.130	0.133	0.182	0.221	0.13	0.128	0.144	0.137
30	0.152	0.152	0.155	0.155	0.152	0.154	0.194	0.238	0.152	0.15	0.168	0.164
50	0.182	0.163	0.170	0.166	0.182	0.177	0.227	0.276	0.182	0.16	0.181	0.180
60	0.201	0.169	0.174	0.177	0.201	0.178	0.228	0.279	0.201	0.167	0.191	0.192
120	0.211	0.207	0.185	0.190	0.211	0.211	0.263	0.314	0.211	0.185	0.203	0.214

20% Ca $(NO_3)_2$

	0	1	3	5	0	1	3	5	0	1	3	5
10	0.160	0.158	0.160	0.173	0.160	0.165	0.207	0.249	0.160	0.153	0.152	0.174
30	0.192	0.195	0.192	0.222	0.192	0.211	0.248	0.284	0.192	0.183	0.197	0.197
50	0.225	0.228	0.243	0.237	0.225	0.225	0.257	0.290	0.225	0.209	0.215	0.223
60	0.235	0.231	0.248	0.252	0.235	0.262	0.290	0.315	0.235	0.216	0.221	0.235
120	0.282	0.273	0.271	0.287	0.282	0.293	0.314	0.334	0.282	0.260	0.263	0.249

30% Ca $(NO_3)_2$

	0	1	3	5	0	1	3	5	0	1	3	5
10	0.179	0.211	0.193	0.195	0.179	0.174	0.226	0.278	0.179	0.169	0.162	0.174
30	0.228	0.244	0.234	0.236	0.228	0.217	0.26	0.303	0.228	0.213	0.231	0.213
50	0.283	0.265	0.272	0.279	0.283	0.241	0.288	0.335	0.283	0.242	0.281	0.249
60	0.300	0.273	0.295	0.302	0.300	0.342	0.348	0.354	0.300	0.264	0.290	0.284
120	0.344	0.340	0.356	0.360	0.344	0.386	0.402	0.417	0.344	0.310	0.336	0.347

6.3.3 Tensile properties

The tensile properties of four compounds are given in Table 6. 2.

Here the effect of different silicates (at different loadings) on tensile strength, elongation at break, modulus at 100 and 300 per cent elongation are given. In the case of amorphous filler, tensile strength values decrease as the loading increases. This decrease may be attributed to its high particle size. In the case of modulus, almost similar behaviour was observed. As the loading increases the elongation at break of the amorphous filler increased. It is to be noted that at low elongation (100%) there is a gradual increase in modulus, which is in the order English Indian clay < bentonite < fluorohectorite.

Table 6.2 Tensile properties of PVNRL containing different silicates

| Properties | Material | Loading, phr | | | |
		0	1	3	5
Tensile strength, MPa	English Indian clay	24.7	23.8	22.5	23.4
	Bentonite	24.7	24.9	25.0	25.7
	Fluorohectorite	24.7	25.0	25.8	26.6
Elongation at break, %	English Indian clay	837	842	850	1039
	Bentonite	837	821	773	747
	Fluorohectorite	837	810	782	732
100% modulus, MPa	English Indian clay	0.64	0.63	0.62	0.59
	Bentonite	0.64	0.72	0.83	1.02
	Fluorohectorite	0.64	0.84	0.90	1.10
300% modulus, MPa	English Indian clay	0.97	0.99	1.11	1.02
	Bentonite	0.97	1.01	1.39	2.10
	Fluorohectorite	0.97	1. 23	1.75	2.14

There is an increase in modulus with fluorohectorite at 300 per cent elongation followed by bentonite. However, at the same elongation the magnitude of the modulus value at 5 phr loading is higher when compared to that at 3phr loading especially with layered silicates. In the case of commercial clay-filled vulcanizates this difference is negligible. The silicate layers may favour the formation of immobilized or partially immobilized polymer phases, which may contribute for high modulus [25]. In the vulcanizate containing layered silicate, a part of the silicate was exfoliated which offered high surface area for reinforcement. The fine sheets of silicate layers orient along the strain direction, which increases with increased strain. The low stiffening effect of commercial clay can be attributed to its high particle size and poor dispersion.

6.4 Conclusion

The dipping characteristics of prevulcanized latex compounds containing layered silicates showed that they behave almost similar to conventional latex compounds. Parameters such as immersion rate, withdrawal rate, dwell time and concentration of coagulant etc have found effect on film thickness. Bentonite, with filler network showed higher compound viscosity and greater film thickness. The thickness of the deposit was found to increase with dwell time as well as increased concentration of coagulant. The thickness of latex deposit increased as the speed of withdrawal increased. Superior mechanical properties were observed with layered silicate incorporated vulcanizates.

6.5 References

1. D. C. Blackely, Polymer Latices, Volume 3, Eds. Chapman & Hall, John Wiley, London, 150, 1997

2. A. D. Roberts, Natural Rubber Science and Technology, Oxford Science Publishers, London, 1989

3. M. Kato, A. Usuki, Polymer-Clay Nanocomposites, Ed. T. J. Pinnavaia, G.W. Beall, J. Wiley, New York, 97, 2000

4. B. B. Boonstra, *Polymer*, **20**, 691 - 704,1979

5. S. Varghese, J. Karger-Kocsis, *J. Appl. Polym. Sci.*, **91**, 2, 813 - 819, 2004

6. F. Schon, W. Gronski, *Kautschuk Gummi Kunststoffe*, **56**, 166 - 171, 2003

7. M. Arroyo, M.A. López-Manchado, B. Herrero. *Polymer*, **44**, 8, 2447 - 2453, 2003

8. A. Usuki, A. Tukigase, M. Kato, *Polymer*, **43**, 2185 - 2189, 2002

9. Y. Kojima, A. Usuki, M. Kawasumi, A. Okada, T. Kurauchi, O. Kamigaito, *J. Appl. Polym. Sci.*, **49**, 7, 1259 - 1264, 1993

10. M. Alexandre, P. Dubois, *Mater. Sci. Eng.*, **28**,1 - 63, 2000

11. S. Varghese, K. G. Gatos, A. A. Apostolov, J. Karger-Kocsis, *J. Appl. Polym. Sci.*, **92**, 543 - 551, 2004

12. J. W. Gilman, T. Kashiwagi, Special Polymers and Applications, Eds. T. J. Pinnavaia, G.W. Beall, 127, 2000

13. S. Mathew, S. Varghese, *J. Rubb. Res.*, **8**, 1, 1 - 15, 2005

14. Y. Wang, L. Zhang, C.Tang, D.Yu, *J. Appl. Polym. Sci.*, **78**, 1879 -1883, 2000

15. M. Chen, N. J. Ao, Y. Chen, H. P.Yu, H. L. Qian, C. Wang, H. L. Zhou, J. L. Qu, C. K. Guo, *J. Appl. Polym. Sci.*, **82**, 338 p, 2001

16. S. Varghese, J. Karger-Kocsis, *Polymer*, **44**,17 4921 - 4927, 2003

17. G. Heinrich, M. Kluppel, *Adv. Polym. Sci.*, **160**, 1 - 44, 2002

18. J. Oberdisse, B. Deme, *Macromolecules*, **35**, 4397 - 4405, 2002

19. Z. Wang, J. Massam, T. J. Pinnavaia, Epoxy-Clay Nanocomposites. Eds T. J. Pinnavaia, G. W. Beall, J. Wiley, New York, 127, 2000

20. R. S. Dargo, Physical Methods in Chemistry (Saunders, W.B Company), West Washington Square, Philadelphia., 600, 1977

21. K. K. Sasidharan, R. Joseph, G. Rajammal, P. Viswanatha Pillai, K. S. Gopalakrishnan, *J. Appl. Polym. Sci.*, **81**, 3141- 3148, 2001

22. A. D. T. Gorton, G. C. Iyer, *J. Rubber Res. Inst. Malaya.*, **23**, 263 - 276, 1973

23. T. D. Pendle, Natural Latex Dipping Technology; Herts, ALSTEF, England, 1996

24. A. D. T. Gorton, *J. Rubb. Res. Ins. Malaya.*, **20**, I, 27-35, 1967

25. M. Ganter, W. Gronski, P. Reichert, R. Mulhaupt, *Rubb. Chem. Technol.*, **74**, 2, 221- 235, 2001

Degradation Behaviour of Natural Rubber Layered Silicate Nanocomposites

The degradation behaviour of natural rubber latex nanocomposites against various degrading agents *viz.* thermal, γ and UV radiations, chlorination, sterilization, ozone and solvents were studied in detail. It was found that layered silicate nanocomposites performed well against most of the degrading agents and such materials are suitable for processes like chlorination, sterilization etc. It was found the degrading action was arrested either due to the hindrance exerted by clay layers against crack propagation or due to the barrier effect against the degrading agents. Kraus plot showed a strong filler rubber interface in rubber nanocomposites. Schematic representation of degradation of the nanocomposite demonstrated the effect of nanofillers in chain scission or cross linking that may occur during degradation.

7.1 Introduction

Oxygen, ozone, heat, solvents and high energy radiations are the most common agents, which cause degradation of polymers. Unsaturation in elastomer makes it more susceptible to oxidation. Prolonged exposure to heat causes thermo-oxidative degradation of rubber and results in the deterioration of its physical properties eventually leading to premature failure. Thermo-oxidative ageing of rubber is believed to occur either by the main chain or by the crosslink scission. In routine technological evaluation, rubber compounds were subjected to accelerated ageing tests to get information about their service life.

Fillers are used in latices either to reduce the cost or to modify the viscosity, and also as reinforcing agent. One interpretation is that during the process of mastication polymer free radicals are produced from the disintegrating rubber molecules, and these radicals being very labile, are able to interact with reactive sites on the periphery of the filler particles. The commonly used fillers in latex include clay, whiting and silica. Recently, polymer layered silicates composites have been studied due to their enhanced mechanical and barrier properties [1-2]. The most commonly used layered silicates belong to bentonite, hectorite and montmorillonite. The important characteristics of these layered silicates are their ability to undergo ion exchange reactions with inorganic and organic cations and to disperse as single layers. According to the interaction between the polymer matrix and layered silicates, three different types of polymer layered silicate nanocomposites can be thermodynamically possible and are named as intercalated, flocculated and exfoliated nanocomposites. Due to the high contact area, layered silicate-natural rubber nanocomposites showed good mechanical and barrier properties [3-4].

Layered silicates get easily exfoliated in latex due to the hydration of interstational cations [5-7]. Hence in latex–layered silicate nanocomposites, the hydrocarbon chains are well surrounded by clay layers which will suppose to increase the thermal stability of the composites [8-11]. In this study the degradation behavior of nanocomposites prepared from layered silicates and natural rubber latex was undertaken.

7.2 Results and discussion

7.2.1 Characterization of NR nanocomposites

7.2.1.1 XRD analysis

The XRD spectrum of pure clay and that of the NR latex nanocomposites (5 phr loading) is given in Figure 7.1.
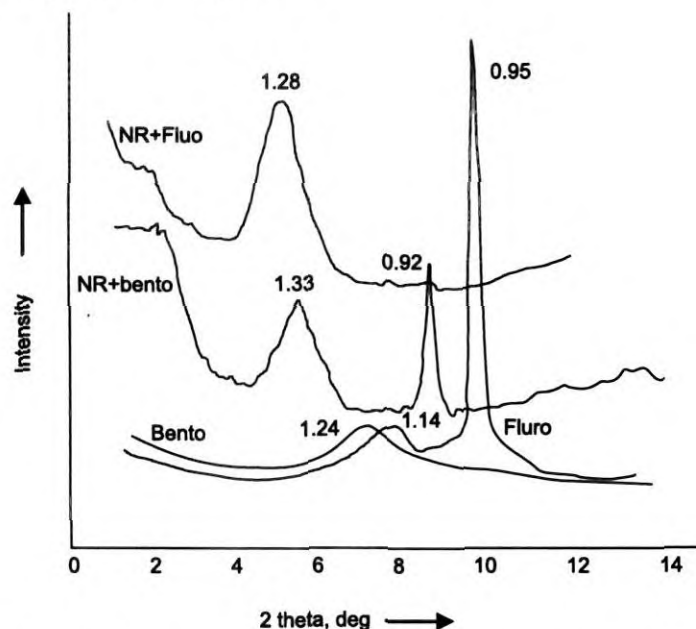
Figure 7.1 XRD pattern of pristine layered silicates (fluorohectorite and bentonite) and that of the corresponding NR nanocompsites at 5 phr loading

Sodium bentonite exhibits a single peak at 7°, which corresponds to a basal spacing of 1.24 nm. Sodium fluorohectorite has two peaks, one at 8° and the other 9.5° corresponding to a basal spacing of 1.14 and 0.95 nm respectively. As shown in Figure 7.1, the basal spacing of Na- bentonite filled NR is shifted to 1.33 nm, indicating that the NR chains get intercalated into the galleries of Na-bentonite. The peak at 0.92 might result from the un-intercalated clay layers. Fluorohectorite filled NR shows a broad peak at a basal spacing of 1.28 nm.

7.2.1.2 TEM and SEM Analysis

The dispersion of layered silicates in the nanocomposites was observed by TEM and was illustrated in Figures 7. 2a and b.
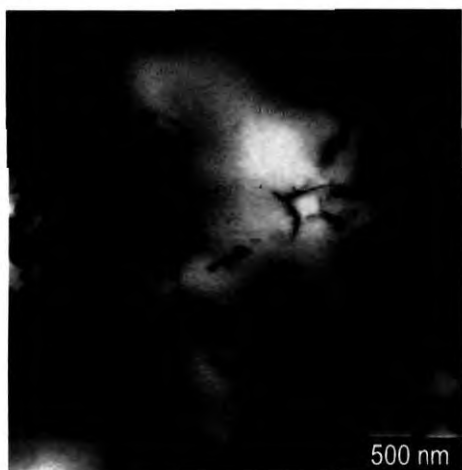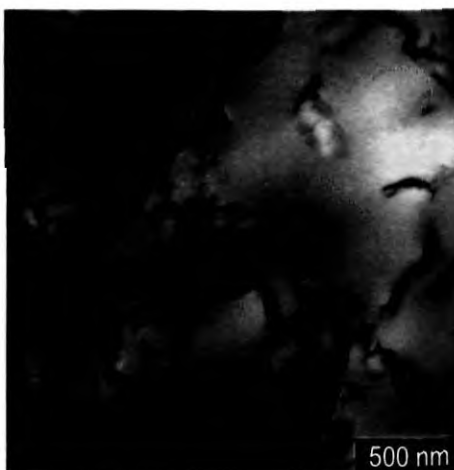
Figure 7. 2a   Figure 7. 2b

Figure 7. 2 TEM photographs of (2a) bentonite and (2b) fluorohectorite at 5 phr loading

Layered silicates showed excellent dispersion in NR latex as compared to conventional composites. The related TEM pictures represent the bentonite clay (7.2a) and sodium fluorohectorite filled NR (7.2b) composites, respectively.

In the bentonite filled composites, the filler was dispersed as intercalated particles (Figure 7. 2a) whereas fluorohectorite exist as thin silicate sheets (Figure7.2b).

Fluorohectorite 10 x 7500   ⊢— 5 μm —⊣   Bentonite 10 x 20,000   ⊢— 2 mm —⊣   ɜntonite 10 x 20,000i----------2 m

Figure 7. 3a   Figure 7. 3b
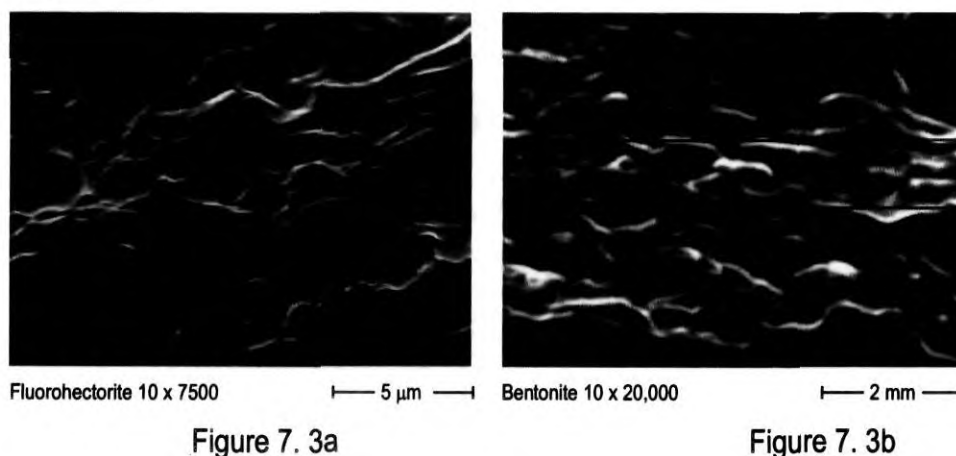
Figure 7.3 SEM photographs of (3a) fluorohectorite and (3b) bentonite at 5 phr loading

In the corresponding SEM pictures (Figures 7. 3a and 3b) bentonite was dispersed as loose aggregate mass whereas fluorohectorite has more compact well dispersed structure.

7.2.1.3 TGA analysis

Thermogravimetric analysis measures the change in weight of the material when it is heated in an inert atmosphere or in the presence of air/ oxygen. When a rubber compound is heated at lower temperature the volatile components will move out. At 100°C moisture present in the rubber will get evaporated. When the heating continues the polymer part will get degraded and converted into gaseous products, a corresponding loss in weight is reflected in the curve. Further heating will remove other components which will be reflected in the TGA curves.
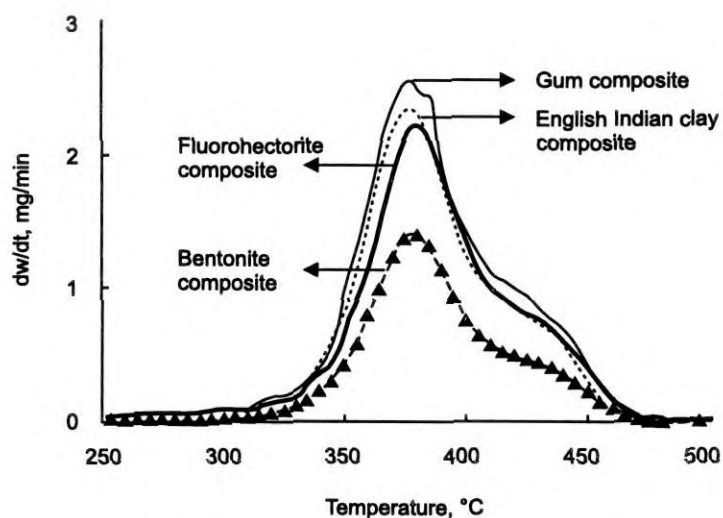
Figure 7. 4 Thermogram of the layered silicate nanocomposite prepared
from sulphur prevulcanized NR latex nanocomposites   at a
loading of 5 phr

Figure 7.4 shows the effect of nanosilicates against thermal degradation.
It is clear that the dw/dt values are in the order gum composite> English Indian
clay composite> fluorohectorite composites> bentonite composite.

Table7.1 Per cent weight loss with temperature (°C) of nanocomposites

Sample	Degradation temperature (°C)				
	10%	30%	50%	70%	90%
NR gum composite	337.5	365.1	376.6	378.9	428.6
NR composite with English Indian Clay	339	366.1	379	398.4	434
NR nanocomposite with bentonite	343	367.5	381	399.6	437
NR nanocomposite with fluorohectorite	342.8	368.7	383.6	403.4	442.4

From the Table 7.1 it is clear that the degradation temperature at 10 to 90
per cent weight loss is higher for layered silicates than the gum and amorphous

clay composites. At lower temperature, filled NR shows slight difference in thermal stability but at higher temperature nanofilled NR showed enhanced thermal stability. This may be attributed to the improved layered silicates- matrix interaction. Nanosilicates can interact better with the matrix due to their higher surface area. This makes the matrix stiffer and the diffusion of heat and gases through the bulk more difficult which retards the degradation of the composite.

7.2.2 Degradation studies

7.2.2.1 Effect of hot air ageing

Figure 7.5 shows the percentage retention of tensile strength after thermal ageing at 100°C for 24 and 48h. After 48h, though the retention values of the composites were decreased to more than 50 per cent of the original, fluorohectorite and bentonite showed comparatively better retention values. This might be due to the protection of polymer chains by surrounding silicate platelets.
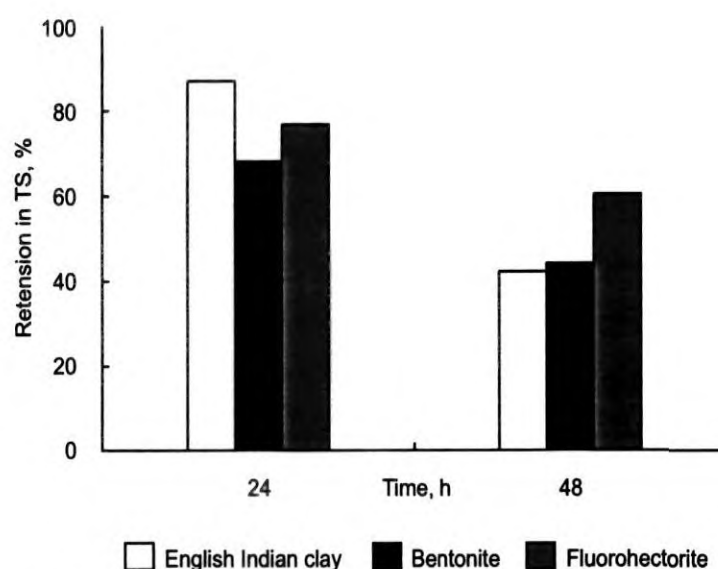
Figure 7.5   Percentage retention of tensile strength after ageing at 100°C

The percentage retention of elongation at break at 100°C for two different intervals is given in Figure 7. 6.
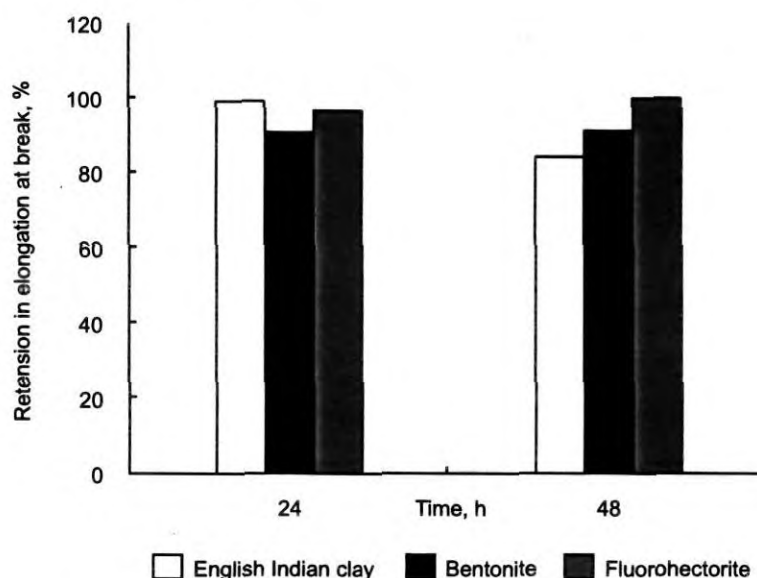
Figure 7. 6 Percentage retention of elongation at break after ageing at 100°C

At 24h, the elongation values are almost unaffected. On prolonged ageing (48h) percentage retention in elongation at break follows the order fluorohectorite > bentonite > English Indian clay. Even though the layers are 'inorganic' in nature, because of their very large aspect ratio and nanometer thickness, they behave mechanically more like thin sheets rather than thick rigid plates. This flexibility (elastic nature) of the silicate layers contributes to the elongation at break of the composites. It has been reported that intercalated and exfoliated clay layers in rubber orient along the strain direction during stretching [12]. After 24h of thermal ageing significant reduction in tensile strength was noted for English Indian clay loaded composites, whereas the reduction is comparatively less in nanocomposites. The better retention in

physical properties of nanocomposites during thermal ageing was due to evenly distributed network of silicate layers (Figures 7. 2a and 2b)

    Both the cross-link formation and main chain scission at high temperature influence the reduction in polymer elongation. The degradation action of oxygen with natural rubber is activated by heat. The mechanism of oxidative degradation can be explained in Figure 7.7.
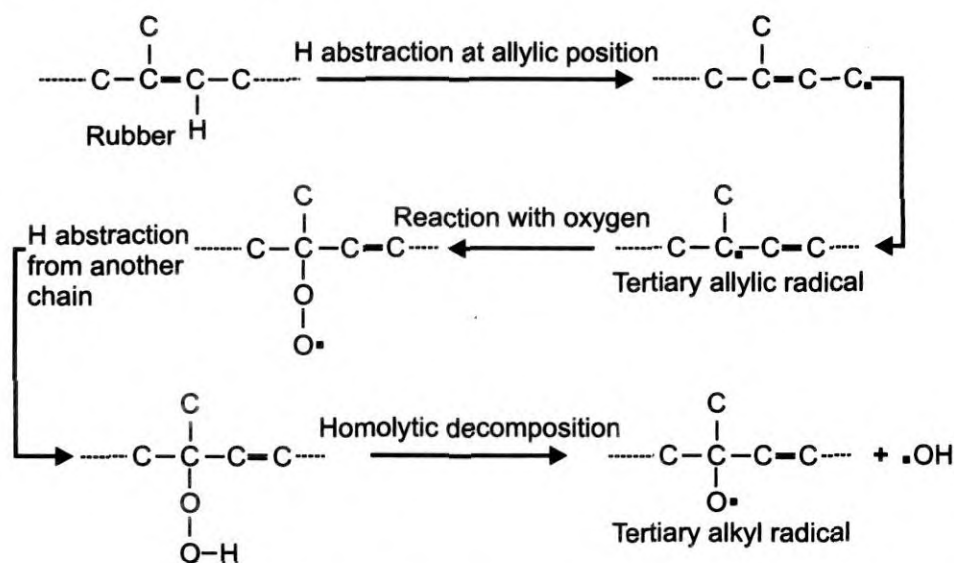
Figure 7.7 Mechanism of thermal degradation of natural rubber [13]

Isoprene   Dipentene   P-Menthene
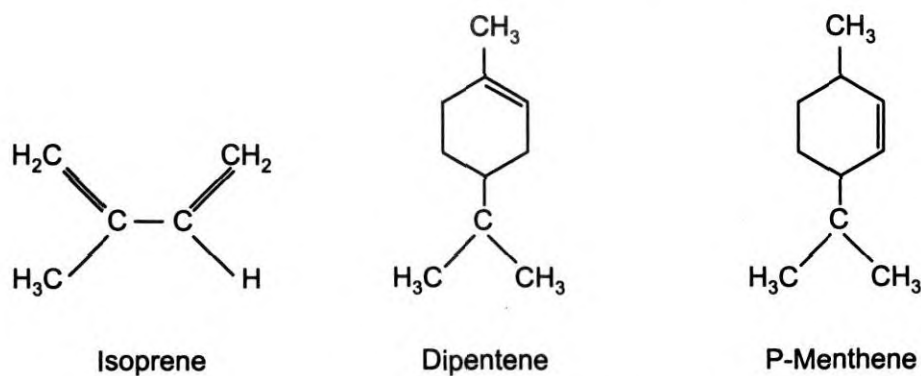
Figure 7.8 Thermal degradation products of natural rubber

The main products of thermal degradation of natural rubber are isoprene, dipentene and p- menthene (Figure 7.8).

In rubber compounds, high temperature cause two competing reactions namely the crosslink formation and scission of chains. In nanocomposites (fluorohectorite or bentonite filled compounds), crack propagation due to chain scission is hindered by clay platelets distributed throughout the matrices. It is reported that the layered silicates filled polymer matrix can improve thermal stability and is explained to the hindered diffusion of volatile decomposition products of the rubber [14-16]. Hence nanocomposites showed comparatively higher tensile strength after thermal ageing.

7.2.2.2 Heat ageing in autoclave

The performances of the latex films in autoclave conditions are important and are given in Table 7.2. Retention of modulus and elongation at break are better for nanocomposites.

Table 7.2 Percentage retention of tensile properties after autoclave ageing

Sample	Elongation at break	500% Modulus
English Indian clay	95.47	87.30
Bentonite	100.53	101.50
Fluorohectorite	98.69	93.00

This indicates that natural rubber latex nanocomposites have good retention of tensile properties after autoclave ageing. It indicates that the products such as gloves made from these materials are suitable for sterilization

and their properties can be retained. Percentage retention in modulus is maximum for nanocomposites especially bentonite. It may be because of the clay platelets act as barriers against the steam and oxidation residues which resist the rubber from further degradation.

7.2.2.3 Exposure to γ- radiation

The effect of γ- radiation on tensile properties of amorphous filler and two layered silicate incorporated vulcanizates are given in Figure 7.9.
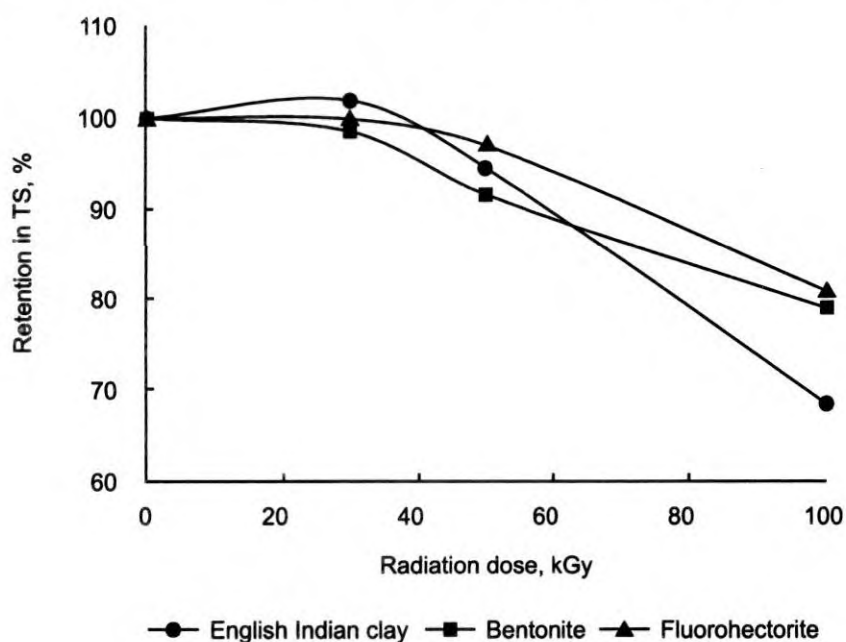
Figure 7.9 Percentage retention of tensile strength after gamma radiation

Being a high energy radiation, gamma irradiation cause a decrease in tensile strength of all composites, but the extent of decrease is different [17]. Though gamma radiation can cause crosslinking and polymer degradation,

the reduction in tensile values showed that chain scission leading to polymer degradation is the predominating reaction.

7.2.2.4 Exposure to UV- radiation

Figure 7.10 showing the effect of UV irradiation on percentage retention of modulus at 500 per cent elongation. During UV irradiation chain scission may occur as a result of the following reactions [17].

$$\text{Polymer} \xrightarrow{h\gamma} R^*$$

$$R^* + O_2 \longrightarrow RO_2^*$$

$$RO_2^* + RH \longrightarrow ROOH + R^*$$

$$2\,RO_2^* \longrightarrow \text{Non radical products}$$
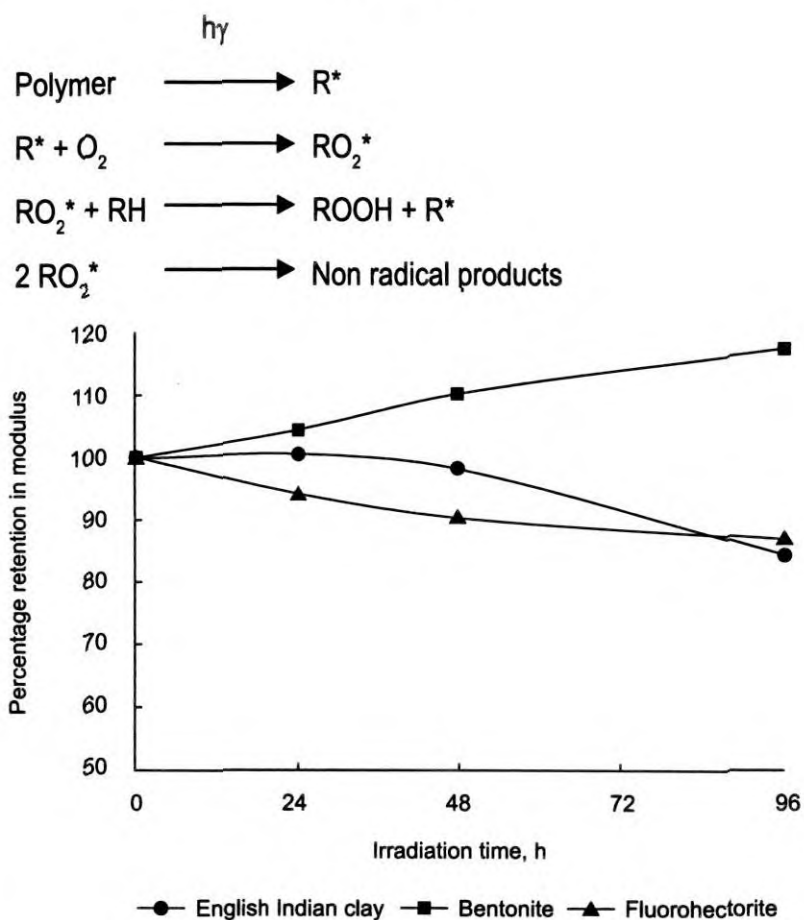
Figure 7.10 Percentage retention in 500 per cent modulus after UV radiation (for 48 h in 30 W).

The imporatance of hydroperoxide in the photo-oxidation process is well established and the photo-oxidation rate is proportional to the initial hydroperoxide concentration. In this case tensile retention decreases as the radiation time increases. Here all the composites showed good retention which might be due to the action of antioxidant (Wingstay). Wingstay has enhanced catalytic activity against hydroperoxide decomposition, UV absorption and deactivation of the absorbed light. The critical region of sun's spectrum responsible for sensitization of photo-oxidation is from 290-350 nm [18]. Slightly higher retension rates shown by fluorohectorite and bentonite might be due to the barrier effect of the layered silicates [19]. It is observed that the sample becomes opaque and sticky on UV- exposure and this may be due to the surface oxidation.

7.2.2.5 Effect of chlorination

Chlorination is a common method used for deprotenization and sterilization of medical goods like latex gloves, catheters, surgical tubing etc. The effects of chlorination on tensile properties of nanocomposites are shown in Table 7.3.

Table 7.3 Percentage retention of tensile properties after chlorination

Sample	Tensile properties		
	Tensile strength	Elongation at break	500 per cent Modulus
English Indian clay	94.5	92.6	95
Bentonite	99.4	96.4	104.5
Fluorohectorite	98.1	95.5	102.1

Here the retention of tensile properties of nanocompsites is better than amorphous filler.

7.2.2.6 Effect of solvent

Figure 7.11 shows the mol percentage of toluene absorbed by the composite at 25°C. The gum vulcanizate has the greatest toluene uptake at equilibrium swelling.
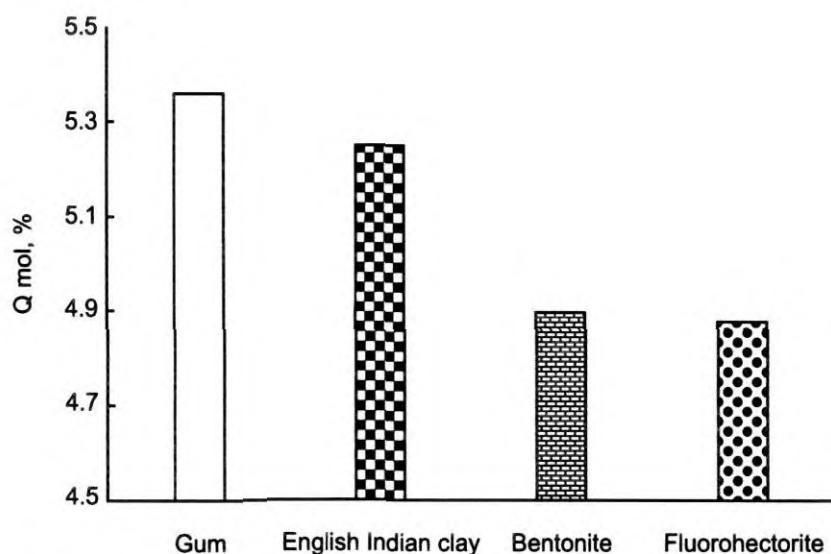
Figure 7.11 Mol per cent of solvent absorbed by the nanocomposites at equilibrium swelling

There is less restriction for the solvent absorption through the vulcanizate filled with microfiller. At equal volume loading of filler [20], the amount of solvent absorbed at equilibrium swelling is less for the composites containing layered silicates-especially with fluorohectorite. The presence of impermeable clay platelets decreases the migration by increasing the effective diffusion path in the specimen [20].

In commercial clay filled rubber, the solvent uptake is greater because of the weak interface and also due to poor clay dispersion. The Kraus plot, which shows the ratio of the crosslink-density of the unfilled material (V_{ro}) to that of the filled vulcanizate (V_{rf}), is given Figure 7.12.
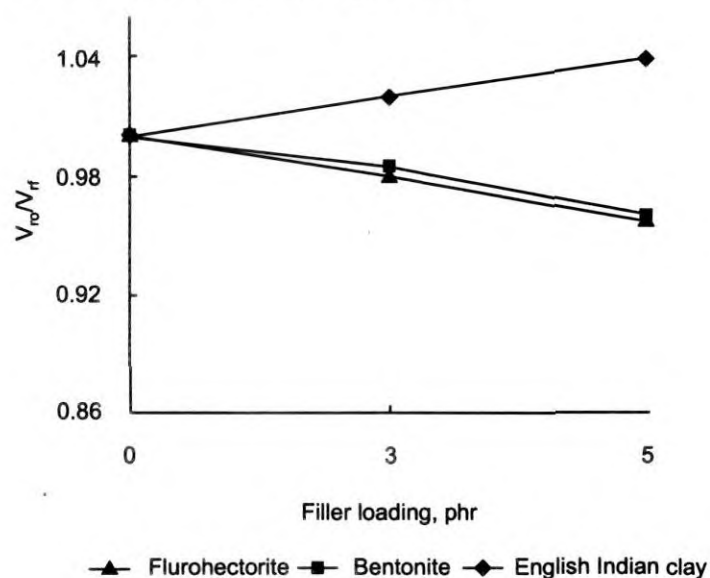
Figure 7.12 V_{ro}/V_{rf} against filler loading

If the value V_{ro}/V_{rf} is less than unity the filler rubber interactions are more and vice- versa. It is interesting to note that for layered silicates V_{ro}/V_{rf} is always less than one and the magnitude of the ratio decreases with filler loading. However in the case of English Indian clay the V_{ro}/V_{rf} is always higher than 1 and these composites showed low reinforcement and poor mechanical properties.

7.2.2.7 Exposure to ozone

Figure 7.13 shows the percentage retention of tensile strength with ozone. The percentage retention of tensile strength is high for fluorohectrite containing vulcanizate at different concentrations of ozone.
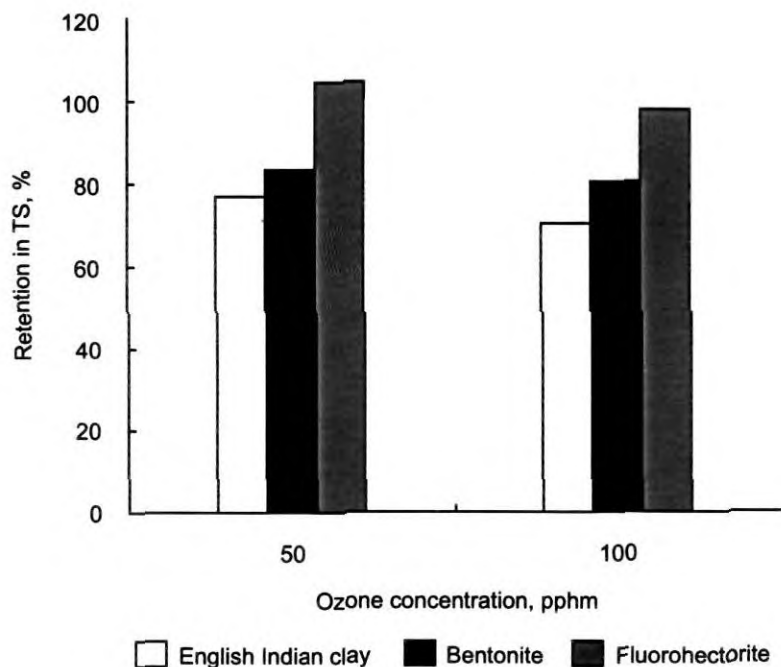
Figure 7.13 Percentage retention of tensile strength of latex vulcanizates with ozone concentration

This may be due to the protection of polymer matrix by exfoliated silicate platelets. Nanocomposites have very good ozone impermeability as the penetration of ozone was arrested by the silicate layers and the scission of rubber chain will be less especially at the bulk of the material.

Figure 7.14 shows schematic representation of degradation in polymer matrix containing layered silicates. This figure explains the comparatively better properties registered by layered silicates towards different degradation processes. This is because in nanocompsite the silicate layers are evenly distributed in the polymer matrix, which in turn gives a good reinforcement. During ageing process, natural rubber products generally undergo two types of

elongation at break of nanocomposites hardly affected on thermal ageing. Nanocomposites retained their tensile properties up to a radiation dose of 40 kGy and thereafter it decreased. On exposure to UV–radiation fluorohectorate showed inferiior properties compared to the ordinary clay compounds. As the penetration of oxygen through the nanocomposite was hindered by silicate layers, they showed good retention of tensile properties on ozone exposure. The retention effect was more pronounced in bentonite- nanocomposites, which might be due to the high level of exfoliation. The silicate platelets in nanocomposites prevent the penetration of degrading agents which protects the chains from oxidation.

7.4 References

1.   K. M. Lee, C. D. Hann, *Macromolecules*, **36**, 19, 7165 - 7178, 2003

2.   E. P. Giannelis, R. Krishnamoorti, E. Manias, *Adv. Polym. Sci.*, **138**, 107 - 147, 1999

3.   R. A. Vaia, G. Price, P. N. Ruth, H.T. Nguyen, J. Lichtenhan, *Appl. Clay. Sci.*, **15**, 67 - 92, 1999

4.   K. Yano, A. Usuki, A. Okada, T. Kaurauchi, O. Kamigatio, *J. Polym. Sci. Part A; Polym. Chem.*, **31**, 2493 - 2498, 1993

5.   T. Lan, P. D. Kaviratna, T. J. Pinnavaia, *Chem.Mater.*, **7**, 2144 - 2150, 1995

6.   X. Kornmann, Synthesis and Characterization of Thermoset-Layered Silicate Nanocomposites, Ph.D Thesis, Lulea University of Technology, Sweden, 2001

7.   S. Varghese, J. Karger-Kocsis, *Polymer*, **44**, 17, 4921 - 4927 2003

8.   P. A. Tarantili, Nanocomposites and Polymers with Analytical Methods,

Ed. John Cuppoletti, ISBN 978-953-307-352-1 ch 7, 149 - 180, 2011

9.   J. K. Pandey, K. R. Reddy, A. P. Kumar, R.P. Singh, *Polym. Degr. Stab.* **88**, 234 - 250, 2005

10.   A. Das, D. Wang, K. W. Stockelhuber, R. Jurk, J. Fritzsche, M. Klu ppel, G. Heinrich, *Adv. Polym. Sci.,* **239**, 85 - 166, 2011

11.   R. Alex, C. Nah, *J. Appli. Polym. Sci.,* **102**, 4, 3277 - 3285, 2006

12.   X. Dai, J. Xu, X. Guo, Y. Lu, D. Shen, N. Zhao, X. Luo, X. Zhang, *Macromolecules,* **37**, 15, 5615 - 5623, 2004

13.   K. J. Kurien, Studies For Improving The Degradation Resistance of Natural Rubber Latex Vulcanizates with Special Reference to Heat and UV- Radiation. Ph.D Thesis, 44, 2002

14.   J. W. Gilman, C. L. Jackson, A. B. Morgan, R. Harris, E. Manias, E. P. Giannelis, M. Wuthenow, D. Hilton, S. H. Phillips. *Chem.Mater.,* **12**, 7, 1866 - 1873, 2000

15.   Z. K. Zhu, Y. Yang, J. Yin, X. Y. Wang, Y. C. Ke, Z. N. Qi, *J. Appl. Polym. Sci.,* **73**, 2063 - 2068, 1999

16.   A. Leszczynska, J. Njuguna, K. Pielichowski, J. R. Banerjee, *Thermochimica Acta,* **454**,1, 1 - 22, 2007

17.   V. R. Gowariker, N. V. Viswanathan, J. Sreedhar, Polymer Science, chap 10, 278, 1996

18.   J. C. Salamone, Polymeric Materials Encyclopedia, Boca Raton, CRC Press, 8684, 1996

19.   S. Komarneni, *J. Mater. Chem.,* **2**, 1219 - 1230, 1992

20.   S. Mathew, S.Varghese, *J. Rubb. Res.,* **8**, 1 - 15, 2005

.

Mechanical and Morphological Properties of Natural/Chloroprene Latex Blends Nanocomposites

Natural rubber latex (NRL), chloroprene rubber latex (CRL) and their blend nanocomposites were prepared using layered silicates. Dispersions of fluorohectorite (synthetic) and bentonite (natural) were mixed with respective rubbers in the prevulcanized stage was used for the production of nanocomposites. An amorphous grade of clay (English Indian clay) was also mixed with the same combination of latices for comparison. The latex based composites were characterized using X-ray diffraction (XRD), transmission electron microscopy (TEM) and Fourier transform infrared spectroscopy (FTIR). From the shift in wave number to the lower regions from the stretching ν (Si-O) and bending δ (Si-O) vibrations of fluorohectorite and bentonite, it is understood that layered clays are well intercalated in NR, CR and 80/20NRCR blends. It was found that fluorohectorite and bentonite improves the mechanical properties of NR, CR and also their blends. Addition of layered silicates also improved the ageing resistance of the component rubbers and their blends. This suggests that these latices and their blends are good intercalation material for fluorohectorite and bentonite.

8.1 Introduction

Layered silicates, being hydrophilic will undergo hydration in aqueous solutions, resulting an increase in interlayer distance. Rubber latices being fine dispersion of rubber particles in aqueous medium can penetrate in the expanded (due to hydration) regions of layered silicates (gallery space), which is considered to be an easy way of producing rubber nanocomposites. Nanocomposites of natural rubber latex were produced both from compounded and prevulcanization routes [1-7].

It has been found that uniform distribution of nanoscale-silicate layers imparts better mechanical and barrier properties to NR latex film. Methods are also reported to produce nanocomposites from solution mixing of latex and layered silicates followed by coagulation [8]. However the slow rate of drying of the coagulated mass and processing difficulties thereafter diminished the production of rubber nanocomposites through this route. Due to the enhanced modulus and reduced barrier properties, unlike the virgin rubber, nanocomposites have got a wide spectrum of applications. Comparatively lower level of loading and the identical colloidal properties of the latex nanocompounds with the conventional micro-dispersions made it more acceptable to the latex dipping industry [9].

Blending of polymers in the latex stage has provided an easy and efficient way to produce new types of high performance materials which results in a molecular level dispersion of materials [10-13]. The enhancement in properties by the addition of layered silicate to latex depends on nature of the polymer (polar or non polar), type of clay (hydrophilic or hydrophobic)

and it's loading. The level of exfoliation rather than the amount of layered silicate decides the composite properties. Blending of CR latex with NR latex will increase the polarity of NR latex (thereby increases the compatibility with layered silicates) which is expected to impart good mechanical properties to the resulting nanocompounds. Hence a study was undertaken to evaluate the composites properties of NR/CR latex blends.

8.2 Experimental

Materials and the equipment used are given in chapter 2. In this study blending of latices and then film was casted. Latex blends (*viz.* 50/50 and 80/20) were prepared by blending the respective latices. Aqueous dispersions of layered silicates were mixed with the latex blends in definite proportions. It was then cast on raised glass plates having dimensions of 13cm x l0cm x 2mm. The casting was allowed to dry at room temperature until transparent and post vulcanized at 70°C for 2h in an air-circulated oven. The samples thus obtained were kept in a desiccator for mechanical testing.

The composites are denoted as given below.

CR- Chloroprene rubber	NR- prevulcanized natural rubber
CRF- CR with fluorohectorite	NRF- prevulcanized NR with fluorohectorite
CRE- CR with bentonite	NRE- prevulcanized NR with bentonite
CRC- CR with China clay	NRC- prevulcanized NR with China clay
50/50NRCR- 50:50 prevulcanized NR/ CR blend	**80/20NRCR -** 80:20 prevulcanized NR /CR blend

8.3 Result and discussion

8.3.1 The XRD studies of NR, CR and their blends nanocompsites

The XRD spectra of the composites are given in Figure 8. 1. The XRD method involves the monitoring of the position, shape, and intensity of the basal reflections from the distributed platelets of layered silicates within the polymer matrix. A shift of the characteristic diffraction peak to lower angles suggests an increase in interlayer spacing of the clay, which is referred as intercalation. Disappearance of this peak may indicate a possible exfoliation of the clay platelets from stacks. Other change might be peak broadening which is considered to be a result of certain level of intercalation and exfoliation [14].

The spectra of pure fluorohectorite and its nanocomposites with NR, CR and 80/20NRCR blends are shown in Figure 8.1A. Sodium fluorohectorite has two peaks corresponding to the 2θ values 7.8° and the other at 9.23° corresponding to the interlayer distances 1.16 and 0.95 nm respectively. The sharp peak at 9.23° suggests that bulk of the fluorohectorite has the characteristic interlayer distance of 0.95nm.

Fluorohectorite filled NR showed a broad peak at 7.7° (d =1.17nm) and a less broad peak at 3.4° (d= 2.6nm.) This suggests that peak at 9.23° (fluorohectorite) has shifted to the lower angles 7.7° indicating an increase in the interlayer distance from 0.95nm to 1.17nm. Similarly the minor peak at 7.8° was shifted to 3.4° causing an increase in interlayer distance from 1.17 to 2.6nm in the composite. All these suggest that NR hydrocarbon intercalated well with fluorohectorite.
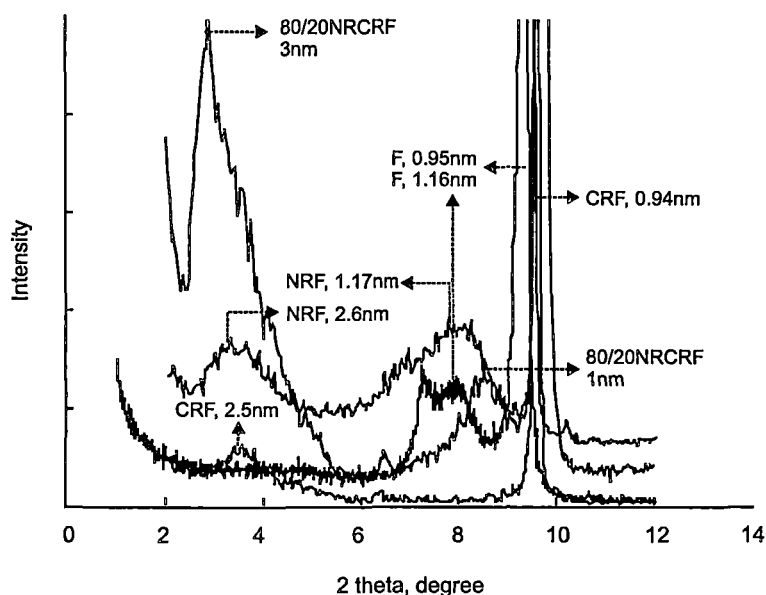
Figure 8.1(A) XRD spectra of fluorohectorite (10 phr) of NR, CR and 80/20NRCR blend. Spectrum of pure fluorohectorite is also given.

In the case of CR nanocomposite 2 peaks were resolved one at $9.4°$ and another at $3.5°$ which corresponds to the d distance 0.94 nm and 2.5 nm respectively. The peaks are less prominent compared to the NR-fluorohectorite composite.This suggests almost complete exfoliation of fluorohectorite in CR latex. The reason for the higher intercalation of CR with fluorohectorite might be due to the polar nature of CR molecules. However in an 80/20 blend of NR latex with CR latex (80/20NRCRF) two peaks were observed. The strong peak at $2.9°$ (d= 3nm) and a less broad peak at $8.6°$ (1nm). In this case also there is a visible shift in the peaks which suggests that the blend is good intercalating with fluorohectorite.
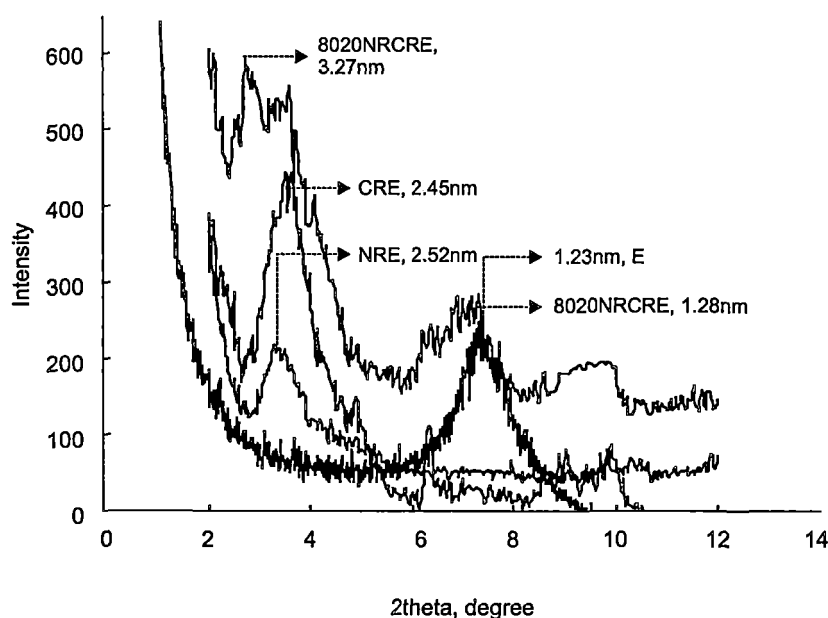
Figure 8.1 (B) XRD spectra of bentonite (10 phr) of NR,CR and 80/20
NRCR blend. Spectrum of pure bentonite is also given.

The spectra of pure bentonite and its nanocomposites with NR, CR
and 80/20NR CR blends are shown in Figure 8.1B. The only one peak at 7.2°
suggests that bulk of the bentonite has the characteristic interlayer distance
at 1.23 nm. Bentonite filled NR showed a prominent peak at 3.5° (d =2.52nm). This
suggests that the characteristic peak of bentonite (7.2°) has shifted to the lower
angles (3.5°) in the composite indicating an increase in the interlayer distance
from 1.23 to 2.52nm. This suggests that the NR hydrocarbon intercalated well
in to the bentonite clay layers.

In the case of CR nanocomposite one peak was observed at 3.62°
which corresponds to the d distance 2.45 nm. Since there is a shift in the peak
from 1.23 to 2.45nm, CR intercalates well with the bentonite layers. However

in an 80/20 blend of NR latex with CR latex (80/20NRCRE) two peaks were observed. The strong peak at 2.7° (d= 3.27nm) and a less broad peak at 6.88° (1.28nm). In this case also there is a visible shift in the peaks suggesting that the blend is a better intercalation material for bentonite, compared to the pure natural rubber latex.

8.3.2 FTIR analysis of NR, CR and their blends nanocomposites.

The absorption bands in the infrared (IR) spectrum of various layered silicates depend on their chemical composition. Differences between the FTIR spectra of pure clay and their nanocomposites were analyzed among peaks corresponding to the vibrations of the macromolecular chains of either CR, NR or in their blend. The vibration of the Si-O bond in the clays was found to be sensitive to stress (here better adhesion between rubber and silicate) indicating a shift to lower wave numbers with increasing level of strain.
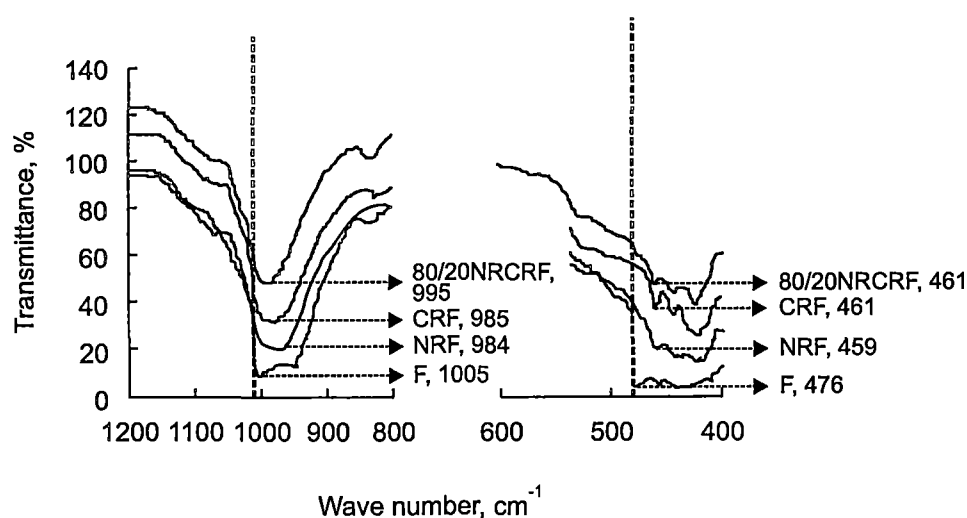
Figure 8.2(A) FTIR spectra of fluorohectorite at 10 phr loading in NR,CR and 80/20NRCR blend vulcanizates

In fluorohectorite (F), the IR spectrum presents mainly two peaks corresponding to the Si-O stretching vibration, ν(Si-O) at 1005 cm^{-1} and the Si-O bending vibration, δ (Si-O) at 476 cm^{-1}(Figure 8. 2A). As presented, the Si-O stretching vibration at 1005 cm^{-1}, in the case of CR/fluorohectorite system is appearing at 985 cm^{-1} whereas, it is at 984cm^{-1} in NR/fluorohectorite. The blend 80/20 NRCR with fluorohectorite showed that the peak is at 995cm^{-1}. The bending vibration of fluorohectorite δ (Si-O) at 476 cm^{-1} is shifted to 461 in CR and 459 in NR and 461 in the blend nanocomposites. These changes in the peaks to lower wave numbers indicated the higher energy required in the stretching and bending vibrations of Si-O bond due to the intercalation with polymer chains.

In the case of bentonite nanocomposites (Figure 8.2 B), the effect of intercalation is very much visible in the FTIR spectra.
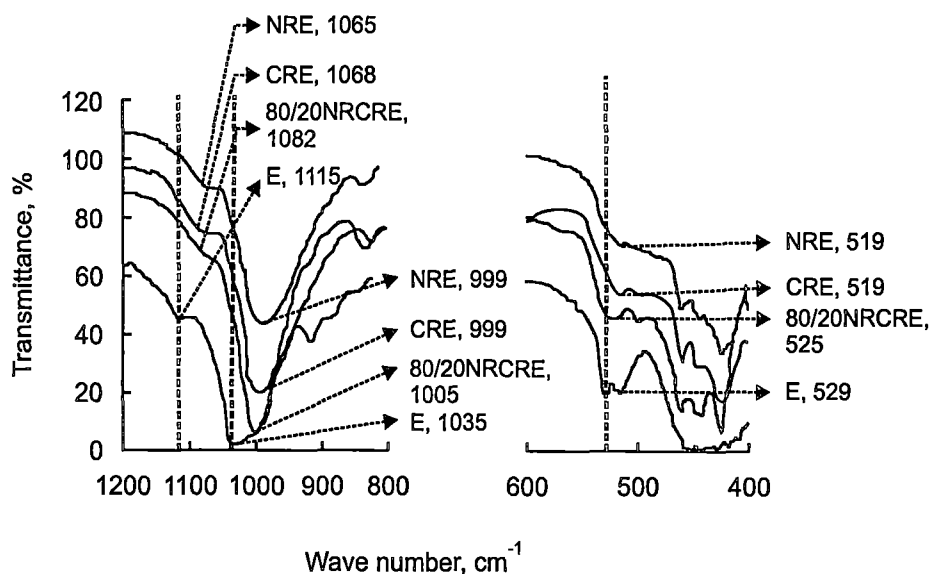
Figure 8. 2(B) FTIR spectra of bentonite at 10 phr loading in NR,CR and 80/20NRCR blend vulcanizates

The IR spectrum of bentonite (E) presents mainly two peaks, two of them corresponding to the Si-O stretching vibrations, ν (Si-O) at 1035 cm^{-1} and stretching / wagging ω (Si-O) at 1115 cm^{-1}. Here 1035 cm^{-1} band corresponds to the in-plane stretching (ν) and 1115 cm^{-1} band corresponds to out-of plane stretching/wagging vibrations (ω). The Si-O bending vibration of bentonite, δ (Si-O) is at 529 cm^{-1}. Sensitivity of these peaks to intercalation/ exfoliation phenomena is discussed here. As presented in Figure, the in-plane Si-O stretching vibration (δ) of pure bentonite clay at the 1035 cm^{-1} is appearing at 999 cm^{-1} in the case of both CR/bentonite and NR/bentonite systems . The blend, 80/20 NRCR with bentonite showed ν (Si-O) at 1005 cm^{-1}. The out-of plane stretching vibration band (ω) of (Si-O), at 1115 cm^{-1} of bentonite is shifted to 1065 cm^{-1} in NR/bentonite, 1068 cm^{-1} in CR/bentonite and 1082 cm^{-1} in 80/20NRCR blend bentonite system. The bending vibration of bentonite δ (Si-O) at 529 cm^{-1} is shifted to 519 in both CR and NR and 525 in 80/20NRCR blend [Figure 8.2(B)] [15]. The visible shift to lower wave number regions in all these cases explains the intercalation of polymer with silicate layers.

8.3.3 Swelling studies of NR, CR and their blends nanocomposites

The swelling curves of the composite were given in Figures 8.3. As the equilibrium swelling (Q_α) values are smaller, higher will be the $1/Q_\alpha$ values, which indirectly show the crosslink density of the polymer
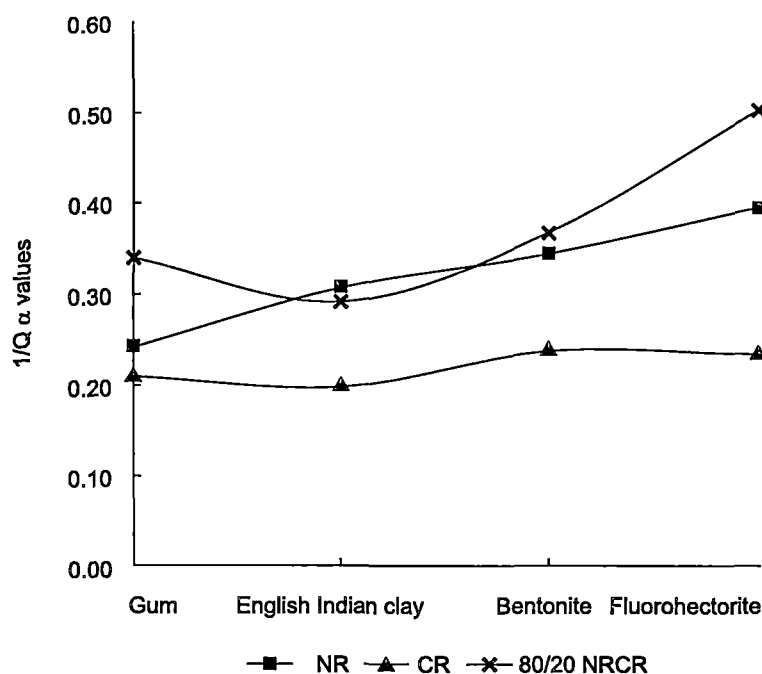
Figure 8. 3 1/Q values of latex vulcanizates of NR, CR and 80/20NRCR
blends nanocomposites

In the case of nanocomposites the intake of solvent is lower compared to gum compounds (Figure 8. 4). This was expected, since there was less restriction for the solvent penetration in gum vulcanizate. At equal volume loading of filler, the amount of solvent absorbed at equilibrium swelling is less for the composites containing layered silicates - especially with fluorohectorite - compared to that containing commercial clay. During swelling the solvent can enter in the polymer along or transverse direction to the aligned silicate platelets. The presence of impermeable clay layers decreases the solvent migration by increasing the average diffusion path length in the specimen [16]. In commercial clay filled rubber, the solvent uptake is restricted to a lower extent because of the weak interface and also due to poor clay dispersion.
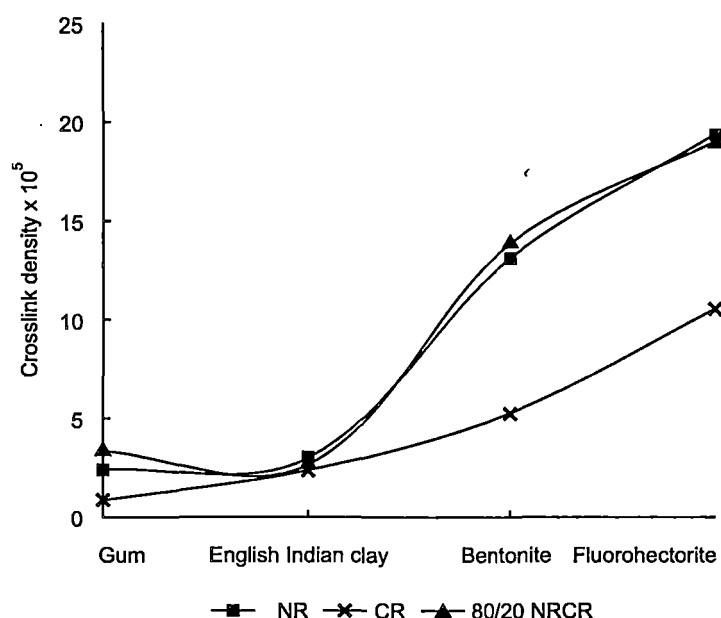
Figure 8. 4 Crosslink density values of NR, CR and 80/20NRCR blend nanocomposites

In well-oriented composites, the penetration perpendicular to the orientation of clay platelets is highly restricted.

A strong polymer- filler interaction reduces the voids at the interface which in turn, leads to less solvent pockets. An enhancement of $1/Q_\alpha$ values may be due to the combined effects of reinforcement, additional crosslinking in presence of filler and the decrease in polymer fraction in the composites. Equilibrium swelling in solvents can be taken as a means to evaluate rubber-filler adhesion, because filler if bonded is supposed to restrict the swelling of the elastomers. Generally in blend system, uneven distribution of crosslinks can be observed due to the difference in affinity of the two phases [17]. When the nanoclays are mixed with the rubber blend, swelling decreases due to the

delaminated clay platelets. In the case of amorphous clay there is only marginal increase in crosslink density due to the uneven distribution of filler particles. In all these cases crosslink density is higher in layered silicate nanocomposites compared to the amorphous clay.

8.3.4 NR and CR nanocomposites

The tensile strength of NR and CR loaded with 10 phr of fluorohectorite and bentonite are shown in Figure 8. 5.

As NR is a strain crystallizing rubber addition of layered silicates does not make any difference in the tensile values of the nanocomposites. However in the case of CR, tensile strength increased from 13 to 18 MPa on addition of 10 phr fluorohectorite. This increase in tensile strength of CR may be because of the reinforcing action of clay platelets in polychloroprene rubber. In NR and CR, bentonite nanocomposites showed maximum properties compared to the amorphous clay. This might be due to the high interlayer distance (1.25nm) of bentonite and better intercalation of the rubber. Amorphous clay (English Indian clay) imparts lower properties in both NR and CR due to the larger particle size.

The moduli at different elongations of the composites are given in Figures 8.6a & 6b. Unloaded NR shows very low modulus at all elongations. It is to be noted that the addition of fluorohectorite causes sharp increase in modulus. Bentonite also showed the same trend. However, unfilled and English Indian clay filled material showed minimum change in modulus. In CR, (Figure 8. 6 b) the unfilled and the English Indian clay composites showed almost similar pattern with modulus.
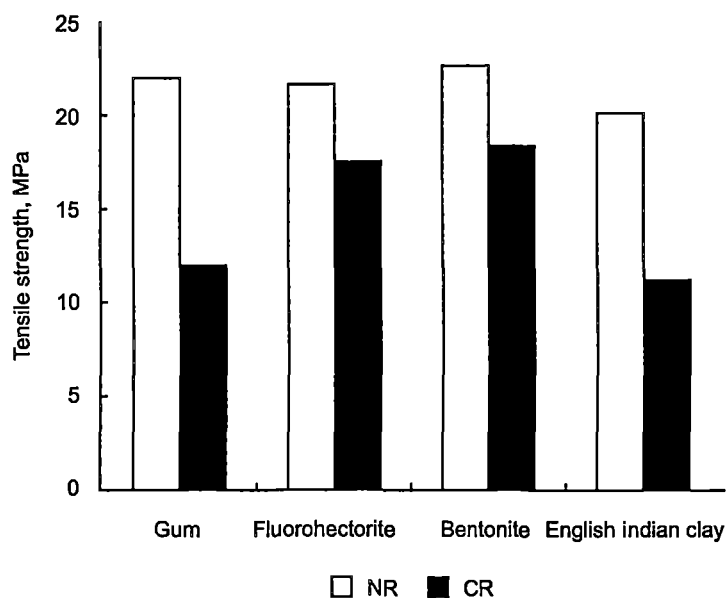
Figure 8.5   Tensile strength values of NR and CR with different silicates nanocomposites at 10 phr loading.
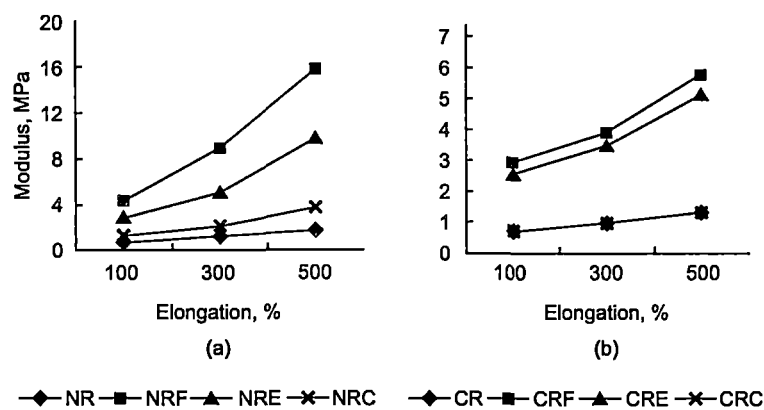
Figure 8.6   Modulus at various elongations of a) NR nanocomposites b)CR   nanocomposites at 10 phr of silicates loading.

The corresponding CR nanocomposite (CRE and CRF) showed sharp increase in modulus at all elongation. However, compared to NR nanocomposites (NRF and NRE) the magnitude of the modulus values is less.

The stress relaxation of the NR and CR composites of different silicates are given in Figures 8.7a and b respectively. In the case of pure NR vulcanizate σ_t/σ_0 is initially 1 and on loading with filler it declines slowly and remains almost constant.
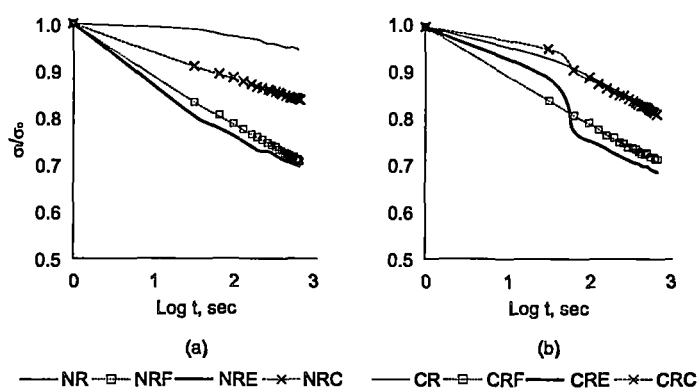
Figure 8.7 Stress relaxation behaviour of a) NR nanocomposite b) CR nanocomposite at 10 phr of silicate loading

For CR vulcanizate stress relaxation is faster than NR vulcanizate. This may be because of the partially crosslinked (prevulcanised) nature of the CR latex particles. It has a single stage relaxation pattern. For amorphous filler, the relaxation of stress is faster compared to gum vulcanizate. In nanocomposite (NRF, NRE, CRF & CRE) the stress decay is much faster and slightly higher in bentonite nanocomposites. In the case of nanocomposites in NR and CR a two stage relaxation mechanism can be seen. It must arise from the progressive failure of rubber- filler attachment either at the surface of the filler or by the rupture of the rubber molecules attached to them. Though the filler loading in nanocomposites and ordinary amorphous clay composite are the same (10 phr), due to exfoliation of the layered silicate (fluorohectorite and bentonite) the effective surface area is very high in nanocomposites. This

might be the reason for the faster relaxation of stress in both NR and CR nanocomposites.

Effect of layered silicates on tension set and tear strength in NR and CR are given in Table 8.1.

Table 8.1 Tear strength and tension set of blends

Sample	Tear strength (N/mm)	Tension set (%)
NR	47.98	1
NRF	28.9	6.67
NRE	23.2	12
NRC	41	6
CR	14.4	8
CRF	25.7	18
CRE	19.4	15.2
CRC	4	10
50/50NRCR	25.4	2
50/50NRCR F	30	14
50/50NRCR E	31.7	26
50/50NRCR C	26.1	4
80/20 NRCR	44.8	2
80/20 NRCR F	35.6	6
80/20 NRCR E	46	24
80/20 NRCR C	33.7	4

In all the cases the layered silicate has high tension set. As the filler rubber interphase increases the chain slippage will be high. This loosely bound interface is responsible for the high tension set in nanocomposites. Tension set values are inversely proportional to 1/Q.

8.3.5 NR/CR blend nanocomposites

The 50:50 virgin blends of NR and CR gave very low tensile strength (Figure 8. 8) whereas corresponding nanocomposite showed sharp increase in the tensile strength values.
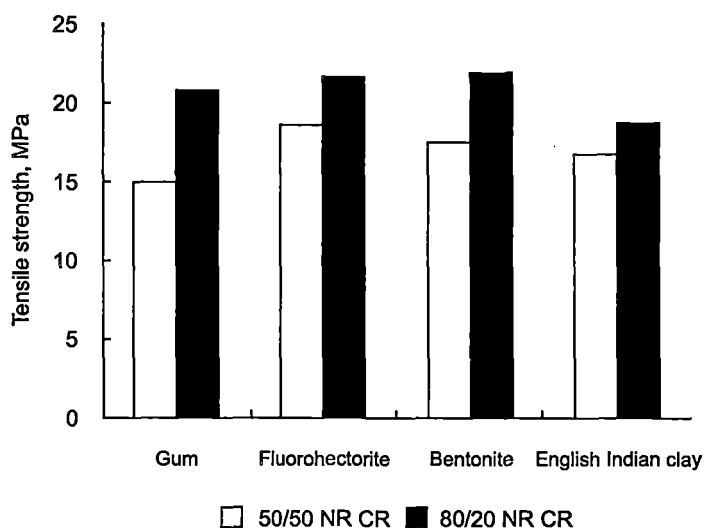
Figure 8.8   Tensile strength values of NR/CR blend nanocomposites with different silicates at a loading of 10 phr

In the case of 80:20 NR/CR blend the pure blend showed a tensile value of 23 MPa and the corresponding nanomaterials also showed almost the same tensile value. This indicates that the virgin blend and the composites showed high TS value when NR phase is predominating. The polarity of the latex (CR)

seems to be influenced by the composite properties. However the effect cannot be assessed in blends as the strain crystallizing effect also comes to effect.
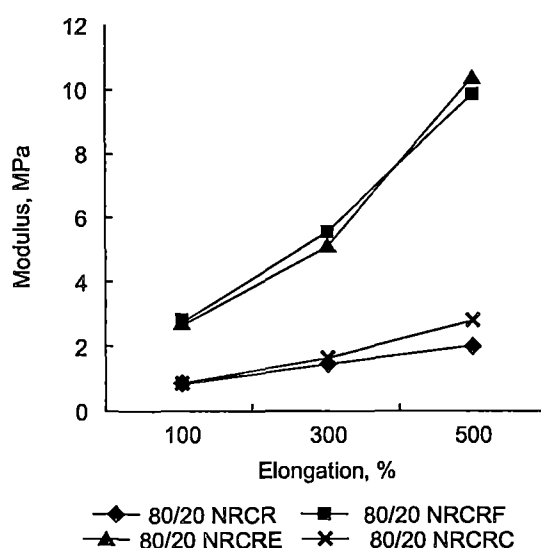
Figure 8.9 Modulus at different elongations of NR/CR blend nanocomposites at 10phr loading

Figure 8.9 shows the modulus at different elongations of the 80/20NRCR blends. The high modulus of the fluorohectorite composite was resulted from the high in- plane strength and large aspect ratio of the fluorohectorite clay platelets.

Figure 8.10 shows the comparative analysis of the after ageing tensile strength values of 50:50 and 80:20 NR, CR blends containing 10 phr of layered and amorphous silicates. The layered silicates nanocomposites show high ageing resistance. This might be due to the higher crosslink formation at the elevated temperature. After 24h of thermal ageing significant reduction in tensile strength was noted for English Indian clay loaded composites, whereas the reduction is comparatively less in nanocomposites.
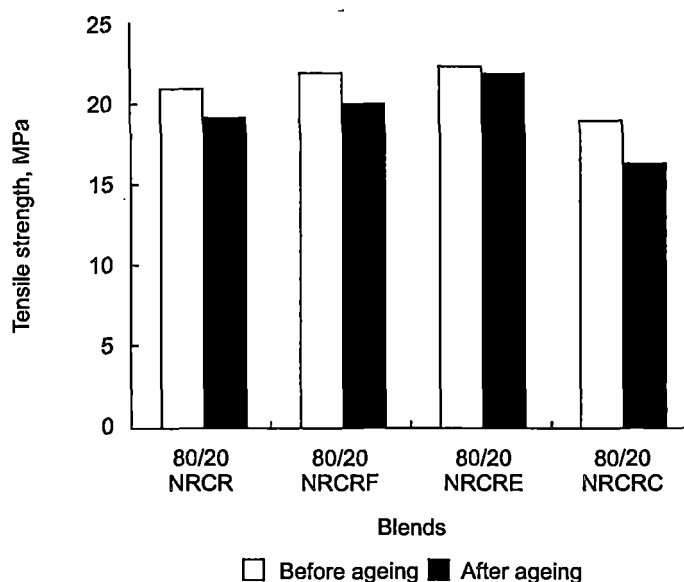
Figure 8.10 Effect of ageing on tensile values of 80/20 NRCR blends
nanocomposite at 10 phr silicate loading

The better strength retention of nanocomposites during thermal ageing was due to evenly distributed network of silicate layers. It is reported that the layered silicates filled polymer matrix can improve thermal stability by preventing the diffusion of volatile decomposition products of the rubber to the bulk [18].

The stress relaxation of the blends composites is given in Figure 8.11. The relaxation of the composites of virgin rubber blends is slow. In the 80/20 blend loaded with layered clays, the relaxation is fast and it follows the same trend as that of pure NR and CR nanocomposites (Figure 8.7).
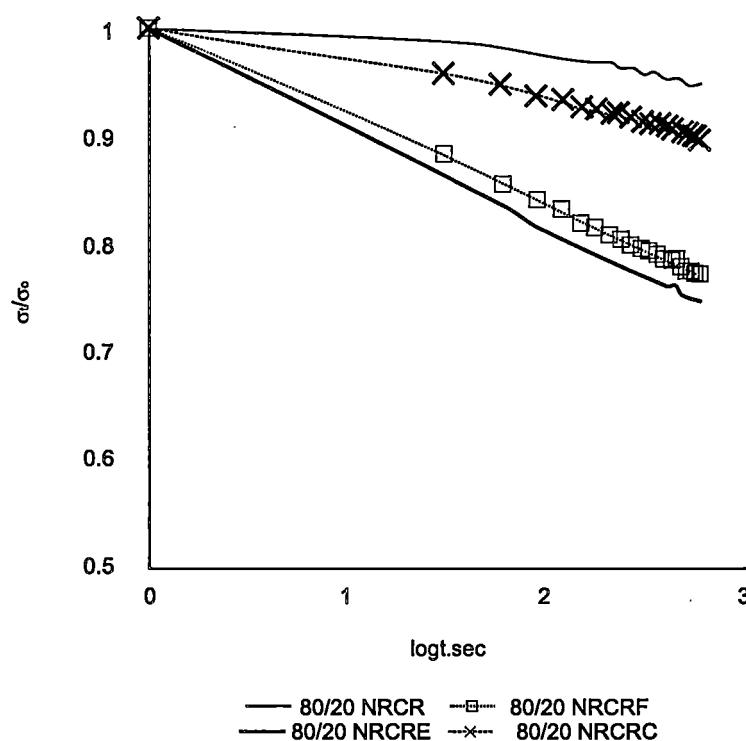
Figure 8.11 Stress relaxation pattern of 80/20 NRCR blends nanocomposite at 10 phr silicate loading

8.4 Conclusion

As observed from the shifting of peaks from higher to lower 2θ values in XRD spectra and also from higher to lower wave numbers in FTIR spectra, it is concluded that layered silicates delaminate in NR, CR and its blends. It was also observed that, the performance of a layered silicate in polymer depends on the nature of the polymer and also on the interlayer distance of the clay. The tensile strength of NR and CR and their blends loaded with 10 phr of layered silicates showed superior TS value when NR is a major component. The nanofillers are polar hence it is more compatibile with CR and 50:50 NR CR blends than pure

NR and 80/20NRCR blend. In blend latices, layered silicates show low elongation values than their corresponding gum and amorphous clay vulcanizates. The layered silicates show high ageing resistance due to the silicate platelets distributed in the matrix. The relaxation of the composites of virgin rubbers and their blends are slower than their corresponding nanocomposites. In all cases the solvent swelling of nanocomposites is lower than the virgin compounds, since there was restriction for the solvent absorption in nanocomposites. As the amount of NR in the blend increases, tear strength values increases. In all cases, crosslink density is higher in layered silicate nanocomposite than the amorphous clay composites.

8.5 References

1.   G. C. Psarras, K. G. Gatos, J. Karger-Kocsis, *J. Appl. Polym. Sci.*, **106**, 2, 1405 - 1411, 2007

2.   Y. Wang, H. Zhang, Y. WU, J. Yang, L. Zhang, *J. Appl. Polym. Sci.*, **96**, 318 - 323, 2005

3.   E. P. Giannelis, *Adv. Mater.*, **8**, 29 - 35, 1996

4.   T. Pojanavaraphan, R. Magaraphan, *Euro. Polym. J.*, **44**, 7, 1968 - 1977, 2008

5.   S. Mathew, S. Varghese, *J. Rubb. Res.*, **8**, 1, 1 - 15, 2005

6.   R. Stephen, S. Varghese, K. Joseph, Z. Oommen, S. Thomas, *J. Membrane Sci.*, **282**, 162 - 170, 2006

7.   Z. Gu, G. Song, W. Liu, P. Li, L. Gao, H. Li, X. Hu, *Appl. Clay Sci.*, **46** ,3 241 - 244, 2009

8.   J. Karger-Kocsis, C. M. Wu, *Polym. Eng. Sci.*, **44**, 1083 - 1093, 2004

9.   S. Mathew, S. Varghese, G. Rajammal, P. C. Thomas, *J. Appl. Polym. Sci.*, **104**, 1, 58 - 65, 2007

10.   S. Varghese, J. Karger-Kocsis, *Polymer*, **44**, 4921 - 4927, 2003

11.   J. T. Varkey, P. R. Chatterji, S. S. Rao, S. Thomas, *J. Appl. Polym. Sci.*, **68**, 1473 - 1483,1998

12.   Japan Synthetic Rubber Ltd., Brit. Pat., 1, 046, 215, 1966

13.   R. Stephen, K. V. S. N. Raju, M. Rao, B. Francis, K. Joseph, S.Thomas., *J. Appl. Polym. Sci.*, **104**, 2528 - 2535, 2007

14.   M. Yoonessi, H. Toghiani, W. L. Kingery, C. U. Pittman, Jr., Macromolecules, **37**, 2511-2518, 2004

15.   H. A. Patel, R. S. Somani, H.C. Bajaj, R.V. Jasra, *Res. Commun. Curr. Sci.*, **92**, 7, 1004- 1009, 2007

16.   Y. Kojima, K. Fukumori, A. Usuki, A. Okada, T. Kurauchi, *J. Mater. Sci. Letters*, **12**, 889 - 890, 1993

17.   L.E. Nielsen, R.F. Landel, Mechanical properties of polymers and composites, 2nd Edition, Marcel Dekker, New York, USA, 1994

18.   Z. K. Zhu, Y. Yang, J. Yin, X. Y. Wang, Y. C. Ke, Z. N. Qi, *J. Appl. Polym. Sci.*, **73**, 2063 - 2068, 1999

Design and Development of Foley Catheter from Natural Rubber Latex Nanocompound

Natural rubber latex products are found applications in health care area for decades due to their outstanding barrier and strength properties. Nanoclays impart higher modulus and better impermeability to rubber films. Latex Foley catheters require good modulus and strength properties, which is usually met by blending suitably compounded NR latex with synthetics. In this work, nanoclay was tried in NR latex to meet the specific strength properties required for Foley catheter. Since the dipping process of catheter is different from other products, the suitability of the latex nanocompound was followed by studying the surface finish and strength of the latex film. The compound was fine tuned to meet the physical and non-toxic properties.

9.1 Introduction

Plenty of consumer and healthcare products are produced from natural rubber, either from latex or dry rubber. With the advent of universal precautions against AIDS, hepatitis B, hepatitis C, etc., many regulatory bodies advocate the use of gloves and condoms both among health care workers and the general public. Another major use of NRL is in urological devices like the Foley catheters. Other medical applications also include vaginal diaphragms, tubes for intravenous (IV) drips, stethoscope tubing, baby bottle nipples, syringe plungers, vial stoppers, etc.

Among the various elastomers available, natural rubber latex (NRL) remains the material of choice for manufacturing gloves and other products owing to the excellent wet gel strength, tactile characteristics, tear resistance, elasticity, and barrier properties [1-6].

Catheter is a flexible tube made of latex, silicone, or teflon that can be inserted into the body creating a channel for the passage of fluid for the entry of a medical device. Now-a-days, there are many specialized catheter designs. For example, specific catheter designs allow catheters to be used in pulmonary, cardiac (vascular), neonatal, central nervous system, and epidural tissues. Catheters are designed to perform tissue ablation (tissue removal) and even serve as conduits for thermal, optics, and various medical devices. The three major types of catheters are coronary, renal, and infusion.

The best-known renal catheters are Foley catheters, which have been commercially available since the 1930s. These catheters are equipped with an inflatable balloon at the tip and are used for urine incontinence and bladder

drainage following surgery or an incapacitating injury or illness. The Foley catheter is relatively easy to use and used throughout the world in hospitals, nursing homes, and home-care settings. From a patient care point, the easiness to insert the catheter in to human body and retrieval from the body must be a very sensitive issue. The modulus of the product must be very critical so as to prevent tissue damage [7, 8].

Foley catheters were designed by Dr. Frederick Foley, a surgeon working in Boston, Massachusetts in the 1930s, when he was a medical student. His original design was adopted by C. R. Bard of Murray Hill, New Jersey, who manufactured the first prototypes and named them in honor of the surgeon. The Foley catheter came into existence in the 1930s. Frederick E. B. Foley began to experiment with different catheters and he realized that urinary catheters would easily slip out of the bladder because there was no way to hold them in place. Foley experimented with different methods of securing the catheter until he came up with the idea of attaching a balloon-like device to the end of the catheter. The device would then be able to be placed and then inflated from the outside. By 1934, Foley catheters were on the market. Other than in material, the Foley catheter remains relatively unchanged in design today.

Foley catheters are flexible (usually latex) tubes that are passed through the urethra during urinary catheterization and into the bladder to drain urine. They are retained by means of a balloon at the tip which is inflated with sterile water. The balloons typically come in two different sizes: 5 cc and 30 cc. The products specifications by various standard organizations are addressing the factors such as size, integrity of the balloon, load carrying capacity and so on [9-10].

In this study a nanoclay latex formulations was developed to meet the specific strength properties of a Foley catheter.

The formulation is designed in such a way that it shall meet the specifications of the catheter by adjusting the amount of layered silicates and other ingredients.

9.2. Result and Discussion

All the chemicals were made to dispersions and compounded in double centrifuged latex using the formulation given in Table 9.1

Table 9.1 Formulation of the latex layered silicate nanocomposite for catheter

Sl.no	Ingredients	Wet wt
1.	60% Double centrifuged latex	167.0
2.	10% Potassium oleate solution	1.0
3.	50% Sulphur dispersion	2.4
4.	50% ZDC dispersion	2.0
5.	50% Anti oxidant dispersion	1.0
6.	50% ZnO dispersion	1.0
7.	50% ZMBT dispersion	0.3
8.	10% Bentonite nanoclay dispersion	10

9.2.1. Optimization of catheter compound

9.2.1.1. Flow properties

The viscosity of latex compound has a critical role in most of the manufacturing processes. Bentonite incorporated latex compound showed

high viscosity than other latex compounds at all loadings [11]. When bentonite is mixed with water, it undergoes considerable swelling due to hydration [12]. Moreover, the ion-exchange capacity of bentonite is comparatively higher which also influences the intercalation process.

Figure 9.1 shows the variations of shear stress of bentonite-loaded composites at three different temperatures 25, 35 and 45°C at (1 phr loading). There is a tremendous increase in stress with strain for bentonite at 25°C compared to other temperatures. This might be due to the hindrance exerted by entangled silicate layers to the flow. At high strain rate exfoliated silicate layers align along the direction of the rubber hydrocarbon.
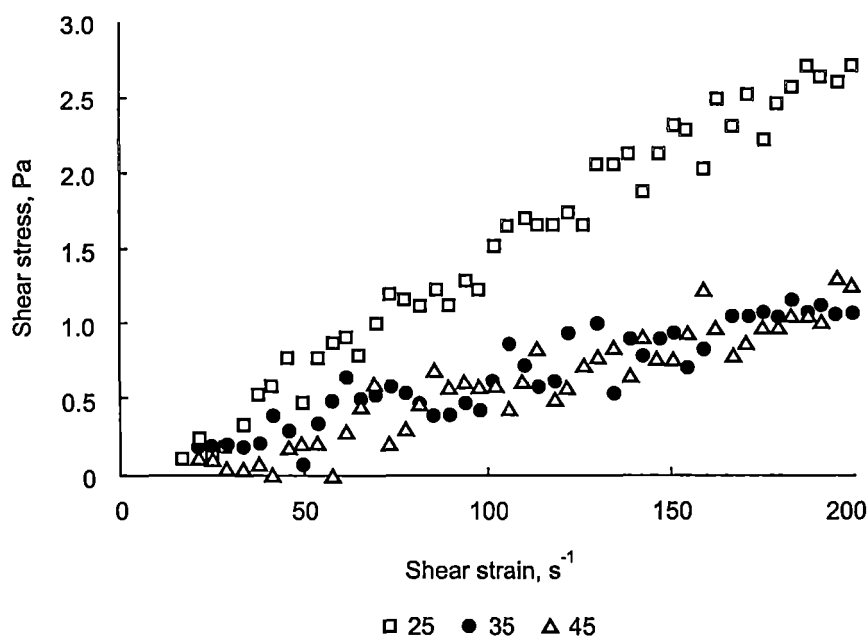
Figure 9. 1 Variations of shear stress at different temperatures of latex compound (1phr bentonite) used for the preparation of latex Foley catheter

9.2.1.2 Optimization of dipping conditions

9. 2.1.2.1 Withdrawal rate of former

The dipping characteristics of the catheter compound were studied with a glass former at constant dwell time and immersion speed. The concentration of the coagulant also kept constant. Figure 9.2 shows the variation in latex film thickness with the rate of withdrawal of the glass former loaded with bentonite (1 phr). A formulation without bentonite was used as control compound.
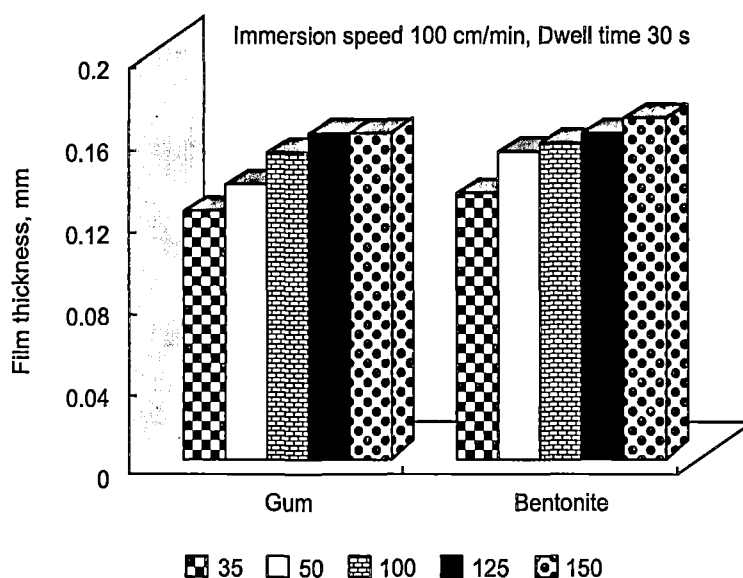
Figure 9.2   Thickness of latex deposit with different rate of withdrawal of the former at constant immersion rate and dwell time

9.2.1.2.2 Immersion rate of the former

Effect of varying immersion rate (cm/min) of the former in to the gum and bentonite (1phr) latex compounds are shown in Figure 9.3. In both cases there was a threshold value above which the thickness decreases. Above the

threshold level the dripping of the latex compound increases since the film holding capacity of the former decreases.
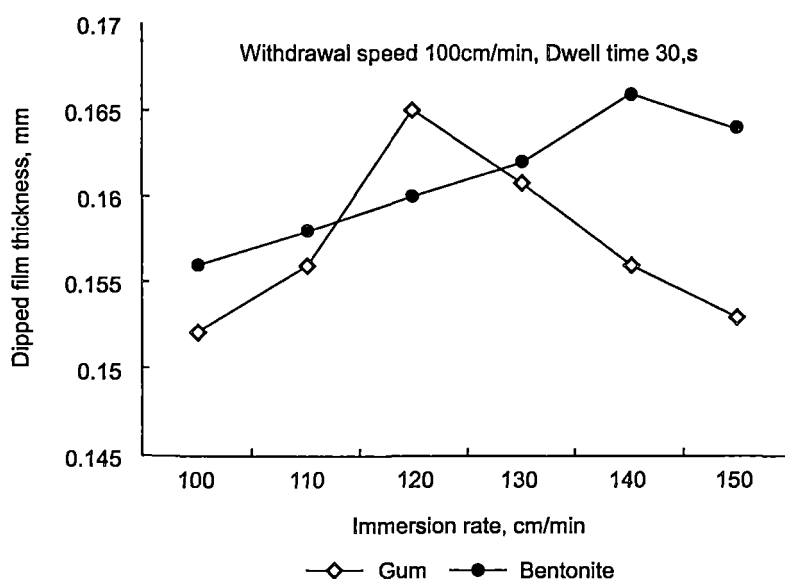
Figure 9.3 Effect of immersion rate (cm/min) of the former on latex film thickness

9.2.1.2.3 Dwell time

Effect of varying dwell time on film thickness was shown in Figure 9.4. As the dwell time increases thickness also increases. This is due to the fact that as the dwell time increases the amount of coagulant deposit on the former increased which intern lead to thick deposit.
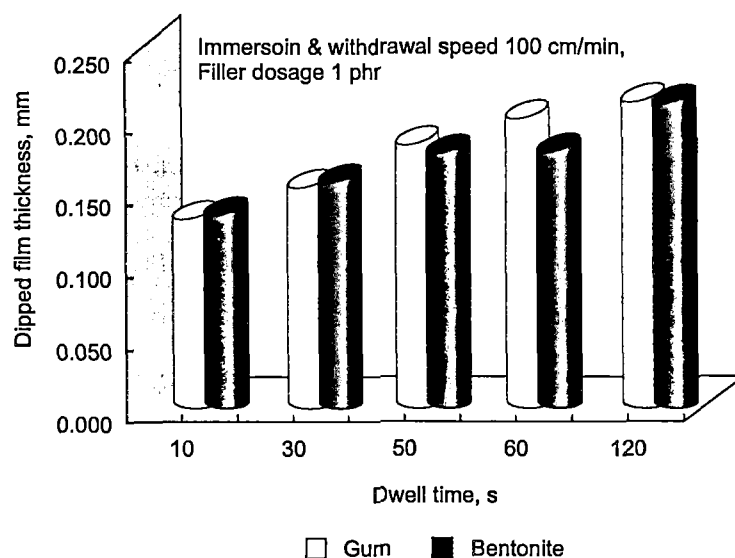
Figure 9. 4 Effect of varying dwell time on film thickness

9.2.1.2.4 Concentration of coagulant

In order to get an idea about the thickness of the latex film with coagulant concentration, an experiment is performed with different coagulant concentration and the results are tabulated in Table 9.2. The dwell time was also optimized during this experiment.

As concentration of the coagulant increases (10-30 per cent) thickness also increases. At high coagulant concentration, the amount of coagulant deposit on the former increased and, hence the rate of diffusion of the coagulant into the latex was higher, which lead to a thick film.

Table 9.2 Effect on film thickness with different concentration of coagulant at different dwell time

Dwell time, s	Bentonite , phr					
	10% Ca (NO$_3$)$_2$		20% Ca (NO$_3$)$_2$		30% Ca (NO$_3$)$_2$	
	0	1	0	1	0	1
10	0.130	0.133	0.160	0.165	0.179	0.174
30	0.152	0.154	0.192	0.211	0.228	0.217
50	0.182	0.177	0.225	0.225	0.283	0.241
60	0.201	0.178	0.235	0.262	0.300	0.342
120	0.211	0.211	0.282	0.293	0.344	0.386

9.2.1.3 Optimization of dipping parameters

From the above experiments the dipping conditions ideal for the catheter compound have been optimized and are listed in Table 9.3

Table 9.3 Dipping characteristics of the catheter compound

Sl. no	Parameters	Value
1.	Immersion speed, cm/min	100
2.	Withdrawal speed, cm/min	100
3.	Dwell time, s	30
4.	Concentration of the coagulant [Ca(NO$_3$)$_2$], %	25

The properties of the catheter compounds (nanocompound and commercial micro compound) are also tested and tabulated in the Table 9.4

Table 9.4 Properties of catheter compound

Sl.no	Tests done	Nanocomposite	Microcomposite
1.	Total solid content, %	45	58
2.	Viscosity, cPs	130	105
3.	pH of the compound	10.15	10.56

9.2.2 Preparation of catheter

The clean dry steel mould was first dipped into the coagulant followed by drying. The coagulant coated steel mould was then immersed into the latex nanocompound according to the conditions given in Table 9.3. After 2 dips in latex compound and coagulant, a thread was fixed and again dipping continued and after partial drying at 80°C for half hour remove the thread. Then placed the latex tube for balloon in the correct position and then also dipping continued for 2 times. (This process is repeated till the deposit gets the desired thickness. Normally this will take 4-5 dipping.) The product is then stripped and leached in several hours in fresh water to remove the residual chemicals. Any material deemed to be defective is discarded. Since the product is directly related to human health, the material must fulfill all quality conditions prescribed. The layer to layer adhesion of the latex film formed by multiple-dipping and strength of the catheter balloon are also checked as per specifications. Figure 9.5 is the process flow chart for the manufacture of Foley catheter from latex nanocompouind.

9.2.2.1 Process flow chart
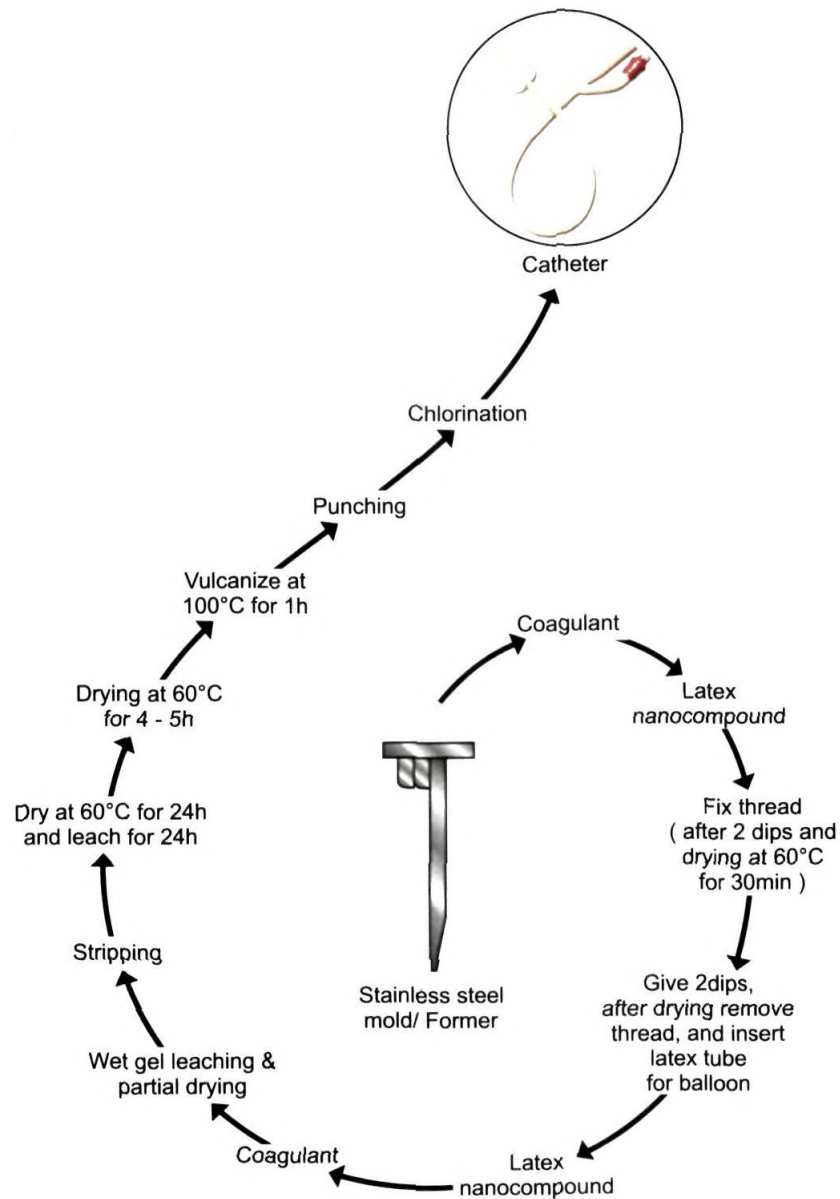
Figure 9. 5 Process flow chart for the manufacture of latex Foley catheter

Table 9.5 Technical properties of vulcanized catheter compounds

Tests done	Microcomposite (Conventional formulation)	Nanocomposite (Designed formulation)	Specification IS 7523/1974 [9]
1. Before ageing as per ASTM D 412-1980			
a) Tensile strength, MPa	18.5	25.01	10 (Min)
b) Elongation at break,%	823	810	400 (min)
c) 300% modulus, MPa	1.24	1.23	-
2. After ageing as per ASTM D 412-1980 (at 100°C for 22h)			
a) Tensile strength, MPa	26.5	28.4	-
b) Elongation at break, %	955	1010	-
c) 300% modulus, MPa	1.08	1.23	-
3. Tension set, %	8	6	10 (Max)
4. pH of water extract	7.5	7.4	7±0.5
5. Extracts colour	colourless	colourless	colourless
6. Extractable protein [content, µg/dm² [13]	56	<50	-
7. Powder content [14]	nil	nil	-
8. Bioburden test	No fungal or bacterial growth	No fungal or bacterial growth	-

Table 9. 5 shows the technical properties of the catheter, done as per IS specification for latex catheter (As per IS 7523/1974Re affirmed date 09 /2001Ammendment No1 [9]) and it was found that all the properties were well within the limits.

9.3 Conclusion

Foley balloon catheters are currently being imported to India and a large volume of this is used in hospitals. In this study nanocomposites were introduced to improve the technical properties of the catheter. The main intention of this study was to know the effect and appearance of the product with nanocomposites, since the mould design and catheter preparation is complicated than the other dipped products. Suitable latex nanocomposite using bentonite was developed and its rheological properties and dipping characteristics were analyzed and a suitable formulation was finalized that the technological properties were also noted. Which was suited for the production of catheter and that meets the physical and non-toxic properties. In order to get correct knowledge about factory problems this work was mainly done in collaboration with M/s Kodi Rubbers, Kerala. The photographs of the catheter prepared are given in Figure 9.6.

Conventionally latex catheters are prepared with certain amount of high styrene SBR latex for getting the required modulus. In the preparation of nanocomposite catheters, the required modulus was met with layered silicates and the production completely bio- compatible. Moreover, the nanocomposite catheters are completely transparent so that the transfer of fluids through the catheter can be viewed externally.
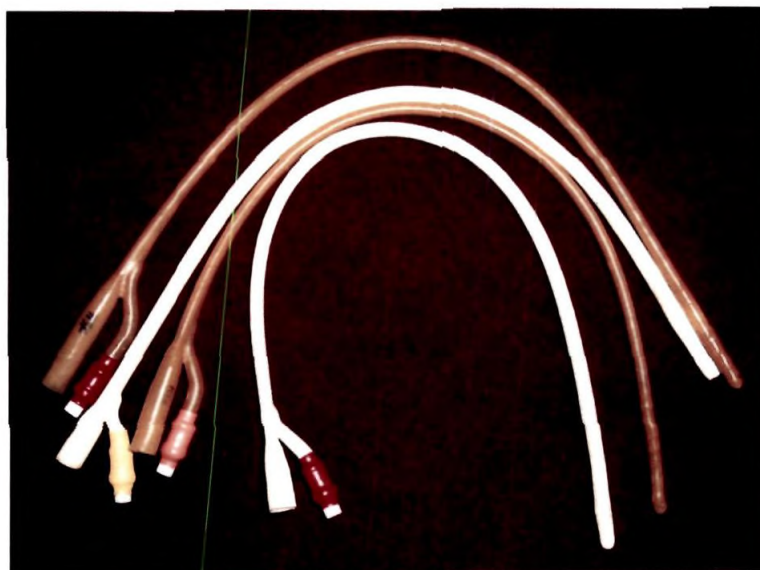
Figure 9.6 Optical photograph of Foley catheters made from natural
rubber latex-layered silicate nanocomposite

9.4 References

1.   E. K. Abraham, P. Ramesh, *Polymer Reviews*, **42**, 2, 185 - 234, 2002

2.   H. R. Kotilainen, J. L. Avato, N. M. Gantz, *Appl. Environ. Microbiol.*, **56**
      6, 1627 - 1630, 1990

3.   M. J. Cox, W. J. Bromberg, R. D. Zura, P. A. Foresman, R. G. Morgan,
      R. F. Edlich, *J. Appl. Biomat.*, **5**, 257 - 264, 1994

4.   J. G. Neal, R. F.Edlich, E. M. Jackson, F. Suber, *J. Long-term Effects
      Med. Impl.*, **8**, 3 & 4, 233 - 240, 1998

5.   G. T. Rodeheaver, D. B Drako, J. G. Neal, E. M. Jackson, F. Suber, P.
      A. Foresman, R. F. Edlich, *J. Long-term Effects Med. Impl.*, **8**, 3 & 4,
      241 - 248, 1998

6.   C. P. Hanman, J. R. Nelson, *Am. J. Infect. Control*, **21**, 6, 289 - 296, 1993

7.   D. F. Williams, Biocompatibility in Clinical Practice: Vol II. CRC Press. Florida, Ch 7, 108 - 120, 1982

8.   D. J. Stickler, R. J. C. McLean, *Cells and Materials*, **5**, 167 - 182, 1995

9.   IS 7523:1974, Specification for Rubber catheter (urinary), 09, 2001

10. ASTM F623 -99, Standard Performance Specification for Foley Catheter, 2006

11. S. Mathew, S. Varghese, G. Rajammal, P. C. Thomas, *J. Appl. Polym. Sci.*, **104**, 1, 58 - 65, 2007

12. D. C. Blackely, Polymer Latices, Volume 3, Eds. Chapman & Hall, John Wiley, London, 150, 1997

13. ASTMD5712-10 Standard Test Method for Analysis of Aqueous Extractable Protein in Natural Rubber and its Products using the Modified Lowry Method

14. ASTM D 6124-2006, Standard Test Method for Residual Powder on Medical Glove

Conclusions and Future Outlook

The major conclusions that are drawn from the present study are summarized in this chapter. Future scope and possible applications are also mentioned herewith.

10.1 Conclusions

Nanotechnology is a future manufacturing technology that will make most products lighter, stronger, cleaner, less expensive and more precise.

Over the past decade, nanomaterials have been the subject of enormous interest. These materials, notable for their extremely small size, have the potential for a wide range of industrial, biomedical and electronic applications. Nanomaterials can be metals, ceramics, polymeric or composite materials. Their defining character is its very small feature size in the range of 1-100 nanometers (nm).

At the nanomaterial level, some material properties are affected by the laws of atomic physics, rather than behaving as traditional bulk materials do. Physical substances with at least one characteristic dimension between 1-150nm can be defined as nanomaterials. Nanomaterials properties can differ

from those of the same materials with micron scale dimensions. Nanomaterials are the building blocks of practical nanotechnology and can be physically and chemically manipulated for specific applications.

Nowadays, composite materials have replaced traditional ones in a variety of applications. Lightweight coupled with enhanced properties are the main reasons for their market acceptance and growth, and the optimization of their performance is a challenge worldwide. Composite materials are engineered or naturally occurring materials made from two or more constituent materials with significantly different physical or chemical properties which remain separate and distinct at the macroscopic, microscopic, nanoscale within the finished structure. Composites are made up of individual materials referred to as constituent materials, namely matrix and reinforcement. The high aspect ratio of the reinforcing particle and its adhesion to the matrix are of great importance, because they control the final properties of the composites.

Polymer/clay nanocomposites are formed through the union of two very different materials with organic and mineral pedigrees. The hybrid compositions, however, exhibit large increase in tensile strength, modulus, and heat distortion temperature as compared with the pristine polymer. Polymer/ clay nanocomposites meet these requirements due to the shape (platelet, disc) and nanometer- scale dispersion of the clay layers in the polymeric matrix. This type of composite has raised significant scientific interest due to the improved physical properties that can be achieved by adding a small fraction of clay (<10wt. %) into the polymer matrix. Among the nanocomposites, polymer/ clay nanocomposites have received a lot of attention due to their excellent mechanical and barrier properties. Organically modified layered silicates are also used as excellent reinforcing materials in elastomers.

Best performance of the polymeric nanocomposites is achieved when the silicate layers are dispersed in the polymer matrix without agglomeration. An essential step in the preparation of a nanocomposite is the delamination of the layered silicates (LS), which is usually termed exfoliation in literature. Both the layer thickness and the space (galleries) between the layers are of ca. 1nm. The galleries are occupied by hydrated cations, which counterbalance the negative charge of the layers generated by the isomorphic substitution of some atoms in the silicate crystals.

The environment of the galleries is hydrophilic and thus inappropriate for the hydrophobic macromolecular chains to penetrate therein. The replacement of the inorganic cations by organic onium ions (surfactant, intercalant) overcomes this inconvenience. The cationic head of, *e.g.*, an alkylammonium compound is tethered to the layers *via* coulombic interactions, leaving the aliphatic tail to hover between the layers. The longer the surfactant chain length and the higher the charge density of the clay, the further apart the clay layers will be forced. The presence of these aliphatic chains in the galleries renders organophilic, the originally hydrophilic silicate. A value that characterizes each LS is the cation exchange capacity (CEC), expressed in meq/100g, referring to the moderate negative charge of the clay layer surface. The effect of CEC has been checked for different types of clay. It was claimed that a well exfoliated silicate structure can be obtained in polymers when layered silicates of optimum CEC (ca. 90 meq/100g) are rendered organophilic.

Various models have been developed to trace the parameters forcing the macromolecular chain in the silicate layers and then causing their delamination. The interplay of entropic and energetic factors determines the outcome of

polymer intercalation/exfoliation. The entropy decrease due to confinement of the polymer molecules when entering between the galleries is over-compensated by the increase in the entropy of the tethered chains of the surfactant while the silicate layers are moving apart prior to their final separation. In addition, energetically favored interactions between the surfactant and polymer molecules may yield a negative mixing enthalpy. It should be noted that a molecular dispersion requires that the Gibbs' free energy of mixing become negative.

Vulcanized rubbers are usually reinforced by carbon black and inorganic fillers. Carbon blacks are excellent in reinforcement owing to the strong interaction with rubbers, but their presence often reduces the processability of rubber compounds, especially at high volume loadings. On the other hand, minerals of various shapes (e.g., fibrous, platy) are suitable for rubber filling, but they have a poor interaction with rubbers ("inactive fillers"). Therefore, it is of paramount interest to disperse layered silicate in rubber on a nanometer level. The required level of reinforcement in rubbers can be achieved at very low LS loadings, which offers easier processing without any property deterioration compared to traditional "active" fillers.

Sulphur prevulcanized natural rubber latex (PVNRL) nanocomposites were produced by mixing dispersions of layered silicates with prevulcanized latex. Layered silicates used were bentonite and fluorohectorite along with English Indian clay as reference material. Nanocomposites based on sulphur prevulcanized natural rubber latex and layered silicates were subjected to mechanical, swelling, XRD and TEM analysis. Rubber nanocomposites showed higher modulus and tear strength with incorporation of layered silicate and 3 phr loading was found to be the threshold level for optimum mechanical properties.

Higher loading leads to agglomeration or filler networking in the rubber. The rate of relaxation of stress and tension set were higher for layered silicate incorporated composites. The solvent resistance of the rubber nanocomposites was better compared to the microcomposite. The filler-rubber interactions are strong in layered silicate-incorporated vulcanizate. It was found that the fine silicate layers form a skeleton network structure (house of cards) in the vulcanizates.

Radiation prevulcanized natural rubber latex (RVNRL) nanocomposites were produced by mixing dispersions of layered silicates with radiation vulcanized latex. The XRD and TEM analysis of radiation vulcanized natural rubber nanocomposites revealed the NR chains get intercalated into the galleries of the layered silicate. Dynamic mechanical analysis revealed that layered silicates nanocomposite has higher storage modulus and minimum tanδ values when compared to the corresponding non-layered grade. From the TEM photomicrograph, it was clear that the layers form a network structure and was concentrated around the boundary of the rubber particles. The air permeability studies showed that the layered silicate nanocomposites had higher gas impermeability than radiation vulcanized natural rubber gum vulcanizates and their composite with commercial clay.

The rheological behavior of sulphur prevulcanized natural rubber (NR) latex nanocomposites was compared with the nonlayered clay latex compound. The flow behavior of latex nanocomposites was depend on the nature of the silicates (layered or non-layered). It was found that viscosity decreased with shear rate and layered silicates registered the higher shear viscosity values. The higher viscosity of layered silicates nanocomposites was due to the intercalation/

exfoliation of rubber hydrocarbons. Natural rubber latex nanocomposites showed shear thinning behaviour at higher shear rates due to orientation of the exfoliated or intercalated structure along the direction of shear. As the loading of layered silicate increased, the viscosity of the compound also increased especially at lower shear rates. The intercalation/ exfoliation can be related to the higher zeroshear viscosity, high yield stress, high activation energy and high pseudoplasticity index.

The dipping characteristics of prevulcanized latex compounds containing layered silicates behaved almost similar to conventional latex compounds. The effect of variation in the speed of immersion and withdrawal of the glass former, dwell time and concentration of the coagulant etc on the thickness of the latex deposit was investigated using a semi- automatic dipping machine. The results of the studies showed that the deposit thickness depends on the withdrawal speed of the glass former, and the viscosity of the latex compound. Bentonite, formed filler network in NR latex showed higher compound viscosity and greater film thickness. The thickness of the deposit was found to increase with dwell time as well as increased concentration of the coagulant. Swelling studies showed that fluorohectorite incorporated vulcanizate (dipped film) have high reinforcement. Superior mechanical properties were observed with layered silicate incorporated vulcanizates.

The degradation behaviour of natural rubber latex nanocomposite against various degrading agents *viz.* thermal, gamma and UV radiation, chlorination and solvents was investigated. During thermal ageing, layered silicate nanocomposite showed better retention of tensile strength especially after prolonged ageing periods. Modulus and elongation at break of nanocomposites

were hardly affected by thermal ageing. Nanocomposites retained their tensile properties up to a radiation dose of 40 kGy and thereafter it decreased. On exposure to UV radiation the performance was inferior for ordinary clay compounds. Kraus plot revealed a strong rubber-silicate interface. As the penetration of oxygen through the nanocomposite was hindered by the silicate layers, they showed good retention of tensile properties after ozone atmosphere. The retention effect was more pronounced in fluorohectorite nanocomposites, which might be due to the high aspect ratio of the platelets. The introduction of nanoclays improved the thermal stability of the nanocomposites compared to microcomposites. This was confirmed by XRD, TEM, SEM and TGA analysis.

Prevulcanized natural rubber latex, chloroprene latex and their blend nanocomposites were prepared using layered silicates. It was observed that layered silicates delaminate in NR, CR and also in their blends. This was evident from the shifting of peaks from higher 2θ values to lower in XRD spectra and also from higher to lower wave numbers in FTIR spectra. It was also observed that, the performance of a layered silicate in a polymer system depends on the nature of the polymer and also on the interlayer distance of the clay. The tensile strength of NR and CR and their blends loaded with 10 phr of layered silicates showed superior TS value when NR phase predominates (strain crystallizing effect). Due to the polar nature of layered nanosilicates they are more compatible with CR and 50/50 NR/ CR blends than pure NR and 80/20 NR/CR blends. The blend showed low elongation values than their corresponding gum and amorphous clay vulcanizates. The layered silicate composite showed high ageing resistance. This might be due to the higher crosslink formation at the elevated temperature. NR nanocomposites showed faster relaxation compared

to the composites of virgin rubbers and their blends. In all cases the solvent intake of nanocomposites was lower than the virgin compounds, since there was less restriction for the solvent absorption in the gum compound. In the blend as the amount of NR increased tear strength values decreased. In NR, CR and their blends crosslink density was higher in layered silicate nanocomposites than the amorphous clay.

Latex Foley catheters requires good modulus and strength properties which are usually met by blending suitably compounded NR latex with synthetic polymers. As latex nanocomposites have good modulus and strength properties Foley catheters were developed from the latex nanocomposite which confirms to BIS (Bureau of Indian Standards) specification.

10.2 Future outlook

The development of organoclay/ rubber composites is still in its embryonic stage. The methods practiced so far are related to various solution (including the latex route) and melt intercalations. No direct (*in situ*) intercalation during rubber synthesis was reported in the literature. Irrespective of the success with latex and solution assisted compounding, the research and development activities in the near future will likely to focus on rubber melt intercalation techniques. Here the target issues are to clarify the role of polar rubbers as additives and the effects of curing components, to perform sulfurless vulcanization, to study the effects of processing oils, and to get experience with in situ melt intercalation (rendering the clay organophilic and achieving its intercalation/exfoliation during mixing/curing).

Since the related research in the field of nano-reinforcement is far more advanced with thermoplastic resins than rubbers, attention should be paid to the related achievements, which may serve as guidance for the development of rubber- based nanocomposite. Latex compounding will likely to focus on rubber blends, whereas for solution intercalation, pristine layered silicates will be tried in the future. The other critical issues in the area of nanocomposites are given in section 1.5.1 (page-66).

CURRICULUM VITAE

SHERA MATHEW

Pulimoottil

4B Unity Towers

Collectorate P.O, Kottayam, Kerala

India-686002

E- mail: sheramathew@gmail.com & shera@pulimoodans.com

Present Address	: Scientific Assistant
	Technical Consultancy Division
	Rubber Research Institute of India
	Kottayam, Kerala
	India –686009
	Phone. No. 0481-2303653
Father's name	: Prof. C.M. Mathew
Husband's name	: Er. Jotty P Thomas
Children	: Two
Religion and caste	: Christian, Orthodox
Nationality	: Indian

Academic Qualifications

1996-1998	**Degree of Master of Technology in _Polymer Technology_**
	Cochin University of Science and Technology
1986-1988	**Degree of Master of Science in _Chemistry_**
	U.C. College, Alwaye
1983-1986	**Degree of Bachelor of Science in _Chemistry_**
	C.M.S College, Kottayam

Professional experience:

- 21 years of experience in Rubber Board in the field of developing and testing of rubber products, processing of NR.

- Expertize in the quality control of NR latex and dry rubber, latex products, rubber effluents, rubber chemicals etc as per National and International standard specifications.

- Working knowledge about different machinery and equipments used in rubber products manufacture like Universal testing machine, Viscometer, Rheometer, FTIR, TGA, UV Vis Spectrophotometer, Automatic dipping machine etc.

- Expertize in reverse engineering of rubber products

- Proficient in Microsoft Word, Excel, Graphics, Power Point and Internet research.

Publications

- Natural Rubber Latex-based Nanocomposites with Layered Silicates.
  Shera Mathew and Siby Varghese, *Journal of Rubber Research*, 8 (1) 1-15 (2005)

- Dipping characteristics of layered silicates-natural rubber latex nanocomposites
  Shera Mathew, Siby Varghese, G. Rajammal, P. C. Thomas
  Journal of Applied Polymer Science, 104 (1) Pages 58 - 65 (2007)

- Rheological Behavior of Layered Silicate Natural Rubber Latex Nanocomposites
  Shera Mathew, Siby Varghese, George K.E, Tresa Cherian
  Progress in rubber, plastics and recycling technology, 27 (3), 177-192, (2011)

- Stability and vulcanization characteristics of enzyme deprotienized natural rubber latex
Rajammal G, Mariamma K George, **Shera Mathew**, Peethambaran N.R and Mathew N.M, *Natural Rubber research*, 17(2): 95-102.(2004)

- Natural Rubber Latex Nano Composites – Process Control of Dipped Goods
Shera Mathew, Siby Varghese and P Viswanatha Pillai, Asia RubberTech Expo 2006, Cochin, Kerala

- Rheology and Shapability of Natural Rubber Latex layered Silicate Nanocomposites
Siby Varghese and **Shera Mathew**, International Conference on Latex and Synthetic Polymer Dispersions 2008, Madrid, Spain, 23-24 January 2008.